



Provided by the author(s) and University of Galway in accordance with publisher policies. Please cite the published version when available.

Title	Novel functions for the CENP-A N-terminus during male meiosis in <i>Drosophila melanogaster</i>
Author(s)	Collins, Caitriona Mary
Publication Date	2018-03-23
Publisher	NUI Galway
Item record	http://hdl.handle.net/10379/7258

Downloaded 2024-05-23T02:53:03Z

Some rights reserved. For more information, please see the item record link above.



**Novel functions for the CENP-A N-terminus
during male meiosis in *Drosophila
melanogaster***



Caitríona M. Collins

Supervisor: Dr. Elaine M. Dunleavy

A thesis submitted to the National University of Ireland, Galway
for the degree of Doctor of Philosophy

October 2017

The Centre for Chromosome Biology
The School of Natural Sciences,
The National University of Ireland, Galway

Table of contents	i
Acknowledgments	v
List of Abbreviations	vii
Thesis Abstract	x
1. Introduction	Error! Bookmark not defined.
1.1. Centromeric chromatin.....	2
1.1.1 Centromeres and Centromere Protein A (CENP-A)	2
1.1.2 Canonical chromatin and histone H3 containing nucleosomes	4
1.1.3 Histone H3 versus CENP-A containing nucleosomes	7
1.1.4 The CENP-A histone core	8
1.1.5 The CENP-A N-terminus	9
1.2. CENP-A function and requirements in meiosis.....	10
1.2.1 CENP-A is required for chromosome segregation in meiosis	10
1.2.2 CENP-A is required for epigenetic inheritance in the germ-line	13
1.3. The CENP-A N-terminus is rapidly evolving.....	16
1.3.1 Is rapid evolution of the CENP-A N-terminus a response to meiotic drive?	16
1.3.2 Does the hyper-variability of the CENP-A N-terminus represent lineage specific functions?	17
1.3.3 Differing functional requirements for CENP-A N-terminus in mitosis versus meiosis in plants	21
1.4. The role of CENP-A in meiosis - conclusion	22
1.5. Meiosis in the fruit fly <i>Drosophila melanogaster</i>	27
1.5.1 Insects and the order Diptera	27
1.5.2 <i>Drosophila melanogaster</i> as a model system	27
1.6. A description of spermatogenesis in <i>Drosophila melanogaster</i>	28
1.6.1 Prophase I in male Drosophalids – distinct staging and nuclear morphology	32
1.7. Chromosome dynamics in meiosis I.....	34
1.7.1 Prophase I	34
1.7.2 Achiasmy, an unconventional meiosis I	36
1.7.3 Alternative methods of homologue pairing in <i>Drosophila</i> males	37
1.8. Chromatid cohesion during meiosis.....	41

1.8.1	Alternative methods of chromatid cohesion in <i>Drosophila</i> males	41
1.9.	Do <i>Drosophila</i> have combined methods of pairing and cohesion?..	47
1.10.	Conclusion.....	47
1.11.	The mitochondrial F ₁ - F ₀ ATP synthase.....	49
1.11.1	ATP synthase subunits – links to fertility in <i>Drosophila</i>	49
1.12.	Project hypotheses, rationale and objectives.....	52
2.	Materials and methods	53
2.1.	Chemical reagents and experimental kits.....	54
2.1.	<i>Drosophila</i> techniques.....	54
2.1.1	Fly stocks and husbandry	54
2.1.2	Classification of meiotic cell stages in the male germline	54
2.1.3	Generation of transgenic fly lines	55
2.1.4	Genetic manipulation	55
2.1.5	Fertility tests	60
2.2.	Molecular biology techniques (DNA and RNA).....	60
2.2.1	Extraction of whole fly genomic DNA (gDNA)	60
2.2.2	Extraction and purification of tissue specific RNA	60
2.2.3	cDNA synthesis and reverse transcriptase-PCR (RT-PCR)	61
2.2.4	Cloning	61
2.2.5	Generation of polyclonal antibodies	62
2.3.	Molecular biology techniques (protein).....	63
2.3.1	Recombinant protein expression and purification	63
2.3.2	Recombinant protein dialysis and storage	64
2.3.3	<i>In vitro</i> protein direct interaction assay	65
2.3.4	His-ATPsyn- α interaction with CENP-A peptide array	65
2.3.5	SDS-PAGE and western blotting	66
2.4.	Cell biology techniques.....	66
2.4.1	<i>Drosophila</i> Schneider 2 (S2) cell culture	66
2.4.2	Preparation of cytoplasmic and nuclear extracts from adult testes	67
2.4.3	Pull-down and identification of GST-CENP-A N-terminal interacting proteins.	68
2.4.4	ATP determination assay	69
2.4.5	Preparation of testes for immuno-staining	69
2.4.6	Preparation of testes for Fluorescence In-Situ Hybridisation (FISH).	71
2.4.7	Microscopy and image processing	74

2.4.8	Quantitation of fluorescent intensities	74
2.4.9	Assays used to identify and quantify cohesion, pairing and cell cycle defects	75
2.5.	Computational analysis & software programmes.....	75
3.	A search for novel functions of the CENP-A N-terminus in the male germ-line.	77
3.1.	Chapter introduction.....	78
3.2.	Characterisation of CENP-A RNAi knockdown.....	78
3.2.1	Identification of a novel role for CENP-A in meiotic centromeric cohesion	78
3.2.2	Analysis of arm cohesion in CENP-A RNAi knockdowns	84
3.3.	Analysis of the role of the CENP-A N-terminus during male meiosis	87
3.4.	Identification of novel meiotic CENP-A interacting proteins.....	94
3.5.	Summary.....	97
3.6.	Discussion.....	97
3.6.1	Novel roles for CENP-A in the germ-line	97
3.6.2	A meiosis specific role for the CENP-A N-terminus	99
3.6.3	Novel CENP-A protein interactors in the germ-line.	100
4.	A characterisation of the role of ATP synthase F₁ subunits in the male germ-line of <i>Drosophila melanogaster</i>	101
4.1.	Chapter Introduction.....	102
4.2.	Characterisation of the gene <i>ATPsyn-βlike</i>	103
4.3.	Analysis of meiotic progression in the ATPsyn-α, -β, -βlike and -γ RNAi knockdowns.....	110
4.4.	Identification of centromeric cohesion defects in the ATPsyn-α, -β, -βlike and -γ RNAi knockdowns.....	116
4.5.	Identification of chromatid arm cohesion defects in the ATPsyn-α, -β, -βlike and -γ RNAi knockdowns.....	123
4.5.1	2 nd and 3 rd chromosome arm cohesion	123
4.5.2	4 th chromosome pairing and/or cohesion	128
4.5.3	X chromosome pericentromeric cohesion	128

4.6. Analysis of MEI-S332 localisation in ATPsyn- α , - β , - β like and - γ RNAi knockdowns.....	132
4.7. Discussion.....	134
4.7.1 Characterisation of <i>ATPsyn-βlike</i>	134
4.7.2 The role of ATP synthase F ₁ subunits in male fertility.....	135
5. Characterisation of the functional interaction between CENP-A and ATP synthase subunits ATPsyn-α, βlike and -γ.	137
5.1. Chapter introduction.....	138
5.2. Analysis of whole testis ATP levels after RNAi knockdown of ATPsyn- α , - β , - β like and - γ	139
5.3. Analysis of ATP synthase F1 subunit localisation in the germ-line 144	
5.4. Recruitment of GFP-ATPsyn- β like to meiotic centromeres.....	146
5.5. ATPsyn- α directly interacts with CENP-A in vitro.....	153
5.6. Conserved sequence blocks on the CENP-A N-terminus are required to interact with ATPsyn- α	154
5.7. Discussion.....	159
6. Discussion	162
6.1. A brief summary of major findings.....	163
6.2. The model.....	164
6.3. Do ATP synthase subunits have novel nuclear roles outside of Drosophila male meiosis?.....	170
6.3.1 Potential nuclear roles of ATP synthase subunits in Drosophila female meiosis?.....	170
6.3.2 Potential nuclear roles of ATP synthase subunits in Drosophila mitosis?.....	170
6.3.3 Potential roles in chromatid cohesion and/or homologue pairing in somatic cells.....	171
6.4. A meiotic role for the Drosophila CENP-A N-terminus in centromere assembly.....	172
7. Bibliography	175
8. Appendix	185

8.1.	E. M. Dunleavy and C. M. Collins, 2017.....	186
8.2.	Chemical reagents and common buffers	209
8.3.	Fly stocks used during this study.....	213
8.4.	Information on cloning and cloning strategy	215
8.5.	Primary and secondary antibodies	218
8.6.	Fluorescence in-situ Hybridization (FISH) DNA probes.....	220
8.7.	C. M Collins and E. M Dunleavy, under review.....	221
8.8.	IP and MS results from Experiment 1 (FL GFP-CENP-A).....	233
8.9.	IP and MS results from Experiment 2	237

Acknowledgments

The first and biggest thank you to my supervisor Elaine. I am really incredibly grateful to you for giving me the opportunity to come and work in your lab. And for many other things over the past 4 years.... including, (but not limited to!) always understanding how long things take to complete in reality, for giving good advice, for giving me so many good opportunities, for career advice and for encouragement. I have had a fantastic PhD experience in your lab and I'm sad that it is over!

Also, thank you to the other members of the Dunleavy lab. To Lucretia for being a constant source of entertainment! But also for her help and support. To Ada, for giving me loads of encouragement and advice and to Ben for his help and useful suggestions.

I also have to especially thank my family, especially my parents for their constant support and concern. For helping me out, putting me through college, babysitting etc. etc. Thank you to my sister Sarah for her help and encouragement. Thank you to Gerard for being there for me, I hope that your "investment" pays off..... And finally, last but by no means least, thank you to my lovely son Michael for being so good and for being such a fantastic helper while I was trying to finish up the last few mont

List of Abbreviations

ADP	Adenosine diphosphate
ATP	Adenosine triphosphate
ATPsyn	ATP synthase
B 1-3	Blocks 1-3
BDSC	Bloomington Drosophila Stock Centre
BLAST	Basic Logical Alignment Search Tool
bp	Base pair
BSA	Bovine Serum Albumen
CAL1	Chromosome Alignment Defect 1
CATD	CENP-A Targeting Domain
CCAN	Constitutive Centromere Associated Network
cDNA	Complementary DNA
CENP-A	Centromere Protein A
CENP-B	Centromere Protein B
CENP-C	Centromere Protein C
CENP-N	Centromere Protein N
cRNA	Complementary RNA
CTCF	Corrected Total Cellular Fluorescence
RNA	Ribonucleic Acid
DNA	Deoxyribonucleic Acid
ECL	Enhanced Chemiluminescence
FBS	Fetal Calf Serum
FISH	Fluorescence in-situ Hybridisation
FL	Full Length
GAL4	Galactose 4
gDNA	Genomic DNA
GFP	Green Fluorescent Protein
GSC	Germ-line Stem Cell
GST	Glutathione S-transferase
HFD	Histone Fold Domain
HI-FISH	High Throughput-FISH
HRP	Horse Radish Peroxidase
IB	Interaction Buffer

IF	Immunofluorescence
IP	Immunoprecipitation
kb	Kilobase
L 1-3	Loop 1-3
LC-MS	Liquid Chromatography – Mass Spectrometry
MS	Mass Spectrometry
Ms	Male Sterile
MYA	Million Years Ago
NCBI	National Centre for Biotechnology Information
NEB	New England Biolabs
NIH	National Institute of Health
NLS	Nuclear Localisation Signal
PBS	Phosphate Buffered Saline
PBS-Tx	PBS with Triton-X
PCR	Polymerase Chain Reaction
PFA	Paraformaldehyde
PM	Prometaphase
RGB	Red Green Blue
RNAi	RNA interference
RPM	Rotations per minute
RT	Reverse transcription
RT-PCR	Reverse transcription- Polymerase Chain Reaction
S1-S6	Stage 1 – Stage 6
S2	Schneider's 2 (Cell line)
SC	Synaptonemal Complex
SDS-PAGE	Sodium Dodecyl Sulphate-Poly Acrylamide Gel Electrophoresis
SSC	Saline-Sodium Citrate
TBS	Tris-Buffered Saline
TBS-Tw	TBS with Tween 20
Tw	Tween 20
Tx	Triton-X
UAS-RNAi	Upstream activating sequence
VDRC	Vienna Drosophila Resource Centre
v/v	Volume per volume
w/v	Weight per volume
WT	Wild Type



Thesis Abstract

Recent studies in plants and *Drosophila* suggest that CENP-A, the centromeric histone H3 variant and epigenetic marker of centromere localisation may have additional roles during meiosis. By immunoprecipitation and mass spectrometry we have identified components of the mitochondrial ATP synthase F₁ complex as potential meiotic CENP-A interactors. Previous studies have identified a role for ATPsyn- α and ATPsyn- β in *Drosophila* male fertility and in addition, male *Drosophila* express a testes specific paralogue of ATPsyn- β : ATPsyn- β -like, which is essential for male fertility.

We report that testes specific knockdown of ATPsyn- α , ATPsyn- γ and ATPsyn- β -like subunits results in a defect in sister chromatid centromeric cohesion throughout meiosis I. Determination of whole tissue ATP levels after knockdown shows that ATP levels are reduced. However loss of cohesion severity does not correlate with ATP reduction indicating that it is likely that observed defect is not due to ATP depletion.

Knockdown of CENP-A also leads to a similar loss of sister centromere cohesion during meiosis suggesting that a functional link between CENP-A and the ATP synthase F₁ subunits exists. Indeed, using an *in vitro* interaction assay we have identified that CENP-A directly interacts with ATPsyn- α and by immunofluorescence microscopy we have found that ATPsyn- α and GFP-ATPsyn- β -like colocalise with CENP-A at centromeres in the germ-line.

In our model, we hypothesise that centromeric CENP-A recruits ATPsyn- α and ATPsyn- β -like via its direct interaction with the ATPsyn- α subunit, at the centromere these subunits promote sister centromere cohesion in a mechanism independent of ATP production.

1. Introduction

1.1. Centromeric chromatin

1.1.1 Centromeres and Centromere Protein A (CENP-A)

The centromere is a chromosomal locus, first described as the primary constriction visible on condensed chromosomes (Flemming, 1882). It is the site upon which the kinetochore, a multi-protein complex that physically links the chromosome to the microtubule spindle is assembled. Together the centromere and kinetochore are required to facilitate faithful segregation of chromosomes during cell division in both mitosis and meiosis (Alberts *et al.*, 2014).

From yeast to humans, centromeres are characterised by both their underlying DNA sequence and the composition of their chromatin, although centromeric size, complexity, precise DNA sequences and the mechanism of specification varies (Allshire and Karpen, 2008). The basic point centromeres of *S. cerevisiae* are genetically specified by a 125 bp DNA consensus (reviewed by Westermann *et al.*, 2007). In contrast, the regional centromeres of higher eukaryotes (including mammals, most fly and plant species as well as fission yeast) are larger, more complex and although they are usually associated with repetitive DNA are defined epigenetically by the presence CENP-A (McKinley and Cheeseman, 2015).

CENP-A is a variant of histone H3. At the centromere it replaces its canonical counterpart in the central hetero-tetramer of the nucleosome (figure 1.1). In humans (and flies) centromeric chromatin is composed of interspersed CENP-A and histone H3 nucleosomes, at a higher 3-dimensional structure the nucleosomes are arranged in an order which orientates CENP-A towards the surface and histone H3 towards the centre of the chromosome (Blower *et al.*, 2002). CENP-A is essential for viability in organisms as diverse as yeast, insects, plants and mammals and abnormal levels of CENP-A at the centromere result in chromosome segregation defects in both mitosis and meiosis. In mitosis such segregation defects contribute to genomic

instability and malignancy. In meiosis they are a common cause of infertility, birth and developmental defects (Alberts *et al.*, 2014 and reviewed by De Rop, *et al.*, 2012).

In humans, centromere size varies from 500 to 1500 kb and consists of a core of inverse 171 bp repeats called α -satellite DNA (Manuelidis 1978; Musich *et al.*, 1980). Although it is known that these satellite sequences can confer centromere function in some instances (Harrington *et al.*, 1997; Ikeno *et al.*, 1998) experimental evidence has shown that they are neither necessary nor sufficient for centromere function (Earnshaw *et al.*, 1989; Warburton *et al.*, 1997). This is best evidenced by the absence of α -satellite DNA at neo-centromeres (discussed below and reviewed by Rocchi *et al.*, 2012) and the inactivation of α -satellite-containing centromeres on pseudo-dicentric chromosomes (Rivera *et al.*, 1989). The repetitive nature of centromeric DNA is conserved throughout evolution yet the precise sequences are not; interestingly centromeric sequences are amongst the fastest evolving DNA known (reviewed by Henikoff *et al.*, 2001)

In contrast the presence of CENP-A nucleosomes in centromeric chromatin is highly conserved and the evidence that CENP-A provides the key epigenetic mark required for centromere location and function is compelling. Initial evidence came from studies of neo-centromeres, centromeres formed at ectopic non-centromeric sites. Such novel epigenetic events have been observed in many individual human cases (Amor and Choo, 2002) and within several different species (Rocchi *et al.*, 2012); in all studied cases CENP-A is present at the neo-centromere yet other centromeric markers such as α -satellite DNA and CENP-B are not. In these cases neo-centromere formation represents a novel epigenetic event which is maintained through cell division and if present in the germ-line can be transmitted from one generation to the next (Amor and Choo, 2002; Rocchi *et al.*, 2012). Other evidence includes identification that misincorporation of CENP-A at ectopic chromosomal loci by overexpression is sufficient to induce centromere function (Heun *et al.*, 2006; Gonzalez *et al.*, 2014), using

GFPLACI fusion proteins targeted to *LacO* arrays it has been shown that CENP-A is sufficient for centromere establishment, kinetochore function and epigenetic inheritance (Mendiburo *et al.*, 2011). CENP-A is required to recruit many inner kinetochore proteins including CENP-C and CENP-N indicating that CENP-A is the essential base upon which the centromere and kinetochore function (reviewed by Allshire and Karpen, 2008). In the following sections CENP-A structure-function relationships are discussed with emphasis on specific requirements in mitosis and meiosis

1.1.2 Canonical chromatin and histone H3 containing nucleosomes

Canonical nucleosomes (containing H2A, H2B, H3 and H4) are composed of a central (H3-H4)₂ hetero-tetramer located between two H2A-H2B dimers (figure 1.1). Together this octamer wraps 147 bp of DNA in a 1.7 super helical, right handed turn. Each nucleosome is connected by a stretch of linker DNA (of varying length) and together the nucleosome and its DNA form the characteristic 'beads on a string' model of chromatin (Luger *et al.*, 1997).

Within the nucleosome, histone interactions are mediated via the histone fold domain (HFD) of each protein, the HFD is a highly conserved structure located within the core of all histone proteins which is composed of three alpha helices ($\alpha 1$, $\alpha 2$, and $\alpha 3$) separated by two loops (L2 and L3) (figure 1.2). On histone H3, the histone core is preceded by a 64 amino acid N-terminus that protrudes from the nucleosome. The H3 N-terminus contains an alpha helix (αN helix) located adjacent to the HFD and an unstructured N-terminal tail. Deletion studies have shown that the N-terminus of histone H3 is required for histone-DNA interactions and nucleosomal stability (Iwasaki *et al.*, 2013). Furthermore it is well established that the N-terminal tail protruding from the nucleosome has the ability to make contact with adjacent nucleosomes and is a site of essential post-translational modifications (Bannister and Kouzarides, 2011).

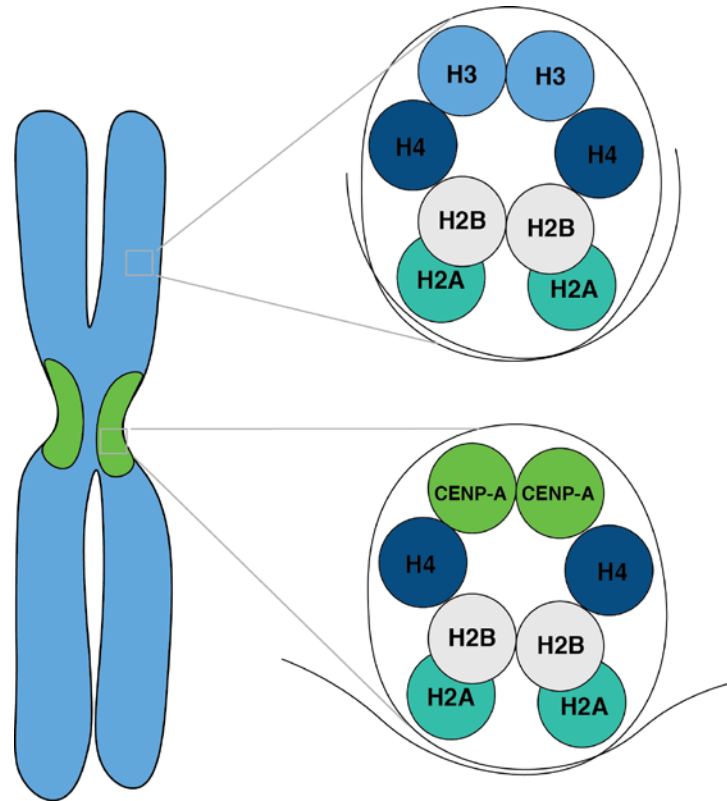


Figure 1.1 The centromere and CENP-A nucleosomes. The centromere composed of CENP-A (green) containing nucleosomes versus canonical histone H3 (blue) containing nucleosomes of non-centromeric chromatin.

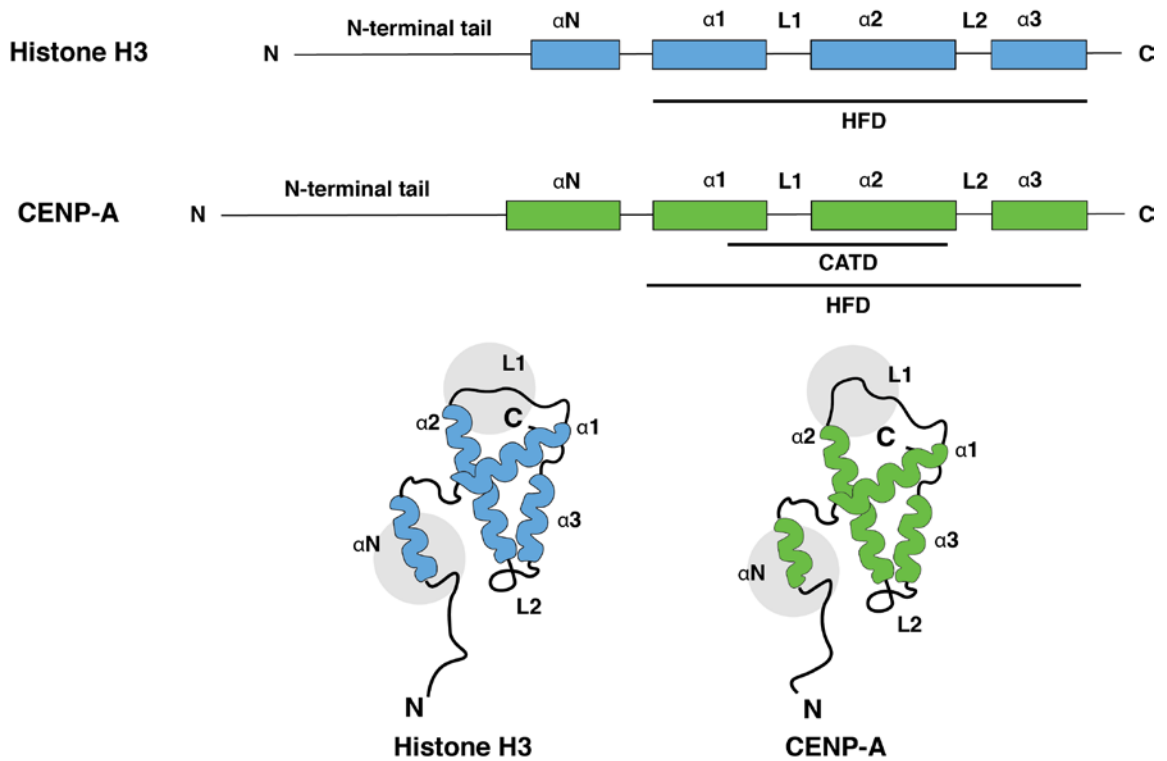


Figure 1.2 Histone H3 versus CENP-A. (A) Schematic representing 2-dimensional structure of histone H3 and CENP-A and the location of functional domains, the histone fold domain (HFD) and the centromeric targeting domain (CATD). (B) A 3-dimensional representation of histone H3 and CENP-A structures, major structural differences between histone H3 and CENP-A are indicated (grey circle).

1.1.3 Histone H3 versus CENP-A containing nucleosomes

In contrast to most histone variants CENP-A and H3 are poorly conserved with 56 and 24 % sequence identities observed between their HFD and N-termini respectively (Loyola and Almouzni, 2007). A large amount of research has been conducted in recent years in order to understand how the cell distinguishes between the CENP-A containing nucleosomes of the centromere and the H3 containing nucleosomes of canonical chromatin. Several different models of CENP-A nucleosome stoichiometry have been described and much debated (reviewed by Henikoff and Furuyama, 2012). However, the most compelling evidence indicates that CENP-A forms canonical octameric nucleosomes *in vivo*. Firstly, human CENP-A containing nucleosomes were reconstituted *in vitro* and crystallised (3.6 Å) as an octamer which wrapped 121 bp of DNA in a right-handed fashion (Tachiwana *et al.*, 2011). In addition, a (CENP-A-H4)₂ hetero-tetramer, the core subunit of an octameric nucleosome was crystallised (2.5 Å) (Sekulic *et al.*, 2010) and disruption of the CENP-A-CENP-A interface within this hetero-tetramer blocked stable incorporation of CENP-A nucleosomes into chromatin (Bassett *et al.*, 2012). Finally, purification of *in vivo* CENP-A nucleosomes from all 23 human chromosomes has revealed that throughout the cell cycle CENP-A chromatin forms homotypic octameric nucleosomes (Nechemia-Arbely *et al.*, 2017).

It is possible that CENP-A containing nucleosomes may exist in other forms (hemisomes/hexasomes) as intermediates. However, studies suggest that it is not an altered stoichiometry which distinguishes CENP-A nucleosomes but the altered structure of the nucleosome itself. Both Tachiwana *et al.*, 2011 and Sekulic *et al.*, 2010 have shown that the structure of the CENP-A containing nucleosome is distinct from that of the H3 containing nucleosome and it has been hypothesised that this structural variation is what confers centromere specific function (Black and Bassett, 2008; Stellfox *et al.*, 2013).

1.1.4 The CENP-A histone core

Compared to histone H3, the histone core of CENP-A displays increased hydrophobicity and two additional residues located at the top of L1 create a bulge in the CENP-A nucleosome (Sekulic *et al.*, 2010; Tachiwana *et al.*, 2011). These altered structures may confer rigidity and compaction to centromeric chromatin (Black and Bassett, 2008; Sekulic *et al.*, 2010) and substitution studies have shown that they are required for long term stability of CENP-A at the centromere (Tachiwana *et al.*, 2011).

Loop L1 and the $\alpha 2$ helix of CENP-A histone core form the CENP-A targeting domain (CATD) (figure 1.2). In human and *Drosophila* cultured cells this domain has been shown to be both necessary and sufficient for targeting of CENP-A to the centromere (Black *et al.*, 2004, Black *et al.*, 2007, Vermaak *et al.*, 2002) and indeed for maintenance of centromere identity (Fachinetti *et al.*, 2013). This function of the CATD does not appear to be conserved in plants as histone H3.3 containing the CATD of CENP-A does not localise to centromeres and cannot rescue lethality in a CENP-A null plant (Ravi *et al.*, 2010). Conflicting evidence has been published regarding the role of the CATD in budding yeast (Morey *et al.*, 2004; Ravi *et al.*, 2010).

Stellfox *et al.*, 2013 propose that it is the unique structure of the CENP-A CATD which allows core components of the constitutive centromere-associated network (CCAN) to “read” centromeric chromatin and indeed in humans CENP-C (via CATD and C-terminus), CENP-N (via CATD) interact specifically with CENP-A via this domain. Furthermore, the CENP-A assembly chaperone HJURP also directly recognises CENP-A via its CATD (Foltz *et al.*, 2009; Bassett *et al.*, 2012) and in human cells and *Drosophila* the CATD has been shown to be sufficient for loading of CENP-A to the centromere during mitosis (Vermaak *et al.*, 2002 Black *et al.*, 2004; Bassett *et al.*, 2012). The dynamics and requirements of CENP-A assembly to the centromere in both mitosis and meiosis are reviewed in Dunleavy and Collins, 2017 (Appendix 8.1 p.186).

1.1.5 The CENP-A N-terminus

The most divergent part of CENP-A is its N-terminus (compared to histone H3) and thus this domain is an ideal candidate for CENP-A specific function. Despite this, at least in human and *Drosophila* cultured cells the N-terminus is not required for centromeric targeting of CENP-A or for maintenance of centromere identity (Black *et al.*, 2007; Fachinetti *et al.*, 2013). The only part of the human CENP-A N-terminus to be crystallised thus far is the α N helix (figure 1.2), which is located adjacent to the histone fold domain. The remainder of the N-terminal tail is thought to be relatively unstructured. On CENP-A the α N helix is approximately 1 helical turn shorter and has a more disordered structure than H3 (Sekulic *et al.*, 2010; Tachiwana *et al.*, 2011). The α N helix of H3 is required for interaction with and maintenance of DNA orientation at the nucleosomal entry/exit points. Alterations of this region on CENP-A suggest a lack of a fixed connection with DNA and indeed this is consistent with the observations that CENP-A nucleosomes wrap less DNA than H3 containing nucleosomes (Sekulic *et al.*, 2010; Tachiwana *et al.*, 2011).

Studies in human cell and fission yeast (*S. pombe*) mitosis have shown that the CENP-A N-terminus is required for long term recruitment of some kinetochore proteins (Fachinetti *et al.*, 2013). Furthermore, the N-terminus of CENP-A is post-translationally modified by phosphorylation at residues Ser 16 and Ser 18 and expression of non-phosphorylatable versions result in increased mitotic segregation defects (Bailey *et al.*, 2013). Finally, in *S. pombe* the N-terminal tail of CENP-A has been shown to be required for long term epigenetic stability (Folco *et al.*, 2015).

In conclusion, centromeric CENP-A is essential in order to maintain the identity of centromere location and function. The CATD, located within the histone core of CENP-A has been shown to be sufficient for major centromere function in mitosis in human and *Drosophila* cells as well as budding yeast. In the following sections the role of CENP-A during meiosis

and fertility is discussed as well as the emerging role of the CENP-A N-terminus.

1.2. CENP-A function and requirements in meiosis

Meiosis is a programme of cell division that occurs in all sexually reproducing organisms, the end goal of which is the production of specialised haploid gametes. In the gonad, a population of germ cells is maintained via the asymmetric divisions of germ-line stem cells and in order to achieve haploidy cells undergo a single round of DNA replication followed by two consecutive rounds of chromosome segregation. In most organisms, homologous chromosomes separate in the first division (reductional event) and sister chromatids separate from each other in the second division (equational event) (Alberts *et al.*, 2014).

In mitosis, the role of CENP-A has been extensively studied. As discussed above, it is well established that normal levels of centromeric CENP-A are required for centromere function including chromosome segregation and epigenetic inheritance of the centromere. In contrast, the role of CENP-A in chromosome segregation and epigenetic inheritance during meiosis and the role of CENP-A during transgenerational inheritance in the zygote is less well understood. Many key questions remain to be answered including, how is CENP-A regulated through two consecutive rounds of cell division and how do CENP-A nucleosomes behave during the prophase I arrest of female meiosis and the histone exchange that occurs during spermiogenesis? Furthermore, a greater understanding of the role that CENP-A plays during transgenerational epigenetic inheritance of the centromere is required.

1.2.1 CENP-A is required for chromosome segregation in meiosis

Studies of CENP-A function during meiosis in humans are limited due to the accessibility of meiotically dividing tissues and for obvious ethical reasons. In mammalian models such as the mouse, studies of CENP-A function are also difficult as *cenp-a* knockout results in embryonic lethality 3.5-8.5 days

post conception (Howman *et al.*, 2000) and traditional conditional knockout or RNAi knockdown approaches are hampered by the stability of pre-existing centromeric CENP-A nucleosomes which must be diluted from centromeric chromatin by DNA replication (Li *et al.*, 2017).

Despite these difficulties, two recent studies in mouse oocytes have identified that CENP-A is present at centromeres throughout meiosis I and II (Smoak *et al.*, 2016; Li *et al.*, 2017) although analyses of CENP-A function in these studies was less clear. In mouse oocytes Smoak *et al.*, 2016 aimed to determine the function of CENP-A by generating a conditional knockout of the *cenp-a* locus in resting primordial follicles of 2 day old mice. Surprisingly, up to 14 months after excision of the *cenp-a* locus no adverse effect on meiotic chromosome segregation or fertility was observed compared to controls. Interestingly, quantification by immunofluorescence microscopy revealed no difference in the level of CENP-A at centromeres in controls versus *cenp-a* knockout mice, indicating that CENP-A nucleosomes assembled in primordial follicles prior to *cenp-a* knockout were stably maintained. Indeed, microinjection of *gfp-cenp-a* cRNA to WT oocytes revealed that no CENP-A assembly occurs between prophase I and metaphase II in mouse oocytes. From this study the authors concluded that CENP-A assembled in primordial follicle cells prior to *cenp-a* knockout must be very stable and sufficient to support normal centromere function during the subsequent meioses (Smoak *et al.*, 2016; Das *et al.*, 2017). In the only other study of the role of CENP-A in mammalian meiosis Li *et al.*, 2017 microinjected anti-CENP-A antibodies into mouse oocytes to perturb CENP-A function. They observed disrupted homologue segregation at anaphase I indicating that CENP-A is required during mammalian meiotic segregation.

In mammals, it is likely that the essential role of CENP-A in mitosis is maintained in meiosis yet with the exception of Li *et al.*, 2017 this has not been shown. The requirement for CENP-A during meiotic segregation has been best studied in the model organisms *C. elegans*, *A. thaliana* and *D. melanogaster*.

In *C. elegans* the orthologue of CENP-A HCP ϵ is required for correct chromosome segregation during mitosis. During meiosis CENP-A was observed to be gradually removed from centromeres during prophase I and was undetectable by anaphase II. Indeed RNAi knockdown of CENP-A in the gonads had no effect on chromosome segregation (Monen *et al.*, 2005). This lack of a requirement for CENP-A during meiosis in the worm is likely related to the holocentric nature of their centromeres. In monocentric organisms, separation of recombined homologues at anaphase I is possible due to the single attachment site of the kinetochore. However as holocentric chromosomes contain centromeres and kinetochore attachments all along their chromosomes it is not possible to bi-orient recombined homologues in this way so holocentric organisms have adapted in a number of novel segregation mechanisms (reviewed by Melters *et al.*, 2012). In *C. elegans* at meiosis I a unique 'cup-like' kinetochore forms at the top of each chromosome independently of CENP-A (Marques and Pedrosa-Harand, 2016), thus considering the adaptations it has to make to ensure homologue segregation *C. elegans* is perhaps not the best model of meiotic CENP-A function in higher eukaryotes.

The fission yeast (*S. pombe*) the CENP-A orthologue Cnp1 is present at centromeres during meiosis and overexpression studies have revealed that ectopic CENP-A is sufficient to recruit the meiotic kinetochore (Gonzalez *et al.*, 2014) suggesting that during meiosis CENP-A is sufficient to induce kinetochore formation as is the case in mitosis. In plants, CENH3 (plant CENP-A orthologue) is also required for accurate chromosome segregation during meiosis. RNAi knockdown of CENP-A levels in germ cells led to unequal segregations and lagging chromosomes during both meiotic divisions and the formation of micronuclei in resulting gametes (Lermontova *et al.*, 2011). In addition several studies in plants have observed meiosis specific defects in plants expressing CENP-A N-terminal mutants (discussed section 1.3.3 p. 21) (Ravi *et al.*, 2010, 2011a; Lermontova *et al.*, 2011). In the insect *D. melanogaster*, the CENP-A orthologue CID is present at centromeres in both male and female meiotic

cells and RNAi knockdown of CENP-A levels in the testes prior to entry into meiosis revealed meiotic chromosome missegregation events, including uneven nuclear segregation at meiosis I and II (Dunleavy et al., 2012).

In conclusion, it seems that with the exception of *C. elegans* a requirement for CENP-A during meiotic chromosome segregation is conserved from yeast to mammals. Furthermore, several studies in plants have indicated that CENP-A has different functional requirements in meiosis compared to mitosis, most notably a meiosis specific role for the CENP-A N-terminus (Reviewed by Dunleavy and Collins, 2017).

1.2.2 CENP-A is required for epigenetic inheritance in the germ-line

To ensure transmission of CENP-A nucleosomes to the next generation CENP-A must be maintained on both the male and female gamete. The exact mechanism of how this occurs, particularly on the male nucleus which undergoes protamine exchange, is not understood. In mammals, it is known that CENP-A is present on the female gamete past meiosis II (Smoak *et al.*, 2016) and that it is stably retained at centromeres past protamine exchange on mature bull spermatozoa (Palmer *et al.*, 1990, Dr. Elaine Dunleavy, unpublished). However the role CENP-A in fertility and/or the establishment of centromere identity in the next generation has not been investigated thus far.

The role of CENP-A in transgenerational inheritance of centromere location and function has been best studied in Drosophalids. In the fruit fly CENP-A is stably retained at centromeres on both the female and male gametes (Dunleavy *et al.*, 2012; Raychaudhuri *et al.*, 2012). Furthermore Raychaudhuri *et al.* have carried out a number of studies in order to determine whether CENP-A assembly in the zygote can occur *de novo* or requires a template. Firstly, depletion of GFP-CENP-A levels on mature sperm using a GFP degradation system resulted in paternal chromosome loss in the first mitotic division of the zygote indicating that

transgenerational inheritance of centromere location requires the presence of CENP-A to act as a template (figure 1.3).

Secondly, after reduction of CENP-A levels on mature sperm to 33 % of control levels corresponding reduction in CENP-A levels was observed in embryonic nuclei and on the mature sperm of the resulting progeny. In addition, WT female eggs fertilised with sperm containing a 7-fold increase in CENP-A levels produced progeny with a 1.7-fold higher level CENP-A at centromeres in embryonic nuclei. Taken together, these results indicate that transgenerational inheritance of the centromere occurs in a template-governed fashion that is dependent of the presence of CENP-A and that the levels of CENP-A at the centromere are quantitatively maintained (figure 1.4).

In Arabidopsis, CENP-A is also stably maintained at centromeres in ovules and pollen and genetic studies expressing GFP-CENP-A mutant and chimeric proteins suggest novel roles for the CENP-A N-terminus both during meiosis and post-fertilisation in the zygote (Ravi *et al.*, 2010; Ravi *et al.*, 2011b).



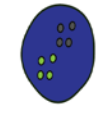



	Sperm (n)	Egg (n)	Early embryo (2n)	Observed	Conclusion
Control				Dilution of CENP-A by half in each of embryonic divisions 1-3.	Paternal CENP-A inherited in the embryo is diluted by maternally supplied CENP-A.
CENP-A Degradation				No GFP-CENP-A assembly at paternal centromeres.	Assembly of CENP-A on paternal centromeres is template governed.

Figure 1.3 An illustration of CENP-A depletion experiments carried out by Raychaudhuri *et al.*, 2012 in order to study transgenerational inheritance of the centromeric CENP-A (Dunleavy and Collins, 2017).



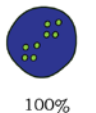




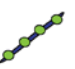



	Sperm (n)	Egg (n)	Early embryo (2n)	Observed	Conclusion
Control					
CENP-A Level:	50%	50%	100%		
CENP-A Reduction					Reduced CENP-A level is inherited.
CENP-A Level:	16.5%	50%	66.5%	72%	
CENP-A Overexpression					Increased CENP-A level is inherited, but not quantitatively.
CENP-A Level:	350%	50%	400%	170%	

Figure 1.4 An illustration of CENP-A overexpression and depletion experiments carried out by Raychaudhuri *et al.*, 2012 in order to study quantitative transgenerational inheritance of centromeric CENP-A (Dunleavy and Collins, 2017).

1.3. The CENP-A N-terminus is rapidly evolving

As discussed above, studies in human cells which have analysed the role of CENP-A in mitosis indicate that the N-terminus is dispensable for centromeric targeting and for epigenetic maintenance of centromere identity (Black *et al.*, 2007; Fachinetti *et al.*, 2013). Studies in both yeast and plants however indicate that this may not be a conserved feature (Ravi *et al.*, 2010). The N-terminus of CENP-A is rapidly evolving and shows little to no similarity in terms of its amino acid composition or length between different organisms (Malik and Henikoff, 2003)(figure 1.5). It remains unclear what drives this rapid evolution of a histone protein with such a conserved function. It has been suggested that rapid changes in the CENP-A N-terminus may be related to the rapid evolution of the underlying DNA sequence (discussed below) (Malik and Henikoff, 2001; Talbert *et al.*, 2004). It is also possible that sequence differences may represent the acquisition of lineage specific functions (Malik and Henikoff, 2001; Torras-Llort *et al.*, 2010; Maheshwari *et al.*, 2015).

1.3.1 Is rapid evolution of the CENP-A N-terminus a response to meiotic drive?

The N-terminus and loop 1 of CENP-A are rapidly adaptively evolving in both *Drosophila* (Malik and Henikoff, 2001) and *Arabidopsis* (Talbert *et al.*, 2002). Both of these CENP-A domains make connections with the underlying DNA sequences and thus the Henikoff laboratory has proposed that rapid changes in the CENP-A N-terminus occur in response to rapidly changing centromeric DNA sequences (Malik and Henikoff, 2001). Changes in the underlying DNA sequences that alter 'centromere strength' would be a strict evolutionarily disadvantage, creating bias by being strongly selected for in the asymmetric divisions of female meiosis. To offset meiotic drive, CENP-A may rapidly evolve to suppress variations in centromere strength and thus non-random segregation during meiosis (Malik and Henikoff, 2001; Talbert *et al.*, 2002; Talbert *et al.*, 2004). Furthermore, in *Drosophalids* it has

been shown that the L1 loop of CENP-A and the N-terminus of its assembly chaperone CAL1 are co-evolving. Strikingly, when expressed in *D. melanogaster* cultured cells, CENP-A from the closely related *D. bipectinia* cannot be assembled to centromeric chromatin (Rosin and Mellone, 2016). Interestingly, Rosin and Mellone, 2016 propose that this co-evolution of CENP-A and CAL1 may represent a mechanism by which the amount of CENP-A deposited at centromeric chromatin and thus centromere strength can be regulated.

1.3.2 Does the hyper-variability of the CENP-A N-terminus represent lineage specific functions?

Despite the hyper variability of the N-terminus, both plants and Drosophalids have evolved a number of conserved sequence blocks (Torras-Llort et al., 2009, Malik et al., 2002, Maheshwari et al., 2015). The N-termini of CENP-A from the Drosophila clade harbor three conserved arginine-rich domains (blocks 1, 2 and 3) (Malik et al., 2002) (figure 1.6). It has been shown that block 3, located adjacent to the histone core of CENP-A is required for recruitment of the kinetochore protein BUBR1 (Torras-Llort *et al.*, 2010) but the function of B1 and B2 remain unknown.

In plants, several conserved sequence blocks have also been identified, at least two of which are conserved on a wide evolutionary scale from green algae to flowering plants (figure 1.7). The emergence of such conserved sequence blocks suggest functionality although the role of these particular domains has not been characterised. Several studies in *Arabidopsis* however have shown that the N-terminus has novel roles during both meiosis and post-fertilisation in the zygote (Ravi *et al.*, 2010, Ravi *et al.*, 2011).

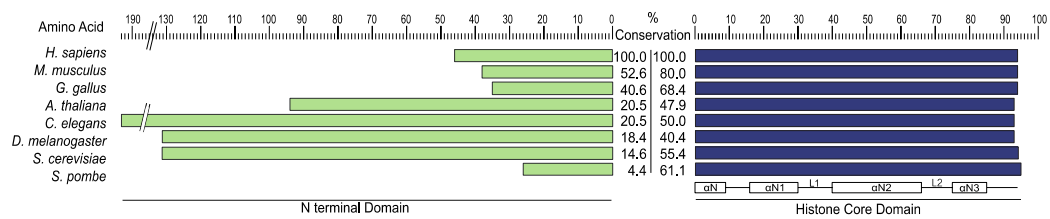


Figure 1.5 A representation of the rapid evolution of the CENP-A N-terminus in terms of length and sequence identity. The length of bars represents the number of amino acids per domain; the N-terminus (green) and the histone core domain (blue) (Dunleavy and Collins, 2017).

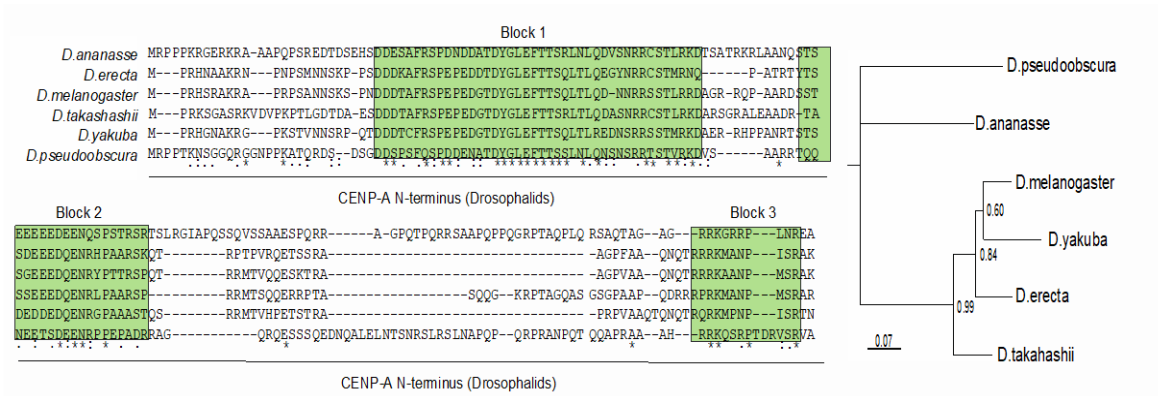


Figure 1.6 Conserved sequences blocks present in the N-termini of plant species. Conserved sequence blocks are indicated in green, * represents full conservation of amino acid, : and . represent strong and partial conservation of amino acid properties. (Dunleavy and Collins, 2017).

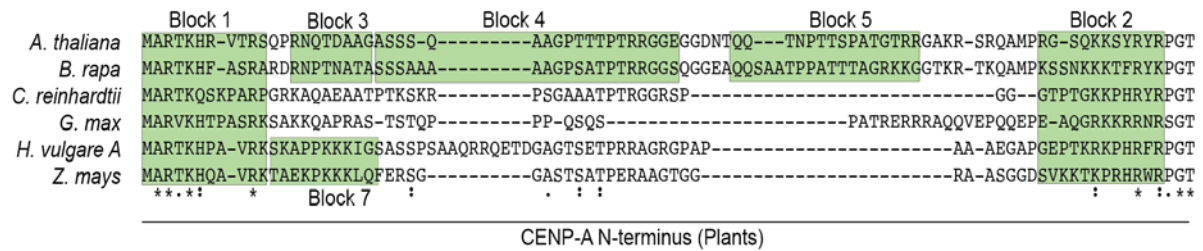


Figure 1.7 Conserved sequences blocks 1-3 present in the N-termini of CENP-A from Drosophilid species. Conserved sequence blocks are indicated in green, * represents full conservation of amino acid, : and . represent strong and partial conservation of amino acid properties. (Dunleavy and Collins, 2017).

1.3.3 Differing functional requirements for CENP-A N-terminus in mitosis versus meiosis in plants

In order to study the functional requirements for CENP-A in *Arabidopsis* the Chan laboratory has expressed an arsenal of different GFP-CENP-A mutant and chimeric proteins in a *cenp-a* null background (figure 1.8). They observed that the CENP-A N-terminus was indispensable for viability in the plant as neither a GFP-H3 protein containing the CENP-A CATD nor a GFP-CENP-A N-terminal deletion was sufficient to rescue a *cenp-a* null phenotype (Ravi *et al.*, 2010; Lermontova *et al.*, 2011). A caveat to these findings is that more recent studies have shown that the GFP-tag in these transgenes was not completely neutral (Maheshwari *et al.*, 2015).

Interestingly, a GFP-CENP-A construct containing the histone H3.3 N-terminal tail 'GFP-tailswap' was sufficient to rescue viability in *cenp-a* null plants but it was not sufficient to rescue fertility (figure 1.8). Fertility was reduced in both male (3.5 %) and female (68.5 %) rescued plants indicating a specific requirement for the CENP-A N-terminus in meiosis. Analysis of meiotic progression in GFP-tailswap revealed meiosis I and II segregation defects as well as abnormal kinetochore formation (Ravi *et al.*, 2010, 2011a). Interestingly, it was observed that without its endogenous N-terminus CENP-A failed to load to the meiotic centromere during meiosis prophase I. This was not the case in somatic cells (root tip) or during gametophyte mitosis (an amplification of gametes post-meiosis that occurs specifically in plants). These results indicate that CENP-A is alternatively recruited to the centromere during meiosis in plants (Ravi *et al.*, 2011b).

In addition to the observed meiotic defect, the Chan laboratory also observed a number of defects post-fertilisation when GFP-tailswap plants were crossed (figure 1.9). GFP-tailswap males were almost completely sterile (3.5 % fertility) compared to *wild type* (Columbia). However, when many anthers were pooled together fertilisation could be achieved. Interestingly, when self-crossed 92 % of the resulting progeny were normal

and diploid while the remainder exhibited some form of aneuploidy. However, when GFP-tailswap pollen was used to fertilise WT plants 34 % of the resulting progeny were haploid, having lost their paternal set of GFP-tailswap containing chromosomes. In addition to this, they found that fertilisation of WT plants with pollen from plants expressing full length GFP-CENP-A also led to an increased frequency of haploid (5 %) and aneuploid (29 %) seeds, albeit at a lower level than what was observed for crosses to GFP-tailswap (Ravi and Chan, 2010) (figure 1.9).

In order to account for any negative effect of a CENP-A GFP-tag Maheshwari *et al.*, 2015 carried out similar experiments using un-tagged native CENP-A proteins from closely related plant species to rescue the CENP-A null mutant. In doing this they were able to rescue viability although it was not possible to fully rescue fertility. Crossing a *cenp-a* null rescued plant expressing CENP-A from closely related species led to genomic instability in the resulting embryo – haploid and aneuploid seeds as well as seeds exhibiting novel genetic arrangements were observed (figure 1.10) (Maheshwari *et al.*, 2015).

Together these results suggest that in the zygote, the presence of different forms of CENP-A N-termini on the maternal and paternal chromosomes leads to incompatibilities in segregation machinery. It is possible that these rapid changes in N-terminal sequence occurred as a way to suppress centromere drive by generating reproductive incompatibility. Maheshwari *et al.* suggest that rapid evolution of the CENP-A N-terminus may also have contributed to speciation.

1.4. The role of CENP-A in meiosis - conclusion

Studies in plants (Lermontova *et al.*, 2011; Ravi *et al.*, 2011b) and *Drosophila* (Dunleavy *et al.*, 2012; Raychaudhuri *et al.*, 2012) have shown that CENP-A is required for correct chromosome segregation during meiosis and for transgenerational propagation of the centromere. Interestingly in

plants, several key differences in CENP-A regulation and requirements during meiosis have been observed compared to mitosis including a meiosis specific requirement for the N-terminus during CENP-A assembly and post-fertilisation during zygotic mitosis (Ravi and Chan, 2010; Ravi *et al.*, 2011b; Maheshwari *et al.*, 2015).

Thus far, the function of conserved sequence blocks present on the CENP-A N-terminus of Drosophalids has not been investigated. It will be interesting to determine if any of the meiosis specific functions of the N-terminus in plants, including a meiosis specific loading and/or transgenerational inheritance are conserved in insects.

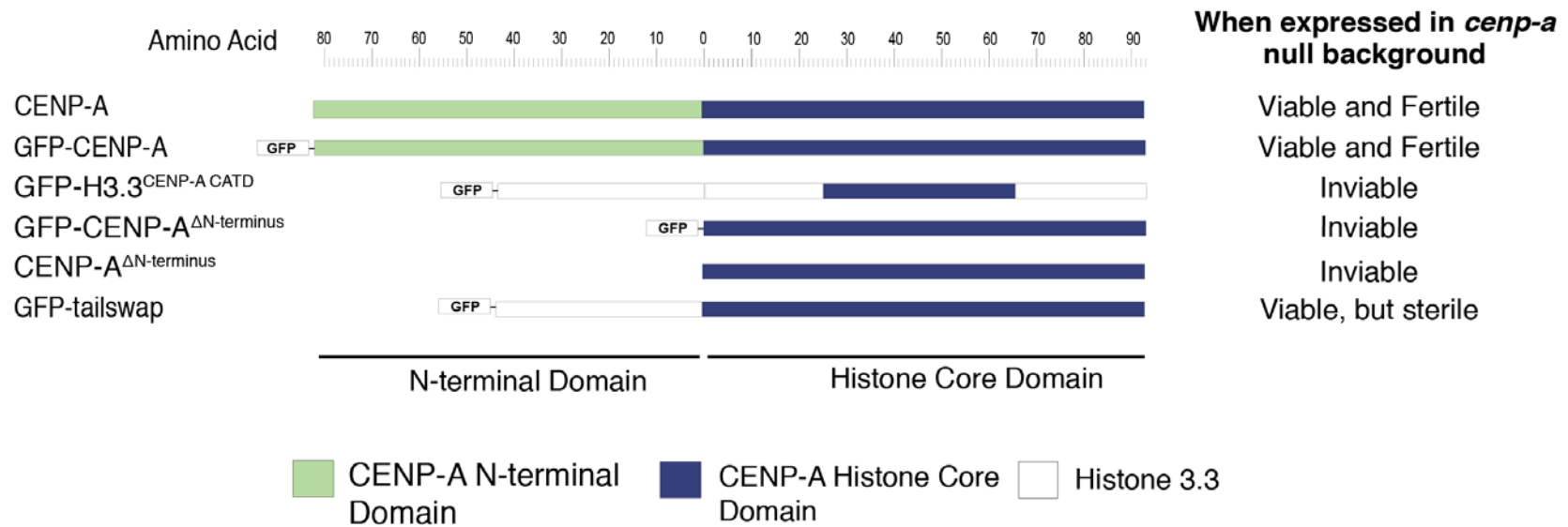


Figure 1.8 A schematic depicting the arsenal of CENP-A deletion and chimeric proteins produced and expressed in a *cenp-a* null background by the Chan laboratory. The location of the GFP-tag is indicated and the ability of these constructs to complement a *cenp-a* null background in plants is indicated.

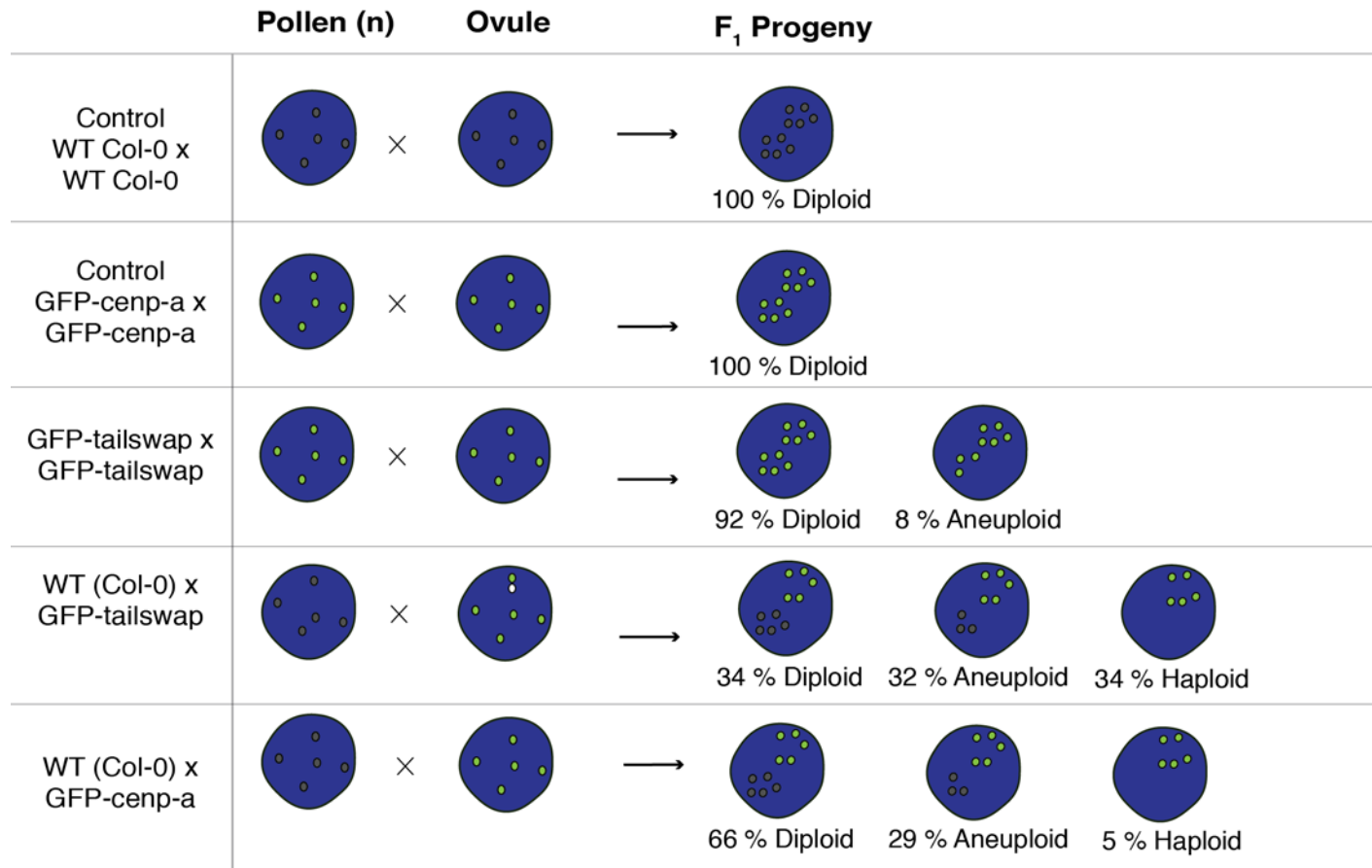


Figure 1.9 Centromere mediated genome elimination. A depiction of the results obtained by Ravi *et al.*, 2010 when crossing plants expressing CENP-As with different N-termini. GFP-CENP-A or GFP-tailswap were crossed to WT Columbia-O, the percentages diploid, aneuploid or haploid first generation (F₁) progeny are indicated.

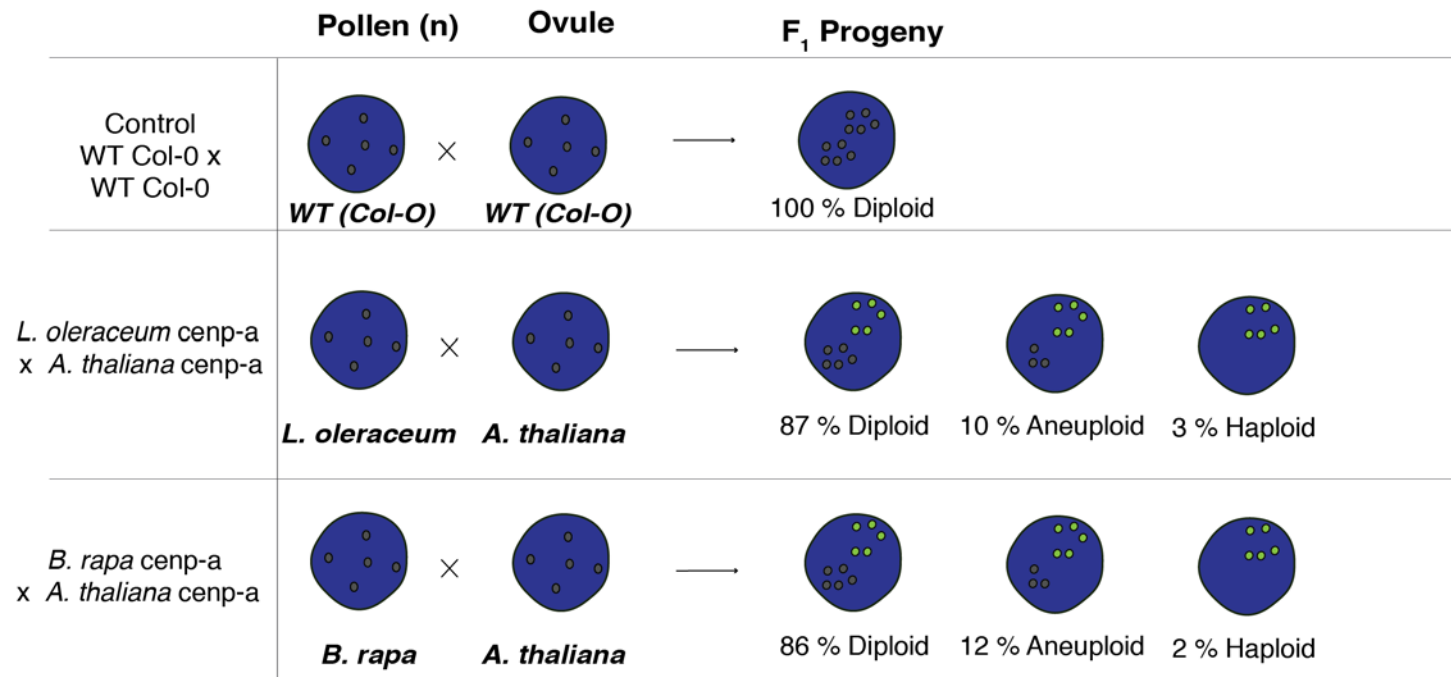


Figure 1.10 Novel genetic arrangements induced by crossing plants expressing evolutionary distant CENP-As. A depiction of the results obtained by Maheshwari *et al.*, 2015.

1.5. Meiosis in the fruit fly *Drosophila melanogaster*.

1.5.1 Insects and the order Diptera

Insects are the largest grouping of arthropods, accounting for at least 50 % of all species diversity on earth. Organisms within this class are characterised by their chitinous exoskeleton, segmented body, compound eyes and single pair of antennae (Halanych, 2004). Family Insecta is divided into four main orders; Coleoptera (beetles), Hymenoptera (ants, wasps and bees) Lepidoptera (butterflies and moths) and Diptera (flies) (figure 1.11). Diptera or true flies are the second largest order within this class containing approximately 20,000 different species. Strikingly, greater than 250 million years of evolutionary divergence separate lower Dipterans (Nematocera) such as mosquitos from higher Dipterans (Neodiptera) such as house flies and fruit flies (Wiegmann *et al.*, 2011)(figure 1.12). Many fly species are ubiquitous and are common household or agricultural pests, many are vectors of serious disease and some represent important biological model organisms.

1.5.2 *Drosophila melanogaster* as a model system

Drosophila melanogaster belongs to a grouping of fruit flies located in the Neo-dipteran sub-group Shizophora (Wiegmann *et al.*, 2011), *Drosophila* are a well-established model organism, the advantages of which are many: firstly, genetic manipulation of *Drosophila* is relatively simple and many mutant alleles and genetic tools are freely available via several stock centers Secondly,. a large amount of genomic and transcriptomic data is available via the ModENCODE consortium (Celniker *et al.*, 2009), the National Centre for Biotechnology Information (NCBI) and the *Drosophila* bioinformatics repository Flybase.

The advantages of using *Drosophila* to study chromosome biology and centromere dynamics during meiosis and development include a high level

of conservation between the processes of chromatin assembly, maintenance and chromosome segregation. Additionally, *Drosophila* have a karyotype of 4 allowing for easy analysis of centromere dynamics on individual chromosomes and finally in *Drosophila* male meiosis progresses sequentially through a tubular shaped testis, this allows for easy identification of the different meiotic cell stages (figure 1.13).

1.6. A description of spermatogenesis in *Drosophila melanogaster*

At the apical tip of the *Drosophila* testis, 6-12 germ-line stem cells (GSCs) surround 'the hub', a group of closely associated regulatory cells. GSCs divide asymmetrically in order to self-renew and to produce a daughter cell called the primary spermatogonium (Fuller, 1998; Spradling *et al.*, 2011). Primary spermatogonia are amplified in number via 4 consecutive rounds of mitosis and incomplete cytokinesis produces cysts of cells containing of 2, 4, 8 and 16 secondary spermatogonia. Once mitosis is complete, the primary spermatocytes of the 16-cell cyst undergo a single round of DNA replication prior to entering meiosis prophase I (Cenci *et al.*, 1994a) (figure 1.13).

As discussed in detail below, *Drosophila* males do not follow the highly conserved meiotic prophase I script whereby homologous chromosomes pair, synapse, recombine and form stable homologue connections called chiasmata. Instead they opt for an alternative and not very well understood method of 'conjoining' their homologous chromosomes in distinct nuclear territories (reviewed by McKee *et al.* 2012). As such this stage is not a true meiotic prophase and so is uniquely characterised (stages S1-S6) based on distinct changes in nuclear morphology and microtubule organisation (described by Cenci *et al.*, 1994) (figure 1.14).

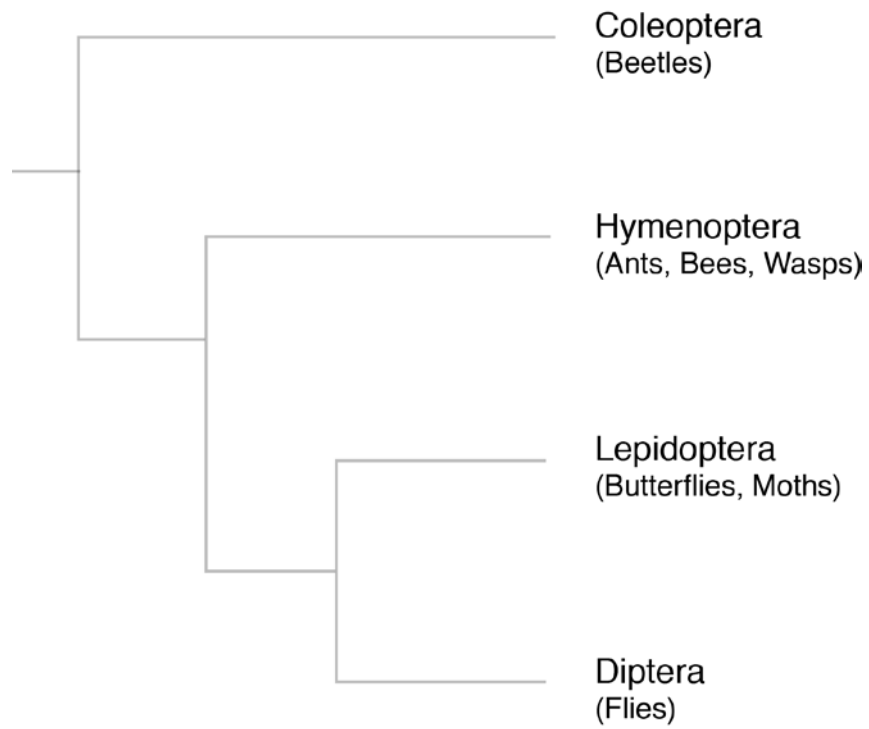


Figure 1.11 A Cladogram illustrating evolutionary relationships within the class Insecta (not to scale).

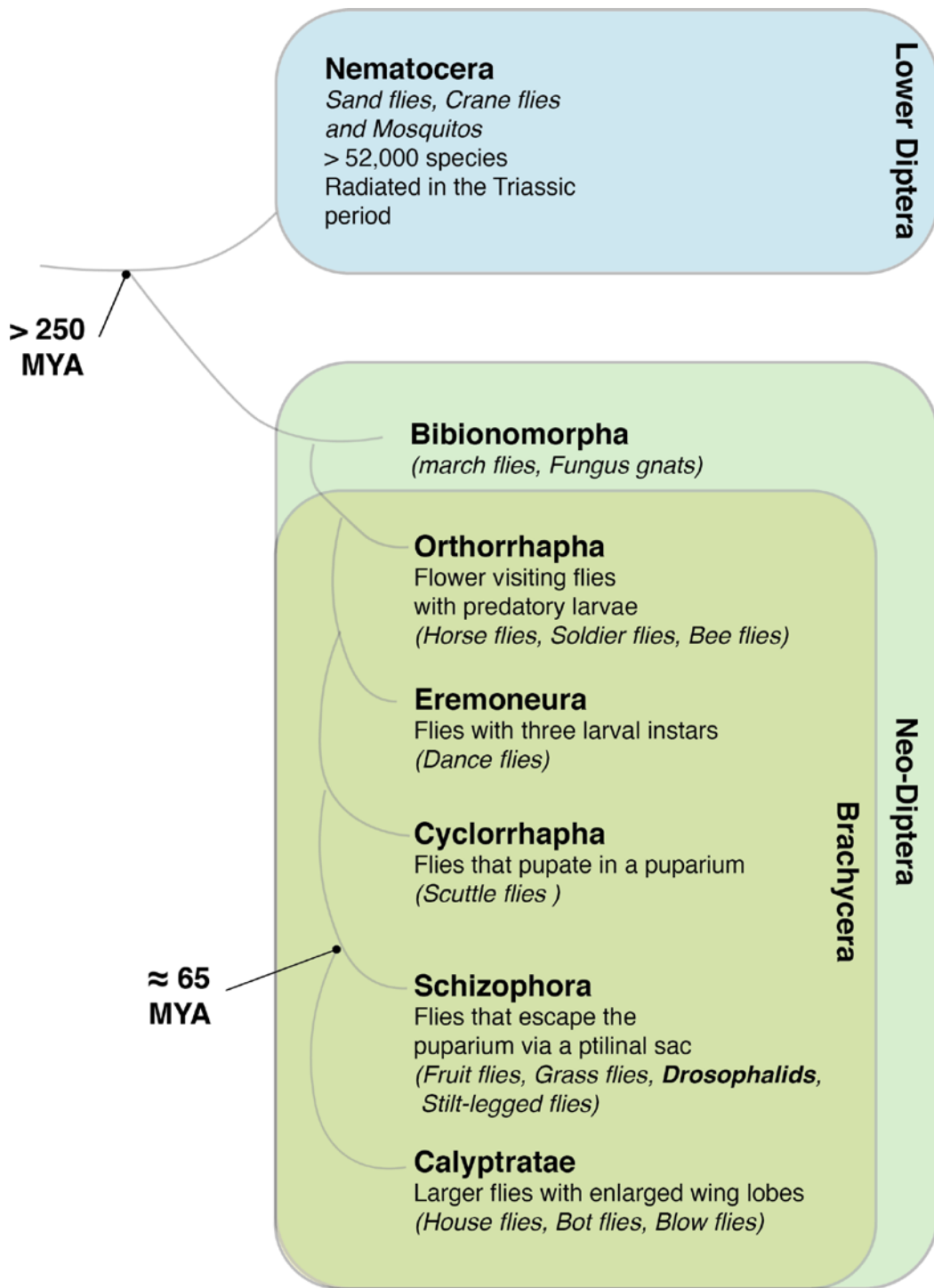


Figure 1.12 Evolutionary relationships and divergence times within the order Diptera.

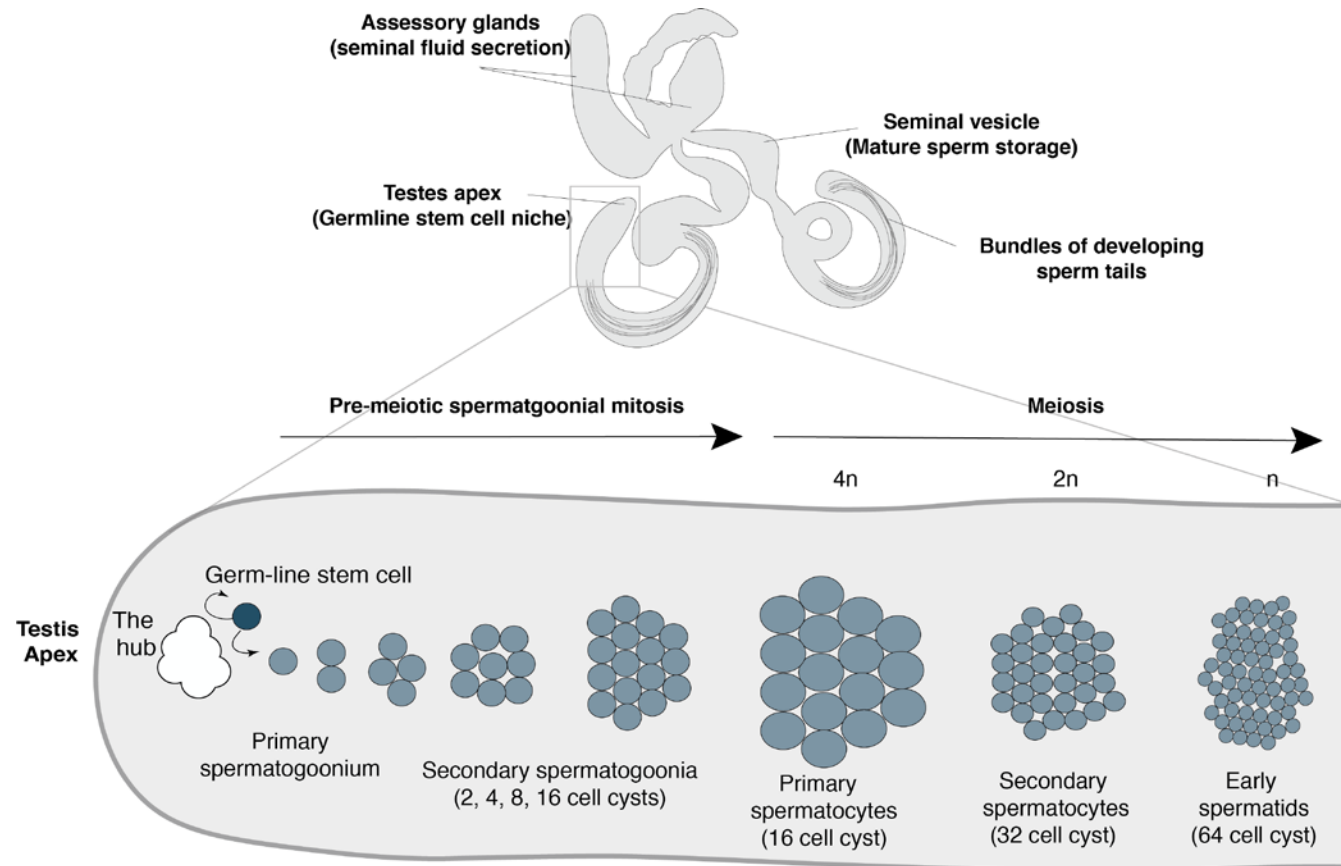


Figure 1.13 Spermatogenesis in the adult *Drosophila* testis. Scheme illustrates sequential progression of meiotic cysts through the tubular shaped testis of *Drosophila melanogaster*. The number of cells per cyst at each point is indicated as well as the ploidy after each meiotic division ($4n$, $2n$, n).

1.6.1 Prophase I in male *Drosophalids* – distinct staging and nuclear morphology

Early prophase I (S1/S2a) nuclei are indistinguishable from those of pre-meiotic secondary spermatogonial cells however the organisation of organelles within the cytoplasm changes. At this stage, the nucleus localises to one pole of the cell and mitochondria cluster to the other, as a result these cells are often referred to as polar spermatocytes. At S3 the nucleus returns to a central location within the cell and the mitochondria become evenly distributed throughout the cytoplasm.

From S1 nuclear volume steadily increases and at S2b 3-4 distinct nuclear territories, separated by a nuclear 'lumen' become apparent. From S4 to S6 the nucleus undergoes a dramatic increase in volume and by S6 nuclei are 25 times their original volume. As nuclear volume increases, the chromatin territories move further away from each other, remaining closely associated with the inner nuclear membrane. Between S3 and S6 chromatin loops of the *Y* chromosome, which are highly transcribed at this time, unfold and locate in the centre of the nucleus between the nuclear territories. This region is resistant to conventional DNA staining due to the level of decondensation and thus appears empty (figure 1.14). At the end of prophase I, the *Y* chromosome loops disintegrate, the chromosome territories condense down and coalesce at the metaphase I plate prior to homologue segregation at anaphase I (Cenci *et al.*, 1994b; White-Cooper, 2004).

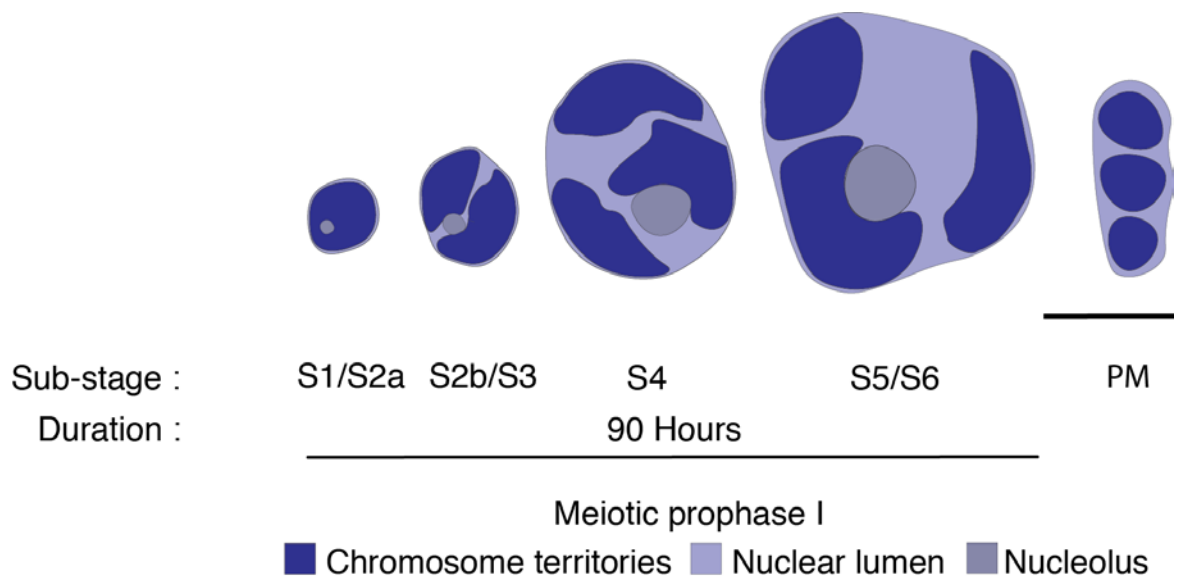


Figure 1.14 A depiction of the distinct nuclear morphology of prophase I in male *Drosophila*. Stages S1-S6 as well as late prometaphase (PM) are indicated. The scale-bar (bold line) represents approximately 10 μm .

1.7. Chromosome dynamics in meiosis I

Chromosome segregation in meiosis I is distinctive in that it is homologous chromosomes which segregate, not sister chromatids. Thus during meiosis I homologous chromosomes which usually mono-orient are required to bi-orient and sister chromatids which usually bi-orient must remain cohesive in order to mono-orient (reviewed by Watanabe, 2012). To achieve this, homologous chromosomes and sister chromatids undergo several meiosis specific adaptations during prophase I. The events of prophase I are well conserved from yeast to humans although several notable deviations from the standard mechanism exist, including male *Drosophalids*.

1.7.1 Prophase I

Cohesion is laid down between newly produced sister chromatids during pre-meiotic replication and remains in place along chromatid arms until anaphase I and at sister centromeres until anaphase II. Conventionally, prophase I is segregated into 5 distinct stages (figure 1.15). In leptotene, homologous chromosomes condense and the synaptonemal complex (SC), a large protein structure that 'zips' homologues together begins to form. During zygotene, homologous chromosomes pair and synapsis is completed. Following this, during pachytene recombination between homologous pairs occurs and cohesion is established along sites of strand invasion forming chiasmata. In most organisms, chiasmata formation is essential for fertility as it allows the kinetochore to form tension generating connections during meiosis I. In diplotene, the SC disassembles and homologous chromosomes are again distinguishable although they remain associated via their chiasmata. Diakinesis, the final stage of prophase I is analogous to prometaphase of mitosis where the bivalents condense and the nuclear envelope begins to break down (reviewed by Baudat *et al.*, 2013).

Prior to homologue segregation at anaphase I, cohesion along the chromosome arms is cleaved by separase, releasing connecting chiasmata. Importantly, at anaphase I cohesion at centromeric regions is maintained by activity of the protector of centromeric cohesion SHUGOSHIN. In the absence of SHUGOSHIN sister chromatids separate prematurely and segregation defects occur in meiosis II (Kerrebrock *et al.*, 1992 and reviewed by Ishiguro and Watanabe, 2007).

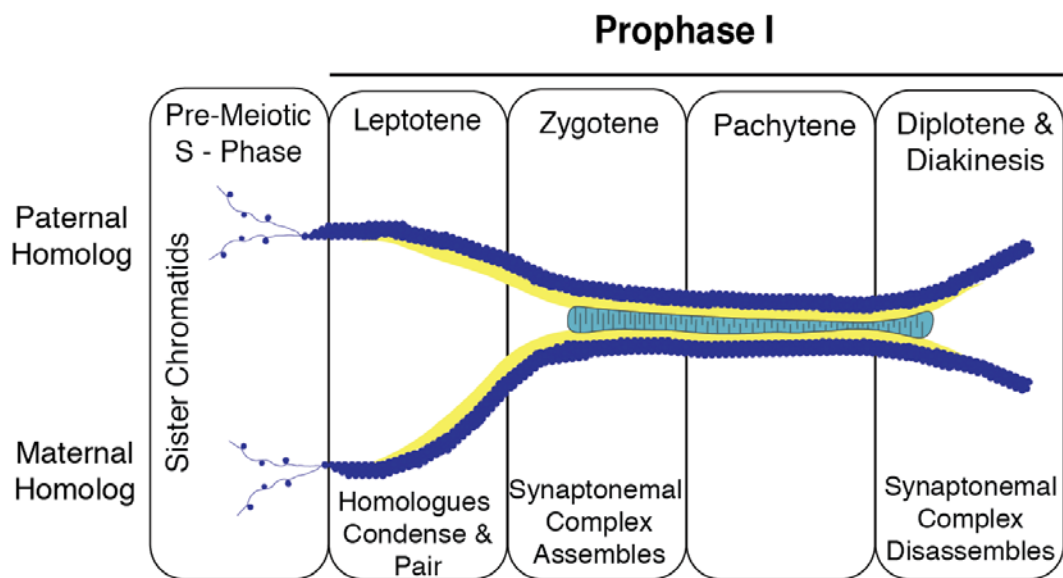


Figure 1.15 A schematic representing homologue pairing and synapsis through meiosis prophase I. Dark blue lines represent chromatin, yellow represents lateral filaments and the light blue structure represents the synaptonemal complex (adapted from Dunleavy and Collins, 2017, figure based on Alberts *et al.*, 2004).

1.7.2 Achiasmy, an unconventional meiosis I

Recombination between homologous chromosomes during meiosis provides a significant evolutionary advantage allowing for genetic diversification and improved population genetics, as well as providing the stable links between homologous chromosomes required at anaphase I (Carvalho, 2003). In spite of this, many species have elected to completely dispense with recombination between homologues (achiasmy), have dramatically different recombination frequencies between sexes (heterochiasmy) and/or have different frequencies of recombination on different chromosomes (John *et al.*, 2016). As mentioned above, *Drosophila* males prophase I occurs in the absence of any SC formation, no recombination events occur and as such stabilising chiasmata do not form between homologous chromosome pairs (Morgan, 1910). The mechanism by which *Drosophila* males manage to faithfully pair and segregate their homologous chromosomes during meiosis I is not well understood (McKee *et al.*, 2012).

Studies investigating the incidence of achiasmate pairing have noted that it is often associated with the heterogametic sex. For example, male *Drosophila* which contain the *X-Y* chromosome pair are achiasmate whereas with the exception of their 4th chromosomes female *Drosophila* are not (reviewed by (McKim *et al.*, 2002). In another example, female Lepidopterans (moths) containing the heterogametic *W-Z* chromosome pair completely dispense with genetic recombination, whereas the *Z-Z* males do not (Turner and Sheppard, 1975). Thus it has been suggested that achiasmy may have evolved as part of a mechanism to suppress recombination between non-homologous sex chromosomes (Yeates and Wiegmann, 2005).

Human sex chromosomes contain a region of DNA homology called the pseudo-autosomal region, this region allows for homology dependent recombination to occur between these normally non-homologous chromosomes (Rappold, 1993). Interestingly, several mammalian species

have been identified which lack this region of homology yet manage to pair and segregate their sex chromosomes in the absence of synapsis and recombination (De La Fuente *et al.*, 2007). It has been suggested that in addition to pairing chromosomes via conventional synapsis and recombination, mammalian species may also possess complementary achiasmate mechanisms (Koehler and Hassold, 1998). Thus an understanding of achiasmate pairing in *Drosophila* males may be of use to understanding such mechanisms in higher eukaryotes.

1.7.3 Alternative methods of homologue pairing in *Drosophila* males

In most organisms, strong association of homologous chromosomes is limited to prophase of meiosis I. In some instances however, homologue pairing can occur in somatic cells albeit transiently and in localised regions. Interestingly, many Dipteran species display high levels of somatic homologous chromosome pairing. This organisation of chromosomes is required for a special type of gene regulation called transvection (Kennison and Southworth, 2002) and for double-stranded break (DSB) repair (Rong and Golic, 2003). Thus in male *Drosophila*, cells enter into prophase I with their homologous chromosomes already paired, avoiding the need for a homology search.

A number of methods have been employed to analyse homologue pairing frequencies; Vasquez *et al.*, 2002 have developed a system employing GFP-LACI proteins which recognise *LacO* sites inserted at 13 different euchromatic genomic locations and Tsai *et al.*, 2011 have used FISH to determine pairing at several heterochromatic loci. In both instances the number of 'allelic spots' visible per nucleus was used to score homologue pairing. Centromeric pairing frequencies were assessed by immuno-staining for CENP-A with number of centromeric foci per nucleus or per nuclear territory indicative of centromeric pairing (Tsai *et al.*, 2011).

At early prophase I S1/S2a, homologous chromosomes are intimately paired with high levels of pairing detected at euchromatic (90 %) and heterochromatic regions. At S1/S2a homologous centromeres are not strictly paired, instead they cluster randomly and thus between 2 and 4 centromeric foci are visible per nucleus. At S3, coincident with the formation of nuclear territories, pairing at all tested euchromatic (Vazquez *et al.*, 2002) and most heterochromatic sites (Tsai *et al.*, 2011) is lost and each homologous pair segregates into a distinct nuclear territory. Also at S3, homologous centromeres transiently pair and then, with the exception of the 4th chromosome un-pair and remain so for the rest of meiosis (figure 1.16)

A 240 bp repeat within the intergenic spacer of the ribosomal DNA (rDNA) genes which is located on both sex chromosomes has been shown to be both necessary and sufficient for X-Y pairing during meiosis I. Deletion of this locus leads to non-disjunction and random segregation at meiosis I (McKee *et al.*, 1992; Thomas and McKee, 2007). In both the male and the female, pairing of the 4th chromosome occurs at a heterochromatic satellite (AATAT, h61). In > 90 % of spermatocytes this locus is visible as a single paired focus (Tsai *et al.*, 2011). Thus far, stably maintained pairing sites on the 2nd and 3rd autosomes have not been identified. FISH analysis at pericentromeric (*dodeca*) and non centromeric heterochromatic regions (1.686g/cm³ satellite) found high levels of pairing through S1/S2a, although past mid prophase S2b/S3 pairing at these sites is only observed < 10 % of the time (Tsai *et al.*, 2011) (figure 1.16).

Three genes have been identified which are required for homologous chromosome pairing during male meiosis. The first, *teflon* was identified as part of a genetic screen to identify meiotic segregation defects. It was observed that mutations in *teflon* induced random segregation of 2nd, 3rd and 4th autosomes at meiosis I in the male but did not appear to effect sex chromosome segregation. There was no effect on female meiosis I segregation (Tomkiel *et al.*, 2000). *Stromalin in meiosis (snm)* and *mdg4 in*

meiosis (mnm) were also identified as part of a genetic screen. *Snm* is a meiosis specific paralogue of the canonical cohesin subunit *scc3/sa* which arose due to a gene duplication. *Mnm* is a gene encoded from the *mod(mgd4)* locus, a complex gene encoding up to 30 different proteins which are involved in chromatin organisation (Gabler *et al.*, 2005; Thomas *et al.*, 2005). Analysis of *snm* and *mnm* null mutants revealed disjunction of autosomes and the sex chromosomes throughout prophase I leading to misalignment at the metaphase I plate and up to 70 % missegregation at meiosis I. (Thomas *et al.*, 2005; Thomas and McKee, 2007). Analysis of SMN and MNM localisation in secondary spermatocytes revealed that both proteins are present in the nucleolus throughout prophase I and colocalise in a single focus on the X-Y bivalent at prometaphase I. Several SNM and MNM foci were also observed in the 2nd and 3rd chromosome territories although they were not associated with any known pairing loci (Thomas *et al.*, 2005).

Thus, it appears that in the absence of chiasmata formation, *Drosophila* have developed novel mechanisms in order to 'conjoin' their homologous chromosomes. The mechanisms of homologue conjunction are as yet poorly understood yet appear to differ between each chromosome pair. Sites of chromosome pairing on the 2nd and 3rd chromosomes are currently unknown as are the mechanisms.

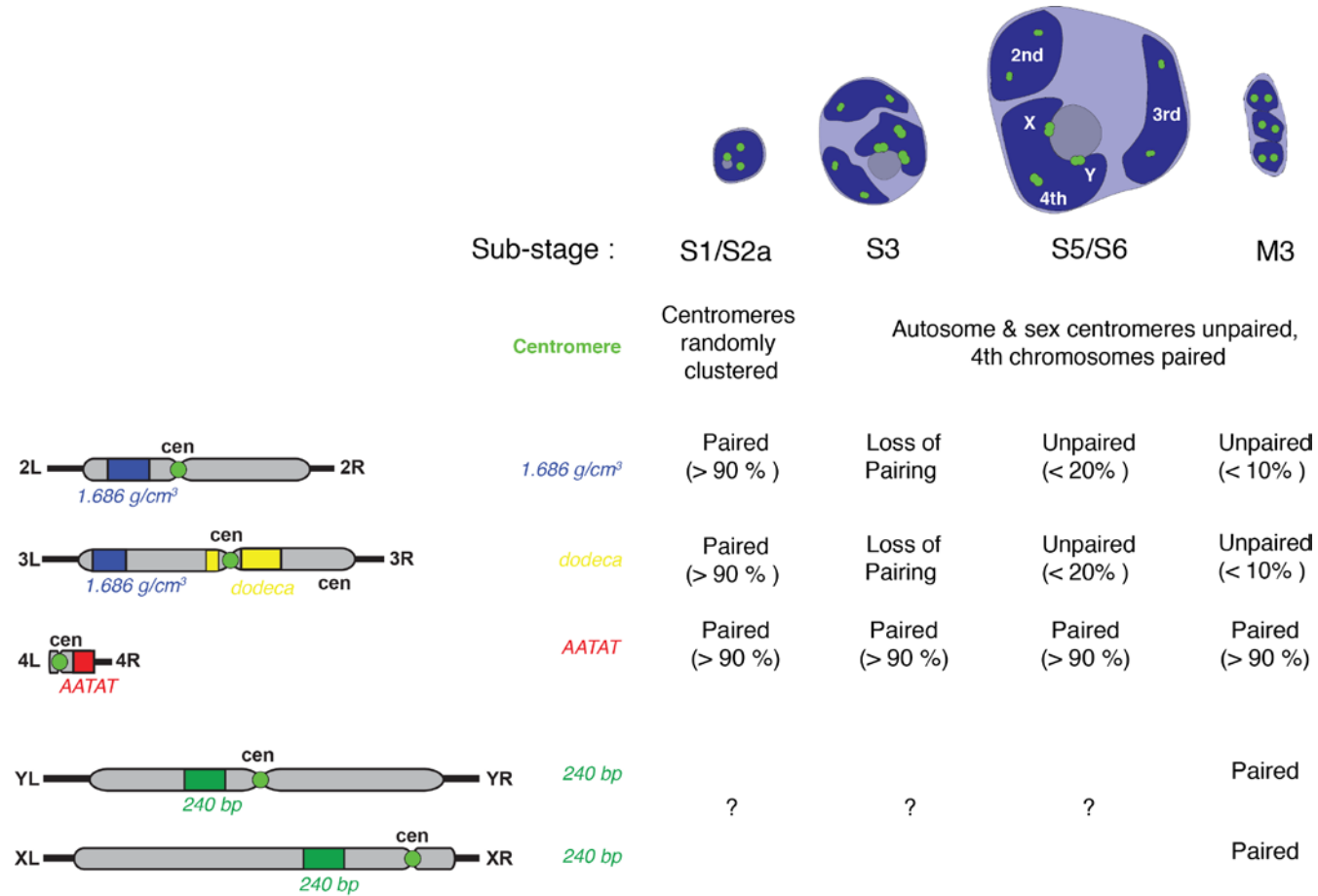


Figure 1.16 Homologue pairing frequencies during prophase I in male *Drosophila* as observed by Tsai *et al.*, 2011.

1.8. Chromatid cohesion during meiosis

Cohesion between sister chromatids is essential in order to tether chromatids prior to chromosome segregation and for the formation of tension generating connections with the kinetochore. In most organisms, cohesion is established by 4 core cohesin subunits Structural Maintenance of Chromosomes 1 and 3 (SMC1 and SMC3), a kleisin family protein double-strand-break repair protein RAD21 homologue (RAD21/SCC3) and an accessory subunit stromal antigen 1 (SA1/2). These core subunits are loaded to the chromosomes during DNA replication and it has been proposed that they form ring-like structures that entrap the chromatids (figure 1.17). At anaphase, cohesion between chromatids is released by the activity of SEPARASE, a specific endopeptidase which cleaves the kleisin subunit (reviewed by Ishiguro and Watanabe, 2007 and Nasmyth and Haering, 2009).

In the germ-line several cohesin proteins are replaced by meiosis specific subunits, most notably the kleisin subunit RAD21 is replaced by meiotic recombination protein REC8 (figure 1.17). At anaphase I, as REC8 is cleaved along the chromosome arms in order to release homologue connections, centromeric REC8 is protected by the activity of SHUGOSHIN (Kitajima *et al.*, 2004). In mitotic cells cohesin localises strongly to the pericentromere but during meiosis, REC8 containing cohesin also localises to the centromere core and mutational analysis has shown that REC8 is required for the functional unification of sister kinetochores and mono-orientation (Watanabe *et al.*, 2004).

1.8.1 Alternative methods of chromatid cohesion in *Drosophila* males

Interestingly, several studies published from the Wu laboratory suggest that in *Drosophalids*, mechanisms of 'cohesin-independent cohesion' may be of significance. Using *Drosophila* cultured cells Joyce *et al.*, 2012 carried out a genome-wide RNAi screen to search for genes that disrupted somatic

homologue pairing and/or sister chromatid cohesion. By probing for two distinct heterochromatic loci they screened the number of allelic spots visible per nucleus using high throughput FISH. Observation of a single spot indicated that both sister chromatid cohesion and somatic pairing was intact, upon RNAi knockdown any variation of this pattern indicated that cohesion and/or pairing was disrupted. Interestingly, of the 105 genes identified which disrupted pairing/cohesion none were known cohesin subunits (Joyce *et al.*, 2012).

In *Drosophila*, the canonical cohesin subunits SMC1, SMC3, RAD21 and SA are conserved, required for viability and localise as expected in mitotic cells (Valdeolmillos *et al.*, 1998; Vass *et al.*, 2003). However, RNAi knockdown studies in cultured cells have shown that although they are required for cohesion during metaphase of mitosis they are completely dispensable for cohesion during interphase (Senaratne *et al.*, 2016). In addition, many accessory cohesin subunits such as *pds5*, *sororin*, *san*, *deco*, *wap*, *mei-s332* and *separase* are also conserved (reviewed by McKee *et al.*, 2012).

In meiosis, the mechanisms by which male *Drosophila* establish and maintain sister chromatid cohesion are not understood. Firstly, the meiosis specific kleisin subunit REC8 is not conserved. The role of SMC3 and SA1/2 during male meiosis have proven difficult to characterise and although SMC1 localises to centromeres from prophase I until anaphase II it is not detectable at any known sites of arm cohesion (Thomas *et al.*, 2005; Yan *et al.*, 2010). It is known that separase is required for both homologue and sister chromatid disjunction at meiosis II (Blattner *et al.*, 2016) however the exact mechanism of release of non-recombined/conjoined homologues and the mechanism of cohesion release in the absence of REC8 is unknown. Finally, *Drosophila* express an orthologue of SHUGOSHIN, called MEI-S322 which localises to the meiotic centromere in late prometaphase I and is required to maintain sister centromere cohesion through the first division (Kerrebrock *et al.*, 1995). However, again in the absence of a REC8

homologue the mechanism of cohesion protection by MEI-S322 is not known.

Drosophila express three specific genes - *orientation disruptor (ORD)* (Mason, 1976), *sisters on the loose (SOLO)* (Yan *et al.*, 2010) and *sisters unbound (SUNN)* (Krishnan *et al.*, 2014) which are required for chromatid cohesion during meiosis. All three of these proteins are required for proper chromosome segregation during both meiotic divisions and mutational analysis revealed premature loss of sister chromatid cohesion and high rates of non-disjunction at anaphase I and II. ORD, SOLO and SUNN colocalise with the cohesin subunit SMC1 at centromeres throughout meiosis until anaphase II and all three are required for stable recruitment of SMC1 (Yan *et al.*, 2010; Krishnan *et al.*, 2014).

Interestingly neither ORD nor SOLO are required to maintain sister chromatid cohesion at early prophase I and no cohesion defects in these mutants have been observed prior to S5. In addition to this, ORD and SOLO and well as SMN and MNM are completely dispensable for arm cohesion throughout meiosis (Thomas *et al.*, 2005). Taken together, these findings suggest that there exist as yet unidentified mechanisms of cohesion establishment and maintenance during male meiosis.

Sites of strong cohesion throughout the *Drosophila* genome have been studied at several euchromatic sites using the GFP-LACI-*lacO* system, with the number of allelic spots visible per nucleus indicative of cohesion frequencies (Vazquez *et al.*, 2002). Cohesion at distinct heterochromatic sites has been determined using site specific FISH and centromeric cohesion has been analysed by immuno-staining for CENP-A and analysing the number of centromeric foci per nucleus (Tsai *et al.*, 2011).

At early prophase I strong cohesion is observed at all analysed euchromatic (Vazquez *et al.*, 2002) and heterochromatic sites as well as at the centromere (Tsai *et al.*, 2011). However at mid prophase S2b/S3, coincident

with the loss of homologue pairing and in a surprising deviation from chromatid cohesion patterns in conventional meiosis, chromatid cohesion at all tested euchromatic and 5 of 10 tested heterochromatic sites was permanently lost (Vazquez et al., 2002, Tsai *et al.*, 2011)(figure 1.18).

Several sites of stable chromatid cohesion through meiosis were identified; firstly sister centromeres were observed to enter into meiosis I fully cohesive and remain so until anaphase II. Secondly, a stable site of chromatid cohesion was observed from entry into prophase I until anaphase II in a heterochromatic region on the arms of the 2nd and 3rd autosomes (1.686g/cm³ satellite) and on a satellite present on the 4th chromosomes (AATAT repeat). Cohesion at three different pericentromeric loci revealed varying states of chromatid cohesion from high cohesion rates at early prophase I to approximately 50 % cohesion at late prophase I and returning to high cohesion rates again at prometaphase I and II (Tsai *et al.*, 2011) (figure 1.19). Taken together these results indicate cohesion establishment and maintenance throughout prophase I in *Drosophila* males is quite a dynamic and variable process. This finding is in contrast to what has been shown, in the case of mouse oocytes where both SMC1b (Revenkova *et al.*, 2010) and REC8 (Tachibana-Konwalski *et al.*, 2010) loaded to sister chromatids during DNA replication is both necessary and sufficient to mediate cohesion in the mature oocyte (reviewed by Jessberger, 2010).

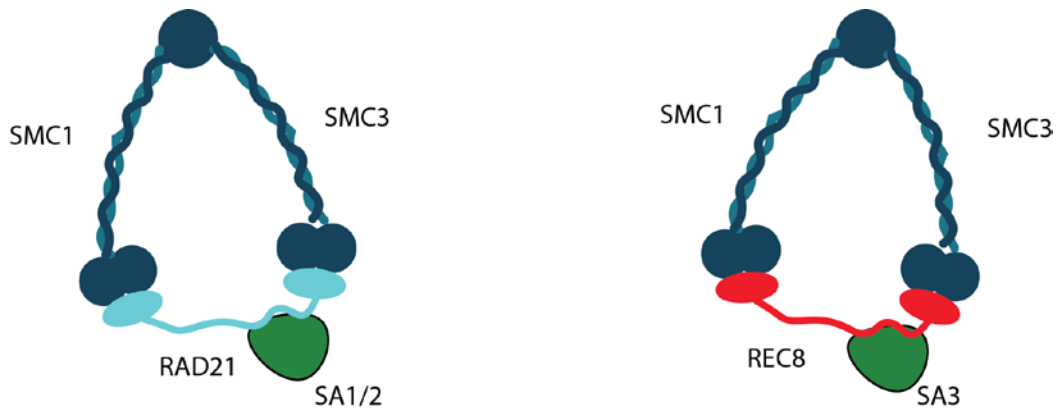


Figure 1.17 The core cohesin components and cohesion structure during mitosis (left) and meiosis (right).

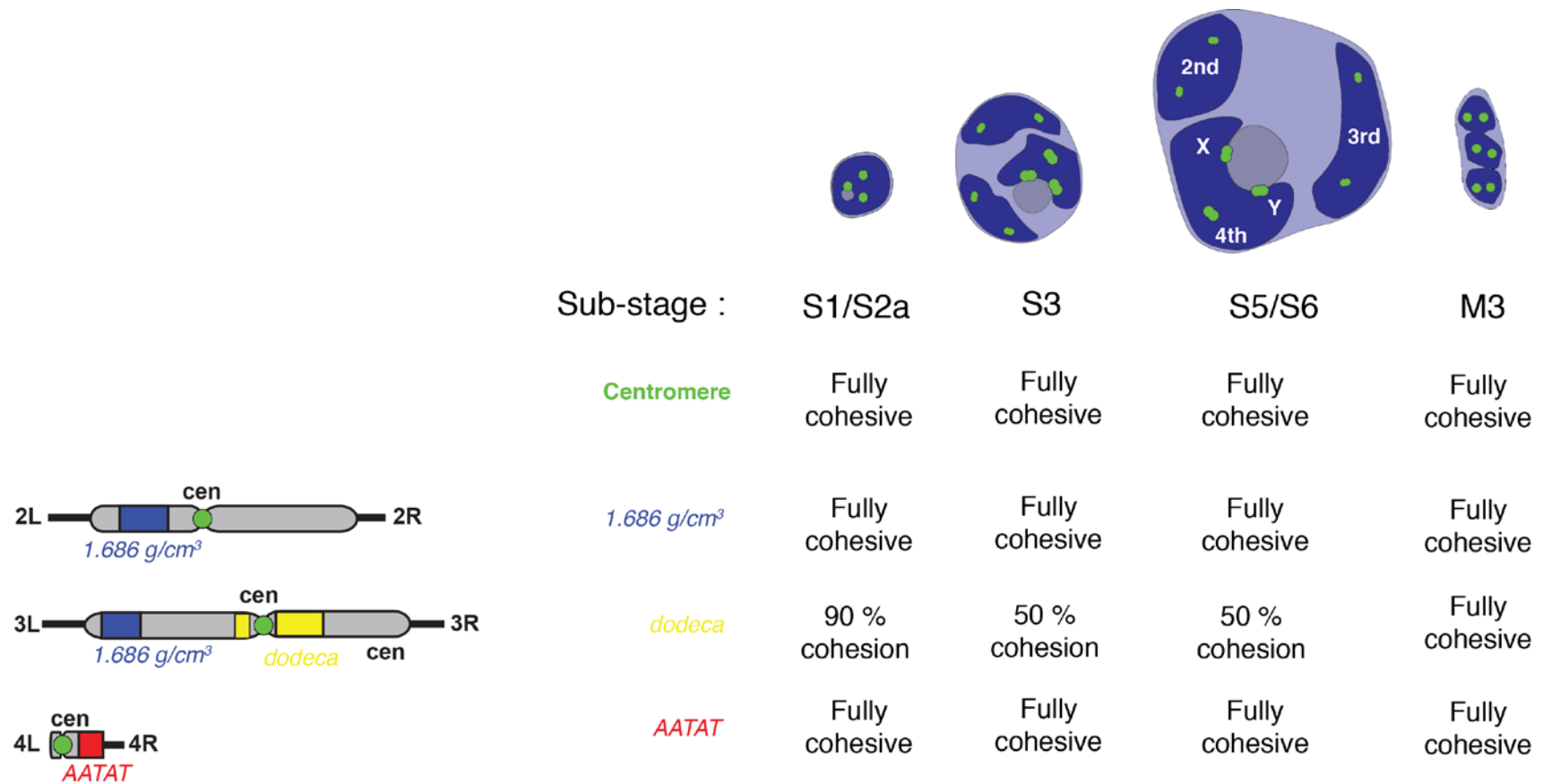


Figure 1.18 Sister chromatid cohesion frequencies during prophase I in male *Drosophila* as observed by Tsai *et al.*, 2011.

1.9. Do *Drosophila* have combined methods of pairing and cohesion?

Several findings from studies of male and female meiosis as well as in cultured cells indicate that the mechanisms which carry out pairing and cohesion in *Drosophila* may overlap. 1) During oogenesis canonical cohesin subunits SMC1 and SMC3 localise to centromeres as well as to chromosome axes and in addition to their role in cohesion they have been shown to be required for SC formation and homologous centromere pairing (Khetani and Bickel, 2007; Tanneti *et al.*, 2011). 2) The cohesin accessory subunits SCC3/SA and PDS5 are required during female meiosis for SC formation and DSB repair. 3) *Drosophila* express several meiosis specific paralogues of canonical cohesin subunits: SNM is a paralogue of SA and C(2)M is a kleisin protein specifically expressed in the female, however both of these paralogues are not required for chromatid cohesion and instead have been implicated in synapsis and recombination (reviewed by McKee *et al.*, 2012). 4) The dynamics of pairing and cohesion at different chromosomal loci during male meiosis display many similarities including strong pairing and cohesion at early prophase I followed by simultaneous loss of both at the mid prophase I transition (S2b/S3) (McKee *et al.*, 2012) and 5) similar pairing and cohesion phenotypes have been observed after RNAi knockdown studies in cultured cells (Senaratne *et al.*, 2016).

1.10. Conclusion

The mechanisms of both homologue pairing and sister chromatid cohesion in *Drosophila* meiosis remain largely unknown. In order to bi-orient their homologous chromosomes at meiosis I, male *Drosophila* have developed a novel mechanism termed 'homologue conjunction'. These mechanisms are dependent on *Drosophila* specific proteins SNM, MNM and TEFLON. Chromatid cohesion in *Drosophila* meiosis is also poorly understood and does not appear to rely on the canonical cohesin subunits, instead employing *Drosophila* specific subunits SUNN, SOLO and ORD. Furthermore,

it appears that in *Drosophila*, the mechanisms of chromosome pairing and cohesion overlap. It is possible that this cooperation may have arisen as a response to achiasmy or to facilitate the intimate homologue pairing that occurs in somatic cells of the fly.

1.11. The mitochondrial F₁ - F₀ ATP synthase

The F₁ - F₀ ATP synthase complex is described as a molecular machine. During respiration it generates ATP from ADP and inorganic phosphate by rotary catalysis (Alberts *et al.*, 2014). The F₀ portion of the complex is embedded within the inner mitochondrial membrane (subunits ATPsyn-a, -b, -c) and is likened a turbine whereas the F₁ portion protrudes from the membrane pore into the inner mitochondrial matrix and is composed of a central stalk (subunits ATPsyn- γ - δ and - ϵ), which stretches from the proton pore to the top of the F₁ subunit. The catalytic core of F is a hexamer of alternating ATPsyn- α and ATPsyn- β subunits, which although they share less than 20 % sequence identity have almost identical structures. The nucleotide binding and catalytic sites of the complex are located at the ATPsyn- α / β interface with the catalytic sites present on ATPsyn- β and non-catalytic sites present on ATPsyn- α . During ATP synthesis, protons translocate through the pore, down the concentration gradient inducing rotation of the ATPsyn-c ring and the central stalk. As the ATPsyn- γ subunit rotates within the catalytic core it induces conformational changes which facilitate catalysis (reviewed by Walker, 2013).

1.11.1 ATP synthase subunits – links to fertility in *Drosophila*

Several links have been made between fertility and subunits of the mitochondrial ATP synthase in *Drosophila melanogaster*. Firstly, male sterile alleles of ATPsyn- α (*bellwether*)(Castrillon *et al.*, 1993) and of a testis specific paralogue of ATPsyn- β (*Ms(3)72Dt/ATPsyn- β like*) (Lindsley *et al.*, 2013) have been identified as part of large-scale mutagenesis screens. In addition, a recent study of endogenous RNAi pathways in *Drosophila* has identified that ATPsyn- β is normally repressed in the testis during spermatogenesis and that disruption of this down-regulation leads to fertility defects (Wen *et al.*, 2015).

Recent large scale *in vivo* RNAi screens carried out in the Lehmann laboratory have identified that components of the ATP synthase F₁-F₀ complex are required for germ cell differentiation in female *Drosophila* (Teixeira *et al.*, 2015; Sanchez *et al.*, 2016). RNAi knockdown of ATP synthase subunits in the germ-line resulted in an arrest which manifested between the 4 and 8 cell cyst stages of pre-meiotic mitosis (Teixeira *et al.*, 2015). Thus these subunits are not essential for stem cell maintenance or for differentiation initiation but they are required during proliferation of the resulting cysts. Furthermore, in the male Sawyer *et al.*, 2017 have identified several testis enriched and/or testis specific paralogues of ATP synthase subunits (ATPsyn-d, ATPsyn-F6 and ATPsyn-g) that are required for fertility. Analysis of mutant alleles and after RNAi knockdown of these genes revealed defects of spermiogenesis and reduced fertility (Sawyer *et al.*, 2017).

Interestingly, both of these studies propose that the observed defects in meiotic progression and fertility are independent of the canonical function of these subunits in oxidative phosphorylation. To show this in the female, Teixeira *et al.*, 2015 alternatively reduced ATP levels in the ovary and observed no defect in germ-line differentiation. In the male, Sawyer *et al.*, 2017 carried out RNAi knockdowns of the testis specific paralogues and observed no change in the membrane potential across the mitochondria. Instead they propose that the defects arise as a result of an ATP-independent role in the maturation of mitochondrial cristae (Teixeira *et al.*, 2015; Sawyer *et al.*, 2017). It is known that several subunits of ATP synthase regulate the maintenance of cristae by promoting dimerization of ATP synthase complexes and that this dimerization promotes curvature of the inner membrane (Walker, 2013). Indeed, in both studies, analysis of the inner mitochondrial morphology after RNAi knockdown revealed immature and rudimentary mitochondrial structures. However, the mechanism of how mitochondrial maturation and cristae formation promotes germ-cell differentiation in the female and spermatid differentiation in the male is not understood.

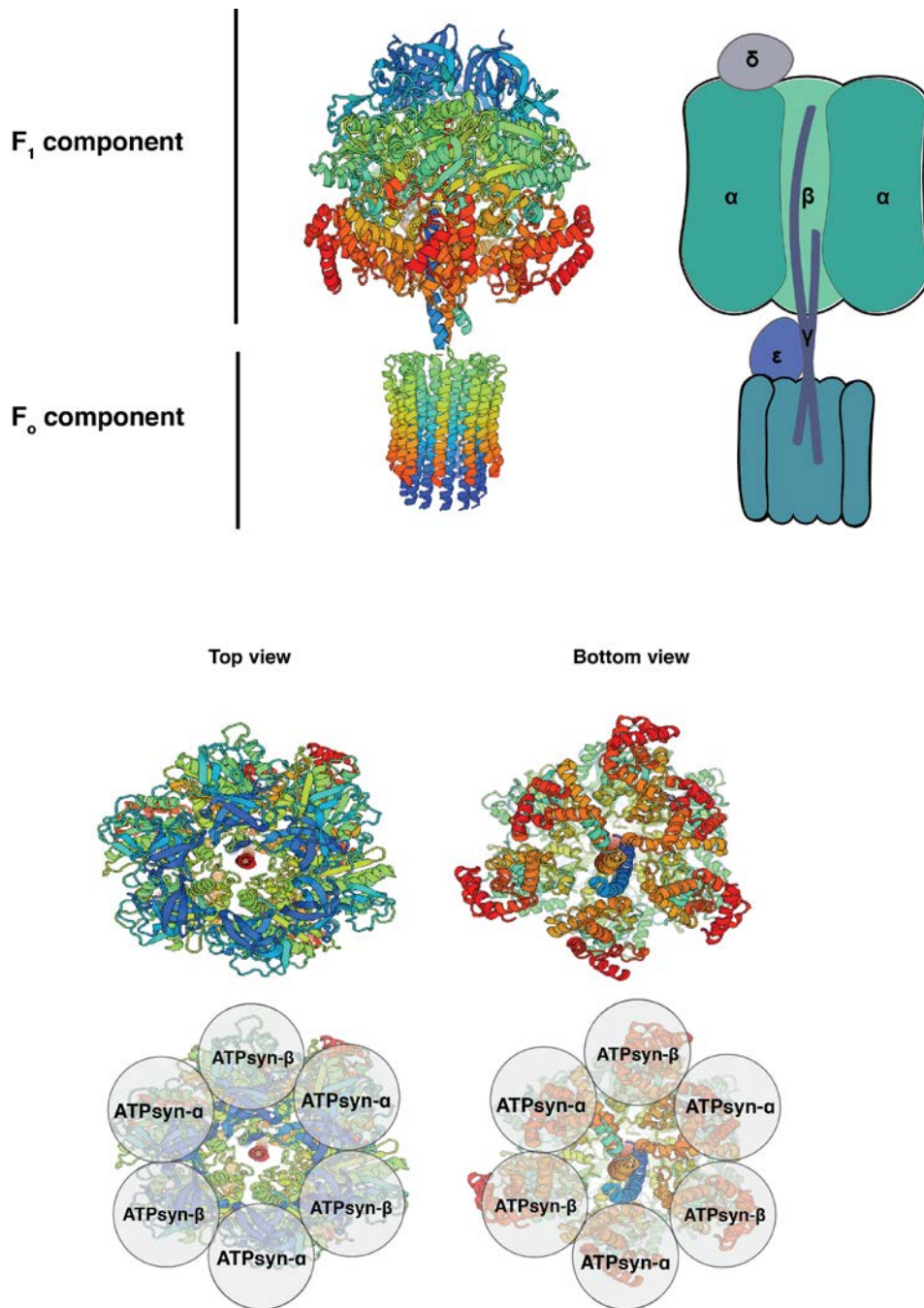


Figure 1.19 Structure of the mitochondrial F_1-F_0 ATP synthase complex. (A) Crystal structure generated by ExPasy Swiss Model and a schematic of a cross section of the complex indicating the location of subunits. (B) Top and bottom views of the F_1 ATPsyn- α and ATPsyn- β hexamer.

1.12. Project hypotheses, rationale and objectives

We hypothesise that the N-terminus of the centromeric histone variant CENP-A has novel functions during male meiosis in *Drosophila melanogaster*.

The rationale for this hypothesis is based on two pieces of evidence. Firstly, studies in the plant *Arabidopsis thaliana* have shown that the CENP-A N-terminus is specifically required in meiosis for centromeric assembly (Ravi *et al.*, 2011b). Secondly, the N-terminus of CENP-A is positively selected for during evolution (Malik and Henikoff, 2001) and 3 conserved sequence blocks have been identified in the N-termini of all Drosophilid species (Malik *et al.*, 2002; Torras-Llort *et al.*, 2010).

This project has 3 objectives:

1. To identify if CENP-A has novel functions in the male germ-line of *Drosophila melanogaster*. To do this we have analysed centromere function and dynamics during meiotic progression after RNAi knockdown of CENP-A in the testis.
2. To identify novel protein interactors of CENP-A in the germ-line. To achieve this we have CENP-A protein complexes from testes protein extracts and analysed interacting proteins by mass spectrometry.
3. To determine if the N-terminus of CENP-A is specifically required for meiotic CENP-A assembly in male *Drosophila melanogaster*. To achieve this we have produced a transgenic fly line expressing a GFP-tagged CENP-A fusion protein lacking its N-terminus.

2. Materials and methods

2.1. Chemical reagents and experimental kits

Unless otherwise indicated, general chemical reagents and experimental kits were obtained from Sigma-Aldrich, Invitrogen and/or Fisher Scientific; specific chemical reagents and experimental kits are indicated within the text. Common reagents and buffers used are listed in appendix 8.2 p.209.

2.1. Drosophila techniques

2.1.1 Fly stocks and husbandry

Stocks were cultured in 25 mm polystyrene vials at 20 °C under a 12 hour light-dark cycle and on standard cornmeal medium (Nutri-Fly™) preserved with 0.5 % propionic acid and 0.1 % Tegosept (APEX Bioresearch Products). ATPsyn F₁ component lines generated by transposable (P) element mediated insertional mutagenesis were obtained from the Bloomington Drosophila Stock Centre (BDSC). UAS-RNAi lines were obtained from the BDSC TRiP collection and from the Vienna Drosophila RNAi Centre (VDRC). All fly stocks used during this study are detailed in appendix 8.3 p.213.

2.1.2 Classification of meiotic cell stages in the male germline

The male germline of *Drosophila melanogaster* has been well described. For identification of different cell stages the following papers were used as reference; Cenci *et al.*, 1994 and White-Cooper, 2004.

In general, cells were selected as being in early prophase I (S1/S2a) if they were located within a 16 cell cyst at the apical end of the adult testis and had not yet begun to form distinct nuclear territories. Cells within a 16 cell cyst that had begun to form distinct nuclear territories but had not yet achieved maximum nuclear size were classified as mid-prophase I (S2b-S4). Late prophase I cells (S5-S6) were identified based on their distinctive nuclear morphology and large nuclear volume. The different stages of prometaphase I and prometaphase II were identified based on nuclear and spindle morphologies and cells dividing by meiosis I and II were distinguished from each other based on their nuclear size, spindle morphologies, and the

presence/absence of CENP-C at centromeres (CENP-C is normally removed after meiosis II).

2.1.3 Generation of transgenic fly lines

Transgenic fly lines expressing mCherry-ATPsyn- β , eGFP-ATPsyn- β like and GFP-CENP-A- Δ 118 were generated by transposable (P) element mediated transformation (injection, selection and balancing was carried out by Bestgene Inc.). *ATPsyn- β* and *ATPsyn- β like* were amplified by PCR from WT *y⁺ry⁺* adult testes cDNA. Both genes were N-terminally tagged with respective fluorescent proteins and placed under the expression of their endogenous promoters and 5' and 3' regulatory sequences (*ATPsyn- β* : 600 bp upstream of start codon and 440 bp downstream of stop codon ; *ATPsyn- β like*: 900 bp upstream of start codon and 600 bp downstream of stop codon).

N-terminally truncated (Δ 118) *cenp-a* (bp 354 – 678) was amplified from whole fly (WT *y⁺ry⁺*) gDNA and N-terminally tagged with *gfp*; a 3 x glycine linker was placed between the GFP-tag and the *cenp-a* start codon. *gfp-cenp-a- Δ 118* was placed under the control of the endogenous *cenp-a* promoter and 5' and 3' regulatory sequences (413 bp upstream of start codon and 417 bp downstream of stop codon). All transgenes were transformed by injection into *w¹¹¹⁸* embryos (Bestgene Inc.).

2.1.4 Genetic manipulation

(a) GAL4-UAS RNAi knockdown

Testes specific knockdown of gene expression was carried out using the well-established GAL4-UAS RNAi system (Duffy, 2002). Briefly, this system involves crossing a line containing an RNAi hairpin targeting a gene of interest which is placed under the control an upstream activating sequence (UAS) to another line expressing the GAL4 transcriptional activator under the control of a tissue specific promoter (figure 2.1). The resulting progeny contain both the UAS-RNAi hairpin and the tissue specific promoter and thus RNAi is induced against the gene of interest.

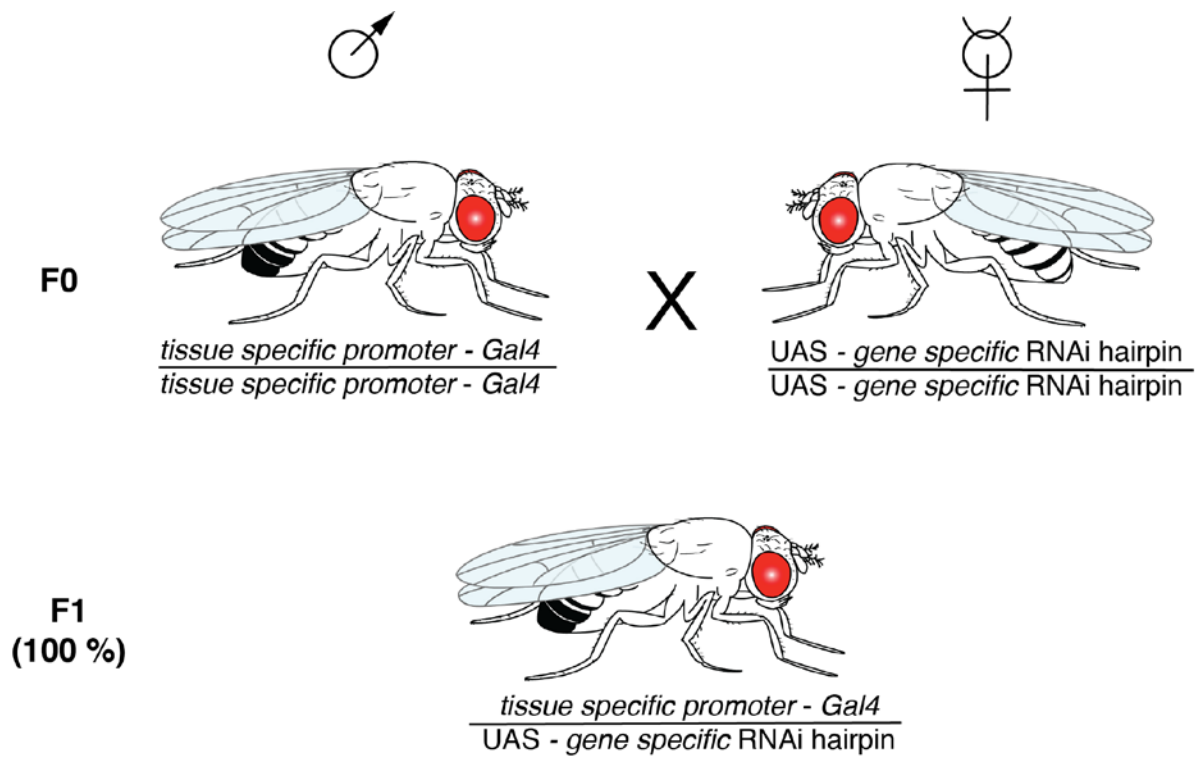


Figure 2.1 A schematic of the *Gal4-UAS* system in *Drosophila melanogaster*.

Unless specifically indicated, for RNAi crosses carried out in this study adult flies were transferred from the main stock (at 20 °C) to the higher temperature of 25 °C in order to induce more efficient RNAi; virgin female progeny from this cross were then isolated and crossed (at 25 °C) to a male 'GAL4-driver' line. To drive expression of GAL4 specifically in the testes the germ-line specific promoter of the gene *bam* was used (*w;; bam-gal4-VP16, UAS-dcr2*).

(b) Crossing scheme: to test functionality of GFP-ATPsyn- β like *in vivo*.

To test the functionality of the eGFP-ATPsyn- β like transgene *in vivo* this line was crossed into an *ATPsyn- β like* P element mutant background and the centromeric cohesion defect observed throughout meiosis I was scored to determine if a rescue had occurred (figure 2.2).

(c) Crossing scheme: placing transgenes into a *UAS-cenp-a* RNAi hairpin background.

To assess the effect of CENP-A depletion on ATPsyn- β like localisation and function, a transgenic line expressing eGFP-ATPsyn- β like was crossed into the background of a line containing a *UAS-cenp-a* RNAi hairpin. *cenp-a* RNAi was then induced by crossing to the *bam-gal4* driver (figure 2.3). The effect of CENP-A depletion on eGFP-ATPsyn- β like, localisation was determined by immunofluorescence microscopy.

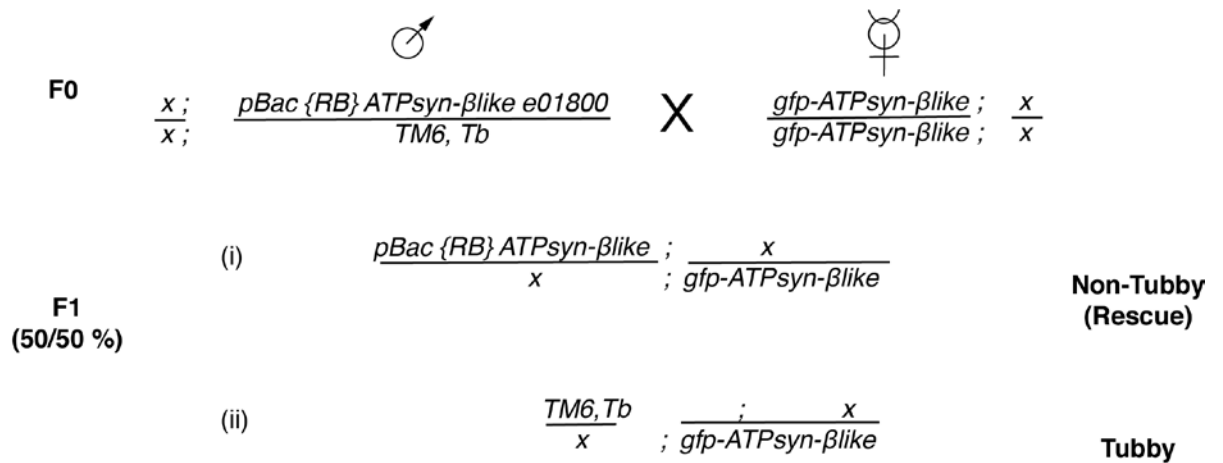


Figure 2.2 Crossing scheme to generate a rescue in the ATPsyn-βlike P element mutant using a GFP-ATPsyn-βlike construct. pBac ATPsyn-βlike is balanced with TM6 with phenotypic marker Tubby (Tb). x/x represents two wild type alleles

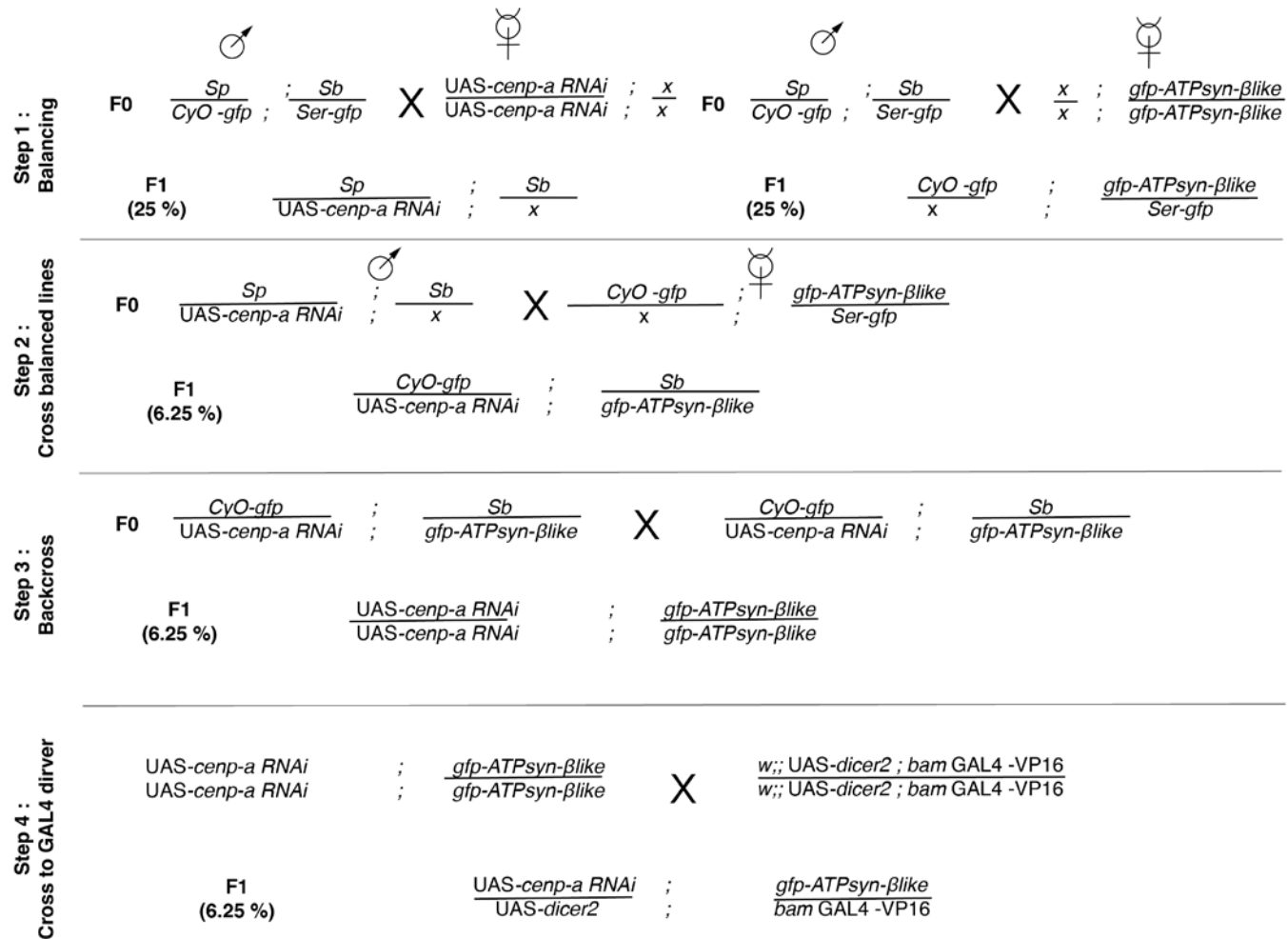


Figure 2.3 Crossing scheme to generate a fly line expressing a CENP-A RNAi hairpin in a *gfp-ATPsyn-βlike* homozygote background. Sb represents the balancer P{B}Sb with phenotypic marker stubble (Sb), Ser represents balancer TM3 with phenotypic marker serrated (ser), CyO represents balancer with phenotypic marker curly (Cy) and Sp represents balancer with phenotypic marker sternoplural (sp)

2.1.5 Fertility tests

Fertility tests were carried out under standard culture conditions at 25 °C. Two virgin adult male/female flies from knockdown experiments were crossed to two virgin female/male control (WT y^+ry^+ or #36303) flies. The number of adult progeny was scored after 20 days. Differences in fertility were analysed statistically using an unpaired students t-test.

2.2. Molecular biology techniques (DNA and RNA)

2.2.1 Extraction of whole fly genomic DNA (gDNA)

30 adult flies were homogenised in 400 µl of grinding buffer (1 % SDS, 100 mM NaCl, 100 mM EDTA and 100 mM Tris-HCl pH 7.5) with a standard plastic pestle until only the cuticles of the fly carcass remained. The sample was then incubated at 65 °C for 30 minutes after which it was transferred to 4 °C and 800 µl of a 6 M lithium chloride : 5 M potassium acetate (1: 2.5) solution was added. The sample was incubated for 30 minutes at 4 °C and then centrifuged at 12,000 x g for 15 minutes at RT. The supernatant, containing gDNA was transferred to a new tube and purified by isopropanol precipitation. Purified DNA was reconstituted in molecular biology grade H₂O (Fisher Scientific), the concentration and purity was analysed using a Nanodrop spectrophotometer. gDNA was stored at -20 °C.

2.2.2 Extraction and purification of tissue specific RNA

For RNA isolation and purification, particular care was taken to avoid contamination with RNases; this included the use of RNase-free tubes (Eppendorf) and filter tips (Fisherbrand). Separate benches and equipment was used for RNA extraction and purification and all equipment and solutions were treated with Diethyl pyrocarbonate (DEPC) prior to use to remove RNases.

Total RNA was extracted from larval brain (150), adult testes (200), adult ovary (100) and *Drosophila* S2 cells (2×10^6). Tissues dissected in PBS were homogenised in 1 ml of Trizol reagent (Invitrogen) using a standard plastic

pestle. The samples were then centrifuged at 4 °C and 12,000 x g for 10 minutes and the supernatant containing the RNA was isolated. To ensure dissociation of nucleoprotein complexes the sample was incubated at room temperature for 5 minutes and subsequently 0.2 ml of chloroform (Trizol:chloroform, 5:1) was added. Phase separation was carried out by centrifugation at 4 °C and 12,000 x g for 15 minutes; the upper aqueous phase containing the RNA was then isolated. To maximise yield, RNA was 'back extracted' by addition of 0.5 ml of H₂O to the phenol-chloroform followed by re-separation.

The RNA was purified by isopropanol precipitation. Precipitated RNA was collected at 4 °C and 12,000 x g for 10 minutes. The RNA pellet was then washed in 75 % ethanol, dried and re-suspended in RNase free molecular biology grade H₂O (Fisher Scientific). Purified RNA was DNase treated to remove any contaminating gDNA. The concentration and purity of RNA was determined using a Nanodrop spectrophotometer. RNA was snap frozen and stored in single use aliquots to minimise degradation.

2.2.3 cDNA synthesis and reverse transcriptase-PCR (RT-PCR)

Reverse transcription (RT) was performed using Super-Script III reverse transcriptase Kit (Invitrogen) according to the manufacturers protocol. 2 µg of purified whole tissue RNA was used for each 20 µl reaction. To produce a full cDNA library oligo dT primers were used in first strand synthesis. 200 ng of cDNA was used in subsequent PCR reactions.

Tissue specific expression of canonical *ATPsyn-β* variants; *ATPsyn-β isoform C* and *ATPsyn-β isoform D* and of the variant *ATPsyn-β; ATPsyn-βlike* was determined by amplification with transcript specific primers from whole tissue cDNA. Amplified transcripts were gel purified and confirmed by sequencing.

2.2.4 Cloning

Taq polymerase (produced in the Dunleavy lab) or Q5 High-Fidelity DNA polymerase (NEB) was used for PCR amplification of DNA. Constructs were

cloned into respective plasmids using either Gibson Assembly and/or conventional restriction cloning. For Gibson Assembly, a 25 bp stretch of sequence with homology to the adjacent DNA fragment was incorporated by PCR to the N and C termini of each piece of DNA. After amplification, each DNA fragment was run on a 1 % (w/v) agarose gel, excised and gel purified. Pure fragments were then assembled in a one-step reaction to their respective plasmids using the Gibson Assembly Mastermix (NEB) according to the manufacturers specifications. For restriction cloning, restriction sites were incorporated by PCR, DNA fragments were then run on 1 % (w/v) agarose gels, excised and gel purified and digested prior to DNA ligation using T4 DNA ligase (NEB) according to the manufacturers specifications.

Assembled plasmids were transformed to chemically competent DH5 α *E. coli* (produced in the Dunleavy lab), cells were grown on selective plates and positive clones were identified by colony PCR. Construction of plasmids used during this study are detailed in appendix 8.4 p.215.

2.2.5 Generation of polyclonal antibodies

An antibody that recognises both *Drosophila* protamine proteins MST35BA and MST35BB (guinea-pig polyclonal) and an antibody that recognises the *Drosophila* transition protein MST77F (rat polyclonal) were produced by immunization of animals with full-length recombinantly expressed proteins (produced as described). Antibody production and affinity purification was carried out by Dundee Cell Products.

An ATPsyn- β like antibody was raised (guinea-pig polyclonal) against two specific ATPsyn- β like peptides; N-terminus (CKTDAELVKKKDE) and C-terminus (GDAPPAKAEAKKDEK). Peptides were BSA and KLH conjugated prior to immunization of animals. Peptide production, conjugation and injection was carried out by Dundee Cell Products. Serum specificity was assessed by western blotting analyses of WT adult testes, ovary and larval brain protein extracts. Specificity was also determined by

immunofluorescent staining in control versus ATPsyn- β like RNAi adult testes.

2.3. Molecular biology techniques (protein)

2.3.1 Recombinant protein expression and purification

All proteins were expressed in BL21 Star Codon-Plus-RIL *E. coli*. For efficient expression a 100 ml starter culture was inoculated with 3-4 colonies from fresh LB agar plates and cultured at 37 °C and 180 RPM for 8 hours. Bacterial cells from the starter culture were collected by centrifugation at 4000 x g for 15 minutes and resuspended in 600 ml of pre-warmed selective LB broth (Lennox). Cultures were grown at 37 °C to an OD₆₀₀ of 0.6 at which point protein expression was induced by addition of 1 μ M IPTG. For expression of GST-CENP-A induction was carried out for 5 hours at 30 °C and 180 RPM. For the expression of His-tagged ATP synthase F₁ components cultures were induced with 1 μ M IPTG for 5 hours at 37 °C and 180 RPM.

After expression, bacterial cells were collected by centrifugation for 20 minutes at 4 °C and 4000 x g; the pelleted cells were then washed in PBS (4 °C) (cell pellets were snap frozen in liquid Nitrogen and stored at -80 °C at this point). Cell lysis was performed in 5 pellet volumes of a PBS buffer containing 200 μ g/ml lysozyme as well as specific protease/phosphatase inhibitors (detailed in table). The lysate was sonicated for a total of 3 minutes (30 seconds on / 30 seconds off) at 20 % amplitude using a digital sonifier (Branson). Following sonication the lysate was supplemented with potassium chloride (0.25 M) and DTT (15 mM) and then centrifuged for 20 minutes at 4 °C and 4000 x g.

GST and GST-CENP-A were expressed as soluble proteins. For purification, 1 ml of washed glutathione-agarose bead slurry was added to the lysate supernatant and incubated for 2 hours at 4 °C and 10 RPM. The beads were collected by centrifugation for 2 minutes at 4 °C and 700 x g and then washed 5 times in 10 ml of wash buffer (PBS with 0.25 M KCL, 0.5 mM DTT and protease inhibitors), after the final wash, any remaining wash buffer

was removed using fine pipette tips. Elution was carried out in 1 bead volume of an elution buffer containing 40 mM glutathione, 0.25 M KCL and 50 mM Tris-HCl pH 8.0 for 5 minutes at 4 °C under gentle agitation.

ATPsyn- α , ATPsyn- β and ATPsyn- β like were expressed as insoluble inclusion bodies, which were isolated after cellular lysis and washed in 50 mM Tris-HCl pH 8.0 with protease inhibitors. ATPsyn- α , ATPsyn- β and ATPsyn- β like were solubilised in 50 mM Tris-HCL pH 8.0 with 5 M Urea and 50 mM DTT for 1 hour at 4 °C and 10 RPM. Solubilised His-ATP synthase F₁ components were then centrifuged for 20 minutes at 4 °C and 20,000 x g. Purification was carried out under denaturing conditions with 1 ml of HisPUR Ni-NTA resin slurry (Thermo Scientific). Binding was carried out for 2 hours at 4 °C and 10 RPM. The beads were collected by centrifugation for 2 minutes at 4 °C and 700 x g and then washed 5 times in 10 ml of wash buffer (50 mM Tris-HCL pH 8.0, 20 mM imidazole), after the final wash any remaining wash buffer was removed using fine pipette tips. The proteins were eluted in 1 bead volume of 50 mM Tris-HCl pH 8.0, 5 M Urea and 200 mM imidazole for 5 minutes at 4 °C and under gentle agitation.

2.3.2 Recombinant protein dialysis and storage

Purified GST and GST-CENP-A proteins were dialysed in a single step overnight at 4 °C to PBS with 20 % glycerol using the Slide-a-lyzer mini dialysis unit (Thermo Scientific). Proteins were stored in single use aliquots at -80 °C.

ATPsyn- α , ATPsyn- β and ATPsyn- β like were re-natured by stepwise dialysis (Du & Gromet-Elhanan 1999; Chen *et al.*, 1992). Dialysis was carried out in slide-a-lyzer mini dialysis units (0.5 ml) as follows; 1. 8 hours at 4 °C to 50 mM Tris-HCl pH 8.0 and 3 M urea. 2. 16 hours at 4 °C to 50 mM Tris-HCL pH 8.0 and 1.5 M urea and 3. 8 hours at 4 °C to 50 mM Tris-HCl pH 8.0. All re-natured His-ATP synthase F₁ components were then stored in single use aliquots at -80 °C.

2.3.3 *In vitro* protein direct interaction assay

Recombinantly produced GST (Control) and GST-CENP-A (bait) were incubated with His-ATPsyn- α , His-ATPsyn- β or His-ATPsyn- β like (prey) at a bait : prey ratio of 10 : 1. The interaction was carried out at 4 °C and 10 RPM for 2 hours in a buffer containing 50 mM Tris-HCl pH 8.0, 250 mM NaCl, 0.05 % NP-40 and 1 % protease inhibitor cocktail. The bait and any interacting proteins were then pulled-down with 25 μ l of blocked (5 % BSA) glutathione agarose beads (50 μ l of bead slurry) for a further 1 hour at 4 °C and 10 RPM. The beads were harvested at 700 x g for 2 minutes and washed 5 times in 1 ml of wash buffer (50 mM Tris-HCl pH 8.0, 400 mM NaCl and 0.05 % NP-40). Proteins were eluted from the beads in 30 μ l of a 40 mM glutathione elution buffer for 5 minutes at 4 °C under gentle agitation. Samples were run on SDS-PAGE gels and co-precipitation of His-tagged ATP synthase F₁ proteins was determined by anti-polyHis western blot.

2.3.4 His-ATPsyn- α interaction with CENP-A peptide array

A series of 18-mer overlapping peptides covering the entire sequence of CENP-A was produced by automatic SPOT synthesis on to Whatman 50 cellulose membrane supports using Fmoc (9-fluorenylmethyloxycarbonyl) chemistry (Frank, 2002). Peptide arrays were produced using the AutoSpot-Rosbot ASS 222 (Intavis Bioanalytical Instruments). Peptide arrays were produced in the laboratory of Dr. P Kiely at the University of Limerick.

To reveal ATPsyn- α binding sites on CENP-A, the CENP-A peptide array was challenged with recombinantly produced His-ATPsyn- α and sites where binding occurred were then revealed by anti-ATPsyn- α western blot. The peptide array binding assay was conducted as follows; the cellulose membrane was activated by incubation in 100 % ethanol for 5 minutes and the membrane was then blocked for 1 hour at RT in 0.1 % PBS-Triton-X (PBSTx) with 5 % (w/v) milk solution. Recombinantly produced His-ATPsyn- α (5 μ g/ml) in 1 % milk (0.1% PBSTx) solution was incubated with the array overnight at 4 °C under gentle shaking. Following binding, the array was washed (3 x 15 minutes in 0.1 % PBSTx) and incubated for 2

hours at RT with an anti-ATPsyn- α antibody. Primary antibody binding was detected using a fluorescently labeled secondary antibody (IRDye 800CW). Fluorescence was detected using an Odyssey CLx Imaging System (LI-COR Biosciences). Fluorescence intensities were quantified using Image Studio Lite Version 5.2.5 (LI-COR Biosciences).

2.3.5 SDS-PAGE and western blotting

For analysis by western blot, protein samples were diluted in NuPAGE LDS sample buffer (Invitrogen) containing 1X Bolt sample reducing agent (Invitrogen) and denatured by incubation at 95 °C for 10 minutes. Protein samples were run on precast Bolt 4-12 % Bis Tris Plus 1.0 mm x 10 well gels (Invitrogen) and in NuPAGE MES SDS running buffer (Invitrogen). Separated proteins were transferred onto nitrocellulose blotting membrane (Amersham Protran 0.45 μ m, GE Healthcare); the membrane was then blocked in 5 % (w/v) milk solution for 1 hour at RT before incubation with primary antibodies. Unless specifically indicated, primary antibody incubations were carried out overnight at 4 °C under gentle rotation (all antibodies used during this study are detailed in appendix 8.5 p.218) and were followed by 3 x 15 minute washes at RT in TBS-Tween 20 (0.1 %). Fluorescent or HRP labeled secondary antibody incubations were carried out for 1 hour at RT under gentle rotation and were again followed by 3 x 15 minute washes at RT in TBS-Tween 20 (0.1 %).

For fluorescently labeled secondary antibodies, binding was revealed using Odyssey CLx Imaging System (LI-COR Biosciences); for HRP labeled secondary antibodies binding was revealed using an ECL western blotting substrate kit (Pierce).

2.4. Cell biology techniques

2.4.1 Drosophila Schneider 2 (S2) cell culture

Drosophila S2 cells are a semi-adherent, macrophage-like cell line that were derived from late stage (20-24 hour old) Drosophila embryos (Schneider, 1972). The cells were cultured in plastic T25 cell flasks in Schneider's

Drosophila medium (Invitrogen) supplemented with 10 % heat inactivated fetal bovine serum (FBS) and standard antibiotics (1 %). The cells were gently passaged every 4-5 days and were cultured at 25 °C in ambient CO₂ levels.

Transient transfection of Drosophila S2 cells with plasmid DNA was carried out using FuGENE HD transfection reagent (Promega) with a ratio of 1 µg DNA : 6 µl transfection reagent. During transfection, cells were transfected in Schnieders Drosophila medium supplemented with 10 % heat inactivated FBS with no antibiotics. For transfection of *gfp-cenp-a* transgenes, cells were harvested for analysis 72 hours after transfection; for transfection of *gfp-ATPsyn-β-like* transgenes, cells were harvested for analysis 48 hours after transfection.

2.4.2 Preparation of cytoplasmic and nuclear extracts from adult testes

Wild Type (WT; strain *y⁺ry⁺*) adult testes were dissected in PBS in batches of 100; the tissue was digested for 30 minutes at 25 °C and 300 RPM in PBS containing 1 mg/ml collagenase 1.5 mM CaCl₂, 2 % BSA and 100 µg/ml DNase. Digested tissue was mechanically disrupted by gentle passage through a large (P1000) pipette tip for 1 minute; cells released were isolated from extracellular material by washing through a 40 µm pore sieve with 10 ml of cold PBS (4 °C). The extracted cells were collected by centrifugation at 300 x g for 15 minutes at 4 °C prior to fractionation.

Two cell fractions were obtained by hypotonic treatment (fraction 1) and nuclear lysis and homogenisation (fraction 2). Briefly, cells were exposed to a hypotonic buffer (10 mM HEPES, 1.5 mM NaCl, 1.5 mM MgCl₂, 0.1 mM EGTA, 1 mM DTT, 0.1 % Triton-X, 1 % protease inhibitor cocktail) for 10 minutes at 4 °C and the supernatant was collected at 1500 x g for 10 minutes at 4 °C. Remaining insoluble material was resuspended in lysis buffer (20 mM Tris-HCl pH 7.5, 300 mM NaCl, 0.5 mM EDTA, 0.05 % Triton-X, 0.1 % NP-40, 1 mM PMSF and 1 % protease inhibitor cocktail) and

homogenised with 10 passes of a tight fitting pestle. Remaining insoluble material was collected by centrifugation at 4000 x g for 10 minutes at 4 °C. Supernatants from fractions 1 and 2 were snap frozen in liquid nitrogen and stored at -20 °C.

2.4.3 Pull-down and identification of GST-CENP-A N-terminal interacting proteins.

Pooled protein extracts from 500 adult testes were used per pull-down experiment. Protein samples were diluted in interaction buffer (IB) (20 mM Tris-HCl pH 7.5, 300 mM NaCl, 0.5 mM EDTA, 0.05 % NP-40, 1 mM PMSF and 1 % protease inhibitor cocktail) and incubated for 2 hours at 4 °C and under 20 RPM with 10 µg of recombinantly produced GST (control) or GST-CENP-A N-terminus (amino acids 1 – 126). 50 µl of glutathione agarose bead slurry was then added for a further 1 hour before the beads were collected by centrifugation at 700 x g and washed 3 x 15 minutes in 1 ml of wash buffer (IB containing 500 mM NaCl). Precipitated proteins from control and bait experiments were eluted by boiling (95 °C) in sample buffer and analysed SDS-PAGE separation followed by silver staining (Invitrogen Silver Quest Staining Kit).

For identification of GST-CENP-A-N terminal interactors, proteins were separated by SDS-PAGE then whole control (GST) and bait (GST-CENP-A N-terminus) gel lanes were excised and subjected to tryptic digestion; this was followed by Nano LC-MS/MS analysis (Mass spectrometry performed by the Proteomics Facility at the University of Bristol).

Proteins detected by MS were analysed based on a number of parameters; (1) the protein area, a measure of the relative abundance of a particular peptide based on the average area scores of the three most abundant peptides. (2) The total number of corresponding peptides detected and (3) the number of specific peptides detected. Proteins were selected for further study based on specificity in the pull-down (versus control lane), the

relative abundance of detected protein and known links to male fertility found from literature searches. ATP determination assay

2.4.4 ATP determination assay

Testes dissected from young adult flies (aged between 3 and 24 hours) were homogenised in a chaotropic buffer containing 6 M guanidine hydrochloride, 100 mM Tris (pH 7.8) and 4 mM EDTA. Lysed samples were boiled for 5 minutes at 95 °C and then spun at 4 °C and 20,000 x g for 5 minutes. The extracted ATP was then diluted 1/10 in 25 mM Tris HCl (pH 7.8) and 100 µM EDTA and spun for a further 5 minutes at 4 °C and 20,000 X g.

The level of ATP in the testes extracts was determined using a luciferase-based assay (kit from Molecular Probes #A22066). Briefly, this light emitting reaction, of which ATP is an absolute requirement, is based on the conversion of D-Luciferin to Oxyluciferin by activity of the firefly luciferase enzyme. The level of ATP in the testes extracts was determined against a standard curve of luminescence versus ATP concentration. The assay was carried out in triplicate in black opaque flat-bottomed 96 well plates (Corning Costar #3915) and luminescence was read at 590 nm using a standard luminometer. ATP levels for all samples were normalised according to the level of protein present in the samples (as determined by Bradford assay). To determine ATP reduction in RNAi knockdowns data was pooled from three independent RNAi experiments and statistical significance was determined using an unpaired students t-test.

2.4.5 Preparation of testes for immuno-staining

For standard immunofluorescence (IF) young adult (< 1 days old) testes or 3rd instar larval testes were dissected from *Drosophila* males in PBS. 10-12 testes per sample were then transferred to 10 µl of PBS on poly-L-lysine coated slides and covered with hydrophobic coverslips (Rain-X rain repellent coated). The samples were lightly squashed before snap-freezing in liquid Nitrogen; coverslips were then quickly removed from frozen slides

using a razor and samples were fixed with 4 % paraformaldehyde (PFA) for 10 minutes at RT. Fixed samples were then treated with a 3 x 2 minute ethanol series in 75 % - 85 % - 95 % ethanol at -20 °C. Ethanol treated samples were then air-dried prior to permeabilisation for 2 x 15 minutes in PBS-TritonX (0.4 %) with 0.3 % sodium deoxycholate.

For cytosolic extraction, testes were dissected and fixed as above, however after squashing and PFA treatment samples were transferred directly to a PBS-Triton-X (0.1 %) wash for 10 minutes at RT. In this case the cytosol was not preserved by ethanol treatment and was washed away by PBS-Triton-X (0.1 %) treatment; fixed nuclei remained adhered to the poly-L-lysine treated slides. Prior to treatment with primary antibodies the samples were blocked in 1 % bovine serum albumen (BSA) in PBS-Triton (0.4 %) for 1 hour at RT.

For tubulin staining, tissues were preserved using methanol-acetone fixation according to (Cenci *et al.*, 1994, White-Cooper, 2004). By this method, testes were dissected in 1X PBS and then transferred to 10 µl of 1X PBS on Poly-L-lysine coated slides. The sample was squashed gently with hydrophobic coverslip before freezing in liquid Nitrogen. Coverslips were removed from frozen slides using a razor, the tissues were then treated with 100 % methanol for 5 minutes at -80 °C, followed by 5 minutes in 100 % acetone at -80 °C. The samples were then incubated for 10 minutes in PBS-Triton-X (1 %) at RT. Samples fixed by this method were blocked for 1 hour at RT in 3 % BSA-PBS-Triton-X (0.4 %).

For primary antibody treatment, antibodies were diluted in blocking buffer (1 % or 3 %, as per fixation method) and incubated with sample overnight at 4 °C. After primary antibody incubation, slides were washed 3 x 15 minutes in PBS-Triton-X (0.4 %). Primary antibodies were detected using fluorescently labeled secondary antibodies; incubation was carried out for 1 hour at RT (all antibodies used during this study are detailed in appendix 8.5 p.218). Afterward slides were again washed 3 x 15 minutes in PBS-

Triton-X (0.4 %). DNA was stained using a 1 µg/ml solution of DAPI (diluted in PBS); staining was carried out for 10 minutes at RT and was followed by a PBS wash at RT for 10 minutes. All slides were mounted in Slow-fade Mounting Medium (Invitrogen) and coverslips were sealed with varnish.

2.4.6 Preparation of testes for Fluorescence In-Situ Hybridisation (FISH).

For FISH analysis, young adult (< 1 days old) testes or 3rd instar larval testes were dissected from *Drosophila* males in PBS. The testes were then transferred to a 10 µl drop of PBS on a poly-L-lysine treated slide, 10 µl of PFA (8 %) was then added to the sample and it was covered with a hydrophobic coverslip allowing fixation in a final concentration of 4 % PFA. Fixation was carried out for 10 minutes at RT after which the samples were squashed lightly beneath the coverslip and then frozen in liquid Nitrogen. Coverslips were removed from frozen slides using a razor blade and the sample was transferred to 70 % Ethanol at -20 °C (where they were stored until later processing).

For FISH, fixed samples were passed through a 3 x 2 minute ethanol series (75 %-85 %-95 % ethanol) at -20 °C. Ethanol treated samples were air-dried and then incubated 2 x 10 minutes in 2X saline-sodium citrate with 0.1 % Tween 20 (SSC-Tw) for 10 minutes at RT. Samples were then incubated in increasing concentrations of formamide at RT as follows; 10 minutes in 2X SSC-Tw with 25 % formamide and 10 minutes in 2X SSC-Tw with 50 % formamide. Pre-hybridisation was carried out in 2X SSC-Tw with 50 % formamide for 2 hours at 37 °C .

Fluorescently labeled oligonucleotides (Alexa flourophores) recognising specific pairing and/or cohesion sites on *Drosophila* chromosomes were obtained from Eurofins. Probes were selected based on a characterisation of heterochromatic pairing and/or cohesion sites throughout the *Drosophila*

genome which was carried out by Tsai *et al.*, 2011 (DNA FISH probes used during this study are detailed in appendix 8.6 and figure 2.4). For 4th chromosome (AATAT)₆ FISH, 40 ng of DNA oligonucleotides was used per sample. For 2nd and 3rd chromosome (1.686 g/cm³ site (AATAACATAG)₃), X chromosome (359 bp repeat) and Y chromosome (AATAC)₆ FISH 20 ng of DNA oligonucleotides was used per sample. DNA probes were diluted in hybridization buffer (3X SSC with 50 % formamide and 10 % dextran sulfate), 20 µl of hybridization buffer was added to each sample, the sample was then covered with a coverslip and sealed with rubber cement (Marabu Fixo-gum). The samples were denatured at 94 °C for 4 minutes and then incubated overnight in a humid chamber at 20 °C.

Post hybridisation, washes were performed in 2X SSC-Tw 50 % formamide as follows; 1 x 10 minute wash at 20 °C and 2 x 30 minute washes at 20 °C. The samples were then gradually diluted back out of formamide by 1 x 10 minute wash in 2X SSC-Tw 25 % formamide at RT and 3 x 10 minute washes in 2X SSC-Tw at RT. Samples were then DAPI treated and mounted as described above. For immunofluorescent staining in combination with FISH (Immuno-FISH) slides were transferred to PBS-Triton-X (0.4 %) and blocking and IF was carried out as described above (Immuno-FISH protocol in detail in Collins and Dunleavy, under review appendix 8.7 p.221).

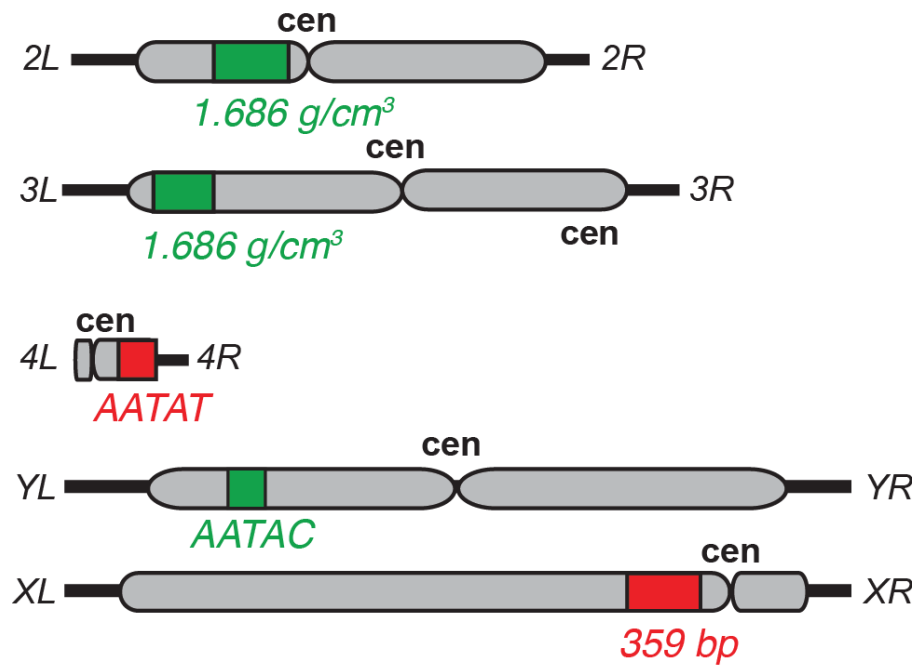


Figure 2.4 An illustration of the genomic location of repetitive and satellite sequences detected by FISH during this study.

2.4.7 Microscopy and image processing

Immunofluorescent microscopy was carried out using a Delta Vision Elite wide-field microscope system (from Applied Precision). Unless specifically indicated, images were acquired as z-stacks with a step size of 0.2 μm ; raw data files were then processed by deconvolution using 10 cycles of a conservative iteration algorithm (SoftWorx). Deconvolved 3D z-stack images were represented in 2D by maximum projection using SoftWorx software. Microscopy images were exported in photoshop (.psd) or .tiff format for further processing and analysis.

2.4.8 Quantitation of fluorescent intensities

Fluorescent intensities were measured as corrected total cellular fluorescence (CTCF) using Image J software (NIH). RGB microscopy images were exported to Image J in tiff format, the composite RGB image was split into individual channels and the signal of interest was analysed by applying a mask and analysing the area and integrated density of the particles. To determine background readings, the average mean grey value of the surrounding area was determined. CTCF was calculated using the following formula:

$$\text{CTCF} = \text{Integrated Density}_{(\text{CENP-A})} - (\text{Area}_{(\text{CENP-A})} \times \text{Average Mean}_{(\text{Background})})$$

Unless specifically indicated, the total centromeric signal per nucleus was determined (as opposed to per centromere) to avoid inconsistencies caused by centromeric cohesion and/or pairing defects. Differences in focal intensities were compared statistically using an unpaired students t-test (focal intensity described in detail in Collins and Dunleavy, under review appendix 8.7 p.221).

2.4.9 Assays used to identify and quantify cohesion, pairing and cell cycle defects

To identify defects in centromeric cohesion during meiosis I, larval or adult testes were immuno-stained with centromeric markers CENP-A and CENP-C. Then using DAPI staining and meiotic cell cyst characteristics as markers of cell cycle stage the number of centromeres per nucleus was counted. To determine defects in 2nd and 3rd chromosome arm cohesion, larval or adult testes were FISH stained using a probe recognising the 1.686 g/cm³ cohesion site, again using DAPI staining and meiotic cell cyst characteristics as markers of cell cycle stage the number of chromosome arms per nucleus with intact cohesion were counted. Differences between samples were determined statistically using an un-paired students t-test and numbers of cells analysed are indicated per experiment.

To determine defects in cell cycle progression, testes from adult flies aged less than 5 hours old were fixed with PFA and ethanol series (as described) and DAPI stained. The number of cell cysts undergoing meiosis I and meiosis II were counted as well as the number of cysts containing maturing spermatids. Differences between samples were determined statistically using an un-paired students t-test and numbers of testes analysed are indicated per experiment.

2.5. Computational analysis & software programmes

DNA plasmid construction and cloning strategies were carried out *in silico* using SnapGene® Software (version 2.6.2) from GSL Biotech. Construction of graphs and charts as well as statistical analyses was carried out using GraphPad Prism 5 (La Jolla, USA). Image processing was carried out using Adobe Photoshop CC 2015 release and figures and schematics were constructed using Adobe Illustrator CC 2015 release.

For bioinformatic analysis DNA and protein sequences were obtained from the database resources of the National Centre for Biotechnology Information

(NCBI). Homology searches were carried out using the basic logical alignment search tool (BLAST) available at the NCBI. Sequence alignments were carried out using Clustal Omega available at EMBL-EBI. Phylogenetic analysis was carried out at Phylogeny.fr. Alignments were performed by Phylogeny.fr using the NCBI alignment tool MUSCLE and trees were constructed using an approximate likelihood ratio test (Anisimova *et al.*, 2006).

**3. A search for novel functions of the CENP-A N-terminus
in the male germ-line.**

3.1. Chapter introduction

This chapter describes the results obtained from an investigation into the role of the N-terminus of the centromeric histone H3 variant CENP-A during male meiosis in *Drosophila melanogaster*. The investigation was carried out using three different approaches;

(i) In the first approach CENP-A protein levels were knocked down in the germ-line and the resulting phenotype was analysed using several different cell markers. This included an analysis of general nuclear and cell division dynamics by DNA and TUBULIN staining and an analysis of centromere dynamics and integrity by immuno-staining for centromeric the markers CENP-A and CENP-C.

(ii) Secondly, by generating a transgenic fly line expressing an N-terminally truncated form of GFP-CENP-A lacking its first 118 amino acids (GFP-CENP-A- Δ 118) we aimed to determine if conserved sequence blocks (B1 and B2) located between amino acids 22-64 and 75-92 are required during meiosis.

(ii) The final approach was biochemical and aimed to identify novel proteins interacting with CENP-A and/or the CENP-A N-terminus in the germ-line. In two independent experiments GFP-CENP-A-FL and an CENP-A N-terminal peptide (amino acids 1-126) were pulled-down from adult testes protein extracts and co-precipitated proteins were then identified by nano liquid chromatography mass spectrometry (nano LC-MS/MS).

3.2. Characterisation of CENP-A RNAi knockdown

3.2.1 Identification of a novel role for CENP-A in meiotic centromeric cohesion

In the male fruit fly, CENP-A protein levels were knocked down in the germline using the GAL4-UAS RNAi system driven by expression of the *bag of marbles* (*bam*) promoter. In the testes, *bam* is switched on during the mitotic divisions of the early secondary spermatogonia and it remains active until late prophase I (White-Cooper, 2012) (figure 3.1 A). The reduction in centromeric CENP-A after CENP-A RNAi was determined by immuno-staining for CENP-A and calculating the total corrected total cellular fluorescence (CTCF) of CENP-A foci per nucleus. Both maternal (isogenic control, genetic background lacking the RNAi hairpin) and paternal (*bam-Gal4* driver) controls were analysed. At late prophase I, a 30 % reduction in total centromeric levels of CENP-A per nucleus was detected compared to control lines *bam-Gal4* and isogenic ($p < 0.0001$) (figure 3.1 B). This 30 % reduction in centromeric levels of CENP-A produced no general nuclear defects prior to prometaphase of meiosis I (as revealed by DNA (DAPI) staining). However immuno-staining for the centromeric markers CENP-A and CENP-C revealed a significant increase in the number of centromeric foci per nucleus throughout meiosis I (figure 3.2).

In control nuclei at early prophase I, as centromeres cluster and sister centromere cohesion is intact an average of 3.65 centromeres are observed per nucleus. After RNAi knockdown of CENP-A, significantly more ($p < 0.0001$) centromeres (average 4.34) were observed per nucleus at this stage immediately following DNA replication indicating a defect of centromere cohesion and/or clustering. This phenotype was also apparent at late prophase I, in control nuclei as homologous centromeres are unpaired (except for the 4th chromosome) yet sister centromere cohesion is maintained, between 6 and 7 centromeres are observed per nucleus (average 6.50) (Schematic: figure 3.1 A). Upon RNAi knockdown of CENP-A an average of 7.73 centromeres were observed per nucleus ($p < 0.0001$)(figure 3.3).

At late prophase I, increased numbers of centromeres were observed in autosomal (2nd and 3rd), 4th chromosome and the sex chromosome

territories indicating that the observed defect was not specific to a particular chromosome. Additionally, as we know that the centromeres of the 2nd and 3rd homologous chromosomes are unpaired during late prophase I, and the fact that more than 8 and up to 11 centromeres were frequently observed per nucleus, this phenotype indicated a loss of sister centromere cohesion rather than a defect of centromere pairing.

Increased numbers of centromeres per nucleus compared to the control ($p < 0.0001$) were also observed in the CENP-A RNAi knockdown at prometaphase/metaphase I. However after the first meiotic division, during interphase, no difference ($p = 0.366$) in centromere number between controls (average 3.63) and CENP-A RNAi knockdowns (average 3.74) were observed (figure 3.2).

Analysis of cell division dynamics by staining tissues for DNA, TUBULIN and centromeric markers (CENP-A and CENP-C) revealed uneven segregations and DNA bridge formation at anaphase I and II (not shown). This is in line with what was previously described by Dunleavy *et al.*, 2012.

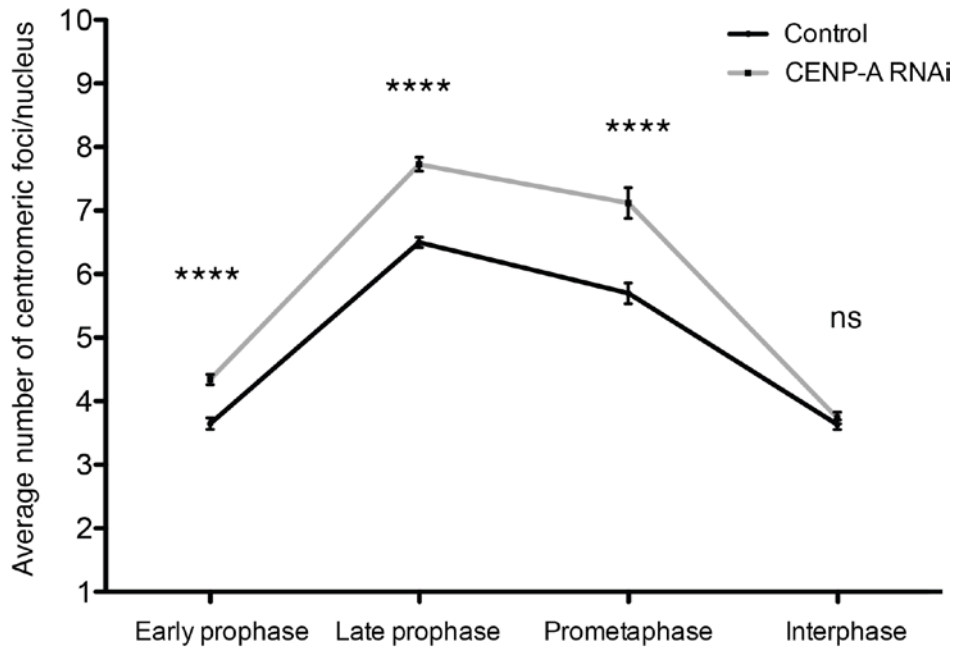


Figure 3.2 A quantification of the average number of centromeric foci per nucleus in control (isogenic) versus CENP-A RNAi. The graph represents the average number of centromeric foci per nucleus at early (S1/S2a) and late (S5/S6) prophase I, prometaphase and interphase in control and CENP-A RNAi lines. n=100 nuclei for each cell stage, error bars represent the standard error of the mean, **** p<0.0001 and ns is a p>0.05.

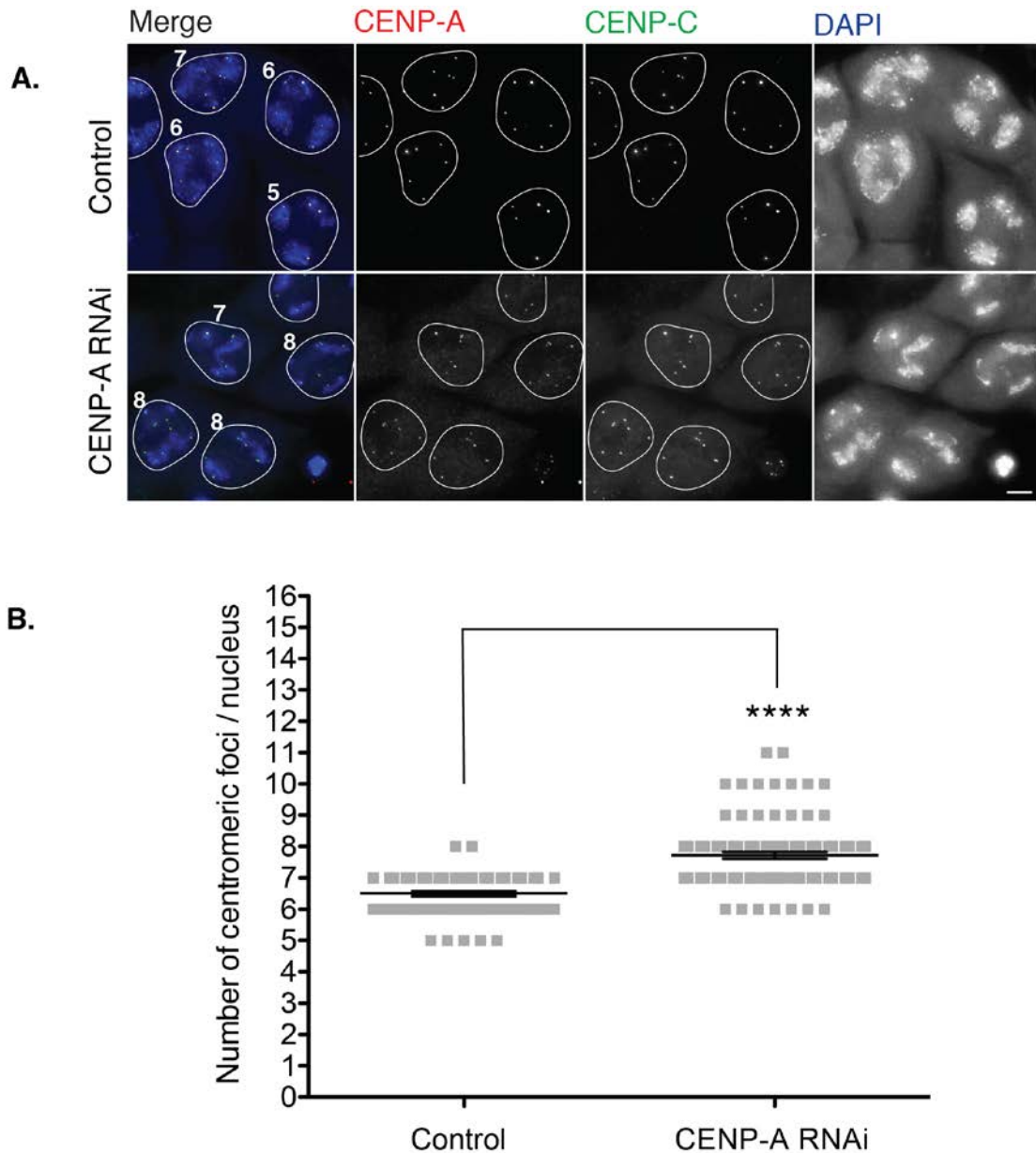


Figure 3.3 Centromeric foci assay at late prophase I in the control versus CENP-A RNAi. (A) Representative image of late prophase I nuclei immunostained for CENP-A (red), CENP-C (green) and DNA (blue). The scale-bar represents 10 μ m, nuclear membranes are indicated (white circle) and the number of centromeres per nucleus is illustrated. (B) Quantification of the number of centromeric foci per nucleus (n=100 nuclei) in control versus CENP-A RNAi. **** p <0.0001, line and error bars represent the mean and standard error of the mean respectively.

3.2.2 Analysis of arm cohesion in CENP-A RNAi knockdowns

To determine if the observed cohesion defect was global or limited to centromeric regions other known sites of meiotic cohesion were analysed using FISH. The 1.686 g/cm³ satellite is a heterochromatic region located on the arms of the 2nd and 3rd chromosomes, it is a known site of strong cohesion retention through meiosis I (Tsai *et al.*, 2011). At late prophase I in control nuclei, between 3 and 4 1.686 g/cm³ foci are observed per nucleus, one spot representing each of the 2nd and 3rd chromosome homologues in which cohesion at this site is intact. Upon RNAi knockdown of CENP-A, no significant difference (p=0.553) in the number of 1.686 g/cm³ foci per nucleus was observed (figure 3.4).

The AATAT repeat, located on chromosome 4R is a known site of 4th chromosome pairing and cohesion throughout meiosis I (Tsai *et al.*, 2011). In control nuclei, a single focus was observed 57.89 % and two closely located (<5 µm) foci were observed 31.57 % of the time, indicating that in the majority (approximately 90 %) of nuclei at late prophase I the homologous 4th chromosomes are paired in a single DNA territory. Of the remainder, 8.77 % of nuclei displayed a diffuse AATAT focus representing cells in which the AATAT focus is not fully condensed or organised and 1.75 % of cells had two AATAT foci that were located > 5 µm apart, indicating a disruption in cohesion and/or pairing. In the CENP-A RNAi knockdown, no difference in the pattern of AATAT foci was observed at late prophase I indicating that 4th chromosome arm pairing and/or cohesion was not disrupted (figure 3.5).

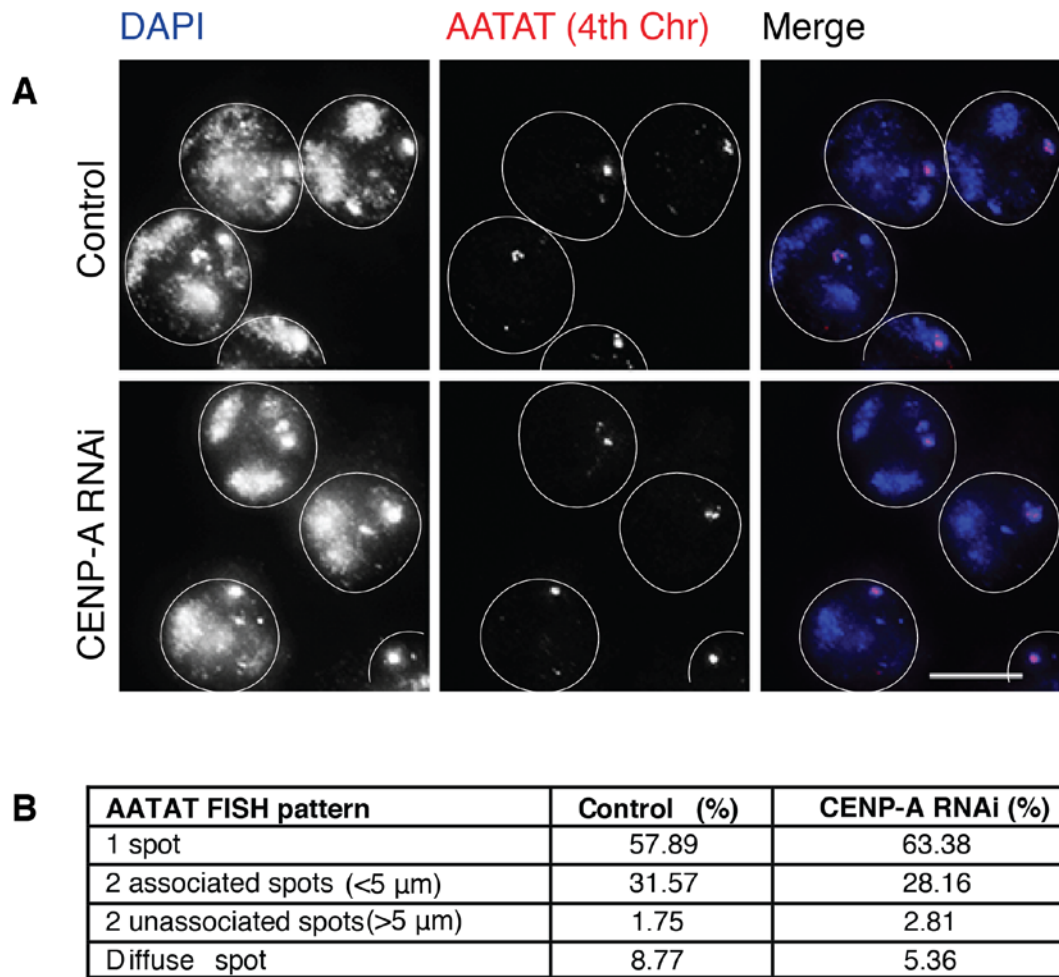


Figure 3.5 FISH at the AATAT satellite repeat of late prophase I nuclei in controls and CENP-A RNAi. (A) Representative image of AATAT loci (red) in DNA stained (blue) late prophase I nuclei. The scale-bar represents 10 μ m and the nuclear membrane is outlined (white circle). (B) A quantification of the percentage of nuclei with a single, two closely associated (< 5 μ m apart), two unassociated (>5 μ m) or diffuse AATAT focus in the control versus CENP-A RNAi.

3.3. Analysis of the role of the CENP-A N-terminus during male meiosis

As discussed in section 1.3, the N-terminus of CENP-A contains three amino acid sequence blocks, which are well conserved in Drosophilid species (Malik *et al.*, 2002) (schematic: figure 3.6 p.89). Block B3 (amino acids 119-124; RRRKAA) is an arginine rich motif located adjacent to the histone core domain of the protein, it is required for centromeric recruitment of the spindle assembly checkpoint protein BUBR1 (Torrás-Llort *et al.*, 2010). The function of conserved sequence blocks B1 (amino acids 22-64) and B2 (75-92) are unknown. The N-terminus of CENP-A in plant species also contains several conserved sequence blocks of relatively unknown function (Maheshwari *et al.*, 2015). Studies in *Arabidopsis thaliana* have shown that the CENP-A N-terminus is required for centromeric recruitment of CENP-A in meiosis, this is in contrast to what has been shown for mitotic centromeric recruitment in plants (Ravi *et al.*, 2011b). Thus, we hypothesised that in *Drosophila* the CENP-A N-terminus may have a similar function.

To study the role of the CENP-A N-terminus, a transgenic fly line expressing an N-terminally tagged GFP-CENP-A lacking its first 118 amino acids (GFP-CENP-A- Δ 118) was produced (figure 3.6 A). As control for this N-terminally deleted construct a transgenic fly line expressing full length GFP-CENP-A was used. GFP-CENP-A-FL (full-length) was tagged internally between amino acids 118 and 119 (figure 3.6 A) and its functionality was previously confirmed by an *in vivo* complementation test for viability (Schuh *et al.*, 2007). Previous *in vivo* studies using this GFP-CENP-A-FL construct have shown that GFP-CENP-A-FL is recruited to centromeres during late telophase/early G1 phase of the cell cycle in mitotic cells and in neural stem cells (Dunleavy *et al.*, 2012) and that GFP-CENP-A-FL is recruited to the centromere in male meiosis during prophase I (Dunleavy *et al.*, 2012; Raychaudhuri *et al.*, 2012).

Prior to generation of transgenic fly lines, localisation of GFP-CENP-A- Δ 118 was determined in WT *Drosophila* cultured (S2) cells. After transient transfection, GFP-CENP-A- Δ 118 was observed at the mitotic centromere (confirmed by co-localisation with anti-CENP-C antibody) (figure 3.6 B) In addition, GFP-CENP-A- Δ 118 signal was also observed throughout the nucleoplasm and the cytoplasm. It is possible that this mis-localisation of GFP-CENP-A- Δ 118 is related to the absence of its N-terminus and/or it maybe as a result of overexpression of the construct in this system. To study GFP-CENP-A- Δ 118 localisation *in vivo* during mitosis and meiosis the *gfp-cenp-a- Δ 118* transgene was placed under the control of the endogenous *cenp-a* promoter and the construct was incorporated into the genome of WT (*w¹¹¹⁸*) embryos (transformation by Bestgene Inc.). Expression and localisation of GFP-CENP-A- Δ 118 was confirmed in the adult germ-line by immuno-staining for GFP and the centromeric marker CENP-C (figure 3.7).

In controls, GFP-CENP-A-FL was detected co-locating with CENP-C at mitotic and meiotic centromeres throughout the germ-line, as expected. GFP-CENP-A- Δ 118 was observed at mitotic centromeres in the germ-line. Co-localisation with CENP-C was observed in the somatic cells of the testis (identified by position at the external epithelium of the testis), in the germ-line stem cells (identified by proximity to the regulatory cells of the hub) and the early spermatogonia (figure 3.7). In meiotic cells from early to late prophase I, GFP-CENP-A- Δ 118 was also present at centromeres (figure 3.8)

Localisation of GFP-CENP-A-FL and GFP-CENP-A- Δ 118 in the germ-line was compared to that of WT CENP-A by immuno-staining with anti-CENP-A antibodies. In addition to centromeric foci both GFP-CENP-A-FL and GFP-CENP-A- Δ 118 localise throughout the nucleus in early and late prophase I nuclei and in the cytoplasm at early prophase I (figure 3.8). This mis-localisation of GFP-CENP-A-FL and GFP-CENP-A- Δ 118 maybe related to the presence of the large fluorescent GFP-tag, which may effect centromeric localisation. It is also possible that the mis-localisation is due to an over-

expression of CENP-A in these flies, which also express two functional copies of WT *cenp-a*.

A quantification of the recruitment of endogenous CENP-A to the centromere during meiosis prophase I was carried out by immuno-staining for CENP-A and then determining the CTCF of centromeric foci per nucleus (figure 3.9). In WT ($y+ry+$) prophase I nuclei a 46 % increase in the level of centromeric CENP-A (per nucleus) was observed and in GFP-CENP-A-FL controls, a 32 % increase in centromeric levels of CENP-A per nucleus was observed between early and late prophase I. This is in line with the previously observed timing of CENP-A recruitment during meiosis (Dunleavy *et al.*, 2012; Raychaudhuri *et al.*, 2012). A 13 % increase in centromeric levels of GFP-CENP-A- Δ 118 was observed from early to late prophase I, indicating that GFP-CENP-A lacking its N-terminal tail can be recruited to the meiotic centromere, albeit at a lower level than what was observed for the full length GFP-CENP-A protein (figure 3.9).

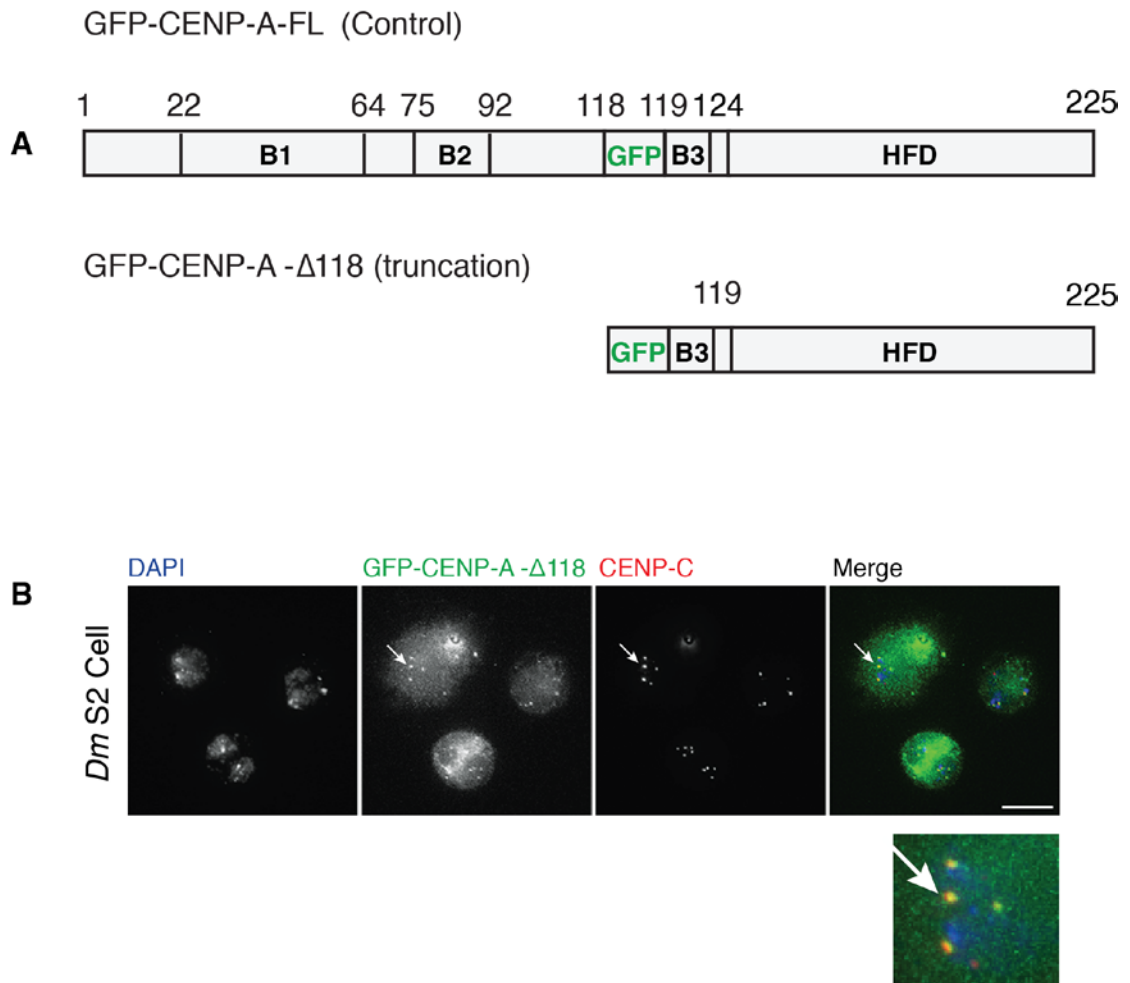


Figure 3.6 Localisation of GFP-CENP-A- Δ 118 in *Drosophila* S2 cells. (A) A schematic illustrating the organisation of GFP-CENP-A-FL (control) and GFP-CENP-A- Δ 118 (truncation). The location of conserved N-terminal sequence blocks B1, B2 and B3 are indicated as well as the position of the GFP flourophore (between amino acids 118 and 119). Location of the Δ 118 truncation is also indicated. (B) *Drosophila* S2 cells after transient transfection of GFP-CENP-A- Δ 118 (green) and co-stained with an anti-CENP-C antibody (red) and DAPI (blue). Co-localisation of GFP-CENP-A- Δ 118 and CENP-C are indicated (arrow) and highlighted. The scale-bar represents 10 μ m.

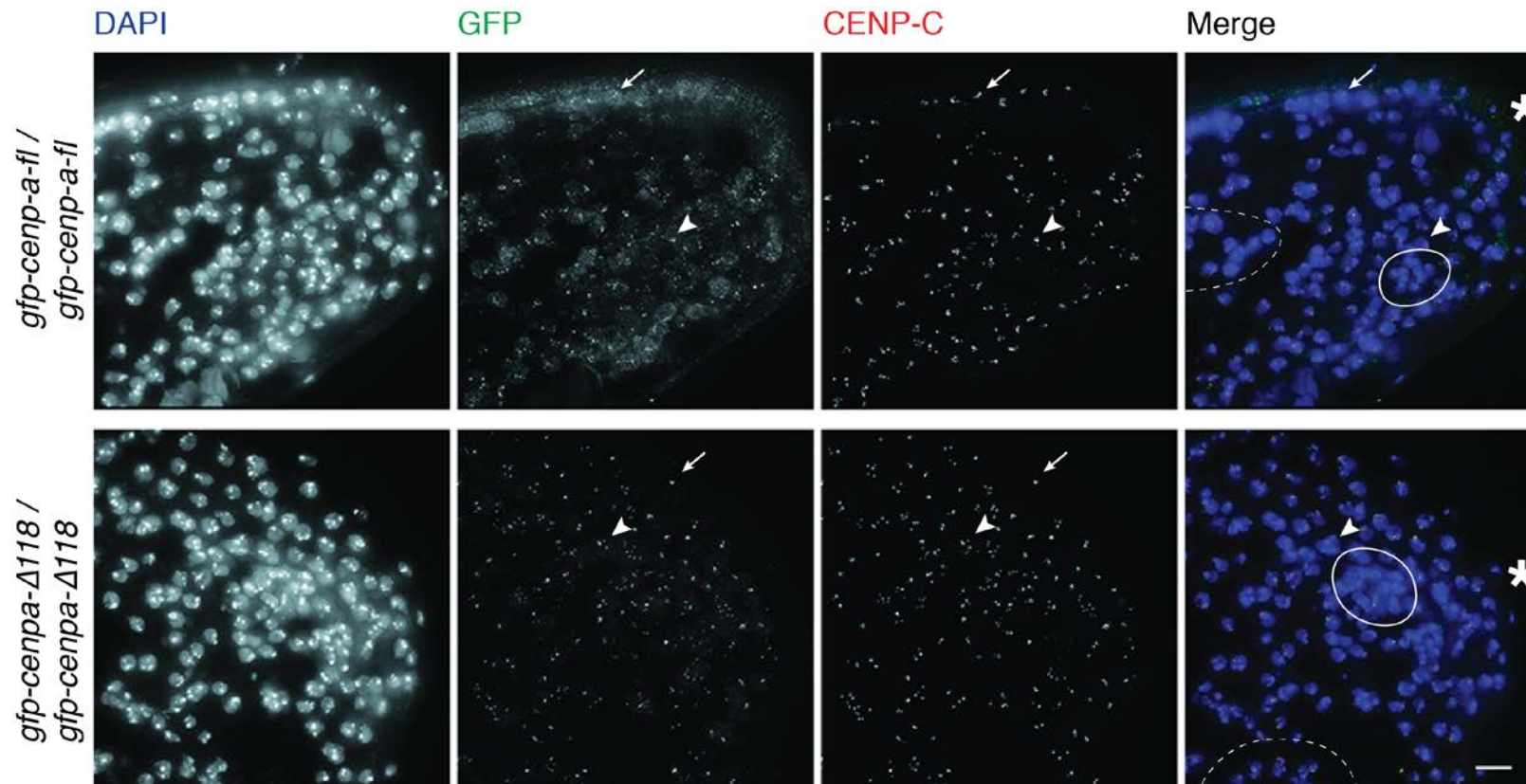


Figure 3.7 Localisation of GFP-CENP-A-FL and GFP-CENP-A- Δ 118 at centromeres by immunostaining for GFP (green), CENP-C (red) and DNA (blue) in adult testes. The apex of the testis is indicated (asterix) as are the hub cells adjacent to the germ-line stem cells (white circle). Co-localisation of GFP-CENP-A-FL and GFP-CENP-A- Δ 118 with CENP-C in somatic cells (arrow), germ-line stem cells (arrowhead) and secondary spermatocytes (dashed circle) are indicated. The scale-bar represents 10 μ m.

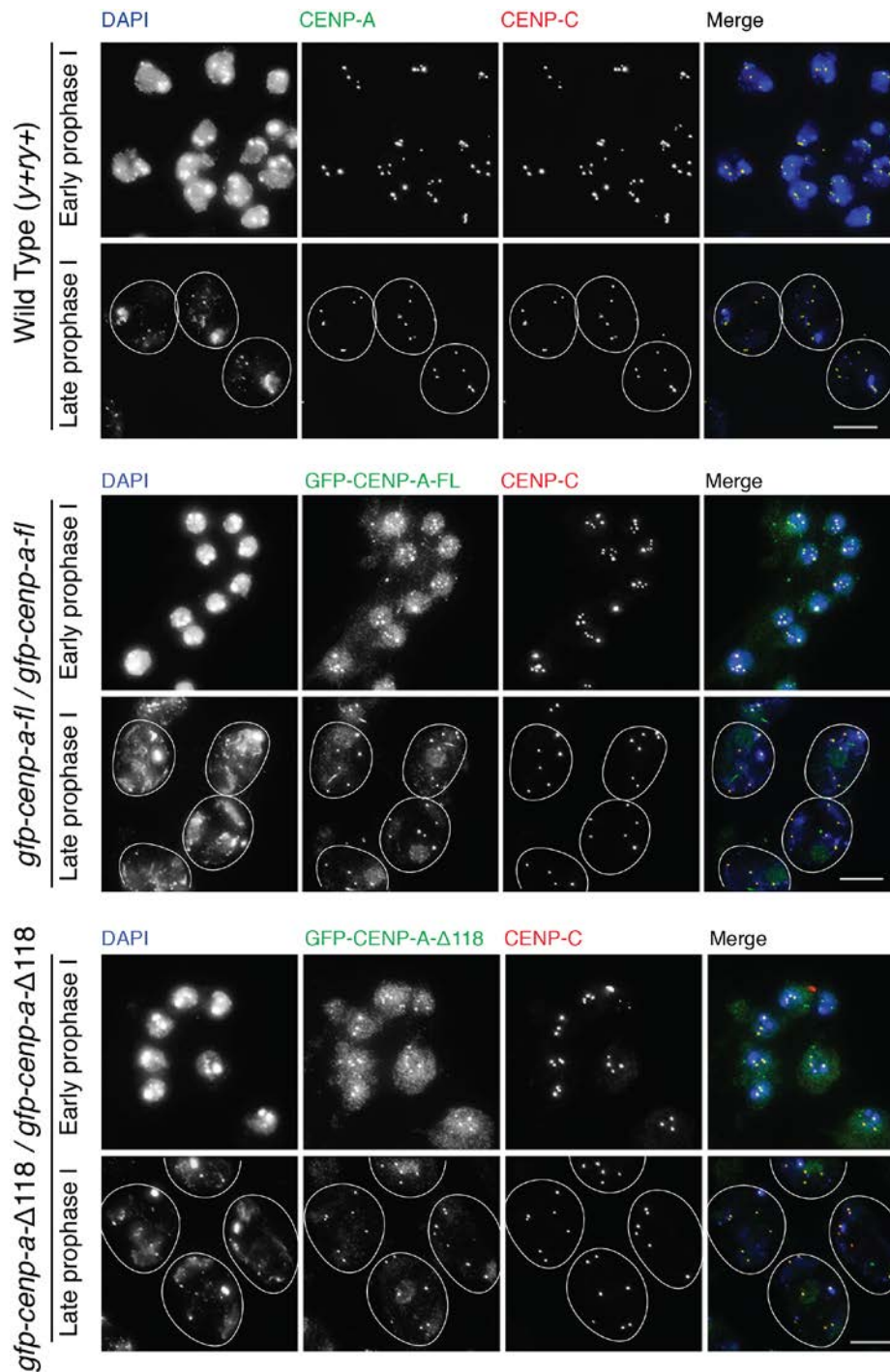


Figure 3.8 Localisation of endogenous CENP-A (anti-CENP-A antibody; green) and GFP-CENP-A-FL and GFP-CENP-A-Δ118 (anti-GFP antibody; green) in early and late meiotic prophase I nuclei. Localisation at centromeres is indicated by immuno-staining for CENP-C (red), DNA is stained with DAPI (blue). The scale-bar represents 10 μm and the nuclear membrane of late prophase I nuclei are indicated (white circle).

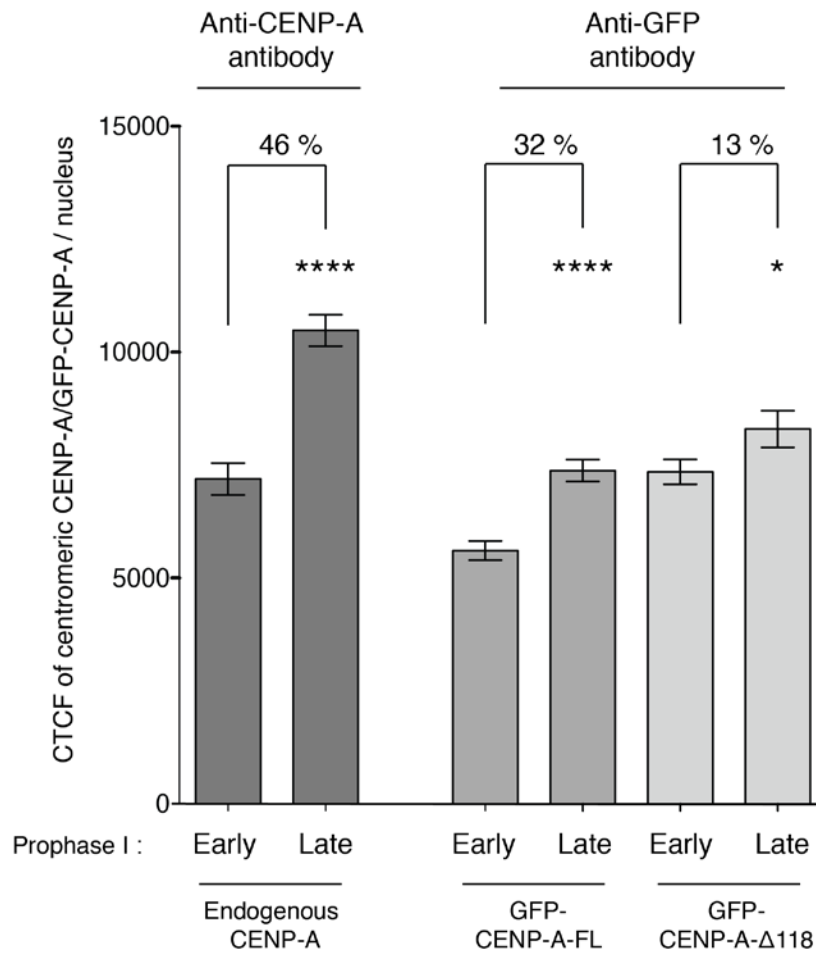


Figure 3.9 A quantification of the CTCF of CENP-A, GFP-CENP-A-FL and GFP-CENP-A-Δ118 at centromeric foci in early and late prophase I nuclei. Error bars represent the standard error of the mean. **** $p < 0.0001$, * $p < 0.05$ and the relative percentage increase in centromeric intensity between early and late prophase I is indicated.

3.4. Identification of novel meiotic CENP-A interacting proteins

The third method employed to identify novel functions of the CENP-A N-terminus during meiosis involved identifying novel interactors of CENP-A. To do this, two independent 'pull-down' experiments were carried out (figure 3.10 A). In 'Experiment 1' GFP-CENP-A-FL was pulled-down from transgenic *gfp-cenp-a-fl* adult testes protein extracts. In 'Experiment 2' proteins interacting specifically with the CENP-A N-terminus were pulled-down from WT (*y+ry+*) adult testes protein extracts using a recombinantly produced CENP-A N-terminal peptide (amino acids 1 – 126) as bait.

For both experiments, precipitated proteins were analysed by SDS-PAGE and gels were silver stained to confirm precipitation of bait and control proteins (figure 3.12 B and C). Co-precipitated proteins, specific to the bait pull-down were identified by nano LC-MS/MS.

In Experiment 1 a total of 28 specific interactors were identified in either cytoplasmic or nucleoplasmic protein pools (appendix 8.8 p.233)(MS analysis performed in the laboratory of Dr. Axel Imhof by Marc Borath and Ignasi Forne). Disappointingly, no well-known CENP-A interacting proteins (such as histone H4, CENP-C or CAL1) were detected and the relative abundance of other proteins pulled down was quite low suggesting that in this instance pull-down using the GFP-Trap® bead system was not very efficient. It is possible that this was due to the internal location of GFP fluorescent protein on GFP-CENP-A-FL. Despite this a number of peptides were pulled down in this experiment, which were also pulled down in Experiment 2.

Analysis of proteins precipitated in Experiment 2 identified a total of 201 specific interactors (appendix 8.9 p.237)(MS analysis performed by the proteomics facility at the University of Bristol, Dr. Kate Heesom). A small number of known CENP-A interacting proteins were found to precipitate with our recombinant CENP-A N-terminal peptide, namely the nucleosomal

binding partner of CENP-A, histone H4 (6 peptides) and the chromatin remodeling protein CAF-1 (1 peptide). However we did not detect commonly identified CENP-A interactors such as CENP-C or CAL1 amongst the precipitated proteins likely due to the fact that these proteins interact with the histone core and C-terminal domains of CENP-A.

Interestingly, proteins identified in both pull-down experiments as potential germ-line CENP-A interactors were members of the mitochondrial ATP synthase F₁ complex. In Experiment 1 (GFP-CENP-A-FL as bait) 2 peptides of ATPsyn- α and 7 peptides of ATPsyn- β were detected. In Experiment 2 (CENP-A N-terminal peptide as bait) a total of 9 peptides of ATPsyn- α , 1 peptide of ATPsyn- β and 10 peptides of the ATPsyn- γ subunit were detected.

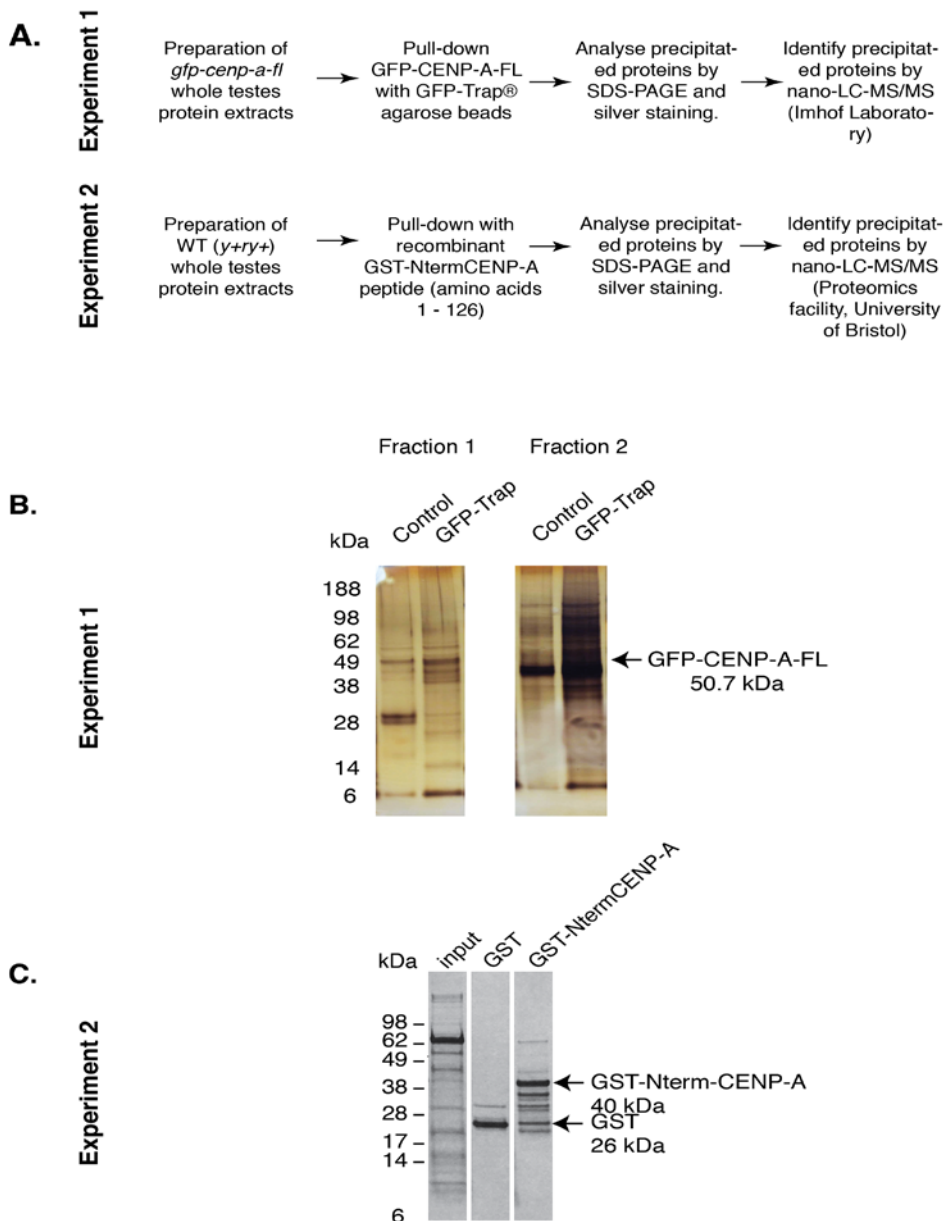


Figure 3.10 Precipitation of novel CENP-A interacting proteins from *Drosophila* adult testes protein extracts. (A) A workflow representing the steps involved in purification of GFP-CENP-A-FL (Experiment 1) and GST-CENP-A N-terminus (amino acids 1-126) (Experiment 2) from adult testes protein extracts and subsequent identification of co-precipitating proteins. (B) A silver stained SDS-PAGE gel containing proteins precipitated in combination with GFP-CENP-A-FL. Fraction 1 contains proteins precipitated from cytoplasmic protein extract and Fraction 2 contains proteins precipitated from nucleoplasmic protein extracts. (C) A silver stained SDS-PAGE gel containing proteins precipitated in combination with GST-CENP-A N-terminus (amino acids 1-126).

3.5. Summary

A summary of the major results presented in chapter 3:

1. A 30 % reduction in centromeric CENP-A levels disrupts sister centromere cohesion throughout meiosis prophase I.
2. An N-terminally truncated GFP-CENP-A, lacking its first 118 amino acids is recruited to both mitotic and meiotic centromeres *in vivo*.
3. In the testes, both GFP-CENP-A-FL and a GST-CENP-A N-terminal peptide (amino acids 1-126) interact with components of the mitochondrial ATP synthase F₁ complex.

3.6. Discussion

3.6.1 Novel roles for CENP-A in the germ-line

After RNAi knockdown of *cenp-a* expression in the germ-line, we have detected a 30 % reduction in the centromeric levels of CENP-A at late prophase I. Considering that pre-existing CENP-A nucleosomes at the centromere must be diluted out by distribution to daughter centromeres during DNA replication (Jansen *et al.*, 2007; Dunleavy *et al.*, 2011) this relatively modest reduction in CENP-A levels is as expected. Thus the 30 % reduction that we have observed here is likely due to a failure to recruit new CENP-A to the centromere during the meiotic prophase I loading phase. Indeed this is consistent with the 36 % increase in CENP-A levels that we have detected during WT (*y+ry+*) prophase I CENP-A loading.

Here we have identified for the first time an unexpected role for CENP-A in sister centromere cohesion establishment and maintenance during male meiosis. A defect of centromeric cohesion was observed from early prophase I, the stage immediately following pre-meiotic replication and the laying down of chromatid cohesion suggesting that CENP-A is required for the establishment of centromeric cohesion. In addition, the defect of

centromeric cohesion was observed through prophase I until prometaphase I indicating that correct levels of CENP-A at the centromere are also required to maintain centromeric cohesion during this window.

In the CENP-A RNAi knockdown a centromeric cohesion defect was not observed during interphase. It is possible that as expression of the *bam-Gal4* driver is switched off by this stage that a recovery in centromeric CENP-A levels may have occurred. However, centromeric recruitment of CENP-A between the end of prometaphase I and meiotic exit was not detected in previous studies (Dunleavy *et al.*, 2012; Raychaudhuri *et al.*, 2012). Sister chromatid cohesion in male *Drosophila melanogaster* is not very well understood process (McKee *et al.*, 2012). Although a number of *Drosophila* specific cohesion proteins which act late in meiosis have been identified, it is possible that these proteins may compensate for reduced levels of CENP-A at centromeres during interphase.

MEI-S332, the *Drosophila* homologue of SHUGOSHIN localises to centromeric and pericentromeric regions during prometaphase and metaphase in both meiosis and mitosis. In meiosis, MEI-S332 is required to prevent premature cleavage of sister centromere cohesion prior to metaphase II (Kerrebrock *et al.*, 1995) and previous studies in *Drosophila* embryonic mitoses have identified that CENP-A is required for the correct centromeric localisation of MEI-S332 (Blower *et al.*, 2001). It is likely that the centromeric cohesion defect observed here upon RNAi knockdown of CENP-A in the germ-line is related to disruption of MEI-S332 localisation and the protection of centromeric cohesion.

Previously observed Meiosis I and II segregation defects in CENP-A RNAi knockdowns were attributed to reduced CENP-C levels and an inability to efficiently recruit the kinetochore (Dunleavy *et al.*, 2012; Kwenda *et al.*, 2016a). It is likely that the centromeric cohesion defects observed here also contribute to these segregation defects, particularly at anaphase II.

3.6.2 A meiosis specific role for the CENP-A N-terminus

Previous studies in plants have shown that the N-terminus of CENP-A is required for its centromeric localisation and recruitment during meiosis, but not mitosis (Ravi *et al.*, 2011b). By generation of transgenic flies expressing an N-terminally truncated version of GFP-CENP-A we have determined that as is the case with Arabidopsis, the N-terminus of CENP-A is not required for centromeric recruitment in mitosis. However in contrast to plants, our preliminary data suggests that the CENP-A N-terminus is dispensable for centromeric recruitment during meiosis in *Drosophila*. In GFP-CENP-A-FL control we observed a 32 % increase in the level of CENP-A at the centromere from early to late prophase I however, in the GFP-CENP-A- Δ 118 line we only observed a 13 % increase in centromeric levels. The expression levels of GFP-CENP-A-FL and GFP-CENP-A- Δ 118 in control and mutant transgenic lines have not been compared in these experiments and thus it is difficult to make any direct comparisons between these two fly lines. Furthermore, both GFP-CENP-A-FL and GFP-CENP-A- Δ 118 express WT copies of *cenp-a* and in the context of an overexpression, centromeric localisation and loading and the role of the N-terminus is difficult to interpret. Several modifications to these experiments and future perspectives are discussed in chapter 6.

Originally, we hypothesised that the CENP-A N-terminus is required for loading of CENP-A to the centromere in meiosis in flies. This was based on the idea that CENP-A loads to the meiotic centromere at a distinct cell cycle stage (late telophase/early G1 in mitosis versus prophase I in meiosis), and that its recruitment occurs at a time when centromeric levels its chaperone protein (CAL1) are reducing (Dunleavy *et al.*, 2012). Furthermore, our hypothesis was based on the observation that in plants the N-terminus of CENP-A is specifically required to load CENP-A to the meiotic centromere (Ravi *et al.*, 2011a). Despite the caveats to our analysis of CENP-A loading during meiosis, our preliminary data appears to disprove this hypothesis.

Recently, Kwenda *et al.*, 2016 have shown that as is the case with mitosis CAL1 and CENP-C are required for localisation of CENP-A to the centromere during meiosis. These results indicate that the molecular chaperones involved in CENP-A assembly during meiosis do not differ from mitosis. Both CAL1 and CENP-C interact with the CATD and C-terminus of CENP-A in flies perhaps allowing efficient recruitment of a CENP-A construct lacking its N-terminus. Recent evidence from the Dunleavy laboratory suggests that it is not alternative recruitment of CENP-A that mediates assembly during meiotic prophase I but alternative cell cycle regulation of its chaperones (Kwenda and Dunleavy, unpublished)

3.6.3 Novel CENP-A protein interactors in the germ-line.

We have identified components of the ATP synthase F₁ complex as potential CENP-A interactors in both of our pull-down and nano LC-MS/MS experiments. No previous links between CENP-A and these mitochondrial proteins have been indicated in the literature. However, interestingly, recent evidence suggests that these subunits may function in the germ-lines of both male and female *Drosophalids* independently of their mitochondrial role in ATP synthesis (Teixeira *et al.*, 2015; Sanchez *et al.*, 2016; Sawyer *et al.*, 2017). Furthermore, both ATPsyn- α (Castrillon *et al.*, 1993) and ATPsyn- β (Wen *et al.*, 2015) have been previously linked to male fertility in the fruit-fly (discussed 1.11.1 p.49).

In chapters 4 and 5 we present a characterisation of the role of a number of ATP synthase F₁ subunits in the male germ-line after RNAi knockdown and we provide evidence for a functional interaction between these mitochondrial subunits and CENP-A.

**4. A characterisation of the role of ATP synthase F₁
subunits in the male germ-line of *Drosophila
melanogaster***

4.1. Chapter Introduction

As discussed in chapter 3, two proteins (ATPsyn- α and ATPsyn- β) were identified as potential germ-line CENP-A interactors in both of our independent pull-down and mass spectrometry experiments. ATPsyn- γ was identified in one experiment. ATPsyn- α , - β and - γ form part of the F₁ catalytic subunit of the mitochondrial ATP synthase and no previous functional links have been identified between these subunits and any centromeric components. Several links have been made however between these subunits and fertility in *Drosophila melanogaster*. Firstly, a male sterile allele of *ATPsyn- α* (*bellwether*) was identified as part of a large scale P element mutagenesis screen (Castrillon *et al.*, 1993). More recently, it has been shown that ATPsyn- α is essential for fertility due to a role in higher order mitochondrial organisation within the inner mitochondrial membrane in both the male (Sawyer *et al.*, 2017) and female (Teixeira *et al.*, 2015) germ-lines. ATPsyn- β has also been implicated in male fertility where its expression has been shown to be tightly regulated in the testis by an endogenous RNAi hairpin pathway. De-repression of ATPsyn- β expression results in male sterility (Wen *et al.*, 2015).

In addition to the commonality between our two pull-down experiments and the links to male fertility our rationale for choosing ATPsyn- α , - β and - γ for further study was also influenced by a previous genetic screen carried out in the Dunleavy laboratory. As part of this study, meiotic progression was characterised in a number of male sterile mutant fly lines; one of which harbored a transposable element insertion in the gene *ms(3)72dt*. *Ms(3)72dt*, also known as '*ATPsyn- β like*' is a paralogue of the canonical *ATPsyn- β* gene, it has been previously linked to male fertility (Castrillon *et al.*, 1993). Immunofluorescence microscopy (anti-CENP-A and anti-TUBULIN antibody staining) carried out as part of this screen identified segregation defects at meiosis I and II (Dr. Elaine Dunleavy, unpublished).

Thus, we aimed to identify the role of ATP synthase subunits ATPsyn- α , - β and - γ , as well as ATPsyn- β like during meiosis in *Drosophila* males. In this chapter we present the results from 1) A bioinformatic and molecular characterisation of *ATPsyn- β like* and 2) A characterisation of the meiotic phenotype after RNAi knockdown of ATPsyn- α , - β , - β like and - γ .

4.2. Characterisation of the gene *ATPsyn- β like*

As discussed, *ATPsyn- β like* (chromosome 3L) is a paralogue of the canonical and highly conserved *ATPsyn- β* (chromosome 4) gene, which likely arose due to a gene duplication. To determine when this duplication event may have occurred and to determine the range of different species in which *ATPsyn- β like* is present; a homology search was carried out. Using the protein sequence of canonical ATPsyn- β , BLAST searches were carried out on specific species and/or clades to determine if *ATPsyn- β like* was present. Using this method, *ATPsyn- β like* was identified in many species of higher Dipterans including both groups of fruit flies (*Drosophilidae* and *Tephritidae*) as well as the house and stable flies (figure 4.1). *ATPsyn- β like* was not identified when carrying out similar searches on lower Dipterans such as the mosquito species *Culex quinquefasciatus* (Southern house mosquito), *Anophyles gambiae* (Malaria mosquito) or *Aedes albopictus* (Asian tiger mosquito). Unexpectedly, considering the absence of *ATPsyn- β like* in lower Dipterans, searches carried out on species in the order Lepidoptera (butterflies and moths) identified *ATPsyn- β like* in the silkworm, *Bombyx mori* (figure 4.1). Similar searches carried out on insect species within the orders Hymenoptera (sawflies, bees, wasps and ants) and Coleoptera (beetles) did not identify any *ATPsyn- β like* homologues.

In *Drosophila melanogaster* ATPsyn- β and its paralogue ATPsyn- β like are well conserved, with an amino acid identity of greater than 75 % within the catalytic core and C terminal helix bundles of the protein (figure 4.2) and the amino acids essential for catalytic activity and nucleotide binding in these domains are highly conserved in both paralogues (figure 4.2). ATPsyn- β like

diverges from ATPsyn- β at its N and C-termini which are <10 % conserved. Throughout evolution, from *Drosophila melanogaster* (Diptera) to *Bombyx mori* (Lepidoptera), the N-terminal extension of ATPsyn- β like is relatively well conserved (30 %), however the C-terminal extension present in *Drosophila melanogaster* is not conserved outside of Drosophilidae (figure 4.3).

Using tissue specific RT-PCR and western blotting it was confirmed that *ATPsyn- β like* is expressed in adult *Drosophila* testes; expression was not detected in the adult ovary, larval brain or in *Drosophila* cultured (S2) cells (figure 4.4). This finding is in line with gene expression data available via the modENCODE consortium (Celniker *et al.*, 2009) and as was reported previously (Lindsley *et al.*, 2013). In addition, the ModENCODE consortium has identified by large-scale mRNA-seq analysis that in addition to moderately high expression in the adult testes, ATPsyn- β like is also expressed at a moderate level during the prepupal stage of the fly life-cycle (figure 4.5). *ATPsyn- β like* *-/-* mutants (produced by transposable element insertions) are viable in the larval stage of development and we have identified that they make up <20 % of the total population..However *ATPsyn- β like* *-/-* are not viable as adults as they die during pupation stages.

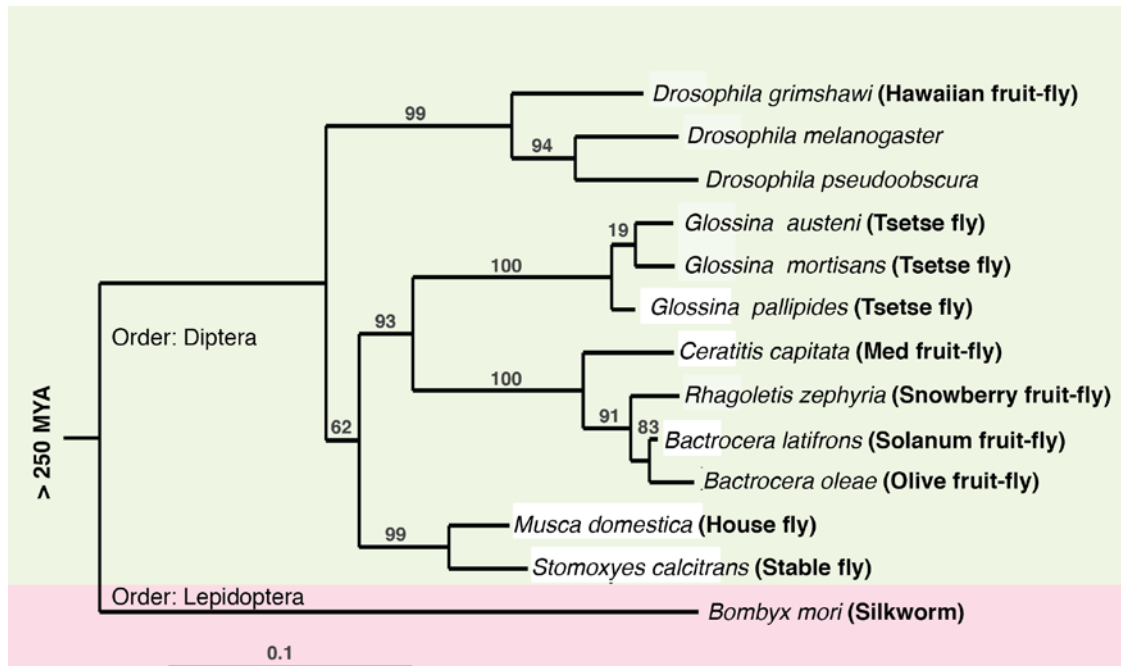


Figure 4.1 Species in which the gene *ATPsyn- β like* was detected. Amino acid sequences were obtained from the NCBI and the alignment was performed using the tool MUSCLE (NCBI). The phylogenetic tree was constructed by Phylogeny.fr using an approximate likelihood ratio test (Anisimova *et al.*, 2006). Node labels are percentages representing branch confidence and the scale bar represents substitutions over time.

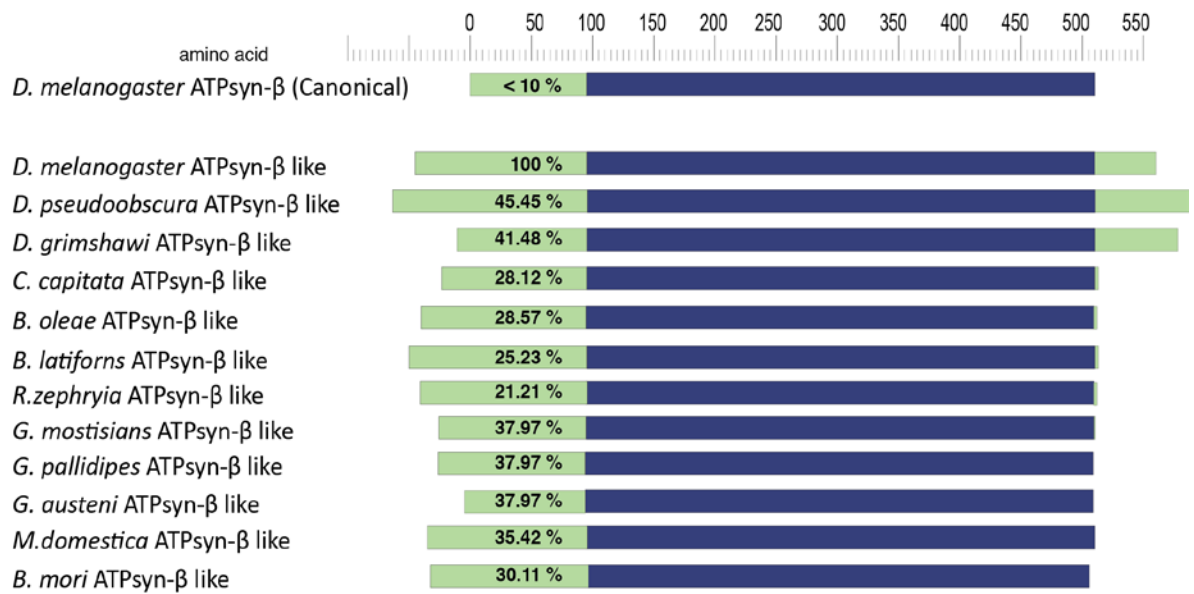


Figure 4.3 Conservation of ATPsyn-βlike from *Drosophila melanogaster* to the silkworm *Bombyx mori*. Alignments and percent identities were calculated using Clustal O (NCBI). Percentages indicate amino acid identity compared to the *Drosophila melanogaster* ATPsyn-βlike amino acids 1-137.

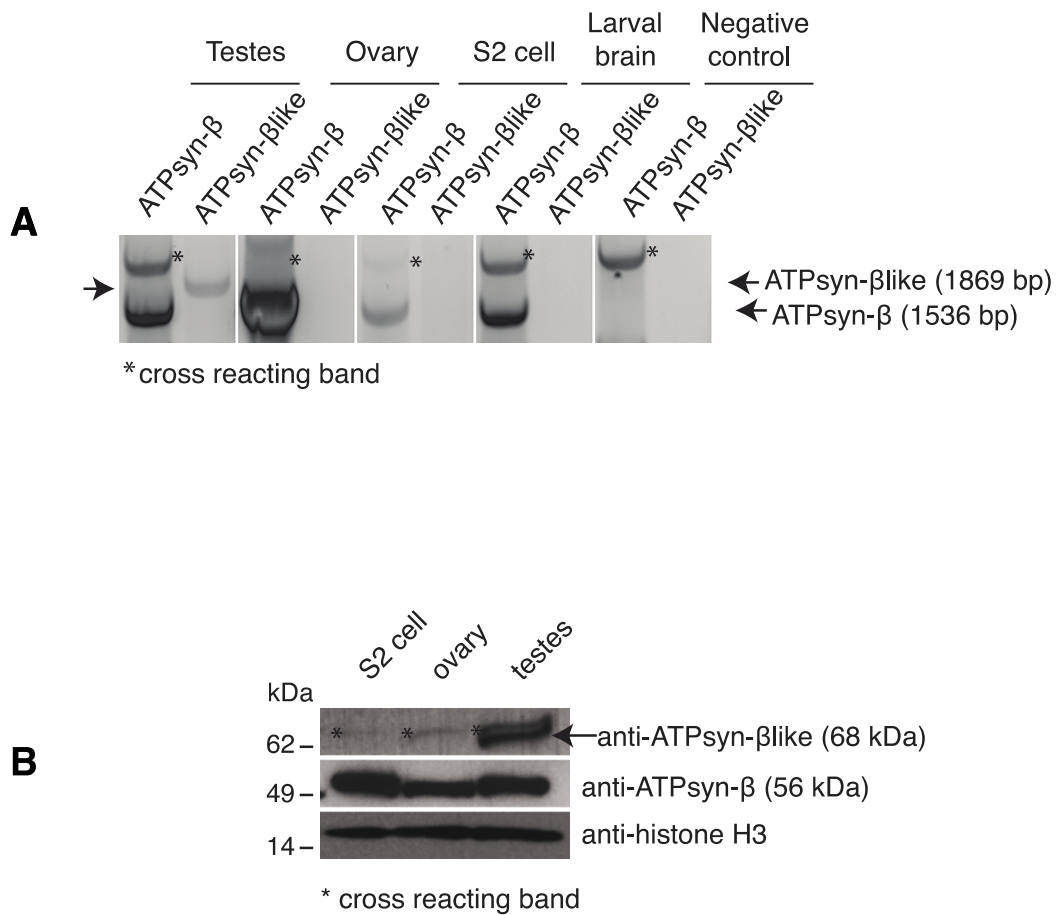


Figure 4.4 Tissue specific expression of ATPsyn- β like. (A) Transcripts of *ATPsyn- β* or *ATPsyn- β like* detected by RT-PCR from adult testes, ovary, S2cell or larval brain DNA extracts. Negative control represents a no template control (B) Expression of *ATPsyn- β* or *ATPsyn- β like* in S2 cell, ovary and testes protein extracts as detected by anti-ATPsyn- β and anti-ATPsyn- β like antibodies. Loading control anti-histone H3.

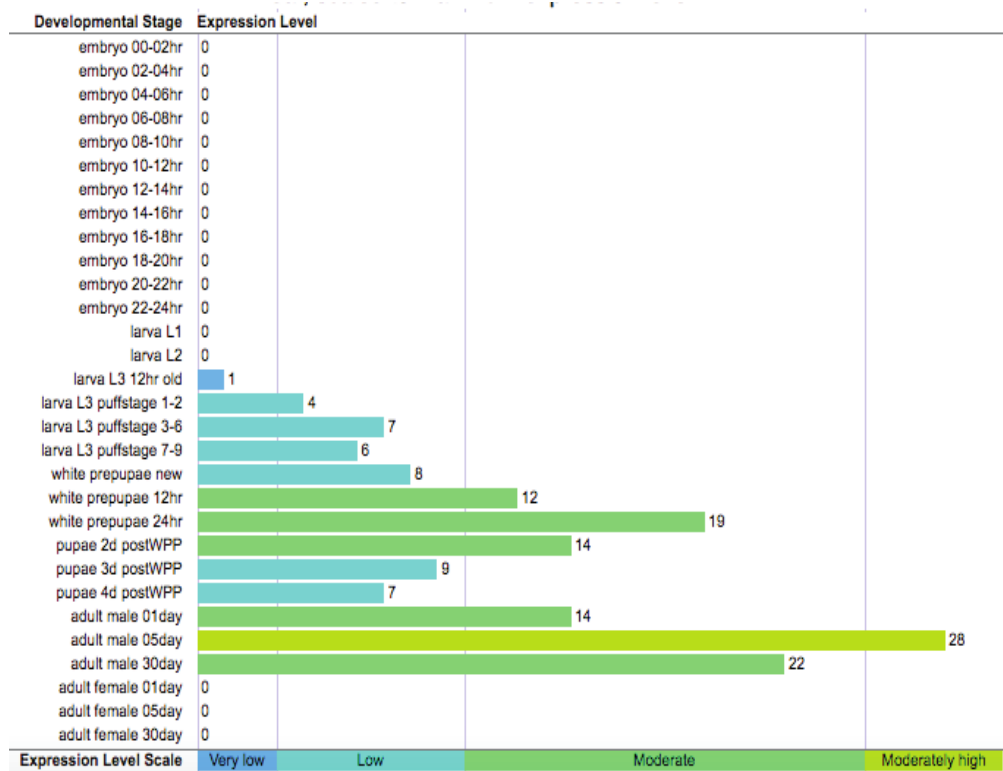


Figure 4.5 Large-scale *ATPsyn- β like* expression data from ModENCODE consortium (Celniker *et al.*, 2009). Data indicates relative expression of *ATPsyn- β like* at different developmental stages and relative expression levels are indicated and colour coded.

4.3. Analysis of meiotic progression in the ATPsyn- α , - β , - β like and - γ RNAi knockdowns

To determine the role of ATPsyn- α , - β and - γ , as well as ATPsyn- β like during male meiosis, testes specific RNAi knockdown of protein expression was carried out using the *bam-Gal4* driver. *Bam-Gal4* expression initiates at the 4-8 cell stage in the secondary spermatocytes and remains activated until late prophase I. Fertility, meiotic progression and centromere dynamics in the germ-line were subsequently analysed. RNAi knockdowns were carried out using two independent UAS-RNAi lines (fly lines are detailed in appendix 8.3) and reduced protein levels were confirmed in meiosis prophase I cells by anti-ATPsyn- α , anti-ATPsyn- β , anti-ATPsyn- β like and anti-ATPsyn- γ immunofluorescence microscopy (figure 4.6).

When crossed to control (WT *y+ry+*) female virgin flies, males with ATPsyn- α , - β like or - γ testes specific RNAi knockdowns were found to be 100 % sterile (figure 4.7). Similar knockdown of canonical ATPsyn- β had no significant effect on male fertility ($p=0.321$). Bright-field imaging of dissected adult testes revealed no striking differences in testes morphology after ATPsyn- α , - β or - γ RNAi knockdowns, however the seminal vesicles of flies with an ATPsyn- β like RNAi knockdown appeared flat and empty and the bundles of sperm tails normally visible within the adult testis were absent (figure 4.8). These changes in morphology indicated that RNAi knockdown of ATPsyn- β like resulted in azoospermia - a failure to produce any sperm.

For the ATPsyn- β like RNAi knockdown, these morphological results were confirmed by assessing meiotic progression (figure 4.9). In ATPsyn- α , - β , - β like and - γ RNAi knockdowns the number of cell cysts between metaphase and telophase of meiosis I and II and the number of cysts of spermatids per testis were quantified. A six-fold reduced number of cells undergoing meiosis I (0.1 cysts per testis) was observed compared to controls (0.6 cysts

per testis) in the ATPsyn- β like RNAi knockdown. In addition, there were no cells undergoing meiosis II and cysts containing spermatids were absent, indicating that a complete meiotic arrest prior to the first meiotic division had occurred.

In the ATPsyn- α and - β RNAi knockdowns meiotic progression did not appear to be affected; the number of cell cysts undergoing meiosis I or II was not significantly reduced and there was no significant difference in the total number of spermatid cysts. In the ATPsyn- γ RNAi knockdown, again there was no significant difference in the number of cysts undergoing meiosis I or II however the total number of spermatid cysts was reduced ($p < 0.01$) from 39.6 cysts per testis in controls to 6.5 cysts per testis in the ATPsyn- γ RNAi knockdown (figure 4.9).

A screen for segregation defects during both meiotic divisions was also carried out by assessing spindle and DNA morphologies by immunofluorescence microscopy and correct homologue segregation at meiosis I using *X* and *Y* chromosome FISH. In the case of the ATPsyn- α and - β RNAi knockdowns no segregation defects were observed by either method. Knockdown of ATPsyn- γ resulted in strong meiosis I and II segregation defects including anaphase bridges and uneven segregation at meiosis I and II (data not shown).

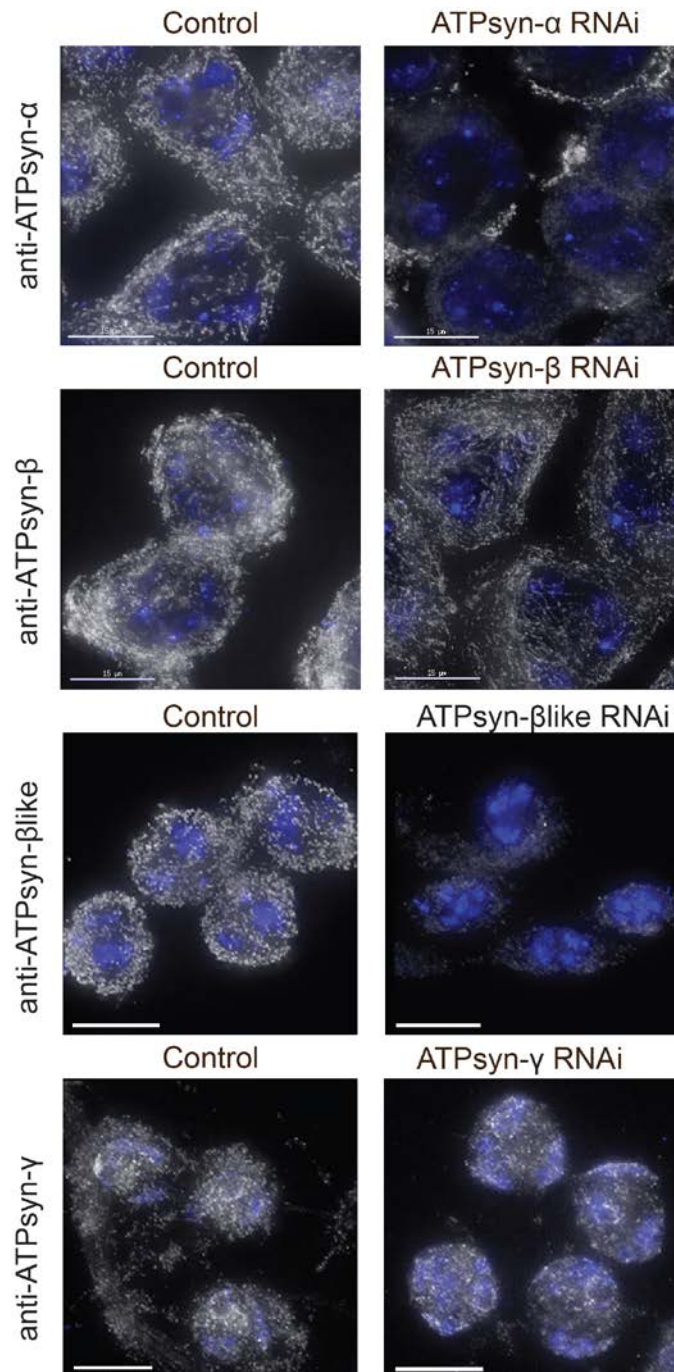


Figure 4.6 Immunofluorescent micrograph indicating expression of ATPsyn- α , - β , - β like and - γ (white) in late prophase I cells of control and RNAi knockdowns. DNA is stained with DAPI (blue) and the scale bar represents 15 μ m. Remaining nuclear signal of ATPsyn- γ after RNAi knockdown may be non-specific binding.

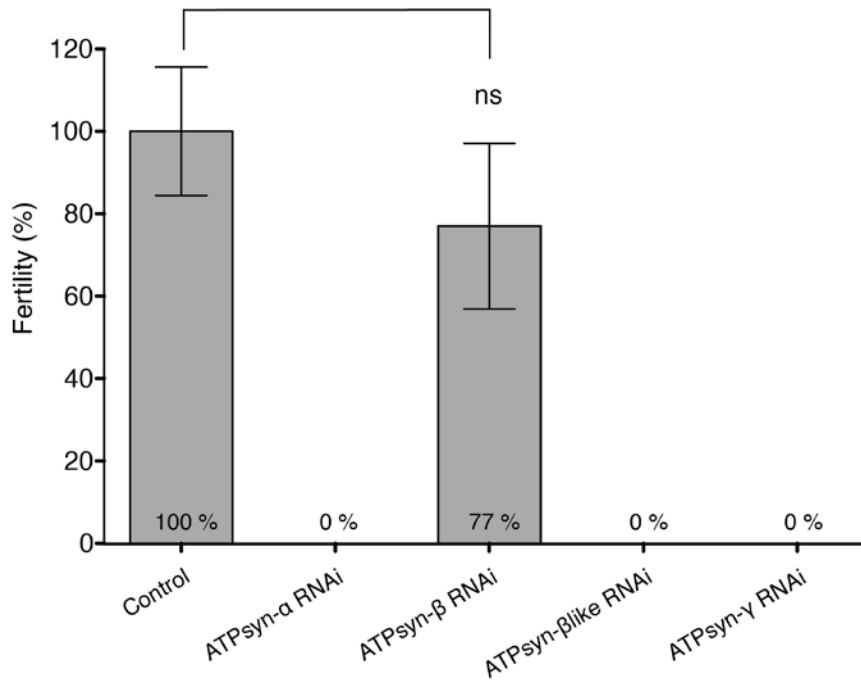


Figure 4.7 Male fertility after RNAi knockdown of ATPsyn- α , - β , - β like and - γ . Fertility is represented as a percentage (indicated) of control (isogenic) fertility, data is pooled from three independent RNAi experiments. Fertility tests were carried out at 25 °C. Error bars represent standard error of the mean, ns $p > 0.05$ was not significant.

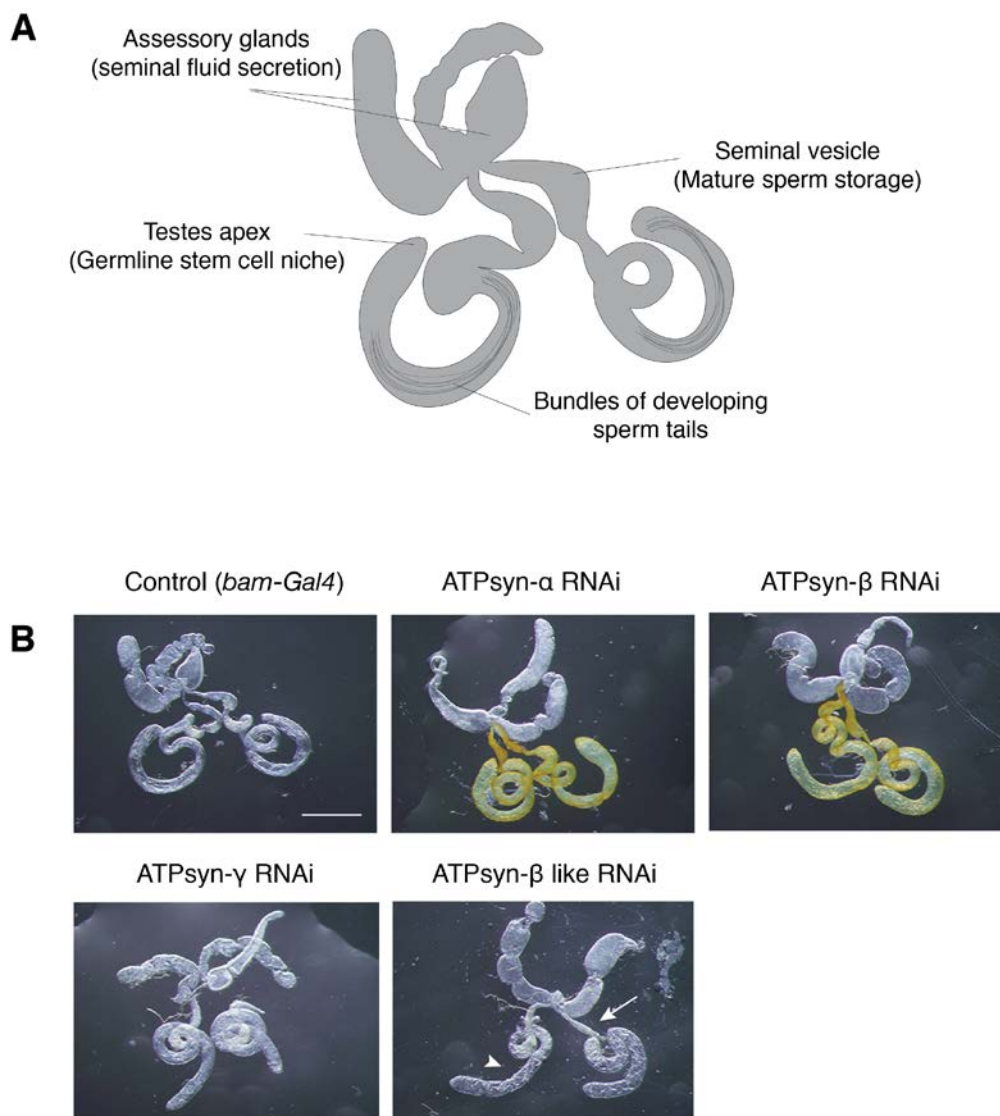


Figure 4.8 Adult testes morphology after RNAi knockdown of ATPsyn- α , - β , - β like and - γ . (A) Schematic illustrating the anatomy of *Drosophila* adult testes. (B) Bright field images of adult (5 days old) control testes and adult testes after ATPsyn- α , - β , - β like and - γ RNAi knockdown. Disrupted morphologies are indicated with arrowheads (absent sperm tails) and arrows (empty seminal vesicles). The scale bar represents 0.5 mm.

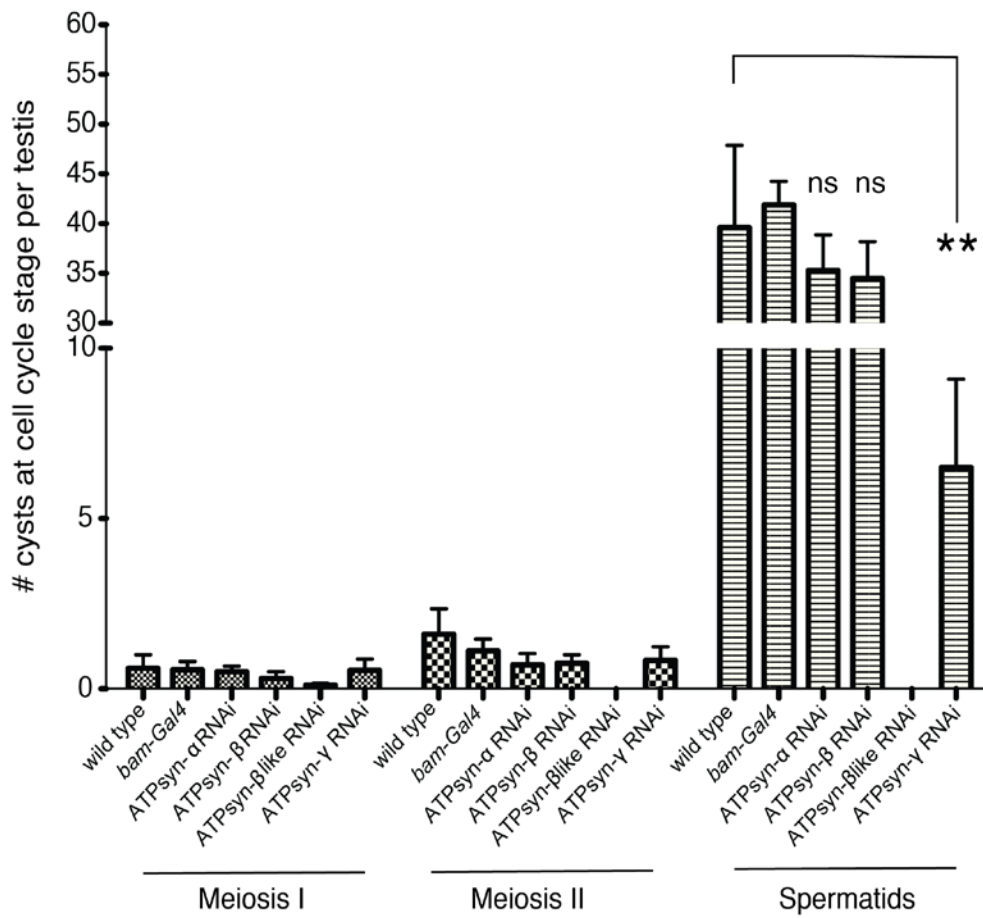


Figure 4.9 Cell cycle analyses after ATPsyn- α , - β , - β like and - γ RNAi knockdown. Data collected from 20 adult testes, the y-axis represents the average number of cell cysts between metaphase and telophase in meiosis I, or II and the average number of spermatid cysts per testis. WT (*y+ry+*) and *bam-Gal4* fly lines used as controls. Error bars represent standard error of the mean. ** represents $p < 0.01$ and ns represents a $p > 0.05$.

4.4. Identification of centromeric cohesion defects in the ATPsyn- α , - β , - β like and - γ RNAi knockdowns

As cell cycle analyses revealed a meiotic arrest in the ATPsyn- β like RNAi knockdown prior to the first meiotic division we analysed cells immediately prior to this stage (prophase I) and searched for defects in centromere dynamics and function by immuno-staining for the centromeric markers CENP-A and CENP-C. Compared to controls, an increased number of centromeric foci were observed per nucleus in the ATPsyn- α , - β like and - γ RNAi knockdowns (figure 4.10 and 4.11).

As discussed previously, early prophase I nuclei generally display between 2 and 4 centromeres per nucleus (average 2.72) due to sister centromere cohesion and homologous centromere clustering at this time. RNAi knockdown of ATPsyn- α , - β like and - γ disrupted this process and led to a significant increase ($p < 0.0001$) in the number of centromeres per nucleus with ATPsyn- α displaying an average of 3.44, ATPsyn- β like displaying an average of 3.21 and ATPsyn- γ displaying an average of 4.07 centromeres per nucleus (figure 4.10). RNAi knockdown of canonical ATPsyn- β did not disrupt ($p = 0.717$) centromere clustering and/or cohesion at early prophase I with nuclei displaying an average of 2.77 centromeres.

This trend was maintained throughout prophase I. In the control, as homologous centromere clustering is lost (except for the 4th chromosome) yet sister centromere cohesion is maintained, late prophase I nuclei display between 6 and 7 centromeres (average 6.5). In the ATPsyn- α , - β -like and - γ RNAi knockdowns the average number of centromeric foci was significantly increased ($p < 0.0001$) to 7.34, 7.80 and 7.87 centromeres respectively (figure 4.11). In these knockdowns, the number of centromeres per nucleus was frequently more than 8 and in many cases up to a maximum of 16, indicating a partial and indeed in some cases complete loss of sister centromere cohesion. RNAi knockdown of canonical ATPsyn- β did not

disrupt ($p=0.102$) centromere clustering and/or cohesion at this stage, with nuclei displaying an average of 6.93 centromeres at late prophase I. At this meiotic stage, the loss of cohesion defect was confirmed using two independent UAS-RNAi lines in order to control for off-target effects.

At prometaphase I as the chromosome territories rapidly condense, sister centromeres of each homologue align along the metaphase I plate and an average of 5.70 centromeres were observed per nucleus in control cells. As reported in figure 4.9, a prometaphase I arrest occurs in the ATPsyn- β -like RNAi knockdown; in these arrested nuclei a significant decrease ($P < 0.05$) in the number of centromeric foci was observed (average 4.82). We propose that this decrease is due to the observed cell cycle arrest at this stage. No significant change in the number of centromeric foci at this stage was observed for the ATPsyn- β or - γ RNAi knockdowns ($P = 0.452$ and 0.355 respectively) and a significant increase ($P < 0.05$) in the average number of centromeric foci was observed for the ATPsyn- α RNAi knockdown (6.5 centromeres) (figure 4.12).

In the ATPsyn- β -like RNAi knockdown late prometaphase/metaphase I arrested nuclei the process of chromatin condensation and alignment is severely disrupted. In controls, by metaphase I chromosomes have condensed and aligned to form a single mass of DNA however in the ATPsyn- β -like RNAi knockdown instead of a single mass of condensed DNA, single sister chromatids which have lost cohesion form several smaller condensed DNA masses (figure 4.13).

The number of centromeres per nucleus in cells after meiosis I, during interphase I was also determined for the ATPsyn- α - β and - γ RNAi knockdowns. Compared to control interphase cells (average number of centromeres 3.63) there was a significant increase in the number of centromeric foci in the ATPsyn- α ($p<0.0001$) and ATPsyn- γ ($p<0.001$) RNAi knockdowns. This phenotype was most severe in the ATPsyn- γ RNAi knockdown, where in many cases cells displayed a maximum of 8

centromeres indicating a complete loss of centromeric cohesion. During interphase I, as was the case throughout meiosis I, there was no significant increase ($p=0.454$) in the number of centromeric foci in the canonical ATPsyn- β RNAi knockdown (figure 4.12).

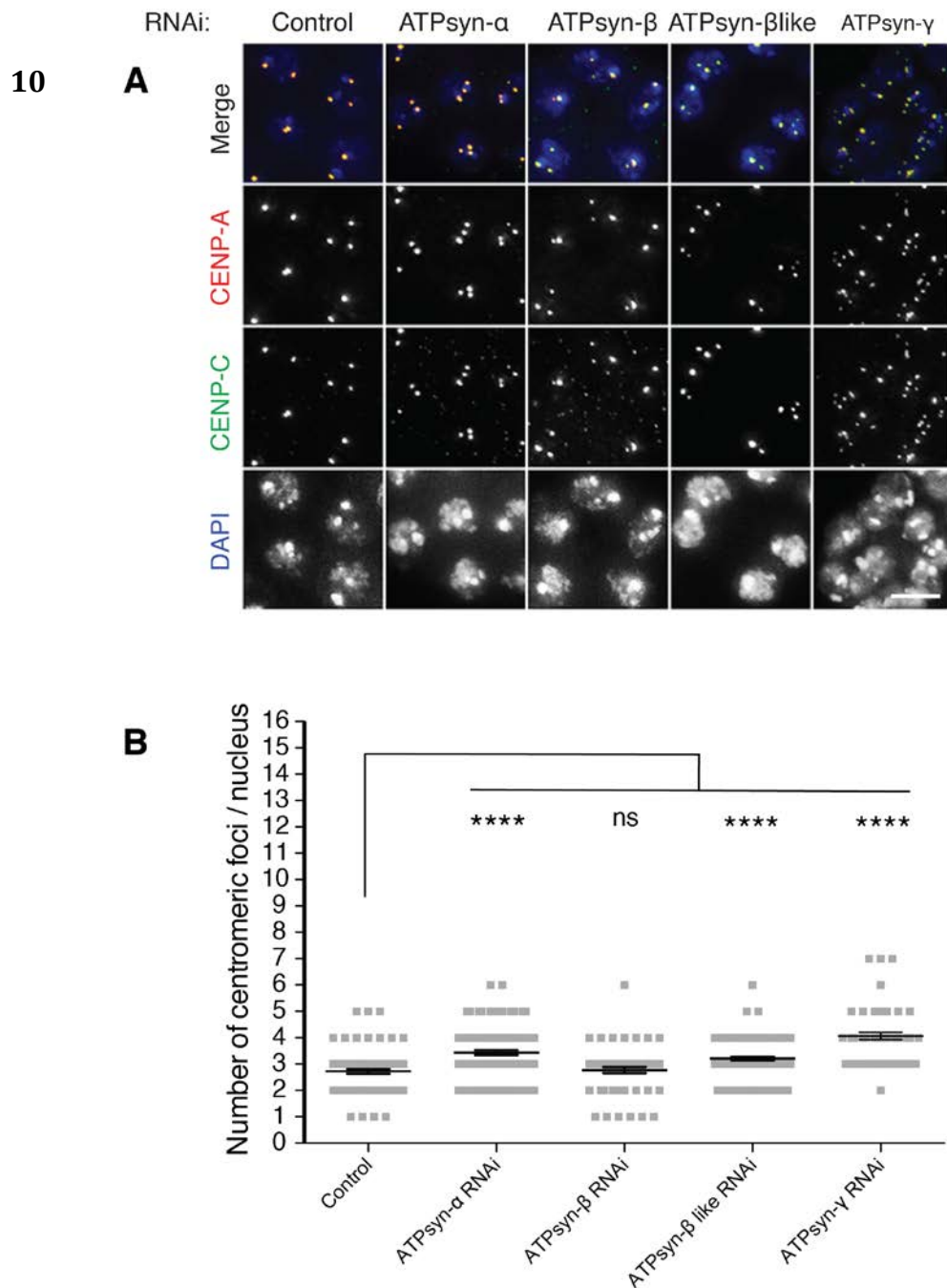


Figure 4.10 Centromere number in early prophase I nuclei after ATPsyn- α , - β , - β like and - γ RNAi knockdown. (A) Early prophase I nuclei in control versus RNAi knockdowns immuno-stained for CENP-A (red) and CENP-C (green), DNA is stained with DAPI (blue). Scale bar represents 10 μ m. (B) Quantitation of the number of centromeric foci per nucleus after RNAi knockdown. > 100 nuclei analysed per sample and line and error bars represent mean and standard error of the mean respectively. **** $p < 0.0001$ and ns $p > 0.05$.

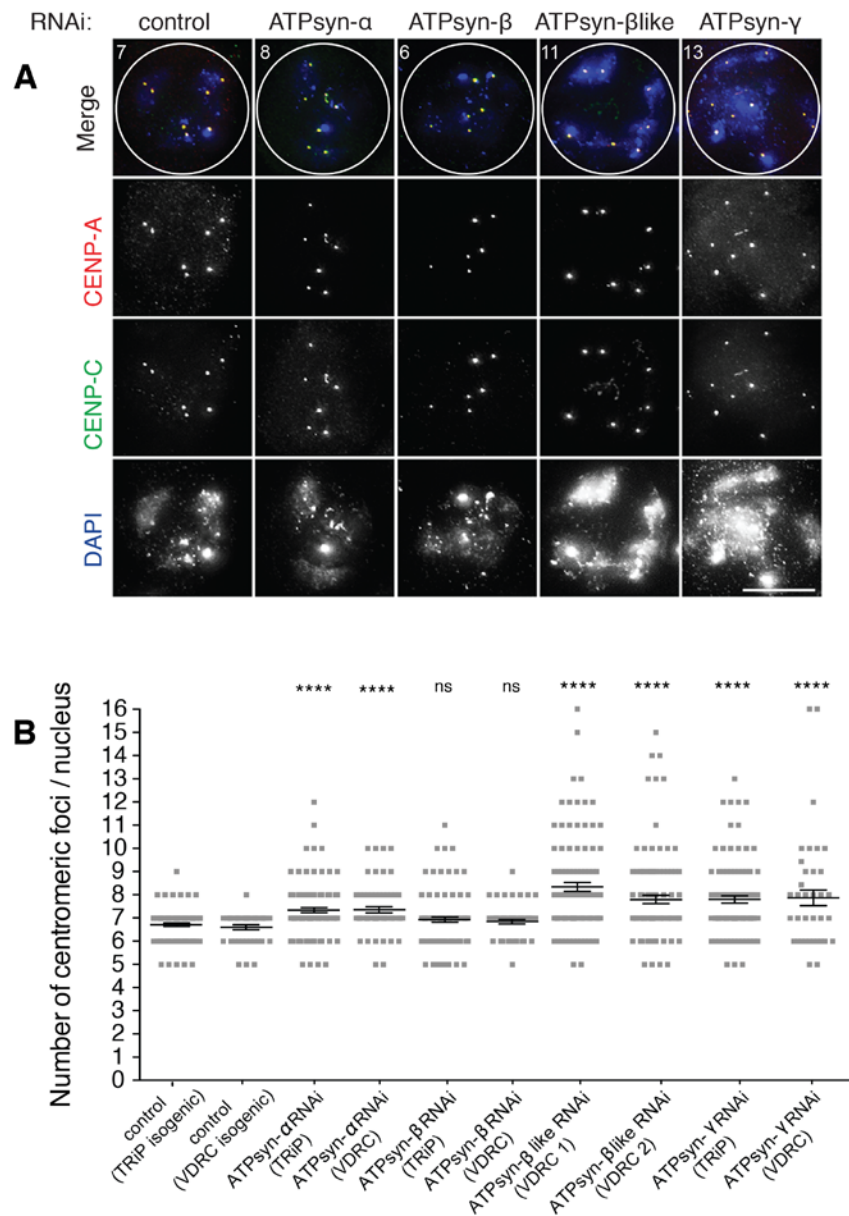


Figure 4.11 Centromere number in late prophase I nuclei after ATPsyn- α , - β , - β like and - γ RNAi knockdown. (A) Late prophase I nuclei immuno-stained for CENP-A (red) and CENP-C (green), DAN is stained with DAPI (blue). The number of centromeric foci per nucleus is indicated, as is the nuclear membrane (white circle). The scale bar represents 10 μ m. (B) Quantitation of the number of centromeric foci per nucleus after RNAi knockdown. > 100 nuclei per sample were analysed for two independent UAS-RNAi lines. **** p<0.0001 and ns p>0.05. Line and error bars represent mean and standard error of the mean respectively.

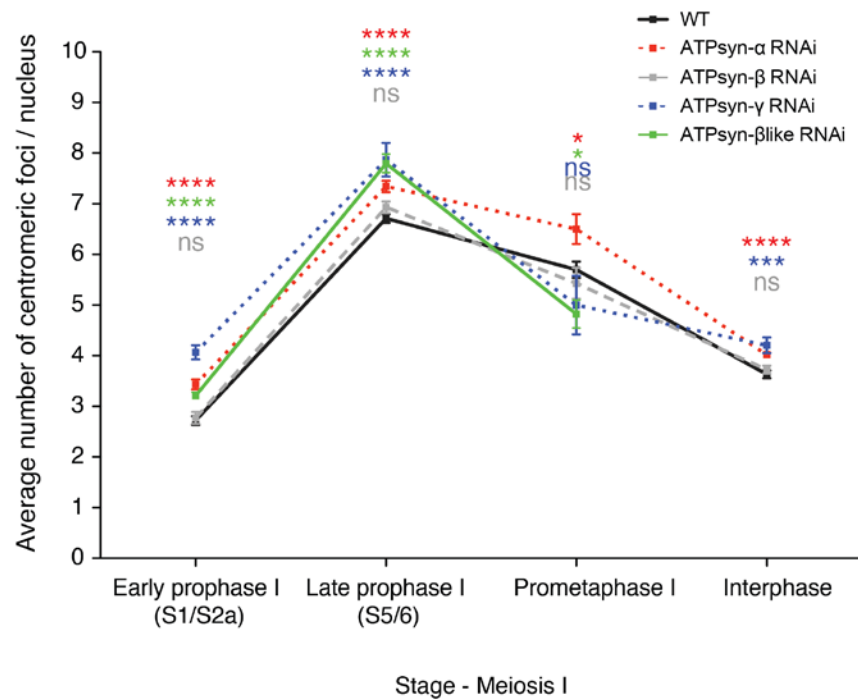


Figure 4.12 The average number of centromeric foci per nucleus in RNAi knockdowns versus control (isogenic). Average numbers of centromeres per nucleus at early and late prophase I, prometaphase I and interphase I after RNAi knockdown of ATPsyn- α (red), - β (grey), - β like (green) and - γ (blue) are represented. $n=100$ nuclei per cell stage, error bars represent standard error of the mean, **** $p<0.0001$, *** $p<0.001$, * $p<0.05$ and ns represents a $p>0.05$.

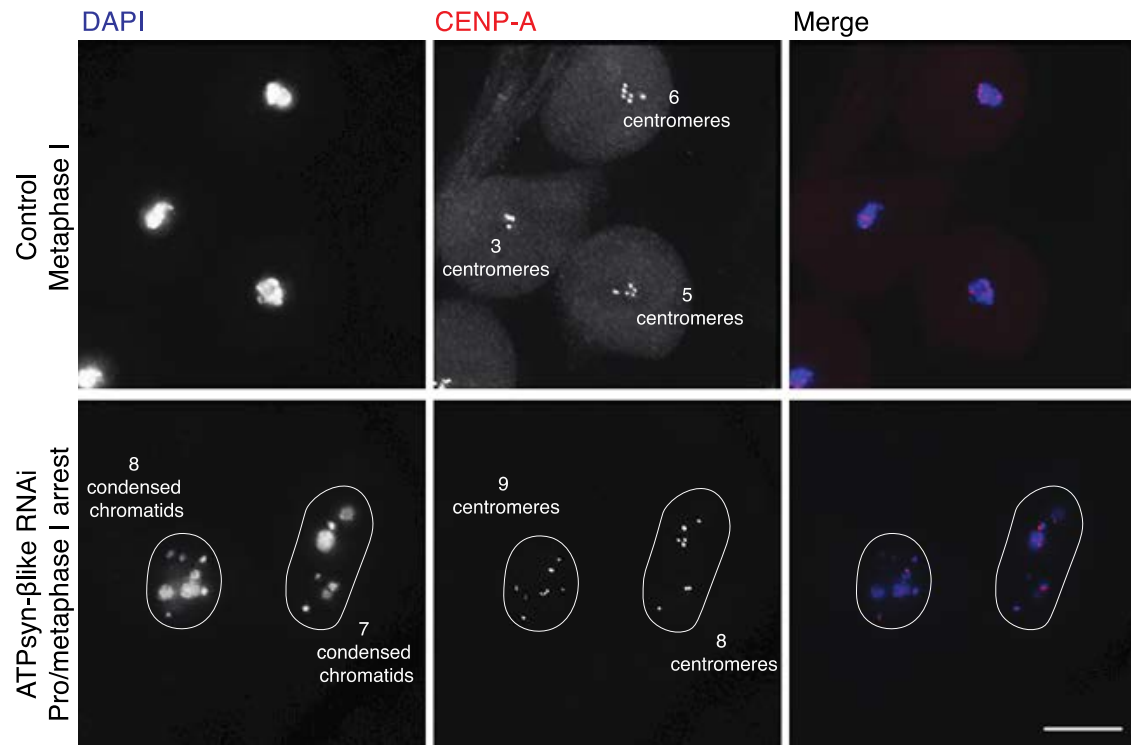


Figure 4.13 Immunofluorescent micrograph of control metaphase I and arrested late prometaphase/metaphase I nuclei. Methanol-acetone fixed cells immuno-stained for CENP-A (red), DNA is stained with DAPI (blue) The number of condensed chromatids per nucleus in the ATPsyn- β like RNAi is indicated as are the number of centromeric foci per nucleus. The nuclear membrane in the ATPsyn- β like RNAi knockdown is indicated (white circle) Scale bar represents 10 μ m.

4.5. Identification of chromatid arm cohesion defects in the ATPsyn- α , - β , - β -like and - γ RNAi knockdowns.

In light of the observed loss of sister centromere cohesion throughout meiosis I, the effect of ATPsyn- α , - β - β -like and - γ RNAi knockdown on chromatid cohesion at several other known cohesion sites was then analysed using DNA FISH.

4.5.1 2nd and 3rd chromosome arm cohesion

Chromatid arm cohesion was assessed using a DNA probe recognising a satellite sequence (1.686 g/cm³) present on the arms of the 2nd and 3rd chromosomes; this heterochromatic region is a site of strong cohesion retention throughout meiosis I (Tsai *et al.*, 2011).

At early prophase I, between one and three 1.686 g/cm³ foci were observed per nucleus due to chromosome cohesion and clustering. At this stage, no significant difference in the number of 1.686 g/cm³ foci per nucleus was observed in the ATPsyn- α , - β and - β -like RNAi knockdowns (p=0.205, 0.056 and 0.660 respectively) (figure 4.14). At late prophase I, as chromosome clustering is lost and chromosome territories form, between three and four 1.686 g/cm³ foci were observed per nucleus (average 3.70). In the ATPsyn- α , - β , - β -like and - γ RNAi knockdowns at this stage there was a significant increase in the number of 1.686 g/cm³ foci per nucleus (p<0.05, p<0.01, p<0.0001 and p<0.01 respectively) (figure 4.15). In many cases the number of 1.686g/cm³ foci per nucleus was greater than 4 indicating a partial loss of arm cohesion in some cells and many cells exhibited up to 8 1.686g/cm³ foci per nucleus indicating a complete loss of chromatid arm cohesion.

In addition to the increased number of 1.686 g/cm³ foci in the ATPsyn- β -like RNAi knockdown at late prophase I these loci also displayed a more diffuse and unorganised pattern. This may indicate that as well as its role is

chromatid cohesion, ATPsyn- β like may have additional roles in chromatin condensation and/or organisation.

In the ATPsyn- β like RNAi knockdown, the number of 1.686 g/cm³ foci at prometaphase/metaphase I was also determined. In control nuclei at this stage the homologous chromosomes condense and align at the metaphase I plate, thus two 1.686 g/cm³ foci are observed per nucleus – one focus representing the paired 2nd chromosomes and the other representing the paired 3rd chromosomes. In the ATPsyn- β like RNAi knockdown the average number of 1.686 g/cm³ foci was significantly increased (P < 0.0001) with prometaphase I nuclei displaying between one and eight 1.686 g/cm³ foci per nucleus (average 2.53) (figure 4.16).

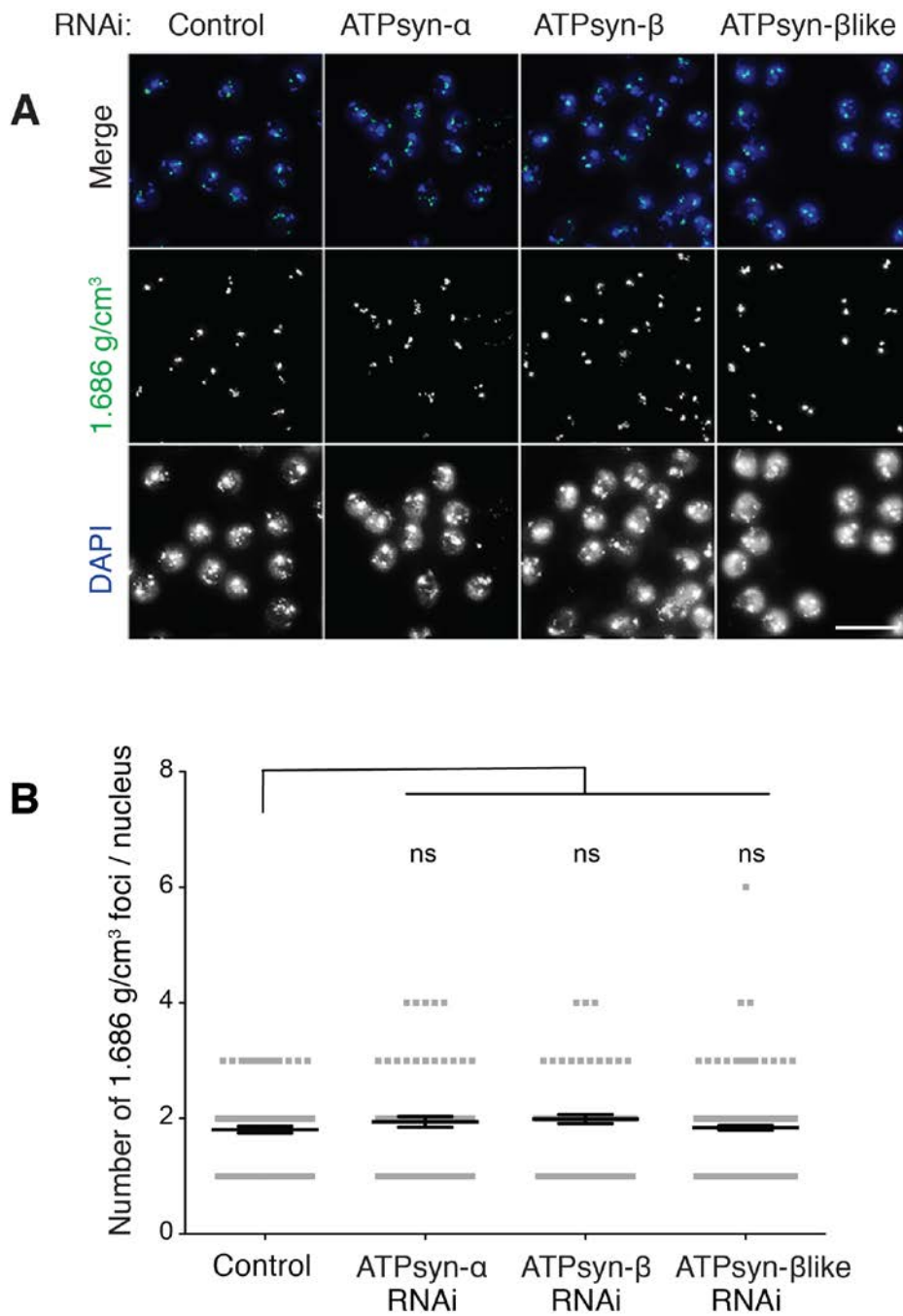


Figure 4.14 Micrograph of FISH on early prophase I nuclei of control and ATPsyn- α , - β and - β like RNAi knockdowns. (A) Representative images early prophase I nuclei with 1.686 g/cm³ foci (green), DNA is stained with DAPI (blue). Scale bar represents 10 μ m. (B) Quantitation of the number of 1.686 g/cm³ foci per early prophase I nucleus (n=100 nuclei). Line and error bars represent the mean and standard error of the mean respectively, ns = p>0.05.

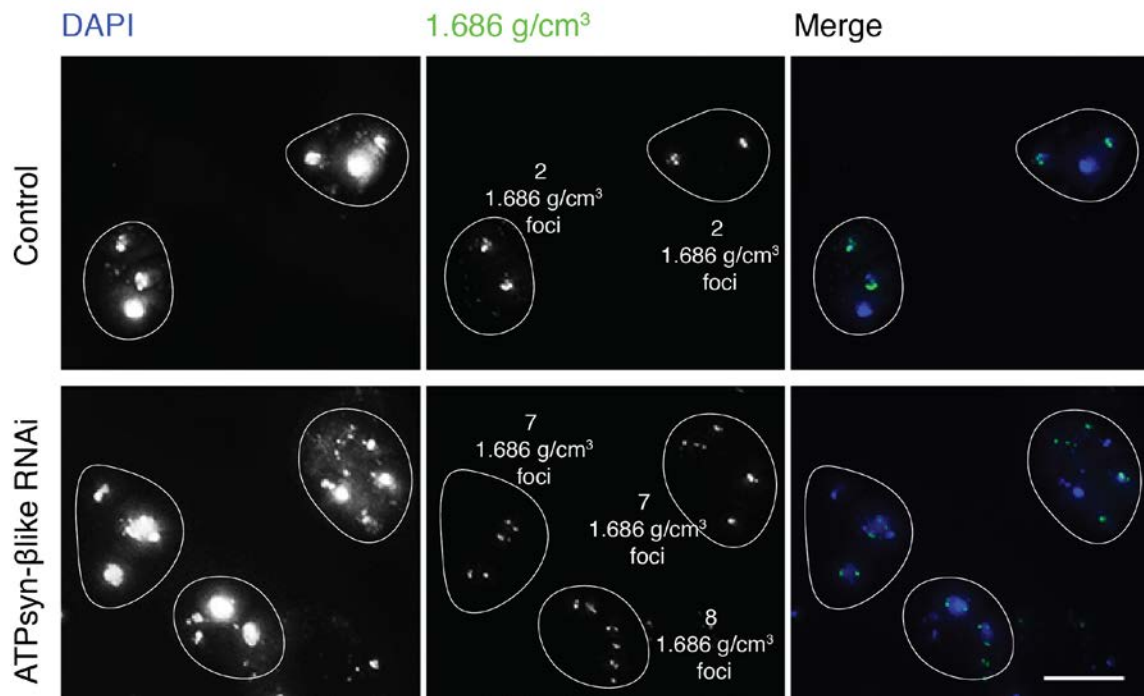


Figure 4.16 FISH analysis of prometaphase/metaphase I arrested nuclei. Representative micrograph of 1.686 g/cm³ foci (green) in control and ATPsyn-βlike RNAi knockdowns. DNA is stained with DAPI (blue). Nuclear membrane (white circle) and the number of 1.686 g/cm³ foci per nucleus are indicated. The scale bar represents 10 μm.

4.5.2 4th chromosome pairing and/or cohesion

Pairing and/or cohesion of the 4th chromosome was assessed using a DNA probe recognising a known pairing site on 4R (AATAT repeat, figure 2.5). In control nuclei at late prophase I 62 % of cells displayed a single bright AATAT focus, representing a single paired 4th chromosome with intact sister chromatid cohesion. 33.4 % of control cells at this stage displayed two closely associated (< 5 µm apart) AATAT foci indicating that the two 4th homologues were located together within a single nuclear territory. A remaining small amount of cells (2.8 %) displayed a diffuse AATAT signal at this stage possibly indicating a disruption of cohesion and/or organisation at the AATAT site (figure 4.17).

In the ATPsyn- α , - β , - β like and - γ RNAi knockdowns the number of cells displaying a single AATAT focus decreased to 37.6, 43, 42 and 41.95 % respectively. There was an increase in the number of cells displaying the two closely associated (< 5 µm apart) spot pattern in the ATPsyn- α and - β like RNAi knockdowns to 45.65 and 41.05 % respectively. In the control nuclei, no cells were observed with 4th chromosome AATAT sites located > 5 µm apart indicating that the homologues and sister chromatids are always located together in a single territory. In the ATPsyn- α , - β , - β like and - γ RNAi knockdowns 3.86, 2.7, 10.71 and 9.67 % of cells displayed AATAT foci that were located > 5 µm apart suggesting that either the 4th chromosome homologues and/or sister chromatids had become detached and were located in separate nuclear territories. In addition the number of cells with a diffuse AATAT signal increased to 12.89, 21.6, 5.35 and 16.29 % respectively (figure 4.17).

4.5.3 X chromosome pericentromeric cohesion

The 359 bp repeat is a non-pairing site located in the pericentromeric heterochromatin of the X chromosome (Tsai *et al.*, 2011)(figure 2.5). Using a DNA FISH probe recognising this site we assessed if X chromosome cohesion

was disrupted upon RNAi knockdown of ATPsyn- α , - β or - β -like (*X* chromosome cohesion was not determined in the ATPsyn- γ RNAi knockdown). In control nuclei at late prophase I 84.45 % of cells displayed a single 359 bp focus, indicating that in the majority of cells at this stage, pericentromeric cohesion is intact. The remainder of cells at this stage (15.55 %) displayed two separate 359 bp foci (figure 4.18). RNAi knockdown of ATPsyn- α and β -like resulted in a decrease in the number of cells displaying a single 359 bp focus from 84.45 % in the control to 64 and 26.5 % respectively, in the ATPsyn- β RNAi knockdown the 359 bp pattern remained unchanged (figure 4.18).

In the control, no nuclei were observed which displayed a diffuse 359 bp signal, however upon RNAi knockdown of ATPsyn- α and - β -like 23.81 and 61.9 % of cells respectively showed spreading of the 359 bp FISH signal. This diffusion of the 359 bp locus was particularly severe in the ATPsyn- β -like RNAi knockdown indicating that a severe chromatin condensation and/or organisation defect had occurred (figure 4.18).

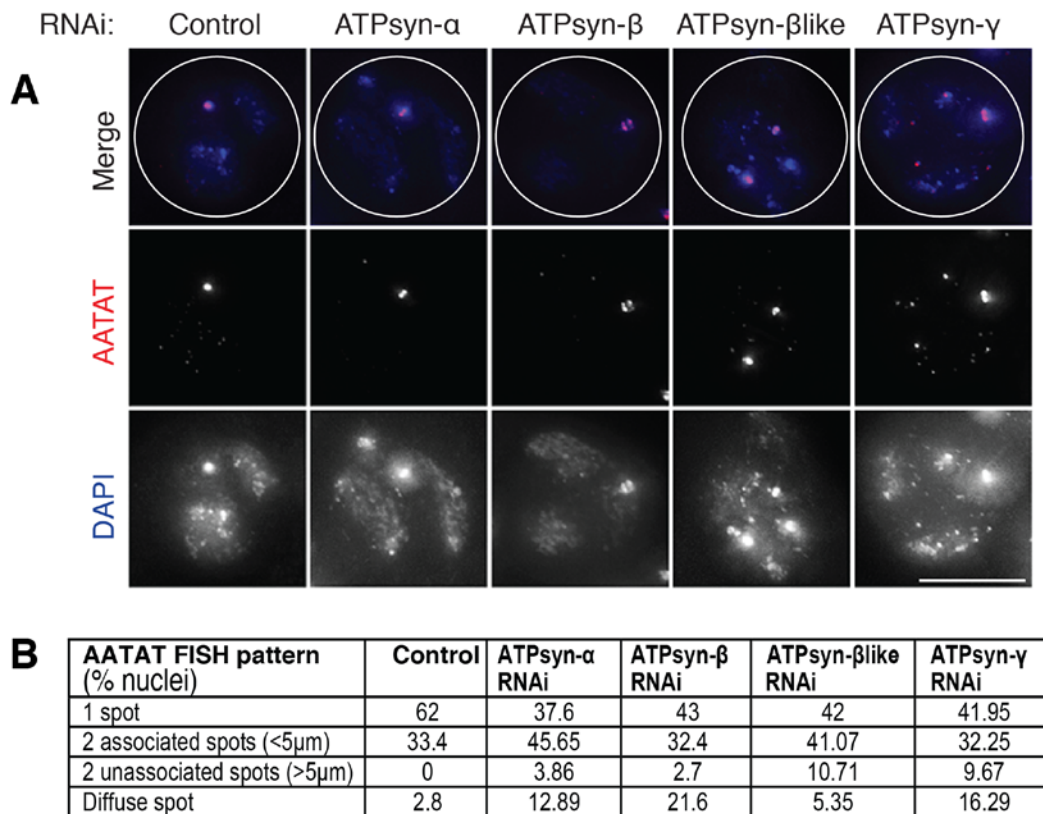
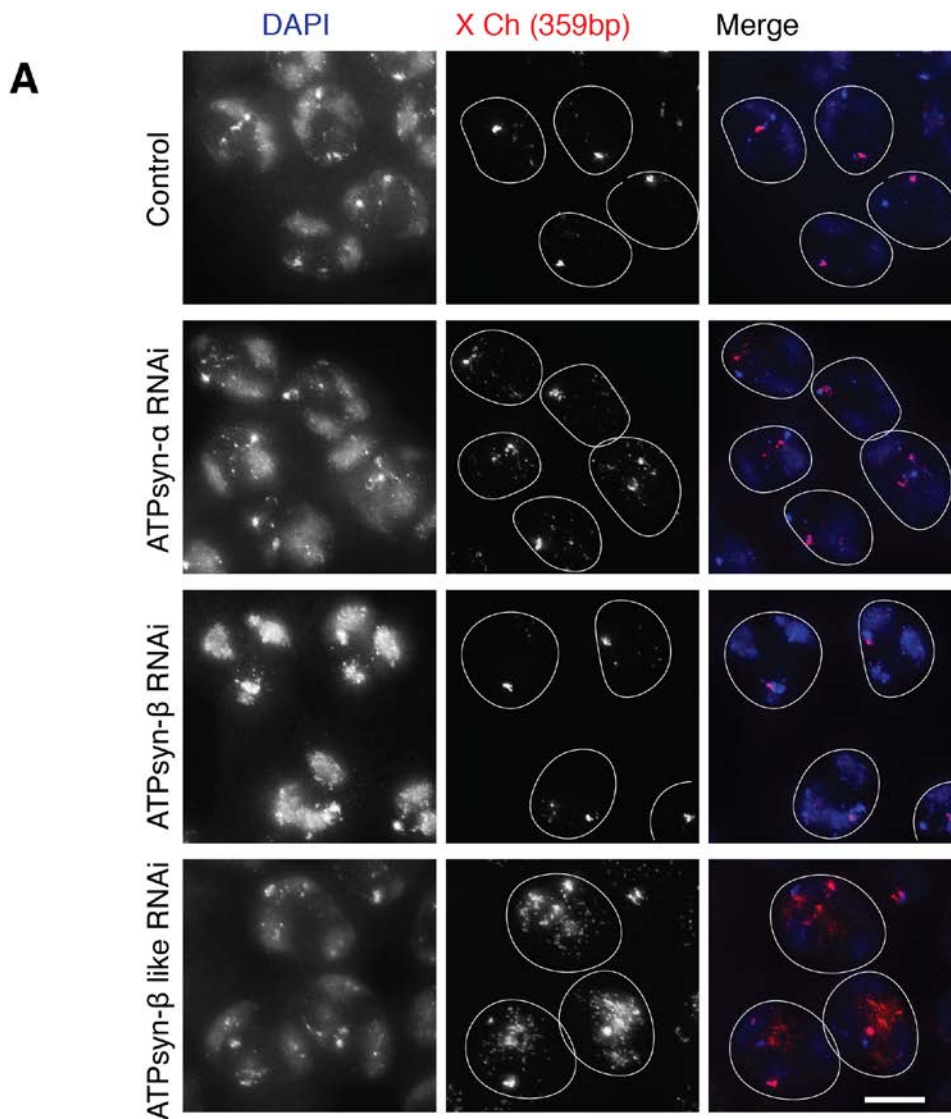


Figure 4.17 FISH on late prophase I nuclei of control and ATPsyn- α , - β , - β like and - γ RNAi knockdowns (A) Representative images of AATAT (red) foci on late prophase I nuclei, DNA is stained with DAPI (blue) and nuclear membranes are indicated (white circle). The scale bar represents 10 μ m. (B) Quantitation of the percentage of late prophase I nuclei containing a single AATAT focus, two foci or a diffuse AATAT pattern, n>50 nuclei per sample.



B

Late Prophase I	1 spot (X)	>1spot (X)	Diffuse signal (X)
Control (n=55 cells)	84.45 %	15.55 %	0 %
ATPsyn- α RNAi (n=42 cells)	64 %	11 %	23.81 %
ATPsyn- β RNAi (n=51 cells)	82.40 %	7.80 %	9.80 %
ATPsyn- β like RNAi (n=105 cells)	26.50 %	4.76 %	61.9 % (Severe)

Figure 4.18 Micrograph of FISH on late prophase I nuclei of control and ATPsyn- α , - β and - β like RNAi knockdowns (A) Representative images of 359 bp foci (red) in late prophase I nuclei, DNA is stained with DAPI (blue). Nuclear membranes are indicated (white circle) and scale-bar represents 10 μ m. (B) Quantitation of the percentage of nuclei with a single, multiple or diffuse 359 bp signals, n>50 nuclei per sample.

4.6. Analysis of MEI-S332 localisation in ATPsyn- α , - β , - β like and - γ RNAi knockdowns

MEI-S332 localises to the centromere and pericentromere during prometaphase and metaphase of meiosis I, its localisation is required to protect the cohesion of sister chromatids allowing for their mono-orientation at anaphase I (Kerrebrock *et al.*, 1995). Given the severe defects and arrest observed upon RNAi knockdown of ATPsyn- β like MEI-S332 localisation in this knockdown was analysed

In control meiotic nuclei as expected, we observed MEI-S332 at pericentromeric regions in late prometaphase and metaphase I nuclei (stage determined by tubulin staining). In prometaphase/metaphase I arrested nuclei of the ATPsyn- β like RNAi knockdown we observed that MEI-S332 was reduced at the centromere and instead was present all over the condensing chromatin. In addition to this, severely abnormal spindle morphology likely due to an inability to form stable kinetochore attachments was observed (Figure 4.19).

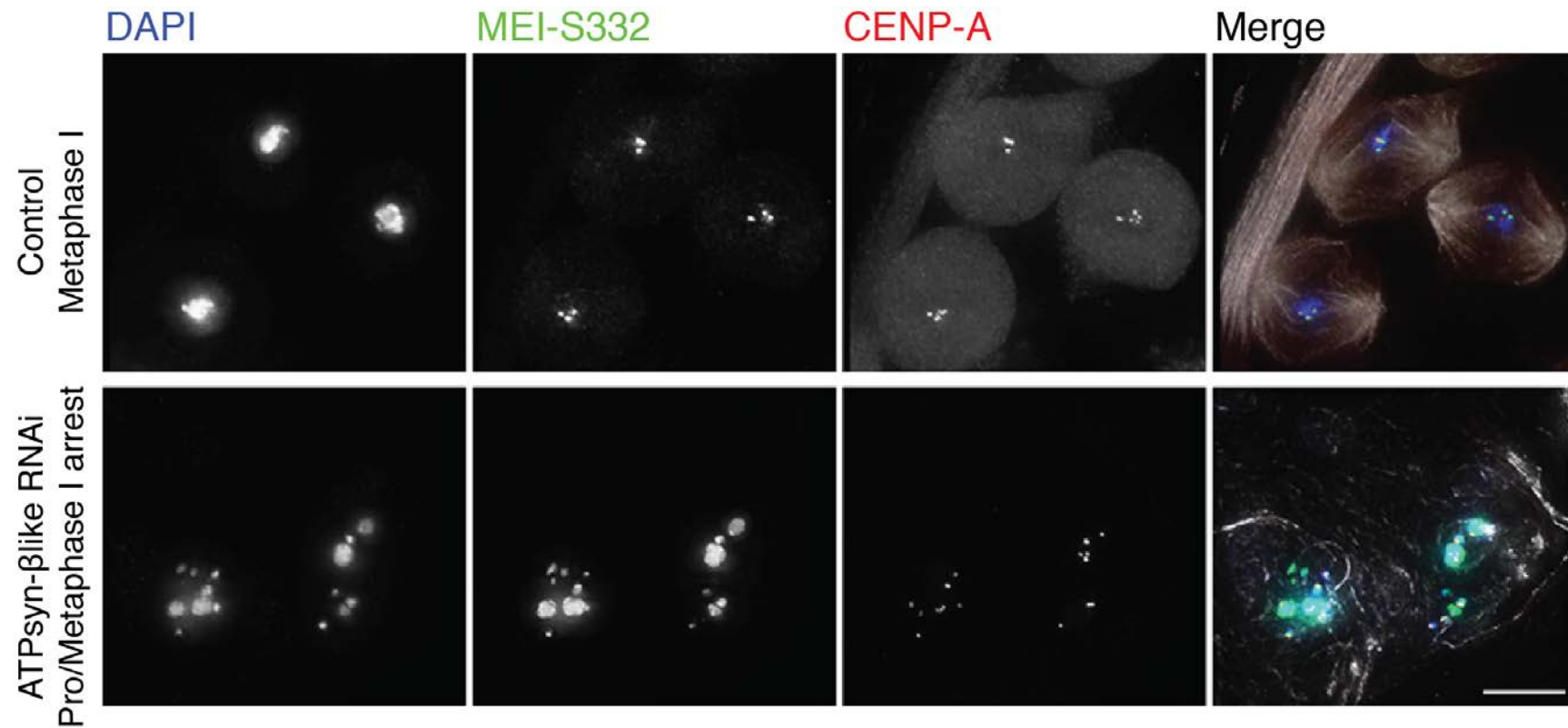


Figure 4.19 **Immunofluorescent micrograph of prometaphase I nuclei in control and ATPsyn-βlike RNAi knockdown.** Cells fixed with methanol-acetone and immuno-stained for MEI-S332 (green), CENP-A (red) and tubulin (white), DNA is stained with DAPI (blue). The scale bar represents 10 μm .

4.7. Discussion

A summary of the major results presented in chapter 4:

1. *ATPsyn- β like* is a paralogue of the mitochondrial ATP synthase F₁ subunit *ATPsyn- β* . It is specifically expressed in the testes where it is required for meiotic progression through prometaphase/metaphase I.
2. Expression of canonical ATP synthase F₁ subunits *ATPsyn- α* and $-\gamma$ as well as the variant *ATPsyn- β like* are required to maintain sister centromere and chromatid arm cohesion throughout meiosis.
3. Expression of *ATPsyn- β like* is required for the centromeric localisation of MEI-S332 at prometaphase/metaphase I.

4.7.1 Characterisation of *ATPsyn- β like*

We have detected *ATPsyn- β like*, a gene essential for male fertility in approximately half of the estimated 150,000 species within the insect group Diptera. In addition to this, we have identified that an *ATPsyn- β like* homologue is present in *Bombyx mori*, a moth species from the closely related group Lepidoptera. The presence of *ATPsyn- β like* in both insect groups and the similarity in *ATPsyn- β like* protein sequence between *Drosophila melanogaster* and *Bombyx mori* suggests that an *ATPsyn- β like* duplication arose in a common ancestor of Dipterans and Lepidopterans. Despite this, we were unable to detect *ATPsyn- β like* homologues in many lower dipteran species such as mosquitos and crane flies. It is possible that *ATPsyn- β like* may have been lost in these species or that the sequence of *ATPsyn- β like* in these species has changed significantly such that more sophisticated search methods are required to identify them.

In the adult fly, we have confirmed that *ATPsyn-βlike* is specifically expressed in the testes, expression has also been detected during the pupal stage of the fly life cycle (ModENCODE consortium; Celniker *et al.*, 2009). Expression of *ATPsyn-βlike* during this window is consistent with the stage at which *ATPsyn-βlike* (-/-) double knockout mutants die indicating that *ATPsyn-βlike* likely has additional, essential roles outside of spermatogenesis during development and/or metamorphosis.

4.7.2 The role of ATP synthase F₁ subunits in male fertility

We have identified that *ATPsyn-βlike*, previously shown to be essential for male fertility (Castrillon *et al.*, 1993; Lindsley *et al.*, 2013) is required to establish and maintain sister chromatid cohesion in meiosis prophase I, this loss of cohesion culminates in an organisation defect and an arrest prior to anaphase I. Knockdown of *ATPsyn-βlike* also leads to a disruption in MEI-S332 localisation to the centromere and pericentromere during prometaphase/metaphase I.

ATPsyn-α has also been previously linked to male fertility (Castrillon *et al.*, 1993; Sawyer *et al.*, 2017). Recently Sawyer *et al.*, 2017 have identified that *ATPsyn-α* has an oxidative phosphorylation independent function in the testes where it is required for in higher order mitochondrial organisation within the inner mitochondrial membrane. Here we have identified that in addition to this, *ATPsyn-α* is also required to establish and maintain sister chromatid cohesion throughout meiosis. In addition, we have found that *ATPsyn-γ* is also required for this process.

In contrast to the *ATPsyn-βlike* RNAi knockdown, knockdown of *ATPsyn-α* and *-γ* does not result in a prometaphase/metaphase I arrest and mature sperm are produced. The observed differences in phenotype severity may reflect differences in RNAi efficiencies or alternatively it is possible that

compared to ATPsyn- α and - γ , ATPsyn- β like has additional roles during prophase I. Results presented in this chapter indicate that ATPsyn- β like may also play a role in chromatin condensation and/or organisation and a combination of chromatid cohesion and condensation defects in the ATPsyn- β like RNAi knockdown may result in a more severe phenotype.

Throughout meiosis, RNAi knockdown of the canonical ATPsyn- β subunit had no observed defect on male fertility or chromosome cohesion. Given that ATPsyn- β expression is down regulated in the testes in meiotic cells (Wen *et al.*, 2015) this result is as expected. Wen *et al.* 2015 have shown that de-repression of ATPsyn- β in the germ-line results in male sterility; it seems likely that increased expression of the canonical ATPsyn- β in these experiments interfered with the correct functioning of the variant ATPsyn- β -like.

It is possible that the observed defects arise as a result of a reduction in the total levels of ATP in the testis. Reduced levels of ATP may disrupt global chromatin organisation and this cohesion and MEI-S322 recruitment. However we think that it is more likely that a functional link exists between CENP-A and this alternative F₁ complex based on the observations that CENP interacts with ATPsyn- α and ATPsyn- β (IP and MS analysis, chapter 3) and that similar cohesion defects are observed upon RNAi knockdown of CENP-A and the ATP synthase F₁ subunits (RNAi knockdown of CENP-A, chapter 3). Furthermore, previous studies indicate that CENP-A also plays a role in the recruitment of MEI-S322 providing a link between CENP-A, ATPsyn- α - β like, - γ and MEI-S322. In chapter 5, the results of an investigation into the mechanism of cohesion establishment and maintenance and the link between CENP-A and the ATP synthase F₁ complex during male meiosis are presented.

**5. Characterisation of the functional interaction between
CENP-A and ATP synthase subunits ATPsyn- α , β like and
 $-\gamma$.**

5.1. Chapter introduction

In chapters 3 and 4 we describe a number of experiments that provide evidence for a functional link between the centromeric histone H3 variant CENP-A and mitochondrial ATP synthase F₁ subunits - ATPsyn- α , - β , - β like and - γ . Firstly, purification of germ-line CENP-A from *Drosophila* testes protein extracts identified a potential protein interaction between CENP-A and ATPsyn- α , - β and - γ . Secondly, phenotypic analysis after RNAi knockdown identified that both CENP-A and the ATP synthase F₁ subunits ATPsyn- α , - β like and - γ are required to maintain centromeric cohesion during male meiosis.

In addition, we have shown that ATPsyn- β like is required for correct localisation of MEI-S332 at prometaphase of meiosis I. MEI-S332, the *Drosophila* homologue of SHUGOSHIN localises to the pericentromere at prometaphase I and is required to maintain sister centromere cohesion at this stage (Kerrebrock *et al.*, 1995). Previous studies in *Drosophila* early embryonic mitoses have shown that correct levels of CENP-A at the centromere are also required for correct MEI-S322 localisation (Blower and Karpen, 2001).

Taken together these results strongly suggest that CENP-A and the ATP synthase F₁ subunits cooperate to establish and maintain sister chromatid cohesion during meiosis and that this function is related to recruitment of the protector of centromeric cohesion, MEI-S332. To advance this model, we aimed to further elucidate the mechanism of how ATPsyn- α , - β like and - γ promote chromatid cohesion during meiosis by addressing the following questions; 1) Is the role of ATPsyn- α , - β like and - γ in meiotic cohesion establishment and maintenance independent of canonical roles in ATP generation? If this is the case, 2) are these subunits re-locating to and acting in the nucleus during meiosis? 3) Are these ATP synthase F₁ subunits directly interacting with CENP-A? And if so, 4) what is the function of this interaction?

5.2. Analysis of whole testis ATP levels after RNAi knockdown of ATPsyn- α , - β , - β like and - γ .

The ATP synthase F₁ complex, normally located within the inner mitochondrial membrane is essential for ATP generation (Alberts *et al.*, 2014). Thus, to determine the effect of ATPsyn- α , - β , - β like and - γ RNAi knockdown on whole testis ATP levels, ATP determination assays were carried out. No difference in ATP level per testis was observed between the two different control fly lines (*bam-Gal4* and isogenic) used in this experiment. In addition, no significant difference ($p=0.726$) was observed between both controls and flies with a CENP-A RNAi knockdown confirming that the level of ATP per testis was reproducibly detectable in different genetic backgrounds (figure 5.1).

RNAi knockdown of ATPsyn- α , - β , - β like and - γ led to a significant reduction in whole testis ATP levels ($p<0.0001$, 0.05, 0.0001 and 0.0001 respectively). Upon RNAi knockdown of ATPsyn- α a 55 % reduction in ATP was detected. RNAi knockdown of the canonical ATPsyn- β and variant ATPsyn- β like subunits led to 6 and 45 % reductions in ATP respectively and RNAi knockdown of ATPsyn- γ produced a 33 % reduction in whole testis ATP (figure 5.1).

To determine if a reduced ATP level alone is sufficient to induce meiotic cohesion defects, ATP levels were reduced by carrying out RNAi knockdowns of several other components of the oxidative phosphorylation and ATP synthesis pathway. Three UAS-RNAi fly lines were identified that induced comparable reductions in whole testis ATP. ATPsyn-b is a peripheral component of the F₀-F₁ ATP synthase complex (Rees *et al.*, 2009), RNAi knockdown of which resulted an ATP reduction of 52 % (figure 5.2 A). ND-23 and ND-51 are core components of NADPH dehydrogenase, which forms complex I of the oxidative phosphorylation pathway (Alberts *et al.*, 2014). RNAi knockdown of these two proteins led to a 36 and 32 % reduction in whole testis ATP respectively (figure 5.2 A). To determine if

this reduction in ATP level was sufficient to induce centromeric cohesion defects the number of centromeric foci per nucleus was assessed by anti-CENP-A and anti-CENP-C immuno-staining. No significant difference was detected during late prophase I between the control and the ATPsyn-b (p=0.185), ND-23 (p=0.893) or ND-51 (p=0.797) RNAi knockdowns (figure 5.2 B) indicating that reduced ATP alone is not sufficient to disrupt meiotic sister centromere cohesion.

To determine if a reduced ATP level was sufficient to impact overall fertility in these male flies, fertility tests were carried out. RNAi knockdown of ATPsyn-b (52 % ATP reduction) resulted in complete male sterility (figure 5.3), this in line with previous reports indicating that knockdown of ATPsyn-b protein levels led to disrupted spermatogenesis and infertility (Chen *et al.*, 2015). In addition, in the female germ-line ATPsyn-b has been shown to have a role in germ-line stem cell differentiation which is independent of its role in ATP generation (Teixeira *et al.*, 2015). RNAi knockdown of ND-23 (36 % ATP reduction) led to an approximate 80 % reduction in male fertility and no significant difference in male fertility was detected in the ND-51 RNAi knockdown (32 % ATP reduction) (figure 5.3). The whole testis ATP levels and fertility data presented here for ND-23 and ND-51 do not correlate; thus far no additional roles in the germ-line have been identified for these proteins however it is possible that the 80 % reduction in fertility detected in the ND-23 RNAi knockdown is due to an additional function of this protein.

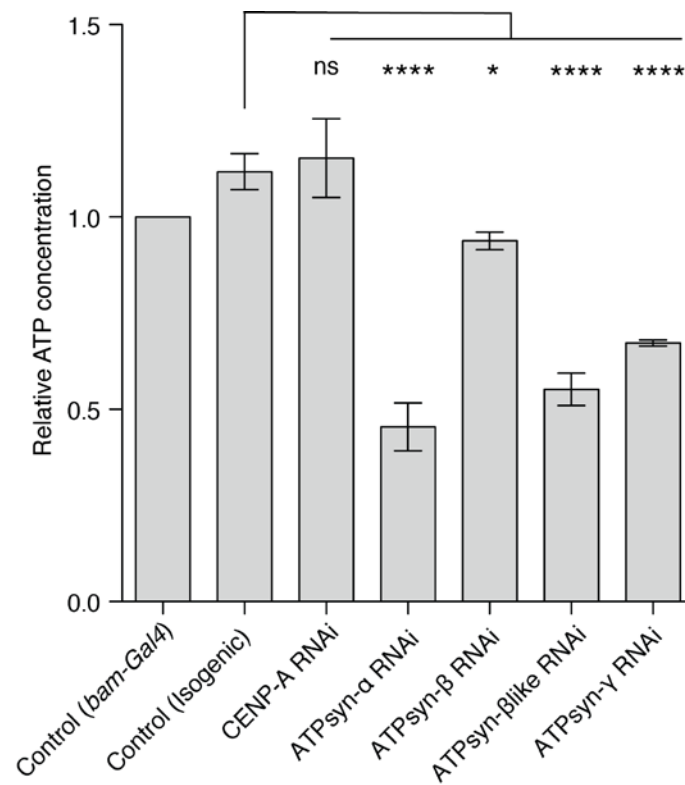


Figure 5.1 Whole testes ATP levels after RNAi knockdown relative to the *bam-Gal4* control line. Error bars represent standard error of the mean. **** $p < 0.0001$, * $p < 0.05$ and ns represents $p > 0.05$.

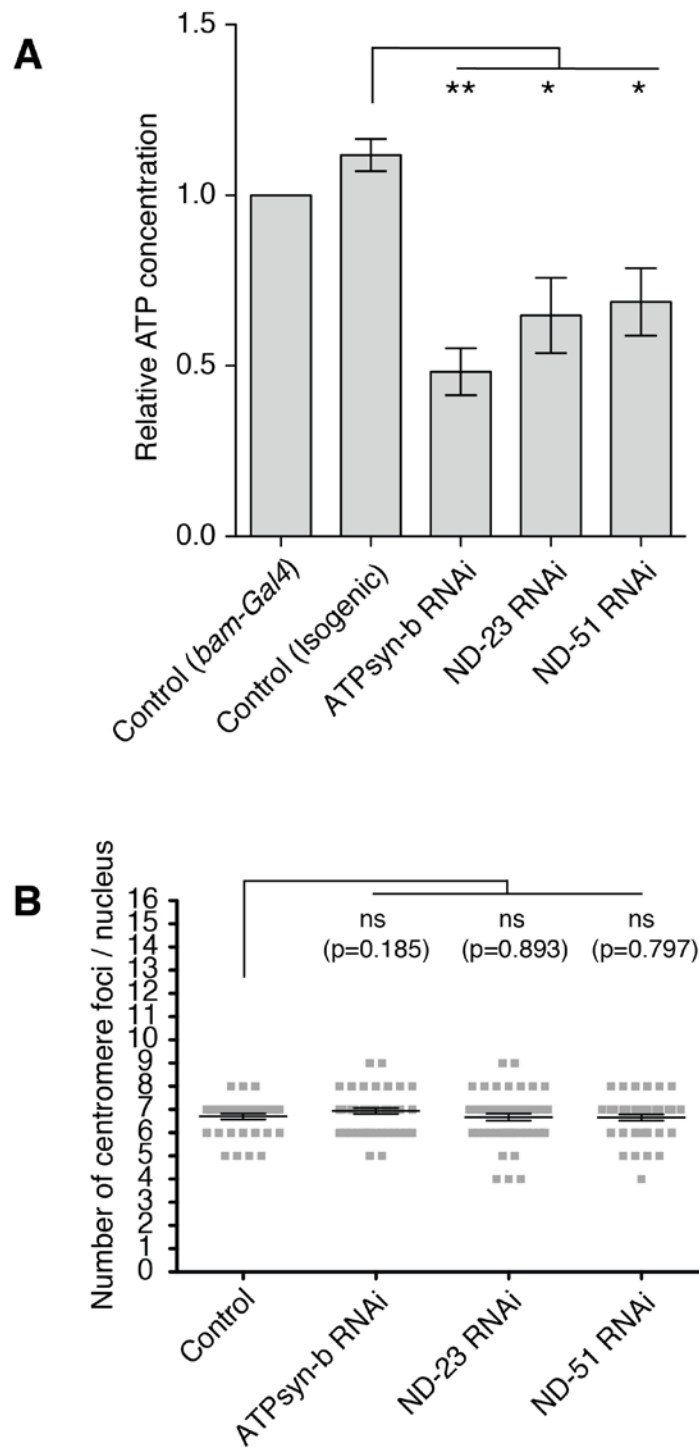


Figure 5.2 Knockdown of ATP levels in the testes. (A) Whole testis ATP level after RNAi knockdown. Values are normalised to the *bam-Gal4* control line. Error bars represent standard error of the mean. ** $p < 0.01$ and * $p < 0.05$. (B) Quantification of the number of centromeric foci per late prophase I nucleus the ATPsyn-b, ND-23 and ND-51 RNAi knockdowns. $n = 100$ nuclei and ns represents $p > 0.05$.

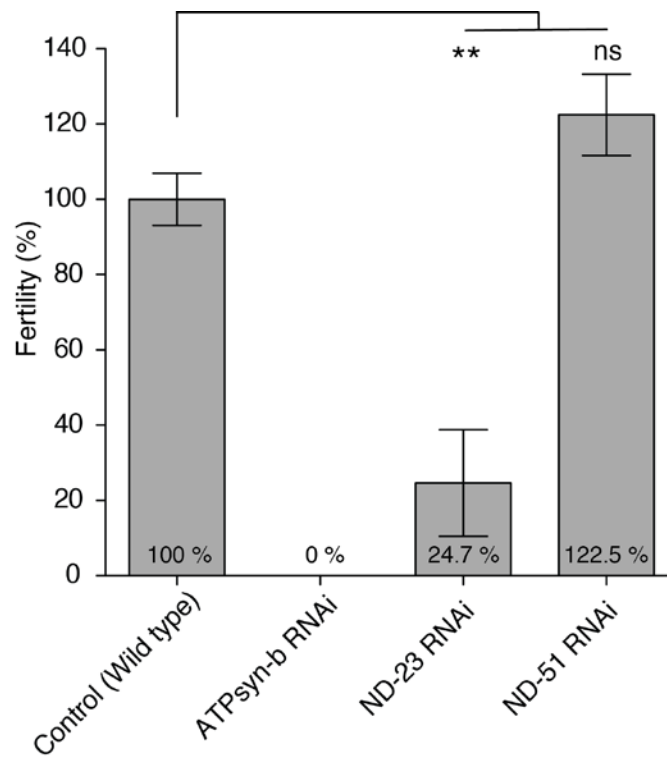


Figure 5.3 Male fertility after RNAi knockdown of ATPsyn-b, ND-23 and ND-51. Fertility is represented as a percentage (indicated) of the control. Error bars represent the standard error of the mean. ** $p < 0.01$ and ns represents a $p > 0.05$.

5.3. Analysis of ATP synthase F1 subunit localisation in the germ-line

The localisation of ATPsyn- α , - β , and - γ was assessed in meiotic prophase I cells using commercially available antibodies. As shown in figure 4.6, ATPsyn- α , - β , and - γ are abundantly present throughout the cytoplasm in the mitochondria. To determine if these subunits localise to the nucleus a cytoplasmic extraction was carried out followed by immuno-staining of the remaining nuclear fraction. Using this method to detect ATPsyn- α , - β , and - γ it was possible to detect nuclear and centromeric signals (not shown), however the signal detected was very weak and results obtained were not reproducible. This may be due to the sensitivity of these antibodies, the level of the endogenous proteins in the nucleus and/or the effect of the cytoplasmic extraction process.

To study the localisation of ATPsyn- β like in meiotic cells an anti-ATPsyn- β like antibody was generated against two specific ATPsyn- β like peptides (methodology section 2.2.5, p 61). To test for specificity, this antibody was used to immunostain adult testes after RNAi knockdown of ATPsyn- β like, a reduction in ATPsyn- β like signal was observed after RNAi compared to controls (figure 4.6). By immunofluorescence microscopy it was identified that ATPsyn- β like is expressed in the germ-line where it co-localises with ATPsyn- α in the mitochondria (figure 5.4 A). The level of ATPsyn- β like in the cell was observed to increase as meiosis prophase I progresses as indicated in figure 5.4 where higher levels of ATPsyn- β like were observed at late prophase I compared to cells at early prophase I. To determine if ATPsyn- β like localises to the nucleus and/or the centromere a cytoplasmic extraction was carried out during fixation (as described in chapter 2.5.5). Nuclei were then co-stained with ATPsyn- β like, DAPI and CENP-C. During late prophase I, many ATPsyn- β like foci were observed throughout the nucleus and in the nucleolus (figure 5.4 B). Several of these foci were observed to co-localise with CENP-A at centromeres.

As was the case with immuno-staining with commercial antibodies recognising ATPsyn- α , - β , and - γ it was unclear how much of the anti-ATPsyn- β like signal was an artefact produced by the cytoplasmic extraction process. In addition, the level of ATPsyn- β like in the nucleus appeared quite low and was not always visible at every centromere. Thus, to confirm centromeric localisation by an alternative method, visualisation was also carried out using a transgenic fly line expressing an N-terminally GFP-tagged ATPsyn- β like transgene.

GFP-ATPsyn- β like was initially characterised by over-expression in *Drosophila* S2 cells following transient transfection. Cytoplasmic and nuclear localisations were then assessed by anti-ATPsyn- α and anti-CENP-A immuno-staining. In S2 cells GFP-ATPsyn- β like foci are present in the cytoplasm, however these foci do not co-localise with the mitochondrial ATPsyn- α signal indicating that GFP-ATPsyn- β like is not transported into the mitochondria (figure 5.5 A). The mitochondrial transport signal (MTS) that transmits ATPsyn- α , - β and β like to the mitochondria is N-terminally located. *In vivo*, following mitochondrial processing this site is cleaved and the mature protein is then transmitted to the inner mitochondrial membrane. In the case of N-terminally tagged GFP-ATPsyn- β like it is likely that the N-terminally located GFP-tag disrupts this process and inhibits efficient mitochondrial transport. However, transport of GFP-ATPsyn- β like (N-terminus unprocessed) to the nucleus does not appear to be disrupted and after transient transfection to S2 cells clear co-localisation of GFP-ATPsyn- β like was observed with CENP-A at centromeres (figure 5.5.B).

In vivo GFP-ATPsyn- β like was placed under the control of its endogenous promoter sequences. As was the case in S2 cells, it appears that GFP-ATPsyn- β like is not processed correctly for mitochondrial transport, as GFP-ATPsyn- β like foci in the cytoplasm did not co-localise with ATPsyn- α in the mitochondria (data not shown). However, after extraction of the cytoplasmic signal, GFP-ATPsyn- β like was observed co-locating with CENP-

A at centromeres (figure 5.6 a). Throughout meiosis, GFP-ATPsyn- β like was visible at centromeres in early and late prophase I nuclei as well as after the first meiotic division during interphase I. To quantify centromeric localisations of ATPsyn- β like we carried out Pearson Coefficient of Correlation analysis and observed a coefficient of $0.5473 \pm \text{sd } 0.0896$ (figure 5.6 b). A coefficient of > 0.5 indicates co-localisation. Co-localisation of GFP-ATPsyn- β like with CENP-A at centromeres was not apparent in the differentiating spermatid (figure 5.6 a).

Using this GFP-ATPsyn- β like transgene it was possible to partially rescue the centromeric cohesion defect previously observed in the ATPsyn- β like P element heterozygote mutant (figure 5.7). This suggests that at least in the case of the proposed nuclear function of this transgene, function is not affected by the presence of the fluorescent tag. It was not determined if a rescue of ATP levels was possible. Since GFP-ATPsyn- β like does not localise to the mitochondria this seems unlikely.

5.4. Recruitment of GFP-ATPsyn- β like to meiotic centromeres

Previous studies have shown that centromeric assembly of CENP-A occurs during meiosis prophase I (Dunleavy *et al.*, 2012; Raychaudhuri *et al.*, 2012; Kwenda *et al.*, 2016). Given the functional link between these two proteins we hypothesised that CENP-A may be responsible for directing GFP-ATPsyn- β like to the centromere. To test this, *gfp-ATPsyn- β like* was crossed into a genetic background containing a UAS-*cenp-a* RNAi hairpin. Upon activation of CENP-A RNAi in this line the nuclear localisation of GFP-ATPsyn- β like became disrupted. GFP-ATPsyn- β like became dispersed throughout the nuclear territories and the colocalisation at the centromere with CENP-A became less apparent indicating that CENP-A maybe required to recruit GFP-ATPsyn- β like (figure 5.8)

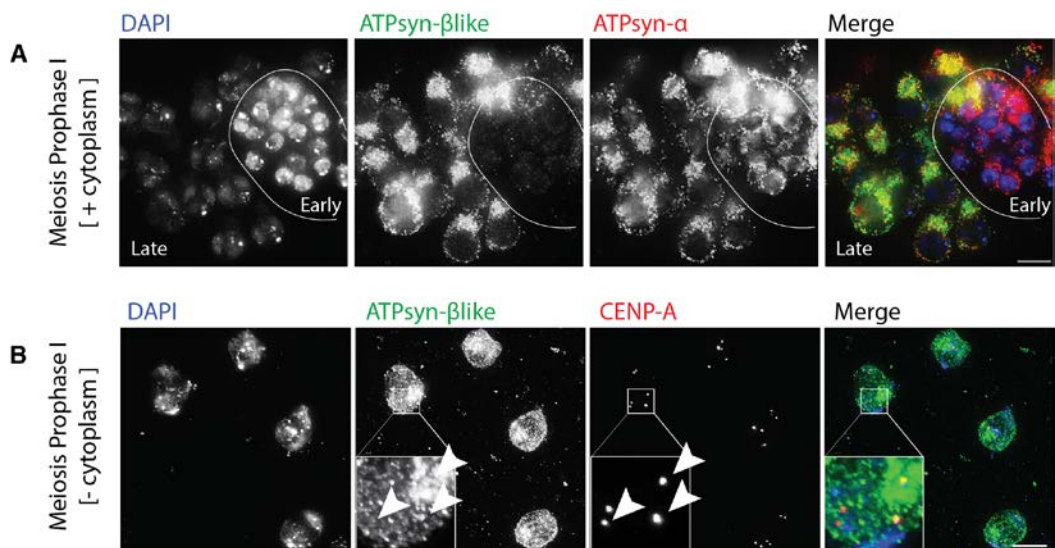


Figure 5.4 Localisation of ATPsyn-βlike in male meiotic cells. (A) Early and late prophase I cells (indicated) stained with anti-ATPsyn-βlike (green) and anti-ATPsyn-α (red) antibodies. (B) Late prophase I nuclei, with the cytoplasmic fraction extracted, nuclei stained with anti-ATPsyn-βlike (green) and anti-CENP-A (red) antibodies. Centromeric co-localisation of ATPsyn-βlike and CENP-A is expanded and visible in yellow and indicated (arrowheads). The scale bar represents 10 μm.

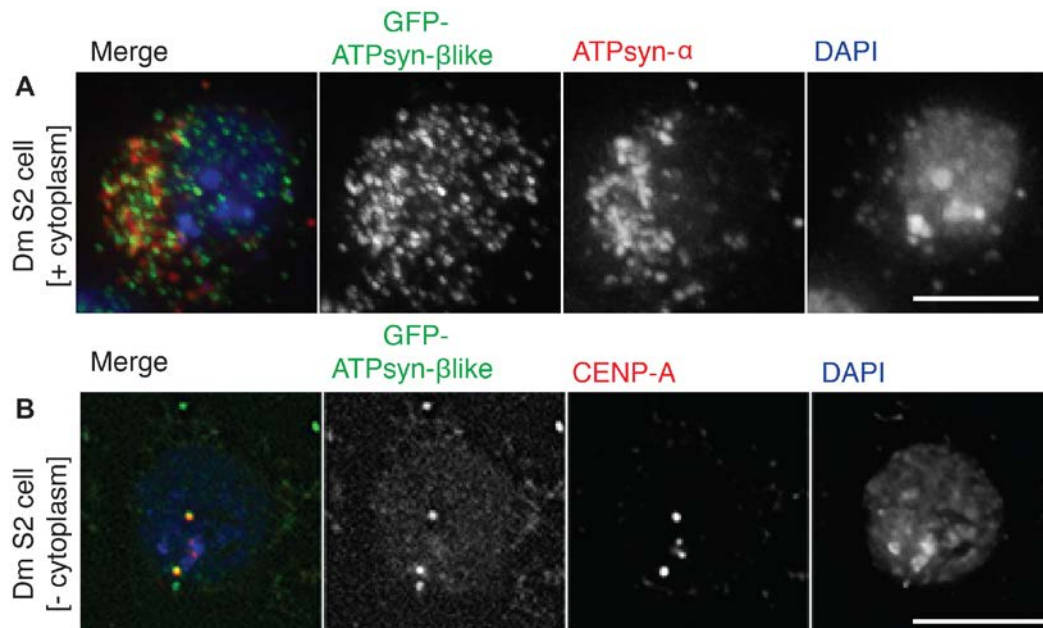


Figure 5.5 Overexpression of GFP-ATPsyn-βlike in Drosophila S2 cells. (A) S2 cells expressing GFP-ATPsyn-βlike (green), co-stained with anti-ATPsyn-α (red) antibodies. (B) S2 cell nuclei, with the cytoplasmic fraction extracted. Cells expressing GFP-ATPsyn-βlike (green) and the nuclei were co-stained with rabbit anti-CENP-A; Rabbit anti-CENP-A antibody was detected using a goat anti-rabbit secondary conjugated to Alexa 647. The scale bar represents 10 μm.

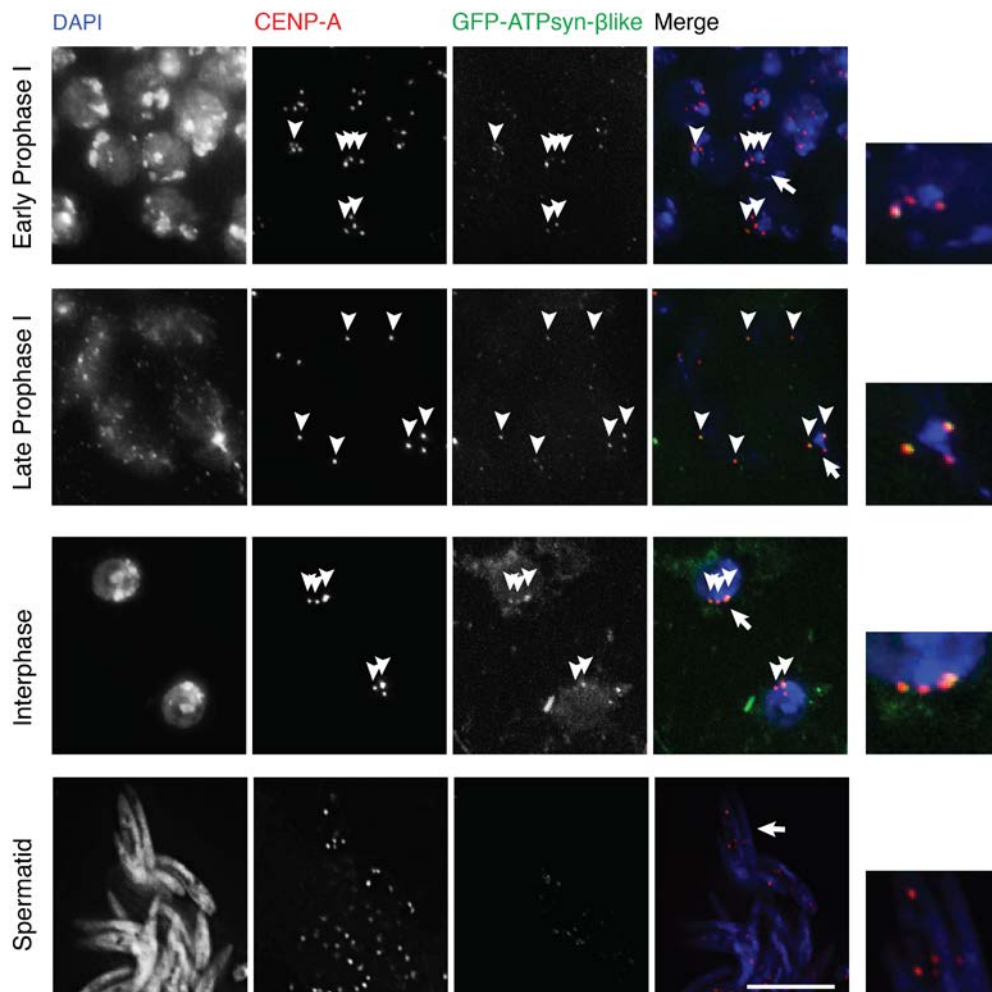


Figure 5.6 (a) Centromeric localisation of GFP-ATPsyn- β like during meiosis. Transgenic GFP-ATPsyn- β like (+/+) adult testes co-stained with rabbit anti-CENP-A antibodies (rabbit anti-CENP-A antibody was detected using a goat anti-rabbit secondary conjugated to Alexa 647). Arrowheads indicate co-localisation of CENP-A and ATPsyn- β like and arrows indicate amplified panel. The scale-bar represents 10 μ m. (B) Graph indicating correlation

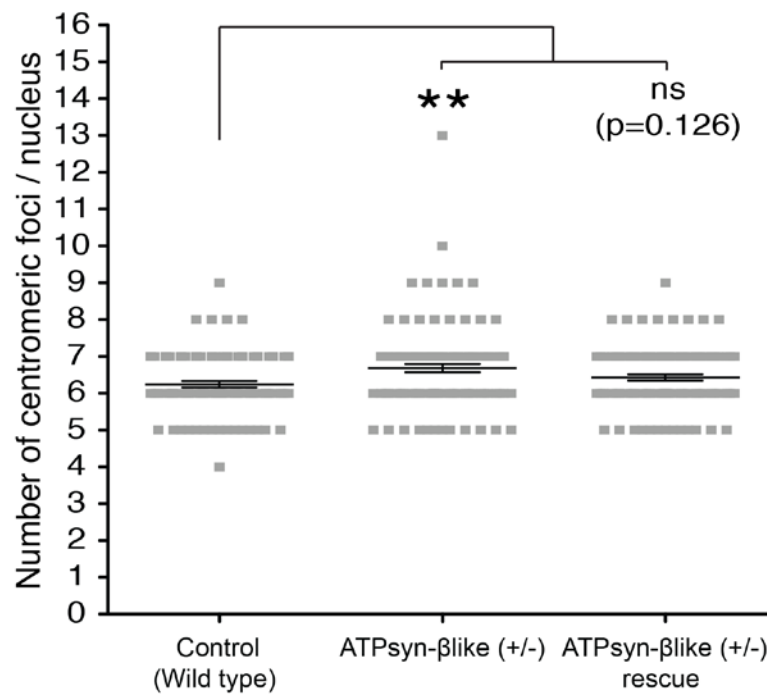


Figure 5.7 Quantification of the number of centromeric foci in control, *ATPsyn-βlike (+/-)* and *ATPsyn-βlike (+/-)* rescue. The line and error bars represent the mean and standard error of the mean respectively. ** $p < 0.01$ and ns represents a $p > 0.05$.

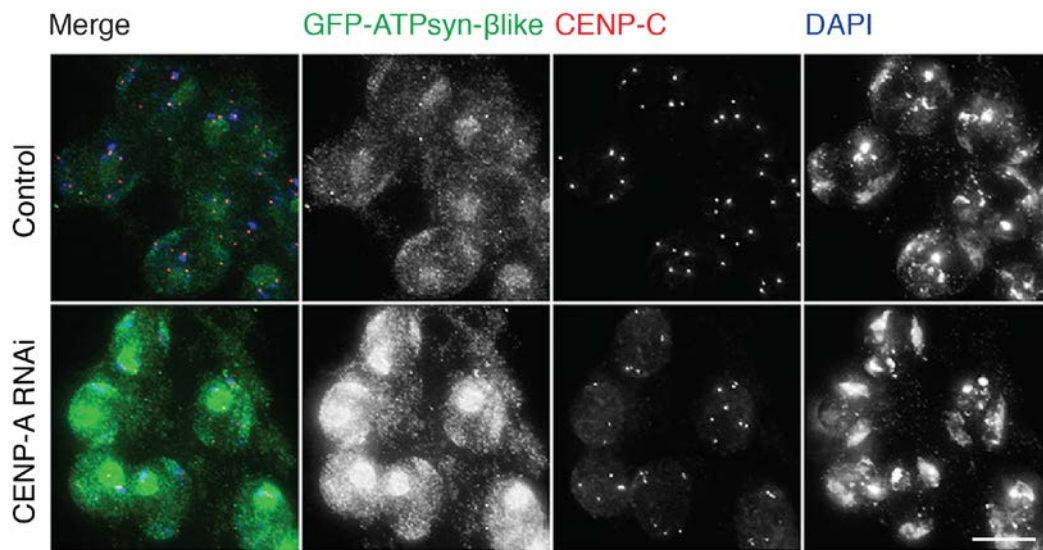


Figure 5.8 RNAi knockdown of CENP-A in a *GFP-ATPsynβlike* genetic background. Representative micrograph of control (*GFP-ATPsynβlike/UAS-cenp-a*, parent line) and RNAi knockdown (*GFP-ATPsynβlike/UAS-cenp-a* crossed to *bam-Gal4* driver). Cells co-stained with anti-GFP (green) and anti-CENP-C (red) antibodies, DNA is stained with DAPI (blue). The scale bar represents 10 μm .

5.5. ATPsyn- α directly interacts with CENP-A in vitro

In vitro interaction assays were carried out in order to determine if the previously identified protein interaction between CENP-A and the ATP synthase F₁ subunits is directly mediated and to test if recruitment of GFP-ATPsyn- β like to the centromere by CENP-A may be due to a direct interaction. To do this GST-CENP-A and HIS-tagged ATPsyn- α , - β and - β like were recombinantly produced in bacterial cells, allowed a period of interaction in a high salt buffer and then GST-CENP-A was purified using GST-agarose beads. *In vitro*, HIS-ATPsyn- α was specifically co-precipitated with GST-CENP-A (but not GST control) as was revealed by anti-HIS western blot. Neither HIS-ATPsyn- β nor HIS-ATPsyn- β like were precipitated in the presence of GST-CENP-A indicating that *in vitro* these proteins do not directly interact with CENP-A (figure 5.9). An interaction assay was not carried out for the ATPsyn- γ subunit due a difficulty in solubilising this protein.

To map the site of interaction between ATPsyn- α and CENP-A to specific CENP-A amino acids, a peptide spot array (18 peptides/spot) encompassing the entire protein sequence of the CENP-A N-terminus was generated (by the laboratory of Dr. P Kiely). This array was then probed using recombinantly produced HIS-ATPsyn- α , interaction sites were revealed by anti-HIS western blotting. A direct peptide interaction was detected between ATPsyn- α and amino acids 29-54 and 73-90 of the CENP-A N-terminus (figure 5.10). Interestingly, these amino acids correspond to the conserved sequence blocks, of previously unknown function, which are located on the CENP-A N-terminus. The CENP-A peptide array was also probed with HIS-ATPsyn- β and after anti-HIS western blotting no direct interaction between CENP-A and HIS-ATPsyn- β was detected. Furthermore, to control for non-specific binding of primary (anti-ATPsyn- α antibody) and secondary (Goat anti-mouse-HRP) antibodies peptide arrays were analysed

by western blotting in the absence of recombinant protein interaction, no non specific binding was detected (data not shown).

5.6. Conserved sequence blocks on the CENP-A N-terminus are required to interact with ATPsyn- α

The results presented in this chapter thus far support a model in which an alternative ATPsyn- α /ATPsyn- β like F₁ complex is recruited to the centromere by CENP-A and that this recruitment is mediated via a direct interaction between the ATPsyn- α subunit and conserved sequence blocks located on the CENP-A N-terminus. To validate this hypothesis *in vivo* we assessed if the expression of an N-terminally truncated version of GFP-CENP-A disrupted centromeric cohesion dynamics during meiosis.

GFP-CENP-A- Δ 118 is an N-terminally tagged CENP-A transgene lacking its first 118 amino acids (figure 5.11 A); *in vivo* its expression is controlled by the endogenous *cenp-a* promoter sequences. GFP-CENP-A- Δ 118 localises to both mitotic and meiotic centromeres *in vivo* (as discussed in chapter 3). A full length GFP-CENP-A transgene (GFP-CENP-A-FL), tagged internally between amino acids 118 and 119 and also placed under the expression of the endogenous *cenp-a* promoter was used as the control in this experiment. This full-length transgene also localises to the centromere during both meiosis and mitosis and has been previously shown to complement a *cenp-a* null phenotype (Schuh et al., 2007).

To determine if GFP-CENP-A- Δ 118 expression (in wild type CENP-A background) has a dominant negative effect on the maintenance of centromeric cohesion during meiosis, testis were immuno-stained with anti-GFP and anti-CENP-C and the number of centromeric foci per late prophase I nucleus was determined. The number of centromeric foci in the GFP-CENP-A- Δ 118 fly-line was compared to flies expressing GFP-CENP-A-FL and to the WT (*y+ry+*).

As has been shown previously, in WT (*y+ry+*) flies an average of 6.41 centromeres was observed per nucleus at late prophase I (figure 5.11). Flies expressing a single copy of the control *gfp-cenp-a-fl* (+/-) displayed an average of 6.63 centromeres per nucleus and flies expressing two copies of *gfp-cenp-a-fl* (+/+) had an average of 6.68 centromeres per nucleus, significantly more ($p < 0.05$) than what was observed in the WT (*y+ry+*) (figure 5.11). Thus, in the control *gfp-cenp-a-fl* fly line it appears that the presence of the GFP-tag alone is disrupting CENP-A function and having a dose dependent, dominant negative effect on centromeric cohesion maintenance.

GFP-CENP-A- Δ 118 was also found to induce a dominant negative effect on centromeric cohesion maintenance however in the case of this N-terminally truncated GFP-CENP-A the observed defect was significantly ($p < 0.01$) more severe than that observed for the control *gfp-cenp-a-fl*. In *gfp-cenp-a- Δ 118* (+/-) flies an average of 6.80 centromeric foci were detected per nucleus, *gfp-cenp-a- Δ 118* (+/+) flies displayed an average of 7.09 centromeres per nucleus (figure 5.11).

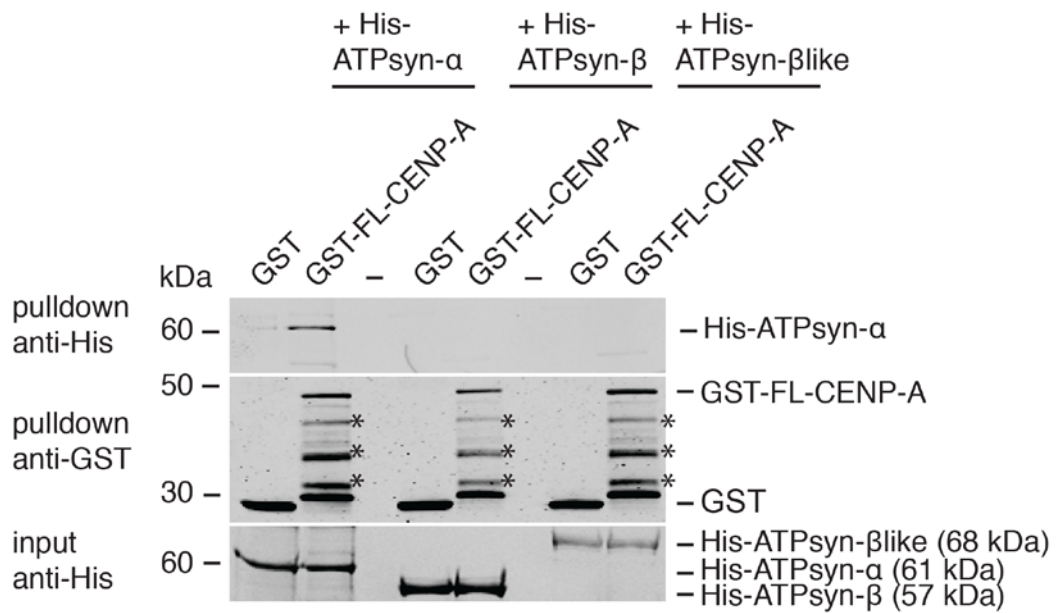


Figure 5.9 *In vitro* direct protein interaction assay. Input panel immuno-stained with anti-poly-HIS antibody detecting His-ATPsyn- α , - β and - β like (molecular weights indicated). Pull-down panel immuno-stained with anti-GST antibodies and detecting GST only control (30 kDa) and GST FL-CENP-A (49 kDa). Pull-down panel immuno-stained with anti-poly-HIS antibody, the presence ATPsyn- α in GST-CENP-A pull-down is indicated. Asterisks indicate protein degradation products.

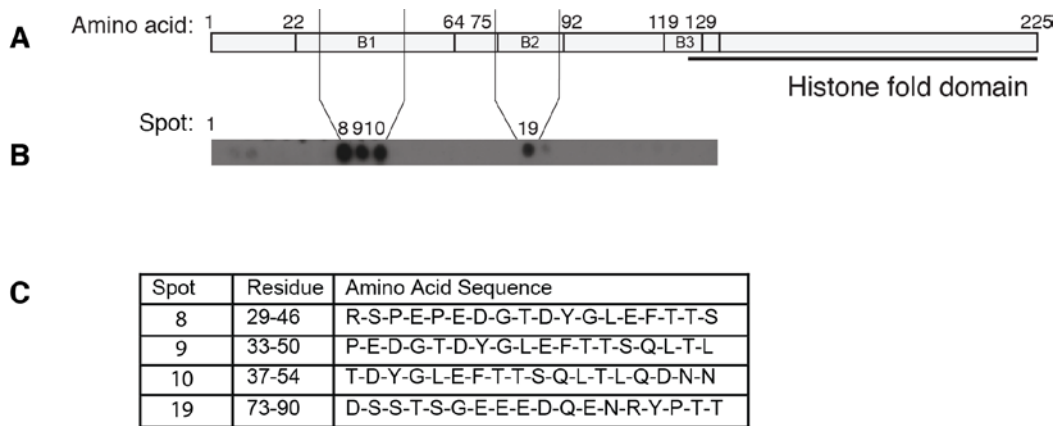


Figure 5.10 Peptide interaction mapping array. (A) Schematic representing the amino acid locations of the histone fold domain and the conserved sequence blocks of the CENP-A N-terminus. (B) HIS-ATPsyn- α binding to the CENP-A N-terminal peptide array as revealed by anti-poly HIS immuno-staining; spots positive for an interaction are indicated, $n=3$ and three independent peptide array membranes were used. (C) A table indicating the residues corresponding to spots positive for interaction - 8, 9, 10 and 19.

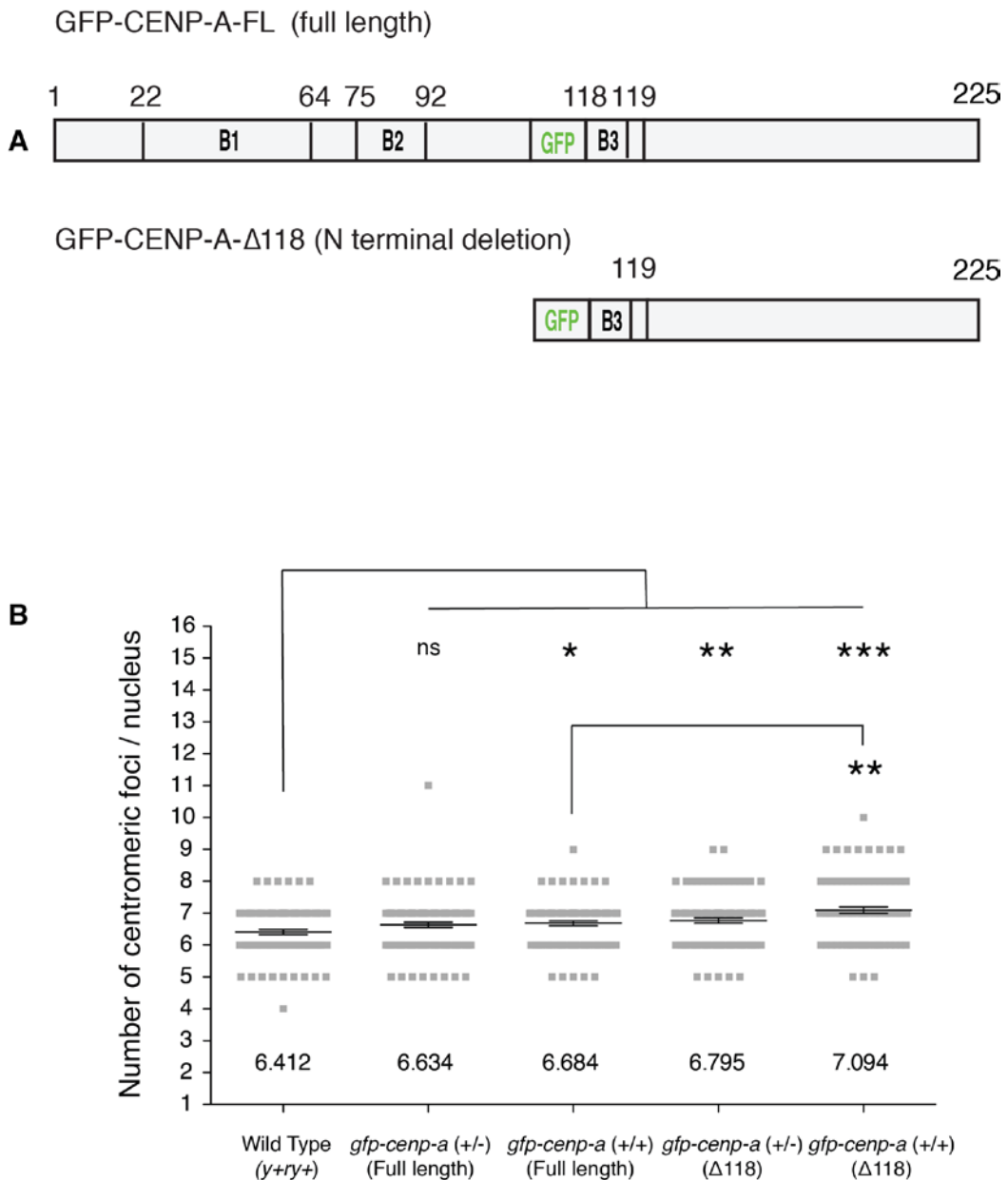


Figure 5.11 Analysis of the effect of GFP-CENP-A-Δ118 expression on centromeric cohesion in late prophase I nuclei. (A) A schematic illustrating the position of GFP on control and N-terminally deleted (Δ118) GFP-transgenes. (B) A quantification of the number of centromeric foci per nucleus in WT (*y+ry+*), control GFP-CENP-A-FL heterozygotes and homozygotes and GFP-CENP-A-Δ118 homozygotes and heterozygotes. The average number of centromeric foci per nucleus is indicated, data pooled from 3 independent RNAi experiments, n=100 nuclei. ***p<0.001, **p<0.01, *p<0.05 and ns is a p>0.05.

Summary

A summary of the major results presented in chapter 5:

1. Whole testes ATP levels are reduced after RNAi knockdown of ATPsyn- α , - β like and - γ , however a reduced ATP level alone is not sufficient to disrupt chromatid cohesion during meiosis.
2. In the testes, ATPsyn- β like fulfills the role of canonical ATPsyn- β ; it localises to mitochondria and is required for ATP synthesis.
3. In germ cells, ATPsyn- β like is present in the nucleus and at the centromere. Inhibition of CENP-A loading during prophase I disrupts GFP-ATPsyn- β like localisation.
4. Conserved sequence blocks within the CENP-A N-terminal tail mediate a direct interaction between CENP-A and ATPsyn- α *in vitro*. *In vivo*, the CENP-A N-terminus is required for centromere cohesion during meiotic prophase I.

5.7. Discussion

As part of this study we have identified two functions of the testes specific paralogue of ATPsyn- β , ATPsyn- β like. Firstly, ATPsyn- β like, present in mitochondria in the germ-line is required for ATP synthesis. ATP determination after RNAi knockdown suggests that ATPsyn- β like fulfills the function of its canonical paralogue ATPsyn- β which is normally down-regulated in the germ-line. Given the localisation and sequence similarities between ATPsyn- β and ATPsyn- β like this function is not surprising. Secondly, we have shown that ATPsyn- β like (as well as ATPsyn- α and - γ) is required to establish and maintain sister chromatid cohesion during meiosis.

Interestingly, knockdown of ATPsyn- β like in the testes resulted in a 45 % reduction in ATP levels and a meiotic arrest at prometaphase/metaphase I, knockdown of ATPsyn- α produced a 55 % reduction in ATP levels and in this instance meiosis proceeded and mature sperm were produced. Thus, there was no correlation between the level of ATP reduction in the testes and the severity of the chromatid cohesion defect suggesting that these two phenotypes are unrelated. Indeed, this independent function was confirmed by alternatively reducing ATP levels in the testes (by 52 %) and observing no detrimental effects on sister chromatid cohesion throughout meiosis.

In addition to its mitochondrial localisation we have shown by anti-ATPsyn- β like immunofluorescence microscopy and by production of a GFP-ATPsyn- β like transgenic fly line that ATPsyn- β like localises to the nucleus. Furthermore by co-staining with centromeric markers CENP-A and CENP-C we have determined that both ATPsyn- β like and GFP-ATPsyn- β like localise to centromeres. We find that inhibition of meiotic prophase I loading of CENP-A disrupts GFP-ATPsyn- β like nuclear localisation. Using *in vitro* interaction assays we have found that this interaction between CENP-A and ATPsyn- β like is not directly mediated. However, a direct interaction was identified between CENP-A and the ATPsyn- α subunit of the F₁ complex. Unfortunately, we have been unable to reproducibly localise ATPsyn- α or - γ at the centromere during meiosis, this may be due to the difficulty of visualizing a small nuclear fraction beneath a large cytoplasmic signal. Despite this, the direct interaction between CENP-A and ATPsyn- α and the observation that ATPsyn- β like localises to the centromere supports our model in which an alternative ATPsyn- α / β like F₁ complex is formed in the germ-line.

By mapping the interaction between CENP-A and ATPsyn- α *in vitro* we have identified a possible first function for the conserved sequence blocks located in the CENP-A N-terminus. It is important to note however that the sequences between amino acids 29 and 54 are highly acidic and that the observed interaction could be due to non-specific hydrogen bonding. We

have carried out binding to the peptide array in the presence of recombinant ATPsyn- β and have not detected any interaction. Use of a scrambled control peptide array would be the best control in this instance.

In vivo we have shown that expression of an N-terminally truncated version of GFP-CENPA (in WT background) is sufficient to disrupt centromeric cohesion. These results suggest that *in vivo* the N-terminus of CENP-A is required for the recruitment of the ATPsyn- α/β like F₁ complex to the centromere, in its absence ATPsyn- α/β like cannot localise efficiently and centromeric cohesion is disrupted. In a caveat to these results we question the suitability of the Δ 118-GFP-CENP-A construct due to the N-terminal location of the GFP tag. It is possible that the location of the tag or indeed the presence of the tag itself may be disruption CENP-A function in this instance. Possible alternative experiments are discussed in section 6.5.

6. Discussion

6.1. A brief summary of major findings

In chapters 3 – 5 we have presented the results from an investigation into the role of CENP-A and specifically the CENP-A N-terminus during male meiosis in the fruit fly *Drosophila melanogaster*. We have identified that in the germ-line CENP-A interacts with subunits of the ATP synthase F₁ complex by IP and MS. Surprisingly, *in vitro* direct interaction assays as well as peptide array mapping have indicated that this interaction is directly mediated via conserved sequence blocks on the CENP-A N-terminus and the ATPsyn- α subunit of the ATP synthase F₁ complex. We have also identified *ATPsyn- β like*, a testis specific variant of canonical *ATPsyn- β* that is required for ATP synthesis in the germ-line and is essential for fertility.

Analysis of centromere dynamics and integrity after testis specific RNAi knockdown of CENP-A as well as ATPsyn- α , ATPsyn- β like and ATPsyn- γ revealed that both of these nuclear and mitochondrial protein complexes are required to establish and maintain sister chromatid cohesion throughout meiosis. Furthermore, expression of an N-terminally truncated version of CENP-A in the male germ-line (in a *cenp-a* WT background) was sufficient to disrupt sister centromere cohesion at prophase I in a dominant negative fashion. Reduced levels of ATP in the testis were detected after RNAi knockdown of ATPsyn- α , - β like and γ , but this reduction alone not sufficient to induce cohesion defects.

Localisation studies using an anti-ATPsyn- β like antibody revealed that as well as localising to mitochondria as expected, ATPsyn- β like also localises to the nucleus. This nuclear localisation of ATPsyn- β like was confirmed by analysis of a transgenic fly line expressing a GFP-ATPsyn- β like transgene with disrupted mitochondrial processing (N-terminal GFP-tag disrupted mitochondrial processing), which localised efficiently to the nucleus. Co-staining with centromeric markers (CENP-A or CENP-C) revealed that in the nucleus, ATPsyn- β like is present at the centromere and inhibition of CENP-A assembly during meiotic prophase I (by RNAi knockdown) revealed

disrupted nuclear localisation of ATPsyn- β like and reduced levels at the centromere.

6.2. The model

We propose that in the male germ-line, mitochondrial ATP synthase subunits ATPsyn- α , - β like and - γ function in the establishment and maintenance of sister chromatid cohesion and that this role is independent of the canonical role in ATP generation. In addition to the observation of chromatid cohesion defects after RNAi knockdown of these subunits, this model is supported by the presence of ATPsyn- α and - β like in the nucleus in male meiotic cells and the observation that reduced ATP levels in the testis alone are insufficient to disrupt chromatid cohesion.

Based on our findings, we predict that ATPsyn- β like undergoes two pathways of processing once translated in the cytoplasm. Firstly, recognition of an N-terminally located mitochondrial transport signal (MTS) by the mitochondrial transport machinery shuttles ATPsyn- β like to the inner mitochondrial membrane where it is assembled to the ATP synthase F_1 - F_0 complex and functions in oxidative phosphorylation. In addition, the presence of a C-terminally located nuclear localisation signal (NLS) directs import of ATPsyn- β like to the nucleus where it functions in chromatid cohesion (Figure 6.1 and 6.2). We assume that ATPsyn- α also undergoes similar pathways of processing in the cytoplasm, as by anti-ATPsyn- α immuno-staining we have been able to detect ATPsyn- α in both the mitochondria and the nucleus however we have not been able to detect any predicted/putative NLS in *Drosophila* ATPsyn- α .

In the nucleus, we hypothesise that an alternative ATPsyn- α /ATPsyn- β like complex is assembled and that via a direct interaction with the conserved sequence blocks on the CENP-A N-terminus, this complex is recruited to the centromere during meiotic prophase I (Figure 6.2). Interestingly, the heat shock protein HSP60C (a homologue of the bacterial ATP synthase assembly

chaperone groEL (Ryabova *et al.*, 2013)) was identified in our IP and MS experiments as a potential germ-line interactor of CENP-A. This could indicate that HSP60C is also present at the centromere where it may assemble the ATPsyn- α /ATPsyn- β like complex. Interestingly, HSP60C is highly expressed in the testes (Celniker *et al.*, 2009) and has been shown to be essential for male fertility (Sarkar and Lakhotia, 2005).

We have not identified the mechanism of how a centromere located ATPsyn- α / β like complex maintains chromatid cohesion in meiosis. It does seem likely that ATPsyn- α / β like forms the cohesin-independent cohesion complex which has been referred to several times in the literature (Joyce *et al.*, 2012; McKee *et al.*, 2012; Senaratne *et al.*, 2016). One possible model is that ATPsyn- α and ATPsyn- β like form a complex that physically entraps sister chromatids in a fashion analogous to canonical cohesin. As we have seen an interaction between CENP-A and HSP60C, this ATPsyn- α / β like complex may be “loaded” onto chromatin at centromeric regions (and elsewhere). We have observed that ATPsyn- β like is present at centromeres through prophase I and is detectable at centromeres until after anaphase II, consistent with localisation patterns of canonical cohesin subunits. Indeed, after knockdown of ATP synthase subunits ATPsyn- α , - β like and - γ we see a disruption in localisation of the protector of centromeric cohesion MEI-S322 providing a further link between ATPsyn- α , - β like and cohesion. Thus far we have not analysed the effect of depletion of MEI-S322 levels on the localisation of centromeric ATPsyn- α or β like, however it would be interesting to determine if MEI-S322 is required to protect ATPsyn- α / β like at centromeres. Interestingly, we have identified a putative separase cleavage site present near the N-terminus of ATPsyn- β like (Figure 6.1); this may be an interesting avenue of investigation to confirm the mechanism of cohesion establishment and maintenance. Indeed if this site is a true separase cleavage site it indicates that ATPsyn- β like is the *Drosophila* functional homologue of REC8.

We have also observed that ATPsyn- α and ATPsyn- β like are required to maintain sister chromatid cohesion along chromosome arms at several sites including the 1.686 g/cm³ heterochromatic locus (2nd and 3rd chromosomes) and the AATAT satellite located on the 4th chromosome and thus we hypothesise that ATPsyn- α / β like is also recruited to these regions where it may act as an alternative cohesion complex. Interestingly, in preliminary experiments we have identified a direct *in vitro* interaction between ATPsyn- α and histone H3, possibly indicating that the ATP synthase subunits can also interact with canonical chromatin.

There are many questions which remain to be answered regarding the mechanism of cohesion establishment and maintenance of the of ATP synthase subunits in male germ cells. Firstly, does the ATPsyn- α / β like complex form a canonical $\alpha_3\beta_3$ hexamer or does it have an alternative stoichiometry? Does ATPsyn- α / β like cooperate/interact with the other known *Drosophila* cohesion subunits SUNN, SOLO or ORD? Does MEI-S322 localisation to the centromere at PM1 protect the ATPsyn- α / β like complex from the activity of separase? Is the putative separase site detected on ATPsyn- β like a true cleavage site and does this site mediate release of sister centromere cohesion at anaphase II?

6.3. Alternative models

As chromatin cohesion and condensation are two process which are highly dependent on ATP (Alberts *et al.*, 2004) it is possible that the observed phenotypes after RNAi knockdown of ATP synthase subunits are due to or are contributed to in some way by a reduction in the availability of ATP. After alternative knockdown of ATP levels in the testes (by RNAi and drug treatment (not shown)) we have detected no disruption in centromeric cohesion. Yet we have not scored the effect of reduced ATP levels on chromatin compaction or on chromatin arm cohesion.

In section 6.2 we propose a model in which the ATP synthase subunits directly effect cohesion both at the centromere and along chromosome arms by forming an alternative cohesion complex. Alternatively, it is possible that this phenotype arises indirectly as a consequence of a more global defect. Indeed, we have observed defects in chromatin condensation and general organisation after RNAi knockdown of the ATP synthase subunits. Yet, because of the identified direct interaction with CENP-A and for many of the reasons outlined above we prefer a 'direct role' model.

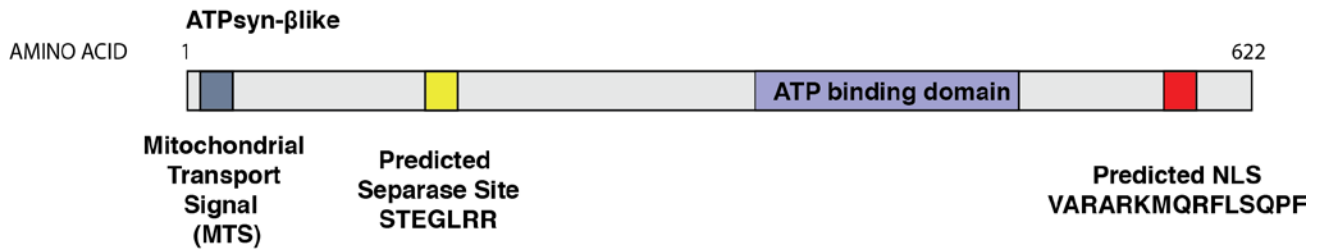


Figure 6.1 Schematic illustrating identified and predicted functional domains in ATPsyn-βlike. Amino acids 1 to 622 are indicated as well as the predicted mitochondrial transport signal (MTS), predicted separase site and the predicted nuclear localisation signal (NLS).

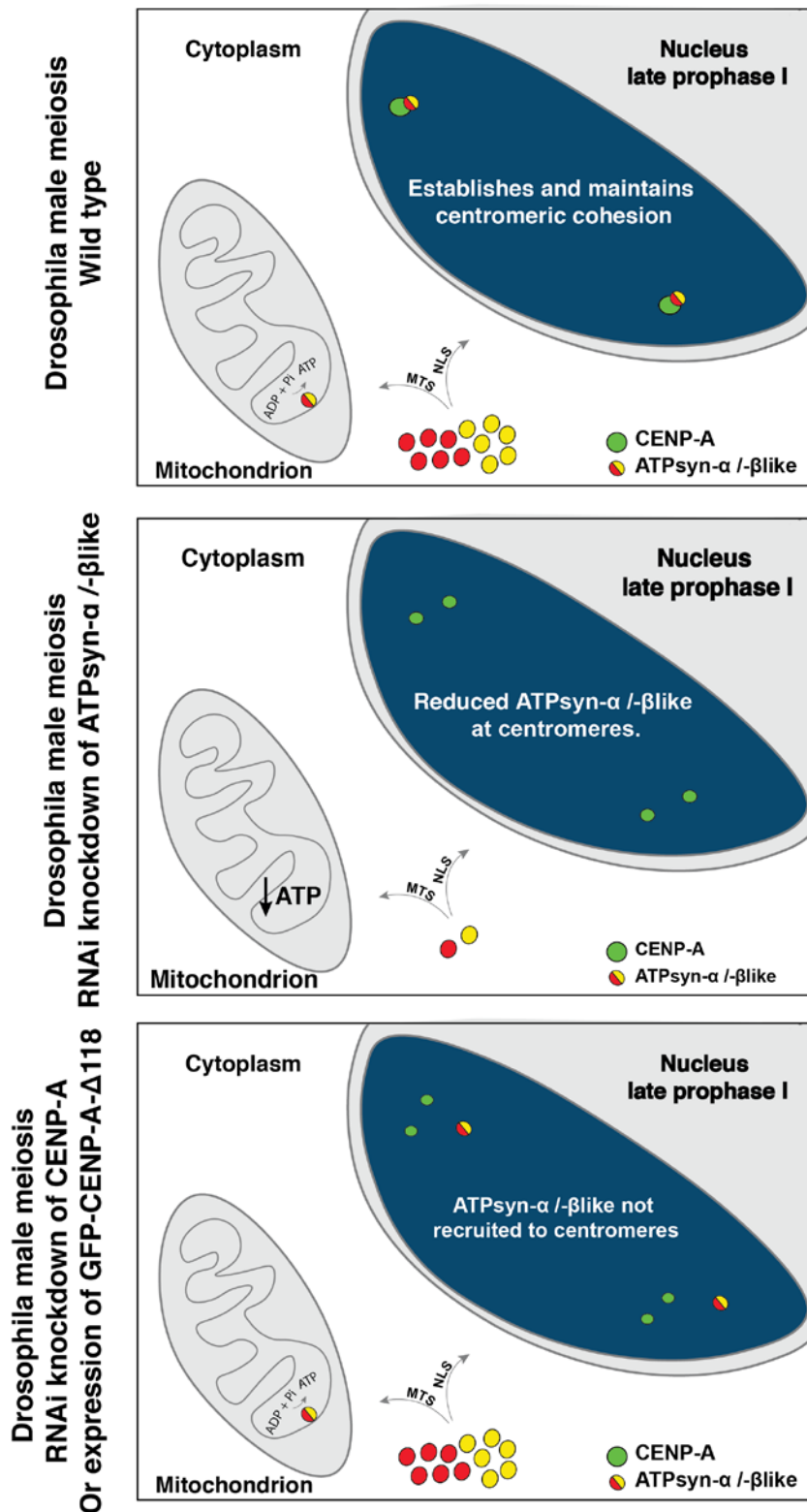


Figure 6.2 Proposed model of cohesion establishment and maintenance by the ATPsyn- α / β like complex.

6.4. Do ATP synthase subunits have novel nuclear roles outside of *Drosophila* male meiosis?

6.4.1 Potential nuclear roles of ATP synthase subunits in *Drosophila* female meiosis?

As discussed in section 1.11.1 recent studies in the female germ-line of *Drosophila* have identified a role for components of the mitochondrial ATP synthase in germ cell differentiation. RNAi knockdown of these subunits in the GSC niche (using *nanos-Gal4* driver) led to an arrest during the pre-meiotic gonial divisions. The Lehmann laboratory have identified that this arrest is related to disrupted mitochondrial cristae formation and propose that it is this failure of mitochondrial maturation which disrupts meiotic progression and furthermore that this role is independent of ATP production.

We have confirmed the results of Teixeira *et al.*, in the female by similar RNAi knockdown of ATPsyn- α , - β and - γ (Dr. Elaine Dunleavy, unpublished). In light of the novel nuclear functions of ATP synthase subunits that we have observed in male meiosis, we hypothesise that similar mechanisms are at play in the female germ-line and that the cell cycle arrest observed in the premeiotic gonial divisions in the female germ-line (Teixeira *et al.*, 2015) may be as a result of pairing and/or chromatid cohesion defects at this stage.

6.4.2 Potential nuclear roles of ATP synthase subunits in *Drosophila* mitosis?

Interestingly, analysis of ATPsyn- β like expression patterns, requirements and evolution has given us many clues regarding potential roles of these subunits outside of *Drosophila* male meiosis. Firstly, transcriptomic data from ModENCODE indicates that as well as its high expression in the male germ-line, ATPsyn- β like is also expressed a several stages throughout

development, including during pupation (Celniker *et al.*, 2009). Interestingly, our analysis of an *ATPsyn-βlike* double knockout mutant revealed that pupae lacking *ATPsyn-βlike* die mid-pupation indicating an essential role for *ATPsyn-βlike* at this time.

Furthermore, we have identified that the *ATPsyn-βlike* gene is present in higher dipteran species and the Lepidopteran species *B. mori* but it is not present in lower Dipteran species such as the mosquito. Interestingly, many higher Dipteran species as well as *B. mori* carryout meiosis in the absence of recombination and chiasmata formation, whereas lower Dipteran species such as the mosquito are not achiasmate. It is possible that the presence of *ATPsyn-βlike* in higher Dipteran and Lepidopteran species is related to achiasmy during their meioses.

Several other publications and screens carried out in *Drosophila* mitotic cells also indicate that ATP synthase subunits may function in the nucleus outside of meiosis. Firstly, it has been shown that *ATPsyn-ε* is required for normal spindle orientation in the syncytial divisions of *Drosophila* embryos (Kidd *et al.*, 2005). In addition, affinity purification of CENP-A nucleosomes from *Drosophila* cultured cells (S2) identified ATP subunits *ATPsynCF6* and *ATPsyn-O* (the OSCP) among 86 proteins which are specifically enriched at centromeres (Barth *et al.*, 2015) and *ATPsyn-α*, *ATPsynβ* and *ATPsyn-γ* were identified amongst approximately 1800 genes associated with the centromere in 9 different purifications from *Drosophila* cultured cells (Barth *et al.*, 2014). Interestingly, components of the ATP synthase complex have also been identified in protein screens to detect chromatin interacting proteins in the African clawed frog *X. laevis*, possibly indicating that an alternative nuclear function for ATP synthase subunits may be conserved outside of insects (Funabiki, Constanzo)

6.4.3 Potential roles in chromatid cohesion and/or homologue pairing in somatic cells

Our analysis of meiotic defects in the male germ-line after RNAi knockdown of ATP synthase subunits ATPsyn- α , - β and - γ has identified that these subunits play a role in sister chromatid cohesion. We have not observed a specific defect of homologue pairing. However, homologue pairing defects in this system are not entirely obvious due to the normal loss of pairing which occurs at centromeres, euchromatin and most heterochromatic sites at mid prophase I. We have analysed a known pairing site on the 4th chromosome using FISH (AATAT site) and observed an increase on the number of AATAT foci per nucleus after RNAi knockdown of ATPsyn- α , ATPsyn- β and ATPsyn- γ . However, the AATAT locus is also a site of strong cohesion retention so it was not possible to distinguish between defects of pairing and or cohesion. We have not analysed X-Y pairing in our RNAi knockdowns. FISH analysis using a probe recognising the X-Y pairing site within the rDNA repeats (240bp repeat) in combination with probes allowing differentiation between both the X and Y chromosomes would allow for dissection of pairing and/or cohesion defects in male meiosis.

As alluded to in section 1.9 p. 47, several similarities have been observed between the mechanisms and proteins involved in homologue pairing and sister chromatid cohesion in both somatic and germ cells in *Drosophila* (Joyce *et al.*, 2012; McKee *et al.*, 2012; Senaratne *et al.*, 2016) Interestingly, a recent RNAi screen of 14,000 *Drosophila* genes identified approximately 400 genes that either inhibited or promoted somatic pairing in *Drosophila* cultured cells (Kc₁₆₇). Interestingly, ATPsyn-b, ATPsyn- β and ATPsyn- γ as well as the centromeric proteins CENP-A, CAL1 and CENP-C were amongst genes identified (Joyce *et al.*, 2012).

6.5. A meiotic role for the *Drosophila* CENP-A N-terminus in centromere assembly

We aimed to determine if the N-terminus of CENP-A is specifically required for centromeric assembly of CENP-A during male meiosis in *Drosophila*. Thus far preliminary analysis of a GFP-CENP-A N-terminal mutant lacking

the first 118 amino acids has not revealed any centromeric loading defects in either mitosis or prophase I loading in meiosis. We have not analysed loading of GFP-CENP-A Δ 118 in the centromeric assembly which occurs after exit from meiosis in the early spermatid, considering that this loading occurs in the absence of centromeric CAL1 and at a time when centromeric CENP-C levels are reducing an alternative mechanism of CENP-A loading at this time, which is dependent on the N-terminus may occur. This Δ 118-GFP-CENP-A mutant may also be useful for analysing the role of the N-terminus during CENP-A retention on differentiating spermatids during protamine exchange. Indeed, preliminary experiments using a GFP-CENP-A- Δ 126 mutant indicate that the N-terminus of CENP-A may be important for the retention of CENP-A on maturing sperm (data not shown).

Analysis of centromeric cohesion in GFP-CENP-FL and GFP-CENP-A- Δ 118 transgenic fly lines revealed defects in both our control (FL) and deletion (Δ 118), indicating that the presence of the GFP-tag interferes with CENP-A function. This result is not entirely surprising given that a 238 amino acid fluorescent tag is placed within a 225 amino acid protein. To conduct a more precise and potential fully functional of the role of the CENP-A N-terminus, CRISPR mediated insertion of a small tag (e.g. 3xFLAG) at the endogenous *cenp-a* locus would be more beneficial. This would remove any concern regarding negative effects of the GFP-tag and of an overexpression induced by introducing additional copies of *cenp-a*.

7. Bibliography

- Alberts, B. Johnson, A. Lewis, J. Morgan, D. Raff, M. Roberts, P. Walter, P. (2014) 'Molecular Biology of the Cell, Sixth Edition. Garland Science.
- Allshire, R. C. and Karpen, G. H. (2008) 'Epigenetic regulation of centromeric chromatin: old dogs, new tricks?', *Nature Reviews Genetics*, 9(12), pp. 923–937
- Amor, D. J. and Choo, K. H. A. (2002) Neocentromeres: Role in Human Disease, Evolution, and Centromere Study', *Am. J. Hum. Genet*, 71, pp. 695–714.
- Bailey, A. O. *et al.* (2013) 'Posttranslational modification of CENP-A influences the conformation of centromeric chromatin', *Proceedings of the National Academy of Sciences*, 110(29), pp. 11827–11832.
- Bannister, A. J. and Kouzarides, T. (2011) 'Regulation of chromatin by histone modifications', *Cell Research*. Nature Publishing Group, 21(3), pp. 381–395.
- Barth, T. K. *et al.* (2014) 'Identification of novel Drosophila centromere-associated proteins', *Proteomics*, 14(19), pp. 2167–2178.
- Barth, T. K. *et al.* (2015) 'Identification of Drosophila centromere associated proteins by quantitative affinity purification-mass spectrometry', *Data in Brief*, 4, pp. 544–550.
- Bassett, E. A. *et al.* (2012) 'HJURP uses distinct CENP-A surfaces to recognize and to stabilize CENP-A/histone H4 for centromere assembly.', *Developmental cell*. NIH Public Access, 22(4), pp. 749–62.
- Baudat, F., Imai, Y. and de Massy, B. (2013) 'Meiotic recombination in mammals: localization and regulation', *Nature Reviews Genetics*. Nature Research, 14(11), pp. 794–806.
- Black, B. E. *et al.* (2004) 'Structural determinants for generating centromeric chromatin', *Nature*. Nature Publishing Group, 430(6999), pp. 578–582.
- Black, B. E. *et al.* (2007) 'Centromere Identity Maintained by Nucleosomes Assembled with Histone H3 Containing the CENP-A Targeting Domain', *Molecular Cell*, 25(2), pp. 309–322.
- Black, B. E. and Bassett, E. A. (2008) 'The histone variant CENP-A and centromere specification', *Current Opinion in Cell Biology*, 20(1), pp. 91–100.
- Blattner, A. C. *et al.* (2016) 'Separase Is Required for Homolog and Sister Disjunction during Drosophila melanogaster Male Meiosis, but Not for Biorientation of Sister Centromeres.', *PLoS genetics*, 12(4) e1005996

- Blower, M. D. and Karpen, G. H. (2001) 'The role of *Drosophila* CID in kinetochore formation, cell-cycle progression and heterochromatin interactions.', *Nature Cell Biology*, 3(8), pp. 730–739.
- Blower, M. D., Sullivan, B. A. and Karpen, G. H. (2002) 'Conserved organization of centromeric chromatin in flies and humans', *Developmental Cell*, 2(3), pp. 319–330.
- Carvalho, A. (2003) 'The advantages of recombination.', *Nature genetics*, 34(2), pp. 128–129.
- Castrillon, D. H. *et al.* (1993) 'Toward a molecular genetic analysis of spermatogenesis in *Drosophila melanogaster*: Characterization of male-sterile mutants generated by single P element mutagenesis', *Genetics*, 135(2), pp. 489–505.
- Celniker, S. E. *et al.* (2009) 'Unlocking the secrets of the genome', *Nature*, 459(7249), pp. 927–930.
- Cenci, G. *et al.* (1994a) 'Chromatin and microtubule organization during premeiotic, meiotic and early postmeiotic stages of *Drosophila melanogaster* spermatogenesis.', *Journal of Cell Science*, 107 pp. 3521–34
- Cenci, G. *et al.* (1994b) 'Chromatin and microtubule organization during premeiotic, meiotic and early postmeiotic stages of *Drosophila melanogaster* spermatogenesis.', *Journal of Cell Science*, 107 pp. 3521–34.
- Chen, Y.-N. *et al.* (2015) 'Knockdown of *ATPsyn-b* caused larval growth defect and male infertility in *Drosophila*', *Archives of Insect Biochemistry and Physiology*, 88(2), pp. 144–154.
- Chen, Z. *et al.* (1992) 'Over-expression and refolding of beta-subunit from the chloroplast ATP synthase.', *FEBS letters*, 298(1), pp. 69–73.
- Das, A. *et al.* (2017) 'Centromere inheritance through the germline', *Chromosoma*, 8 August, pp. 1–10.
- Duffy, J. B. (2002) 'GAL4 system in *Drosophila*: a fly geneticist's Swiss army knife.', *Genesis (New York, N.Y. : 2000)*, 34(1–2), pp. 1–15.
- Dunleavy, E. M. *et al.* (2012) 'The Cell Cycle Timing of Centromeric Chromatin Assembly in *Drosophila* Meiosis Is Distinct from Mitosis Yet Requires CAL1 and CENP-C', *PLoS Biology*, 10(12). e1001460
- Dunleavy, E. M., Almouzni, G. and Karpen, G. H. (2011) 'H3.3 is deposited at centromeres in S phase as a placeholder for newly assembled CENP-A in G₁ phase.', *Nucleus* 2(2), pp. 146–57.
- Earnshaw, W. C., Ratrie, H. and Stetten, G. (1989) 'Visualization of centromere proteins CENP-B and CENP-C on a stable dicentric chromosome in cytological spreads.', *Chromosoma*, 98(1), pp. 1–12.

Fachinetti, D. Folco, HD. Nechemia-Arbely, Y. Valente, LP. Nguyen, K. Wong, AJ. Zhu, Q. Holland, AJ. Desai, A. Jansen, LE. Cleaveland, DW. (2013) 'A two-step mechanism for epigenetic specification of centromere identity and function'. *Nat Cell Biol.* Sep;15(9):pp 1056-66.

Flemming W 1882. *Zellsubstanz, kern und zelltheilung*. F.C.W. Vogel, Leipzig.

Folco, H. D. *et al.* (2015) 'The CENP-A N-Tail Confers Epigenetic Stability to Centromeres via the CENP-T Branch of the CCAN in Fission Yeast', *Current Biology*, 25(3), pp. 348–356.

Foltz, D. R. *et al.* (2009) 'Centromere-Specific Assembly of CENP-A Nucleosomes Is Mediated by HJURP', *Cell*, 137(3), pp. 472–484.

Frank, R. (2002) 'The SPOT-synthesis technique: Synthetic peptide arrays on membrane supports - Principles and applications', *Journal of Immunological Methods*, 267(1), pp. 13–26.

Fuller, M. T. (1998) 'Genetic control of cell proliferation and differentiation in *Drosophila* spermatogenesis', *Seminars in Cell & Developmental Biology*, 9(4), pp. 433–444.

Gabler, M. *et al.* (2005) 'Trans-splicing of the *mod(mdg4)* complex locus is conserved between the distantly related species *Drosophila melanogaster* and *D. virilis*.' *Genetics*. Genetics Society of America, 169(2), pp. 723–36.

Gonzalez, M. *et al.* (2014) 'Ectopic centromere nucleation by CENP-A in fission yeast', *Genetics*, 198(4), pp. 1433–1446.

Halanych, K. M. (2004) 'Invertebrates; Invertebrate Zoology: A Functional Evolutionary Approach', *Systematic Biology*. Belmont, CA : Thomson-Brooks/Cole, 53(4), pp. 662–664.

Harrington, J. J. *et al.* (1997) 'Formation of de novo centromeres and construction of first-generation human artificial microchromosomes', *Nature Genetics*. Nature Publishing Group, 15(4), pp. 345–355.

Henikoff, S., Ahmad, K. and Malik, H. S. (2001) 'The Centromere Paradox: Stable Inheritance with Rapidly Evolving DNA', *Science*, 293(5532), pp. 1098–1102.

Henikoff, S. and Furuyama, T. (2012) 'The unconventional structure of centromeric nucleosomes.', *Chromosoma*. Springer, 121(4), pp. 341–52.

Heun, P. *et al.* (2006) 'Mislocalization of the *Drosophila* centromere-specific histone CID promotes formation of functional ectopic kinetochores.', *Developmental cell*. 10(3), pp. 303–15.

Howman, E. V *et al.* (2000) 'Early disruption of centromeric chromatin organization in centromere protein A (Cenpa) null mice.', *Proceedings of the National Academy of Sciences of the United States of America*, 97(3), pp. 1148–53.

Ikeno, M. *et al.* (1998) 'Construction of YAC-based mammalian artificial

- chromosomes', *Nature Biotechnology*, 16(5), pp. 431–439.
- Ishiguro, K. and Watanabe, Y. (2007) 'Chromosome cohesion in mitosis and meiosis', *Journal of Cell Science*, 120(3), pp. 367–369.
- Iwasaki, W. *et al.* (2013) 'Contribution of histone N-terminal tails to the structure and stability of nucleosomes', *FEBS Open Bio*, 3(1), pp. 363–369.
- Jansen, L. E. T. *et al.* (2007) 'Propagation of centromeric chromatin requires exit from mitosis', *The Journal of Cell Biology*, 176(6), pp. 795–805.
- Jessberger, R. (2010) 'Deterioration without replenishment—the misery of oocyte cohesin.', *Genes & development*. Cold Spring Harbor Laboratory Press, 24(23), pp. 2587–91.
- John, A., Vinayan, K. and Varghese, J. (2016) 'Achiasmy: Male Fruit Flies Are Not Ready to Mix', *Frontiers in Cell and Developmental Biology*. 4, p. 75.
- Joyce, E. F. *et al.* (2012) 'Identification of genes that promote or antagonize somatic homolog pairing using a high-throughput FISH-based screen', *PLoS Genetics*. Public Library of Science, 8(5). e1002667
- Kennison, J. A. and Southworth, J. W. (2002) 'Transvection in *Drosophila*', *Adv Genetics*, 46, pp. 399–420.
- Kerrebrock AW¹, Miyazaki WY, Birnby D, Orr-Weaver TL. (1992) The *Drosophila* mei-S332 gene promotes sister-chromatid cohesion in meiosis following kinetochore differentiation. *Genetics*. 130(4):pp 827-41.
- Kerrebrock, A. W. *et al.* (1995) 'Mei-S332, a *Drosophila* Protein Required for Sister-Chromatid Cohesion, Can Localize to Meiotic Centromere Regions', *Cell*, 83, pp. 247–256.
- Khetani, R. S. and Bickel, S. E. (2007) 'Regulation of meiotic cohesion and chromosome core morphogenesis during pachytene in *Drosophila* oocytes', *Journal of Cell Science*, 120(17), pp. 3123–3137.
- Kidd, T. *et al.* (2005) 'The epsilon-subunit of mitochondrial ATP synthase is required for normal spindle orientation during the *Drosophila* embryonic divisions.', *Genetics*. Genetics Society of America, 170(2), pp. 697–708.
- Kitajima, T. S., Kawashima, S. A. and Watanabe, Y. (2004) 'The conserved kinetochore protein shugoshin protects centromeric cohesion during meiosis', *Nature*, 427(6974), pp. 510–517.
- Koehler, K. E. and Hassold, T. J. (1998) 'Human aneuploidy: lessons from achiasmate segregation in *Drosophila melanogaster*.', *Annals of human genetics*, 62(Pt 6), pp. 467–479.
- Krishnan, B. *et al.* (2014) 'Sisters Unbound Is Required for Meiotic Centromeric Cohesion in *Drosophila melanogaster*', *Genetics*, 198(3), pp. 947–965.

- Kwenda, L. *et al.* (2016a) 'Nucleolar activity and CENP-C regulate CENP-A and CAL1 availability for centromere assembly in meiosis', *Development*, 143(8), pp. 1400–1412.
- Kwenda, L. *et al.* (2016b) 'Nucleolar activity and CENP-C regulate CENP-A and CAL1 availability for centromere assembly in meiosis', *Development*, 143(8), pp. 1400–1412.
- De La Fuente, R. *et al.* (2007) 'Meiotic pairing and segregation of achiasmatic sex chromosomes in eutherian mammals: The role of SYCP3 protein', *PLoS Genetics*, 3(11), pp. 2122–2134.
- Lermontova, I. *et al.* (2011) 'Knockdown of CENH3 in Arabidopsis reduces mitotic divisions and causes sterility by disturbed meiotic chromosome segregation', *The Plant Journal*, 68(1), pp. 40–50.
- Li, L. *et al.* (2017) 'CENP-A Regulates Chromosome Segregation during the First Meiosis of Mouse Oocytes', *J Huazhong Univ Sci Technol*, 37(3), pp. 313–318.
- Lin, H. P. and Church, K. (1982) 'Meiosis in *Drosophila melanogaster*, III. The effect of orientation disruptor (*ord*) on gonial mitotic and the meiotic divisions in males.', *Genetics*, 102(4), pp. 751–70.
- Lindsley, D. L. *et al.* (2013) 'Anent the Genomics of Spermatogenesis in *Drosophila melanogaster*', *PLoS ONE*. Edited by P. Callaerts. Public Library of Science, 8(2), p. e55915.
- Loyola, A. and Almouzni, G. (2007) 'Marking histone H3 variants: How, when and why?', *Trends in Biochemical Sciences*. Elsevier Current Trends, pp. 425–433.
- Luger, K. Mader, A. Richmond, R. Sargent, D. Richmond, D. (1997) 'Crystal structure of the nucleosome core particle at 2.8 Å resolution'. *Nature*. Vol:389 (6648) pp: 251-260.
- Maheshwari, S. *et al.* (2015) 'Naturally Occurring Differences in CENH3 Affect Chromosome Segregation in Zygotic Mitosis of Hybrids', *PLoS Genetics*. 11(1), p. e1004970.
- Malik, H. S. and Henikoff, S. (2001) 'Adaptive evolution of Cid, a centromere-specific histone in *Drosophila*.', *Genetics*, 157(3), pp. 1293–8.
- Malik, H. S. and Henikoff, S. (2003) 'Phylogenomics of the nucleosome', *Nature Structural Biology*, 10(11), pp. 882–891.
- Malik, H. S., Vermaak, D. and Henikoff, S. (2002) 'Recurrent evolution of DNA-binding motifs in the *Drosophila* centromeric histone.', *Proceedings of the National Academy of Sciences of the United States of America*, 99(3), pp. 1449–54.
- Manuelidis, L. (1978) 'Chromosomal localization of complex and simple repeated human DNAs.', *Chromosoma*, 66(1), pp. 23–32.
- Marques, A. and Pedrosa-Harand, A. (2016) 'Holocentromere identity: from the

typical mitotic linear structure to the great plasticity of meiotic holocentromeres', *Chromosoma*, 125(4), pp. 669–681.

McKee, B. D., Habera, L. and Vrana, J. A. (1992) 'Evidence that intergenic spacer repeats of *Drosophila melanogaster* rRNA genes function as X-Y pairing sites in male meiosis, and a general model for achiasmatic pairing.', *Genetics*. Genetics Society of America, 132(2), pp. 529–44.

McKee, B. D., Yan, R. and Tsai, J.-H. (2012) 'Meiosis in male *Drosophila*.', *Spermatogenesis*. Taylor & Francis, 2(3), pp. 167–184.

McKim, K. S., Jang, J. K. and Manheim, E. A. (2002) 'Meiotic Recombination and Chromosome Segregation in *Drosophila* Females', *Annual Review of Genetics*, 36(1), pp. 205–232.

McKinley, K. L. and Cheeseman, I. M. (2015) 'The molecular basis for centromere identity and function', *Nature Reviews Molecular Cell Biology*. 17(1), pp. 16–29.

Melters, D. P. *et al.* (2012) 'Holocentric chromosomes: convergent evolution, meiotic adaptations, and genomic analysis', *Chromosome Research*, 20(5), pp. 579–593.

Mendiburo, M. J. *et al.* (2011) '*Drosophila* CENH3 Is Sufficient for Centromere Formation', *Science*, 334(6056), pp. 686–690.

Miyazaki, W. Y. and Orr-Weaver, T. L. (1992) 'Sister-chromatid misbehavior in *Drosophila* ord mutants.', *Genetics*, 132(4), pp. 1047–61.

Monen, J. *et al.* (2005) 'Differential role of CENP-A in the segregation of holocentric *C. elegans* chromosomes during meiosis and mitosis', *nature cell biology*, 7(12) p.1248-55.

Morey, L. *et al.* (2004) 'The Histone Fold Domain of Cse4 Is Sufficient for CEN Targeting and Propagation of Active Centromeres in Budding Yeast', *Eukaryotic cell*, 3(6), pp. 1533–1543.

Morgan, T. H. (1910) 'Sex Limited Inheritance in *Drosophila*.', *Science*, 32(812), pp. 120–122.

Musich, P. R., Brown, F. L. and Maio, J. J. (1980) 'Highly repetitive component and related alphoid DNAs in man and monkeys', *Chromosoma*. 80(3), pp. 331–348.

Nasmyth, K. and Haering, C. H. (2009) 'Cohesin: Its Roles and Mechanisms', *Annual Review of Genetics*, 43(1), pp. 525–558.

Nechemia-Arbely, Y. *et al.* (2017) 'Human centromeric CENP-A chromatin is a homotypic, octameric nucleosome at all cell cycle points.', *The Journal of cell biology*. 216(3), pp. 607–621.

Palmer, D. K., O'Day, K. and Margolis, R. L. (1990) 'The centromere specific histone CENP-A is selectively retained in discrete foci in mammalian sperm nuclei', *Chromosoma*. 100(1), pp. 32–36.

- Rappold, G. A. (1993) 'The pseudoautosomal regions of the human sex chromosomes', *Human Genetics*, pp. 315–324.
- Ravi, M. *et al.* (2010) 'The rapidly evolving centromere-specific histone has stringent functional requirements in *Arabidopsis thaliana*', *Genetics*, 186(2), pp. 461–471.
- Ravi, M. *et al.* (2011) 'Meiosis-Specific Loading of the Centromere-Specific Histone CENH3 in *Arabidopsis thaliana*', *PLoS Genet*, 7(6). P. e1002121
- Ravi, M. and Chan, S. W. L. (2010) 'Haploid plants produced by centromere-mediated genome elimination', *Nature*, 464(7288), pp. 615–618.
- Raychaudhuri, N. *et al.* (2012) 'Transgenerational propagation and quantitative maintenance of paternal centromeres depends on Cid/Cenp-A presence in *Drosophila sperm*.' *PLoS biology*, 10(12), p. e1001434
- Rees, D. M., Leslie, A. G. W. and Walker, J. E. (2009) 'The structure of the membrane extrinsic region of bovine ATP synthase.', *Proceedings of the National Academy of Sciences of the United States of America*. 106(51), pp. 21597–601.
- Revenkova, E., Adelfalk, C. and Jessberger, R. (2010) 'Cohesin in oocytes-tough enough for Mammalian meiosis?', *Genes*, 1(3), pp. 495–504.
- Rivera, H. *et al.* (1989) 'Alternate centromere inactivation in a pseudodicentric (15;20) associated with a progressive neurological disorder.', *J Med Genet*, 26(10), pp. 626–630. doi: 10.1136/jmg.26.10.626.
- Rocchi, M. *et al.* (2012) 'Centromere repositioning in mammals.', *Heredity*, 108(1), pp. 59–67. doi: 10.1038
- Rong, Y. S. and Golic, K. G. (2003) 'The homologous chromosome is an effective template for the repair of mitotic DNA double-strand breaks in *Drosophila*.' *Genetics*, 165(4), pp. 1831–42.
- De Rop, V., Padeganeh, A. and Maddox, P. S. (2012) 'CENP-A: the key player behind centromere identity, propagation, and kinetochore assembly', *Chromosoma*. 121(6), pp. 527–538.
- Rosin, L. and Mellone, B. G. (2016) 'Co-evolving CENP-A and CAL1 Domains Mediate Centromeric CENP-A Deposition across *Drosophila* Species', *Developmental Cell*, 37(2), pp. 136–147.
- Ryabova, N. A. *et al.* (2013) 'Molecular chaperone GroEL/ES: Unfolding and refolding processes', *Biochemistry (Moscow)*, 78(13), pp. 1405–1414.
- Sanchez, C. G. *et al.* (2016) 'Regulation of Ribosome Biogenesis and Protein Synthesis Controls Germline Stem Cell Differentiation.', *Cell stem cell*. 18(2), pp. 276–90.
- Sarkar, S. and Lakhota, S. C. (2005) 'The Hsp60C gene in the 25F cytogenetic region in *Drosophila melanogaster* is essential for tracheal development and fertility.'

Journal of genetics, 84(3), pp. 265–81.

Sawyer, E. M. *et al.* (2017) 'Testis-specific ATP synthase peripheral stalk subunits required for tissue-specific mitochondrial morphogenesis in *Drosophila*', *BMC Cell Biology*, 18(1), p. 16. doi: 10.1186.

Schneider, I. (1972) 'Cell lines derived from late embryonic stages of *Drosophila melanogaster*.', *Journal of embryology and experimental morphology*, 27(2), pp. 353–365.

Schuh, M., Lehner, C. F. and Heidmann, S. (2007) 'Incorporation of *Drosophila* CID/CENP-A and CENP-C into centromeres during early embryonic anaphase.', *Current biology: CB*, 17(3), pp. 237–43.

Sekulic, N. *et al.* (2010) 'The structure of (CENP-A-H4)₂ reveals physical features that mark centromeres' *Nature* 16;467(7313) p.347-51

Senaratne, T. N. *et al.* (2016) 'Investigating the Interplay between Sister Chromatid Cohesion and Homolog Pairing in *Drosophila* Nuclei', *PLoS Genetics*, 12(8). p. e1006169

Smoak, E. M. *et al.* (2016) 'Long-Term Retention of CENP-A Nucleosomes in Mammalian Oocytes Underpins Transgenerational Inheritance of Centromere Identity', *Current Biology*, 26(8), pp. 1110–1116.

Spradling, A. *et al.* (2011) 'Germline stem cells', *Cold Spring Harbor Perspectives in Biology*, 3(11). p. a002642

Stellfox, M. E., Bailey, A. O. and Foltz, D. R. (2013) 'Putting CENP-A in its place.', *Cellular and molecular life sciences*, 70(3), pp. 387–406.

Tachibana-Konwalski, K. *et al.* (2010) 'Rec8-containing cohesin maintains bivalents without turnover during the growing phase of mouse oocytes', *Genes & Development*, 24(22), pp. 2505–2516.

Tachiwana, H. *et al.* (2011) 'Crystal structure of the human centromeric nucleosome containing CENP-A'. *Nature*. 10;476(7359) p.232-5.

Talbert, P. B. *et al.* (2002) 'Centromeric localization and adaptive evolution of an *Arabidopsis* histone H3 variant.', *The Plant cell*, 14(5), pp. 1053–66.

Talbert, P. B., Bryson, T. D. and Henikoff, S. (2004) 'Adaptive evolution of centromere proteins in plants and animals', *J Biol. BioMed Central*, 3(4), p. 18.

Tanneti, N. S. *et al.* (2011) 'A Pathway for Synapsis Initiation during Zygotene in *Drosophila* Oocytes', *Current Biology*, 21(21), pp. 1852–1857.

Teixeira, F. K. *et al.* (2015) 'ATP synthase promotes germ cell differentiation independent of oxidative phosphorylation', *Nature Cell Biology*, 17(5), pp. 689–696.

Thomas, S. E. *et al.* (2005) 'Identification of Two Proteins Required for Conjunction and Regular Segregation of Achiasmata Homologs in *Drosophila* Male Meiosis', *Cell*, 123, pp. 555–568.

- Thomas, S. E. and McKee, B. D. (2007) 'Meiotic pairing and disjunction of mini-X chromosomes in drosophila is mediated by 240-bp rDNA repeats and the homolog conjunction proteins SNM and MNM.', *Genetics.*, 177(2), pp. 785–99.
- Tomkiel, J. E., Wakimoto, B. T. and Briscoe, A. (2000) 'The teflon Gene Is Required for Maintenance of Autosomal Homolog Pairing at Meiosis I in Male *Drosophila melanogaster*', *Genetics*, 157, pp. 273–281.
- Torras-Llort, M. *et al.* (2010) 'A conserved arginine-rich motif within the hypervariable N-domain of *Drosophila* centromeric histone H3 (CenH3cid) mediates BubR1 recruitment', *PLoS ONE*, 5(10).
- Tsai, J.-H. and McKee, B. D. (2011) 'Homologous pairing and the role of pairing centers in meiosis.', *Journal of cell science*, 124(Pt 12), pp. 1955–1963.
- Tsai, J. H., Yan, R. and McKee, B. D. (2011) 'Homolog pairing and sister chromatid cohesion in heterochromatin in *Drosophila* male meiosis I', *Chromosoma*, 120(4), pp. 335–351.
- Turner, J. R. G. and Sheppard, P. M. (1975) 'Absence of Crossover in Female Butterflies (*Heliconius*)', *Heredity*, 34(70), pp. 265–269.
- VALDEOLMILLOS, A. *et al.* (1998) 'Molecular Cloning and Expression of Stromalin Protein from *Drosophila melanogaster*: Homologous to Mammalian Stromalin Family of Nuclear Proteins', *DNA and Cell Biology*, 17(8), pp. 699–706.
- Vass, S. *et al.* (2003) 'Depletion of Drad21/Scc1 in *Drosophila* cells leads to instability of the cohesin complex and disruption of mitotic progression', *Current Biology*. Elsevier, 13(3), pp. 208–218.
- Vazquez, J., Belmont, A. S. and Sedat, J. W. (2002) 'The dynamics of homologous chromosome pairing during male *Drosophila* meiosis', *Current Biology*, 12(17), pp. 1473–1483.
- Vermaak, D., Hayden, H. S. and Henikoff, S. (2002) 'Centromere Targeting Element within the Histone Fold Domain of Cid', *Molecular and Cell Biology*, 22(21), pp. 7553–7561.
- Walker, J. E. (2013) 'The ATP synthase: the understood, the uncertain and the unknown', *Biochemical Society Transactions*, 41(1), pp. 1–16.
- Warburton, P. E. *et al.* (1997) 'Immunolocalization of CENP-A suggests a distinct nucleosome structure at the inner kinetochore plate of active centromeres.', *Current biology : CB*, 7(11), pp. 901–4.
- Watanabe, Y. *et al.* (2004) 'Modifying sister chromatid cohesion for meiosis.', *Journal of cell science*. 117(Pt 18), pp. 4017–23. doi: 10.1242
- Watanabe, Y. (2012) 'Geometry and force behind kinetochore orientation: lessons from meiosis.', *Nature reviews. Molecular cell biology*, 13(6), pp. 370–82. doi: 10.1038

- Wen, J. *et al.* (2015) 'Adaptive regulation of testis gene expression and control of male fertility by the drosophila harpin RNA pathway', *Molecular Cell*, 57(1), pp. 165–178.
- Westermann, S., Drubin, D. G. and Barnes, G. (2007) 'Structures and Functions of Yeast Kinetochores Complexes', *Annual Review of Biochemistry*. 76(1), pp. 563–591.
- White-Cooper, H. (2004) 'Spermatogenesis: analysis of meiosis and morphogenesis.', in *Methods in molecular biology* 247 pp. 45–75.
- White-Cooper, H. (2012) 'Tissue, cell type and stage-specific ectopic gene expression and RNAi induction in the Drosophila testis.', *Spermatogenesis*. 2(1), pp. 11–22.
- Wiegmann, B. M. *et al.* (2011) 'Episodic radiations in the fly tree of life.', *Proceedings of the National Academy of Sciences of the United States of America*. 108(14), pp. 5690–5.
- Yan, R. *et al.* (2010) 'SOLO: A meiotic protein required for centromere cohesion, coorientation, and SMC1 localization in Drosophila melanogaster', *Journal of Cell Biology*, 188(3), pp. 335–349.
- Yeates, D. K. and Wiegmann, B. M. (2005) *The evolutionary biology of flies*. Columbia University Press. Available at: <https://books.google.ie/books?id=rELP5sNn6IYC&pg> (Accessed: 9 September 2017).

8. Appendix

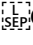
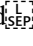
8.1. E. M. Dunleavy and C. M. Collins, 2017.

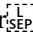
Dunleavy, E. M. and Collins, C. M. (2017) '**Centromere Dynamics in Male and Female Germ Cells**', *Prog Mol Subcell Biol*, pp. 357–375. doi: 10.1007/978-3-319-58592-5_15.

Centromere Dynamics in Male and Female Germ Cells

Elaine M. Dunleavy and Caitríona M. Collins

Abstract In sexually reproducing organisms the germ line is the cellular lineage that gives rise to gametes. All germ cells originate from germline stem cells that divide asymmetrically to generate gonial pre-cursors, which are amplified in number by mitotic divisions, undergo meiosis and eventually differentiate into mature gametes (haploid eggs and sperm). Information transmitted with gametes is inherited by offspring, and potentially by subsequent generations, instructing in organismal development and beyond. Meiosis comprises one round of DNA replication, followed by two rounds of chromosome segregation; homologous chromosomes segregate in the first division (meiosis I) and sister chromatids segregate in the second division (meiosis II). Important mechanistic features of meiosis occur in substages of prophase I and are critical for genetic recombination, including pairing and synapsis of homologous chromosomes (at leptotene and zygotene), crossing-over (at pachytene), and the appearance of chiasmata (at diplotene/diakinesis). Another unique feature of meiosis is the altered centromere/kinetochore geometry at metaphase I, such that sister kinetochores face the same spindle pole (mono-orientation) and stay together at anaphase I. This chapter reviews centromere dynamics in germ cells, focusing on centromere function and assembly in meiotic cell cycles, as well as centromere inheritance in zygotes. Centromeres are functionally defined by the presence of the histone H3 variant CENP-A, the epigenetic determinant of centromere identity. In most eukaryotes, it is well established that CENP-A function is essential for chromosome segregation in mitosis. CENP-A function in meiosis is less well understood and emerging insights into the differential regulation of meiotic and mitotic CENP-A are discussed.

E.M. Dunleavy (&) C.M. Collins  Centre for Chromosome Biology, Biomedical Sciences, National University of Ireland, Galway, Ireland  e-mail: elaine.dunleavy@nuigalway.ie

© Springer International Publishing AG 2017 357 B.E. Black (ed.), Centromeres and Kinetochores, Progress in Molecular  and Subcellular Biology 56, DOI 10.1007/978-3-319-58592-5_15

1 CENP-A Function in Germ Cells

CENP-A function is essential for kinetochore assembly in mitosis (Fachinetti et al. 2013; Black et al. 2007; Takahashi et al. 2000; Blower and Karpen 2001; Buchwitz et al. 1999; Howman et al. 2000; Ravi et al. 2010; Stoler et al. 1995). CENP-A function in meiosis is less well understood and is currently unknown in many organisms, including humans. One of the first investigations into CENP-A function in meiosis was performed in the nematode *Caenorhabditis elegans*. Surprisingly, its function appears to be dispensable in worm meiosis, or at least it is not required at mitotic levels (Monen et al. 2005). Fixed and time-lapse imaging of CENP-A-depleted gonads showed that meiotic chromosome segregation was not perturbed, yet chromosome segregation completely failed in CENP-A-depleted mitotic cells. The lack of a requirement for CENP-A in worm meiosis most likely relates to the fact that this organism is holocentric. As CENP-A is incorporated throughout the length of holocentric chromosomes, they lack a single site to co-orient sister chromatids and to protect cohesins against degradation in the first meiotic division (Marques and Pedrosa-Harand 2016). To overcome this problem, *C. elegans* oocytes have departed from the typical kinetochore-driven mode of chromosome segregation to one in which microtubules between chromosomes mediate separation (Dumont et al. 2010), perhaps excluding a need for CENP-A. In contrast, in the fruit fly *Drosophila melanogaster*, CENP-A is required for centromere function in meiosis, at least in males. RNAi knockdown of CENP-A in pre-meiotic gonial cells in testes revealed meiotic chromosome missegregation events, including uneven nuclear segregation in meiosis I and II (Dunleavy et al. 2012). Moreover, depletion or mutation of key CENP-A assembly factors Chromosome alignment defect 1 (CAL1) and Centromeric protein-C (CENP-C) give rise to defects in meiotic centromere function in both male and female flies (Dunleavy et al. 2012; Raychaudhuri et al. 2012; Kwenda et al. 2016; Unhavaithaya and Orr-Weaver 2013). In the thale cress *Arabidopsis thaliana*, RNAi knockdown of CENP-A to a level sufficient for mitosis leads to partial plant sterility, with lagging chromosomes in meiosis I and II, and gametes (pollen spores) have micronuclei (Lermontova et al. 2011). Indeed, meiosis-specific functions for CENP-A are best illustrated in plants, in which alterations to CENP-A can give rise to haploid progeny (Ravi and Chan 2010). Therefore, aside from worm, the consensus finding from model organisms examined so far is that CENP-A is functionally required for meiosis.

1.1 Germ-Cell-Specific Functions of the CENP-A N-Terminus

The CENP-A N-terminus shares no similarity between eukaryotes, it is highly divergent and is rapidly evolving (Malik and Henikoff 2003) (Fig. 1).

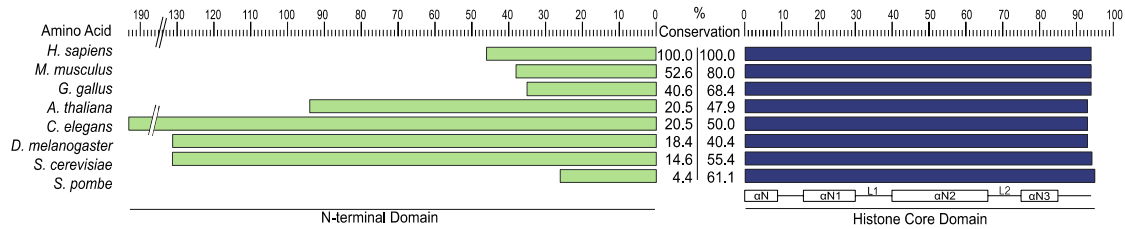


Fig. 1 The CENP-A N-terminal domain is highly divergent in both length and amino acid sequence. Amino acids 1–46 and 47–140 of human CENP-A represent the N-terminal and histone core domain of CENP-A, respectively. Percent identity relative to human CENP-A was determined using TCOoffee (Notredame et al. 2000)

First experiments investigating CENP-A domains critical for centromere specification showed that the centromere-targeting domain (CATD) within the C-terminal histone core domain is both necessary and sufficient for CENP-A deposition and function (Black et al. 2004, 2007; Fachinetti et al. 2013). At this point, the function of the CENP-A N-terminus was not known and it was presumed to be largely dispensable for CENP-A deposition. More recent long-term viability assays in human cultured cells and fission yeast, in which centromere function can be rescued by the expression of chimeric CENP-A/H3 transgenes, now indicate functional requirements for the CENP-A N-terminus in addition to the CATD (Fachinetti et al. 2013). In both organisms, the CENP-A N-terminus supports long-term cellular viability and in human cells it directs CENP-B binding to reinforce kinetochore function. Additional centromere establishment assays in human cells revealed that the CENP-A N-terminus is required for the initial recruitment of the kinetochore proteins CENP-C and CENP-T (Logsdon et al. 2015). Studies carried out in *A. thaliana* first demonstrated an unexpected functional requirement for the CENP-A N-terminus in plant germ cells. Ravi and colleagues isolated a *cenh3* (plant CENP-A) null mutation by ethylmethanesulfonate (EMS) mutagenesis, which was embryo lethal as expected. This CENP-A-lethal mutation could be rescued by the expression of an N-terminally GFP-tagged CENP-A (Ravi et al. 2010). Surprisingly, expression of a modified, GFP-tagged version of CENP-A in which its N-terminus is replaced with that of histone H3.3 (so-called ‘GFP-tailswap’, Fig. 2) complemented lethality in *cenh3* null plants, but the resulting plants were largely sterile (Ravi et al. 2010; Ravi and Chan 2010). Similar experiments, instead performed using fluorescently tagged CENP-A transgenes

completely lacking its N-terminus, showed that ‘tailless’ CENP-A localises to mitotic centromeres (Lermontova et al. 2006; Ravi et al. 2010). Yet, in line with GFP-tailswap plants, plants over expressing the YFP-tagged tailless transgene were sterile or partially sterile (Lermontova et al. 2011). Sterility in tailless and GFP-tailswap plants was attributed to meiotic abnormalities in gametes. GFP-tailswap plants were defective in homolog disjunction in meiosis I, in chromosome alignment at metaphase II and pollen spores display micronuclei (Lermontova et al. 2011; Ravi et al. 2011). YFP-tagged tailless plants displayed lagging chromosomes in meiosis II also resulting in pollen spores with micronuclei (Lermontova et al. 2011). These findings point to critical roles for the CENP-A N-terminus in meiotic chromosome segregation.

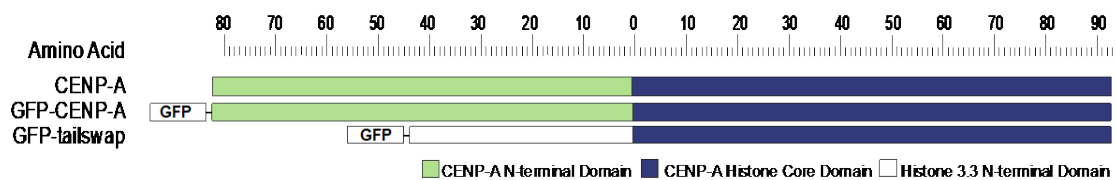


Fig. 2 In *A. thaliana*, GFP-tailswap plants express a GFP-tagged CENP-A transgene in which the N-terminus of CENP-A is replaced with the N-terminus of histone H3.3 (Ravi et al. 2010)

In their analyses of transgenic plants expressing modified versions of CENP-A, Ravi and Chan made a second striking observation. GFP-tailswap plants could be crossed to wild-type plants; however, viable offsprings were haploid and only contained the wild-type set of chromosomes (Ravi and Chan 2010). This phenomenon termed centromere-mediated genome elimination has been exploited for accelerated plant breeding purposes, but has also fuelled research into CENP-A function in germ cells and zygotes in a number of plant species. To explain this uniparental chromosome loss, current models propose that gamete chromosomes with modified CENP-A are ‘weaker’ than those with wild-type CENP-A and either fail to interact with the mitotic spindle or lag in early embryo mitoses (Karimi Ashtiyani et al. 2015; Ravi and Chan 2010). A similar mechanism was also proposed for genome elimination in barley hybrids (Sanei et al. 2011). Plant breeders are now positioned to carry out targeted mutagenesis screens to identify additional CENP-A alterations that might give rise to haploid plants. For example, in *A. thaliana*, a single point mutation within the centromere-targeting domain (CATD) of CENP-A impairs its localisation to both mitotic and meiotic centromeres and can give rise to haploid embryos (Karimi-Ashtiyani et al. 2015), albeit at a lower efficiency than crosses with the

GFP-tailswap. This exact point mutation impairs CENP-A localisation in barley and sugar beet (Karimi-Ashtiyani et al. 2015), raising the possibility that this method for haploid plant induction could be extended to other species. In summary, plant breeding experiments strongly support a germ-cell-specific role for CENP-A and its N-terminus; parents with defective or modified versions of CENP-A generate chromosome loss both in meiocytes and resulting progeny.

A third observation of GFP-tagged CENP-A localisation in plants demonstrated an unexpected role for the N-terminus in meiotic CENP-A dynamics. GFP-tailswap and GFP- or YFP-tailless CENP-As fail to localise to meiotic centromeres; GFP-tailswap was only faintly visible at centromeres during early prophase I (leptotene and zygotene) and was not detected beyond the start of pachytene, nor for remaining phases of meiosis I and II (Ravi et al. 2011; Lermontova et al. 2011). Therefore, it is likely that plants expressing modified or truncated CENP-A are sterile due to a specific failure in meiotic CENP-A retention at centromeres that gives rise to chromosome segregation defects in gametes. Remarkably, the small percent of GFP-tailswap or tailless gametes that survive meiosis were competent to reload CENP-A in subsequent mitotic (gametophytic) divisions of pollen spores that occur in plants (Ravi et al. 2011; Schubert et al. 2014). These findings point to de novo CENP-A assembly after meiotic exit, possibly due to the re-availability of mitotic CENP-A assembly factors. While experiments with GFP-tailswap plants have been extremely informative, it is important to note that presence of the GFP-tag alone compromises CENP-A function (Ravi et al. 2011). Complementation assays with untagged, mutated versions of CENP-A might prove more biologically relevant for future studies (Maheshwari et al. 2015).

Interestingly, despite its hyper-variability among divergent organisms, the CENP-A N-terminus of flies and plants harbour blocks of conserved amino acid motifs (Torras-Llort et al. 2009; Malik et al. 2002; Maheshwari et al. 2015). The N-terminus of CENP-As from the *Drosophila* clade harbour three conserved arginine-rich domains (Malik et al. 2002) (Fig. 3), whereas at least two conserved blocks were identified in nearly all plant CENP-As analysed ranging from green algae to flowering plants (Maheshwari et al. 2015) (Fig. 4). The function of such conserved sequence blocks is largely unknown, but suggest functional specialisation. Indeed, evolutionarily divergent plant CENP-As can complement mitotic and meiotic functions in an *A. thaliana* cenH3 null background (Maheshwari et al. 2015), suggesting that despite sequence differences in N-terminal tails, critical functional features are conserved. Further investigations into requirements of the CENP-A N-terminus and its potential conserved blocks in other organisms might reveal germ-cell-specific functions,

for example in meiotic CENP-A assembly or maintenance.



Fig. 3 Conserved amino acid sequence blocks in the CENP-A N-termini of *Drosophila* species. Alignment was carried out using Toffee (Notredame et al. 2000). Asterix, semi-colon and stop represent full conservation of amino acid, strong conservation and weak conservation of amino acid properties, respectively. Phylogenetic analysis was performed using Phylogeny.fr (Dereeper et al. 2010). Node values and scale represent confidence and number of substitutions, respectively, based on the pairwise alignment

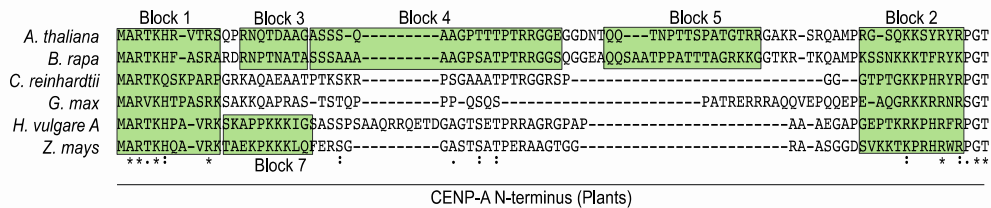


Fig. 4 Conserved amino acid sequence blocks in the CENP-A N-termini of highly divergent plant species. Alignment was performed as shown in Fig. 3

2 Cell Cycle Assembly Timing of Meiotic CENP-A

In the last decade, investigations into the cell cycle timing of centromere assembly in mitosis have proven critical to understanding mechanisms of centromere specification and function. In human cultured cells, seminal first studies showed that CENP-A is assembled at late telophase and early G1 phase (Jansen et al. 2007; Hemmerich et al. 2008) or at anaphase in syncytial divisions in fly embryos (Schuh et al. 2007). Critically, these experiments highlighted the stability of pre-existing CENP-A nucleosomes incorporated at centromeres that are stably retained through mitotic cell cycles. CENP-A assembly in G1 phase was unexpected as it indicated that centromeres are competent for kinetochore

assembly and chromosome segregation with half the total amount of CENP-A. Different from metazoans, CENP-A assembly occurs in G2 phase in plants and fission yeast (Lando et al. 2012; Lermontova et al. 2006, 2007). The significance of pre-divisional CENP-A assembly in most organisms and post-divisional CENP-A assembly in others is currently not clear, but could have mechanistic implications for centromere function and kinetochore assembly at chromosome segregation. What is clear is that new CENP-A deposition should occur at least once per cell cycle to ensure centromere propagation. Given that the meiotic cell cycle comprises two rounds of nuclear division, investigations into meiotic CENP-A assembly have focused on determining if CENP-A is replenished in both divisions, or in only one division, or not at all, i.e., is the pre-meiotic CENP-A level sufficient to support both meiotic divisions?

Earliest investigations into the cell cycle timing of meiotic CENP-A assembly were conducted in *C. elegans*. Fixed and live analysis of oocytes showed that meiotic CENP-A was dynamic (Monen et al. 2005), a result that was unexpected given the stability of CENP-A nucleosomes in mitosis (Buchwitz et al. 1999). Surprisingly, CENP-A was not detected on prophase I chromosomes at early pachytene and was first detected at late pachytene/diplotene (Fig. 5). Unusual CENP-A localisation dynamics in this system might again be related to the finding that CENP-A is largely dispensable for holocentric worm meiosis (Monen et al. 2005). Intriguingly, CENP-A removal in early pachytene and reloading by late diplotene coincides with the timing of key recombination events in prophase I. An unexpected drop in CENP-A signal was also observed between meiosis I and II; however, its functional importance was not tested.

Meiotic CENP-A assembly in prophase I was also observed in *D. melanogaster* males (Dunleavy et al. 2012; Raychaudhuri et al. 2012) (Fig. 5). Quantitation of endogenous and GFP-tagged CENP-A levels from fixed and live testes revealed an increase in CENP-A intensity between early and late prophase I (Dunleavy et al. 2012; Raychaudhuri et al. 2012). CENP-A assembly in prophase I was also observed in *Drosophila* females (between zygotene and diplotene) (Dunleavy et al. 2012). Unlike *Drosophila* males that lack conventional features of meiotic prophase I, *Drosophila* females carry out chromosome synapsis and homologous recombination, indicating that CENP-A assembly at this time is unlikely to be a peculiarity of male fruit flies. In contrast to mitosis, in which the majority of CENP-A is assembled in minutes to hours (Schuh et al. 2007; Jansen et al. 2007; Hemmerich et al. 2008), meiotic CENP-A assembly dynamics appear to be slow in flies. Prophase I lasts over 90 h in *Drosophila* males and gradual increments in CENP-A assembly were measured between early and late substages (Dunleavy et al. 2012; Raychaudhuri et al. 2012). Similar to findings

in worm, an unexpected drop in CENP-A intensity of greater than half was also measured between meiosis I and II (Dunleavy et al. 2012), but again the significance of this drop is not clear. Intriguingly, the localisation of CAL1, the major CENP-A assembly factor in flies, inversely correlates with the dynamics of CENP-A deposition in prophase I. Centromeric CAL1 level is reduced in early prophase I and is undetectable at late prophase I, the time when CENP-A assembly reaches its peak (Dunleavy et al. 2012; Raychaudhuri et al. 2012). It is possible that CAL1 is gradually removed from centromeres once meiotic CENP-A assembly is complete. An additional phase of CENP-A assembly was measured on spermatids post-meiosis II (Dunleavy et al. 2012). Given that neither CAL1 nor CENP-C is detected at centromeres at this time, it is still unclear if either centromere assembly factor is specifically required for this second loading phase.

Consistent with findings in worms and flies, measurements of CENP-A immuno-fluorescent intensities in meiocytes of the rye plant *Secale cereale* also revealed a first major phase of CENP-A assembly in early prophase I (Schubert 2014) (Fig. 5). Additional unloading and loading events were also measured between late prophase and metaphase I, and at interkinesis, respectively. An unexpected drop in CENP-A intensity, comparable to the drop reported in *Drosophila* males, was also reported after anaphase, in this instance in tetrad pollen nuclei immediately after the second meiotic division. Taken together, unusual CENP-A dynamics including loading and unloading events appear to be a common feature of meiotic centromere assembly in worm, flies and plants (Fig. 5). Analysis in *A. thaliana* of GFP-tailswap localisation dynamics has also added to current understandings of such meiotic CENP-A loading and unloading events. Strikingly, GFP-tailswap mutants fail to localise to meiotic centromeres (Ravi et al. 2011). Failure to detect the GFP-tailswap was first observed from leptotene in early pro- phase I, the time when meiotic pairing between homologs initiates (Fig. 5). One hypothesis that might explain such a loss is that CENP-A is gradually removed during prophase I, supporting the notion that numbers and types of CENP-A molecules are normally subject to a quality check at discrete meiotic substages. Given that GFP-tailswap plants express an N-terminally modified version of the CENP-A, it is possible that the N-terminus is a substrate for unloading and might normally direct a quality check (discussed in Sect. 2.1).

CENP-A assembly in early prophase I might also be conserved in mammals. A recent investigation in mouse oocytes failed to detect GFP-CENP-A assembly in prophase I arrested oocytes or upon maturation of oocytes to meiosis II (Smook et al. 2016) (Fig. 5). This result suggests that sufficient CENP-A for meiotic centromere function is already assembled prior to prophase I arrest at

diplotene. Presumably, a round of CENP-A assembly occurs in the last mitosis before entry into meiosis, but additional CENP-A assembly events in early prophase I prior to diplotene remain an open possibility. It is clear that CENP-A incorporated prior to the prophase I arrest is extremely stable, as arrested oocytes in which *cenp-a* was knocked out retain 70% of the pre-existing CENP-A protein one year later (Smoak et al. 2016). Moreover, when bred, the mice were fertile and could support early embryogenesis, reinforcing a model in which CENP-A assembled prior to diplotene is sufficient for meiotic centromere function. However, given that a 30% reduction in CENP-A was measured, some CENP-A was lost after one year and a low level of CENP-A turnover cannot be excluded. Similar investigations into CENP-A assembly and maintenance dynamics in mammalian testes are currently lacking, but will be important to corroborate findings in *Drosophila* and to identify common features of centromere assembly pathways in males. In summary, while in mitosis CENP-A is stably incorporated at centromeres during the cell cycle, its localisation in meiosis is dynamic, with both assembly and disassembly events reported in most model organisms examined so far.

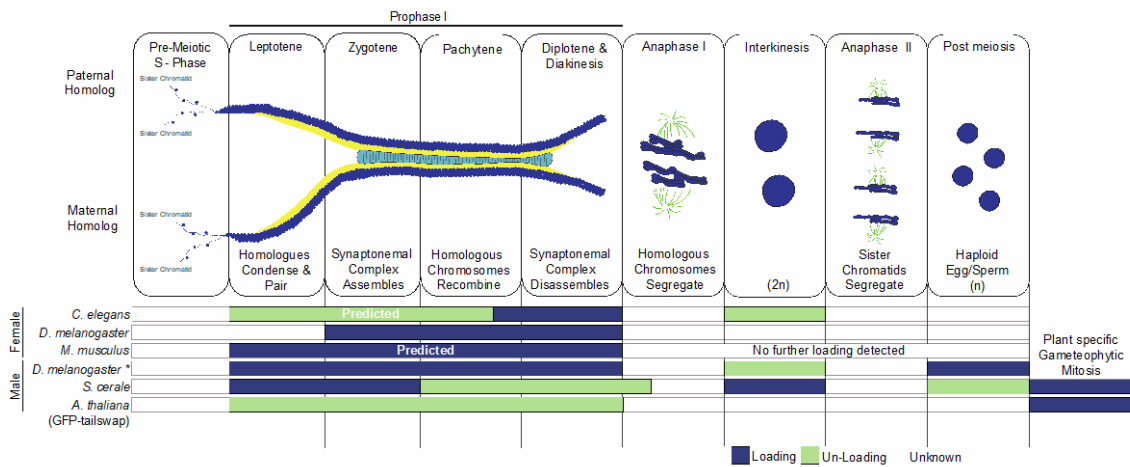


Fig. 5 Chromosome and CENP-A dynamics during meiosis in *C. elegans* (Monen et al. 2005), *D. melanogaster* (Dunleavy et al. 2012; Raychaudhuri et al. 2012), *M. musculus* (Smoak et al. 2016), *S. cereale* (Schubert et al. 2014) and *A. thaliana* (Ravi et al. 2011). *Synapsis and recombination are absent in *Drosophila* male meiosis

2.1 Significance of Unusual CENP-A Dynamics in Meiotic

Prophase I

With the exception of plants and fission yeast, most eukaryotes assemble CENP-A after chromosome segregation in mitosis (Valente et al. 2012). An emerging theme from investigations into the temporal control of meiotic CENP-A is its assembly before chromosome segregation, in the first meiotic division (Fig. 5). Why switch between post-divisional loading in mitosis to pre-divisional loading in meiosis? One hypothesis is that pre-divisional loading in meiosis I might relate to unique mechanistic features of prophase I that result in genetic recombination. In rye and female fruit flies, CENP-A assembly initiates in early prophase (Schubert et al. 2014; Dunleavy et al. 2012) and likely coincides with synaptonemal complex assembly. In worm, CENP-A assembly initiates later in prophase I, at late pachy- tene (Monen et al. 2005), when synapsis is complete and crossing-over takes place. In mouse oocytes, any CENP-A assembly likely occurs prior to diplotene (Smoak et al. 2016), the stage at which chiasmata that mark sites of genetic crossover are clearly visible. Therefore, on the one hand, CENP-A assembly could be coupled to the initiation or completion of homolog pairing, chromosomal synapsis or homologous recombination. This is unlikely to be the case in *Drosophila* males, however, which assemble CENP-A in prophase I despite a lack of synapsis and homologous recombination (Meyer 1960). On the other hand, CENP-A and its associated kinetochore complex may be incompatible with aspects of homologous recombination that necessitate its removal and subsequent reloading.

A second hypothesis is that pre-divisional CENP-A assembly in prophase I prepares the centromere/kinetochore for the mono-orientation of sister chromatids at metaphase I. It is possible that the absolute number of CENP-A nucleosomes is critical to build the kinetochore for the first meiotic division and this number requires adjustment at this cell cycle time. In addition to assembly, evidence for the selective removal of a modified version of CENP-A in early prophase I in plants (Ravi et al. 2011), raises the possibility that CENP-A is turned over at this cell cycle stage. It is possible that CENP-A disassembly removes imperfect or not correctly modified versions of CENP-A before the first meiotic division, as part of a quality control step. Fluorescent recovery after photobleaching (FRAP) experiments with functional fluorescently tagged CENP-A are currently lacking in any organism, but might confirm CENP-A turnover and dynamics in prophase I. Findings that meiotic CENP-A assembly is dependent on an intact CENP-A N-terminus in plants (Ravi et al. 2011) supports models in which the N-terminus directs CENP-A removal. It is possibly subject to meiosis-specific post-translational modifications, or it

interacts with a meiosis-specific chaperone/assembly/disassembly factor, or it directs protein-folding activities that instruct CENP-A stability. Finally, the selective CENP-A drop in interkinesis after meiosis I, so far observed in flies and worms, might reflect CENP-A loss due to the reconfiguration of centromeres/kinetochores from a side-to-side to a back-to-back orientation for sister chromatid segregation in meiosis II (Watanabe 2012). The second major phase of CENP-A assembly after meiosis II, so far observed in *Drosophila* males, is post-divisional and more comparable to the assembly triggered by mitotic exit, for example in human cells (Jansen et al. 2007; Silva et al. 2012). Here additional CENP-A assembly might compensate for excess removal in prophase or anaphase I, or ensure that a sufficient amount of CENP-A is present on mature gametes for epigenetic inheritance in the zygote.

3 Transgenerational Inheritance of CENP-A

In most organisms studied so far, it is apparent that sufficient CENP-A for the two rounds of nuclear division in meiosis is assembled prior to the end of prophase I, with additional CENP-A assembly events immediately after meiotic exit in some organisms (Fig. 5). However, in order to epigenetically specify centromere identity in the next generation, CENP-A must also be maintained on gamete chromatin. Females face the challenge of CENP-A maintenance on egg chromatin arrested at prophase I, which lasts for months to years depending on the species (Von Stetina and Orr-Weaver 2011). Remarkably, a first quantitative analysis of CENP-A protein in mouse oocytes confirms its long-lived stability for at least one year with little turnover (Smoak et al. 2016). Similar analysis of CENP-A stability in arrested human oocytes is of interest, although technically challenging. Male gametes face a different challenge; mature spermatozoa must retain CENP-A despite the dramatic removal and exchange of most other histones for protamines during differentiation. Early immuno-fluorescent studies of fully differentiated bovine spermatozoa first confirmed that CENP-A is retained in discrete nuclear foci in males (Palmer et al. 1990). Moreover, CENP-A was identified as one of the most abundant proteins on bovine sperm, which investigators exploited for its purification and sequencing (Palmer et al. 1991). Subsequent studies confirmed CENP-A localisation on mature sperm in diverse organisms such as *Xenopus*, plants and flies (Zeitlin et al. 2005; Raychaudhuri et al. 2012; Dunleavy et al. 2012; Ingouff et al. 2010), indicating that CENP-A maintenance on male gametes is likely of wide functional importance for epigenetic centromere inheritance.

One of the most extensive investigations into the inheritance of CENP-A from one generation to the next was performed in *Drosophila* males (Raychaudhuri et

al. 2012). These experiments provide support for a template-governed centromere inheritance and assembly model, in which pre-existing CENP-A nucleosomes direct the deposition of new CENP-A nucleosomes (Figs. 6 and 7). First, Raychaudhuri and colleagues crossed male flies expressing only a GFP-tagged copy of CENP-A to wild-type females and observed dilution of GFP-CENP-A by half in each of the early embryonic cell cycles 1–3 (Fig. 6). This result indicates that each cell cycle pre-existing CENP-A on paternal chromosomes is diluted by unlabeled, maternally supplied CENP-A and is in line with the dilution of pre-existing CENP-A by newly synthesised CENP-A in mitotic cell cycles (Jansen et al. 2007). Next, the authors use a genetic approach to generate flies harbouring sperm in which CENP-A was degraded and no longer detectable at centromeres. In embryos generated from ‘CENP-A-degraded’ sperm, paternal chromosomes did not assemble new CENP-A and were lost during the initial embryonic cell cycles (Fig. 6). This result demonstrates that a minimal amount of pre-existing paternal CENP-A is required to direct the assembly of maternal CENP-A. In a second set of experiments, the authors use additional genetic approaches to manipulate CENP-A levels on sperm and track whether high or low CENP-A levels are inherited in the next generation (Fig. 7). They report two major findings. (i) When males with reduced CENP-A on sperm were crossed to control females, resulting progeny had reduced total CENP-A in embryonic nuclei, as well as adult sperm nuclei. Given that half the chromosomes were of paternal origin, the observed drop in total CENP-A level was in line with the expected drop. (ii) When males with a higher CENP-A level on sperm were crossed to control females, resulting progeny had a higher CENP-A level on chromosomes in embryonic nuclei. While the observed CENP-A increase was lower than expected, it is likely that CENP-A is not quantitatively maintained as levels of CENP-A and its assembly factor CAL1 are limiting (Schittenhelm et al. 2010). Alternatively, it is possible that high CENP-A levels at centromeres can gradually revert back to normal levels. Both sets of experiments support template-driven epigenetic memory at sperm centromeres and indicate that CENP-A levels are not reset, at least not in the next generation. Intriguingly, in RNAi experiments reduced CENP-A levels were also measured in wing imaginal discs and mature adult sperm, indicating that quantitative changes in CENP-A at centromeres were maintained beyond embryogenesis. It will be insightful to now investigate CENP-A inheritance in subsequent generations, i.e., in adult tissues and sperm from grandsons and great grandsons. It will also be of interest to determine if mechanisms for resetting CENP-A at centromeres could exist, for example to counterbalance unequal CENP-A inheritance on paternal and maternal homologs.

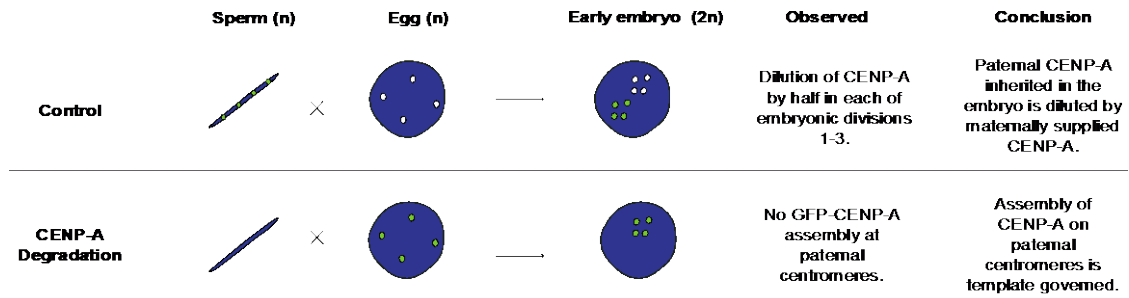


Fig. 6 This experiment suggests that CENP-A inherited on paternal chromosomes acts as a template for subsequent CENP-A loading in the embryo (Raychaudhuri et al. 2012)

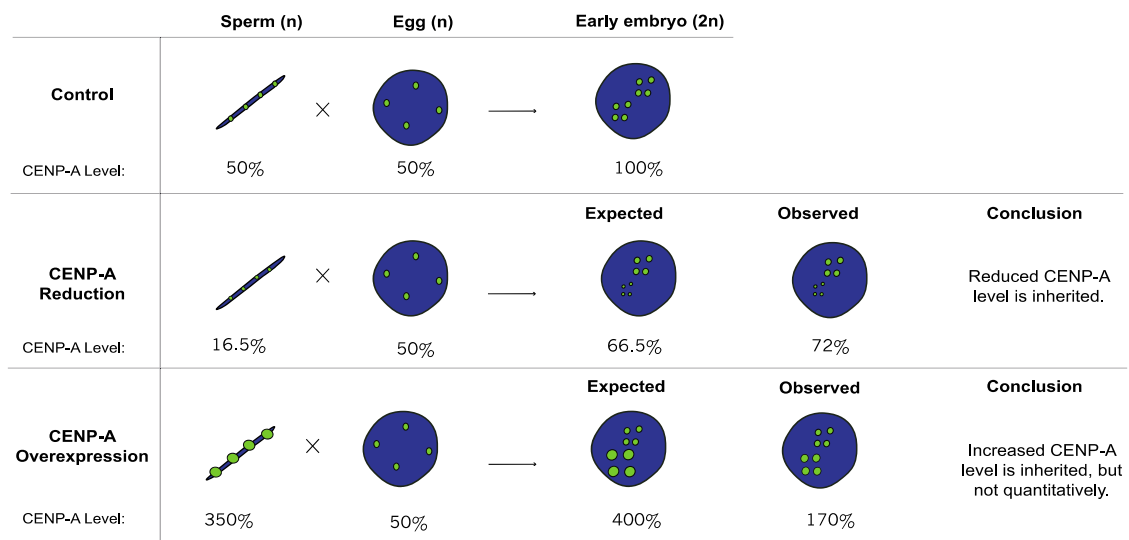


Fig. 7 These experiments suggest that altered centromeric CENP-A levels on sperm are inherited by the embryo (Raychaudhuri et al. 2012)

In striking contrast to many eukaryotes, CENP-A is not retained on mature sperm in *C. elegans*, arguing against a template-governed centromere inheritance mechanism in worms. Indeed, photobleaching experiments show that GFP-tagged CENP-A is turned over in embryo cell cycles and progeny generated from CENP-A-depleted oocytes fertilised with wild-type sperm do not inherit any CENP-A (Gassmann et al. 2012). Instead genome-wide chromatin immunoprecipitation of CENP-A and hybridisation to a tiling microarray (ChIP-chip) experiments show that CENP-A position in zygotes is linked to transcription (Gassmann et al. 2012). Genes transcribed in the germline, or in embryos, are refractory to CENP-A incorporation, whereas genes silent in embryos are permissive for CENP-A incorporation. The link

between de novo centromere specification and transcriptional silencing might be a unique feature of worm holocentric chromosomes. Indeed, an increasing body of evidence supports transcription-coupled CENP-A assembly in somatic cell mitosis in other organisms (Chan and Wong 2012). A second scenario, which argues against a template-driven model for centromere inheritance, comes from a report of de novo CENP-A assembly in zygotic divisions in *A. thaliana* (Ingouff et al. 2010). In this study, analysis of plants expressing a GFP-tagged CENP-A revealed that CENP-A is present on mature sperm, but is absent on mature eggs (Ingouff et al. 2010). Analysis of the earliest divisions post-fertilisation revealed that paternal GFP-CENP-A foci are undetectable after karyogamy (fusion of male and female genomes), and are only detectable at the 16-cell stage of development (Ingouff 2010). These results suggest that CENP-A is assembled de novo in the zygote without pre-existing CENP-A as a guide, the mechanism of which is currently unknown. However, it is possible that a residual amount of CENP-A beyond the limits of detection is retained on egg chromatin or after karyogamy that is sufficient to direct new CENP-A deposition.

A common feature of plant and worm germ cells is the absence of CENP-A on one mature gamete (Table 1); CENP-A is absent from plant eggs (Ingouff et al. 2010), while CENP-A is absent from worm sperm (Gassmann et al. 2012). Alternative mechanisms to assemble CENP-A in zygotes might exist to counter-balance unequal CENP-A loading between male and female gametes; if CENP-A is absent, reduced or not loaded on one gamete, the organism can still reset CENP-A deposition in the zygote. It is also possible that one gamete is more sensitive to CENP-A reduction or modification. For example, GFP-tailswap plants are mostly male sterile; measured fertility was 3.5% for pollen, but 68.5% for ovules (Ravi et al. 2011). This bias in sterility between sexes might reflect different dependencies for meiotic CENP-A and its assembly pathways in males and females.

Table 1 CENP-A maintenance on mature gametes and the major mechanism of CENP-A assembly in early embryonic cell cycles in *D. melanogaster*, *C. elegans* and *A. thaliana*

Species	CENP-A on mature sperm	CENP-A on mature egg	CENP-A assembly in early embryos	References
<i>D. melanogaster</i>	✓	✓	Template-governed	Raychaudhuri et al. (2012)
<i>C. elegans</i>	✗	✓	de novo	Gassmann et al. (2012)
<i>A. thaliana</i>	✓	✗	de novo	Ingouff et al. (2010)

4 Functions, Assembly and Inheritance of CENP-C in Germ Cells

CENP-C is a conserved primary component of the constitutive centromere-associated network and can directly interact with CENP-A chromatin (Carroll et al. 2009, 2010; Foltz et al. 2006; Falk et al. 2015). CENP-C is essential for mitosis and cell viability in diverse organisms (Meluh and Koshland 1995; Heeger et al. 2005; Kalitsis et al. 1998; Kwon et al. 2007), which has hampered investigations into potential roles in meiosis. However, the targeted isolation of point mutants in *cnp3* (fission yeast CENP-C) that leave mitotic functions intact, provide evidence for meiosis-specific functions (Tanaka et al. 2009). Specifically, C-terminal mutations in CENP-C perturb Moa1 (monopolar attachment 1) recruitment, a meiosis-specific protein exclusively required for mono-orientation of kinetochores in meiosis I (Tanaka et al. 2009). Interestingly, Moa1 and its functional equivalent in mammals Meikin share no significant sequence homology, yet Meikin was discovered through its interaction with CENP-C in mouse testes (Kim et al. 2015). Similarly in *D. melanogaster*, the isolation of a C-terminal point mutation in *cnp-C* that renders flies sterile, but leaves mitotic functions mostly intact, has aided dissection of CENP-C's roles in meiosis. In females, functional CENP-C is required for meiotic centromere clustering, pairing and chromosome segregation (Unhavaithaya and Orr-Weaver 2013). In males, CENP-C is also required for meiotic chromosome segregation, with additional roles in meiotic CENP-A assembly and the timely release of CAL1 and CENP-A from nucleoli (Kwenda et al. 2016). Additionally, separation-of-function mutations in other organisms are likely to reveal further meiosis-specific roles of CENP-C. Remarkably, CENP-C appears to be dispensable for worm meiosis, in line with findings reported for CENP-A (Monen et al. 2005).

Compared to CENP-A, CENP-C assembly dynamics in either mitosis or meiosis are less well characterised. Unexpectedly, although CENP-C directly binds to CENP-A nucleosomes, its dynamics do not always follow those of CENP-A. In

human mitotic cells in culture, quantitative FRAP and Fluorescence Correlation Spectroscopy (FCS) experiments show that CENP-C undergoes dynamic exchange in both G1 and G2 phase, but not S phase (Hemmerich et al. 2008). This result contrasts findings for CENP-A in this system, which only recovers in early G1 phase. In mouse meiosis, CENP-C-GFP can assemble in oocytes arrested at pro- phase I or upon maturation, yet CENP-A-GFP cannot (Smoak et al. 2016), further highlighting differential CENP-C and CENP-A dynamics in mammals. In other organisms, CENP-C assembly dynamics appear to align more closely with those of CENP-A. In worm oocytes, like CENP-A, CENP-C is first detected at centromeres in prophase I, at late pachytene/diplotene stages (Monen et al. 2005). In flies, also in line with CENP-A, CENP-C is assembled at anaphase of mitosis in embryonic divisions (Schuh et al. 2007) and at prophase I in meiosis in spermatocytes (Kwenda et al. 2016). Yet, unlike CENP-A, CENP-C level on spermatids drops off after the second meiotic division in male flies (Dunleavy et al. 2012; Raychaudhuri et al. 2012). Intriguingly, the timing of CENP-C ‘removal’ inversely correlates with an increase in CENP-A intensity at this stage, raising the possibility that novel factors participate in this second phase of CENP-A assembly.

One common feature between frogs, worm and flies is the absence of CENP-C on mature sperm (Milks et al. 2009; Gassmann et al. 2012; Raychaudhuri et al. 2012; Dunleavy et al. 2012). Additionally, CENP-C was not detected on plant meiocytes (Ravi et al. 2011). Therefore, it is unlikely that CENP-C is a mark of paternal centromere identity in the next generation, an epigenetic function attributed instead to CENP-A. Indeed, both in vitro chromatin assembly experiments in *Xenopus* (Milks et al. 2009) and in vivo dynamics of GFP-tagged CENP-C in *Drosophila* early embryos (Raychaudhuri et al. 2012), confirm de novo CENP-C assembly from a maternal pool supplied in the egg cytoplasm. Thus, in zygotes, CENP-C assembly is most likely specified by pre-existing or newly assembled CENP-A.

5 Centromere Structure/Function Roles in Homolog Pairing, Clustering and Synapsis in Prophase I

Distinguishing and critical features of meiotic prophase I include the pairing of homologous chromosomes, the assembly of the synaptonemal complex between homologs (synapsis) and homologous recombination leading to genetic exchange, as well as the formation of chiasma that hold homologs together until anaphase of meiosis (Watanabe 2012; Cahoon and Hawley 2016) (Fig. 5). Accumulating evidence suggests centromeres might play structural roles at very early stages of meiotic prophase I. In budding yeast, assembly of the

synaptonemal complex component Zip1 in early zygotene initiates at paired homologous centromeres (Tsubouchi et al. 2008). In *Drosophila* females, assembly of C(3)G, the Zip1 equivalent in flies, is also first detected at centromeres (Tanneti et al. 2011; Takeo et al. 2011). In this system, centromere clustering is coincident with (Tanneti et al. 2011; Takeo et al. 2011) or immediately prior to (Christophorou et al. 2013) the initiation of meiosis. Intriguingly, mutations in cenp-C and call disrupt centromere clustering and homolog pairing in zygotene, as well as the retention of C(3)G at centromeres (Unhavaithaya and Orr-Weaver 2013). In this context, clustered and paired centromeres might serve as an effective structural platform to build and maintain functional associations between chromosomes. It is possible that CENP-A assembly at this time could reinforce such associations.

6 Current and Future Perspectives

Centromere dynamics in germ cells is a relatively new and exciting research field. Investigations into mechanisms of germ cell centromere function, assembly and maintenance in fly, plant, worm and frog model systems are certainly proving fruitful. A common emerging theme is that problems in centromere dynamics in germ cells can give rise to defective gametes, potentially resulting in aneuploidy in the next generation. Yet, experiments in more complex mammalian systems are currently lacking, limited by the accessibility to germ cells, as well as lack of genetic tools for germ cell-specific manipulations and appropriate *in vitro* culture systems. For example, centromere dynamics and functions in human germ cells are relatively unexplored, but are likely to prove important with clinical relevance for fertility and ageing. Major unresolved themes and future research questions include the following:

- . (i) Identifying key players and mechanisms of centromere specification and function in germ cells: Investigations so far have highlighted unexpected differences in CENP-A requirements and assembly dynamics in meiosis compared to mitosis. Given that in many organisms meiotic CENP-A assembles in prophase I, a cell cycle time when cyclin-dependent-kinase (CDK) activity is high, molecular signals must differ from mitosis (Silva et al. 2012). How is CENP-A assembly coupled to the meiotic cell cycle? What is the cell cycle timing of CENP-A assembly in male and female meiosis in mammals and in other species? Do mitotic chaperones and assembly factors function in meiosis or are meiosis-specific chaperones required? Undoubtedly, the targeted generation of separation-of-function mutations via the clustered regularly interspaced short palindromic repeats (CRISPR)/Cas9 system will aid the dissection of meiosis-specific

functions of essential genes. Additionally, genetic screens in model organisms and biochemical purifications of centromere proteins from meiotic cells will identify critical interactions and regulators. It will also be of interest to determine mechanisms and consequences of CENP-A disassembly in meiosis. ^{[[[}_{SEP]}

- . (ii) Identifying the function of the CENP-A N-terminus in germ cells: What is the meiosis-specific role of the CENP-A N-terminus in plants? Are the N-terminal conserved sequence blocks, identified in plants and flies, important for this function? Outside of plants, is the CENP-A N-terminus required for meiosis in other organisms? To answer these questions, the targeted deletion of the motifs by the CRISPR/Cas9 system in transgenic plants and animals is sure to prove informative. Is the CENP-A N-terminus differentially modified in meiosis? Do meiosis-specific CENP-A assembly and maintenance factors interact with the N-terminus? For this, protocols that facilitate precise sorting of meiotic cells improved strategies for biochemical purifications of germ cells from tissues, as well as the development of more sensitive mass spectrometry approaches to identify proteins from reduced ^{[[[}_{SEP]} amounts of material are critical.

(iii) Does the CENP-A N-terminus direct its removal in prophase I? FRAP experiments with truncated CENP-A trans- genes could give insight into potential phases of meiotic CENP-A turnover and provide evidence to support a CENP-A quality control check before chromosome segregation in meiosis I. For this, conditions that enhance the viability of germ cells in tissues for high-resolution time-lapse imaging are key.

Identifying mechanisms that govern the transgenerational inheritance of CENP-A: In most organisms, CENP-A epigenetically marks the position of the centromere on male and female gametes, which likely determines centromere position and function in every cell in the next generation. Therefore, it is critical that this epigenetic information is transmitted with fidelity from one generation to the next. On one hand, evidence from flies strongly supports a template-driven mechanism for CENP-A transmission. It is now important to confirm if this model holds true through multiple generations and in other organisms and if so, which molecular mechanisms determine the quantitative, template-driven inheritance of CENP-A. On the other hand, it is important to consider the possibility that de novo CENP-A assembly in zygotes might occur in other species aside from plant and worm. If so, is CENP-A sufficient to nucleate centromere establishment in this context? It is also important to consider whether the balance of CENP-A inherited with male and female gametes is

critical. For example, what is the relative contribution of egg and sperm chromatin to centromere identity in progeny and subsequent generations? What determines dependencies on specific CENP-A assembly pathways in male and female gametes in a given organism? Investigations into germ cell centromere dynamics in appropriate model organisms with short generational times and accessibility to both male and female gametes are key to the success of such transgenerational studies. Finally it will be important to determine how CENP-A resists protamine exchange during sperm differentiation.

References

- Black BE, Foltz DR, Chakravarthy S, Luger K, Woods VL, Cleveland DW (2004) Structural determinants for generating centromeric chromatin. *Nature* 430:578–582
- Black BE, Jansen LE, Maddox PS, Foltz DR, Desai AB, Shah JV, Cleveland DW (2007) Centromere identity maintained by nucleosomes assembled with histone H3 containing the CENP-A targeting domain. *Mol Cell* 25:309–322
- Blower MD, Karpen GH (2001) The role of *Drosophila* CID in kinetochore formation, cell-cycle progression and heterochromatin interactions. *Nat Cell Biol* 3:730–739
- Buchwitz BJ, Ahmad K, Moore LL, Roth MB, Henikoff S (1999) A histone-H3-like protein in *C. elegans*. *Nature* 401:547–548
- Cahoon CK, Hawley RS (2016) Regulating the construction and demolition of the synaptonemal complex. *Nat Struct Mol Biol* 23:369–377
- Carroll CW, Milks KJ, Straight AF (2010) Dual recognition of CENP-A nucleosomes is required for centromere assembly. *J Cell Biol* 189:1143–1155
- Carroll CW, Silva MC, Godek KM, Jansen LE, Straight AF (2009) Centromere assembly requires the direct recognition of CENP-A nucleosomes by CENP-N. *Nat Cell Biol* 11:896–902
- Chan FL, Wong LH (2012) Transcription in the maintenance of centromere chromatin identity. *Nucleic Acids Res* 40:11178–11188
- Christophorou N, Rubin T, Huynh JR (2013) Synaptonemal complex components promote centromere pairing in pre-meiotic germ cells. *PLoS Genet* 9:e1004012
- Dereeper A, Audic S, Claverie JM, Blanc G (2010) BLAST-EXPLORER helps you building datasets for phylogenetic analysis. *BMC Evol Biol* 10:18
- Dumont J, Oegema K, Desai A (2010) A kinetochore-independent mechanism drives anaphase chromosome separation during acentrosomal meiosis. *Nat Cell Biol* 12:894–901
- Dunleavy EM, Beier NL, Gorgescu W, Tang J, Costes SV, Karpen GH (2012) The cell cycle timing of centromeric chromatin assembly in *Drosophila* meiosis is distinct from mitosis yet requires CAL1 and CENP-C. *PLoS Biol* 10:e1001460
- Fachinetti D, Folco HD, Nechemia-Arbely Y, Valente LP, Nguyen K, Wong AJ, Zhu Q, Holland AJ, Desai A, Jansen LE, Cleveland DW (2013) A two-step mechanism for epigenetic specification of centromere identity and function. *Nat Cell Biol* 15:1056–1066
- Falk SJ, Guo LY, Sekulic N, Smoak EM, Mani T, Logsdon GA, Gupta K, Jansen LE, van Duyne GD, Vinogradov SA, Lampson MA, Black BE (2015) Chromosomes. CENP-C reshapes and stabilizes CENP-A nucleosomes at the centromere. *Science* 348:699–703
- Foltz DR, Jansen LE, Black BE, Bailey AO, Yates JR, Cleveland DW (2006) The human CENP-A centromeric nucleosome-associated complex. *Nat Cell Biol* 8:458–469
- Gassmann R, Rechtsteiner A, Yuen KW, Muroyama A, Egelhofer T, Gaydos L, Barron F, Maddox P, Essex A, Monen J, Ercan S, Lieb JD, Oegema K, Strome S, Desai A (2012) An inverse relationship to germline transcription defines centromeric chromatin in *C. elegans*. *Nature*

484:534–537

Heeger S, Leismann O, Schittenhelm R, Schraidt O, Heidmann S, Lehner CF (2005) Genetic interactions of separate regulatory subunits reveal the diverged *Drosophila* Cenp-C homolog. *Genes Dev* 19:2041–2053

Hemmerich P, Weidtkamp-Peters S, Hoischen C, Schmiedeberg L, Erliandri I, Diekmann S (2008) Dynamics of inner kinetochore assembly and maintenance in living cells. *J Cell Biol* 180:1101–1114

Howman EV, Fowler KJ, Newson AJ, Redward S, Macdonald AC, Kalitsis P, Choo KH (2000) Early disruption of centromeric chromatin organization in centromere protein A (Cenpa) null mice. *Proc Natl Acad Sci U S A* 97:1148–1153

Ingouff M, Rademacher S, Holec S, Soljić L, Xin N, Readshaw A, Foo SH, Lahouze B, Sprunck S, Berger F (2010) Zygotic resetting of the HISTONE 3 variant repertoire participates in epigenetic reprogramming in *Arabidopsis*. *Curr Biol* 20:2137–2143

Jansen LE, Black BE, Foltz DR, Cleveland DW (2007) Propagation of centromeric chromatin requires exit from mitosis. *J Cell Biol* 176:795–805

Kalitsis P, Fowler KJ, Earle E, Hill J, Choo KH (1998) Targeted disruption of mouse centromere protein C gene leads to mitotic disarray and early embryo death. *Proc Natl Acad Sci U S A* 95:1136–1141

Karimi-Ashtiyani R, Ishii T, Niessen M, Stein N, Heckmann S, Gurushidze M, Banaei-Moghaddam AM, Fuchs J, Schubert V, Koch K, Weiss O, Demidov D, Schmidt K, Kumlehn J, Houben A (2015) Point mutation impairs centromeric CENH3 loading and induces haploid plants. *Proc Natl Acad Sci U S A* 112:11211–11216

Kim J, Ishiguro K, Nambu A, Akiyoshi B, Yokobayashi S, Kagami A, Ishiguro T, Pendas AM, Takeda N, Sakakibara Y, Kitajima TS, Tanno Y, Sakuno T, Watanabe Y (2015) Meikin is a conserved regulator of meiosis-I-specific kinetochore function. *Nature* 517:466–471

Kwenda L, Collins CM, Dattoli AA, Dunleavy EM (2016) Nucleolar activity and CENP-C regulate CENP-A and CAL1 availability for centromere assembly in meiosis. *Development* 143:1400–1412

Kwon MS, Hori T, Okada M, Fukagawa T (2007) CENP-C is involved in chromosome segregation, mitotic checkpoint function, and kinetochore assembly. *Mol Biol Cell* 18: 2155–2168

Lando D, Endesfelder U, Berger H, Subramanian L, Dunne PD, McColl J, Klenerman D, Carr AM, Sauer M, Allshire RC, Heilemann M, Laue ED (2012) Quantitative single-molecule microscopy reveals that CENP-A(Cnp1) deposition occurs during G2 in fission yeast. *Open Biol* 2:120078

Lermontova I, Fuchs J, Schubert V, Schubert I (2007) Loading time of the centromeric histone H3 variant differs between plants and animals. *Chromosoma* 116:507–510

Lermontova I, Koroleva O, Rutten T, Fuchs J, Schubert V, Moraes I, Koszegi D, Schubert I (2011) Knockdown of CENH3 in *Arabidopsis* reduces mitotic divisions and causes sterility by disturbed meiotic chromosome segregation. *Plant J* 68:40–50

Lermontova I, Schubert V, Fuchs J, Klante S, Macas J, Schubert I (2006) Loading of *Arabidopsis* centromeric histone CENH3 occurs mainly during G2 and requires the presence of the histone fold domain. *Plant Cell* 18:2443–2451

Logsdon GA, Barrey EJ, Bassett EA, Denizio JE, Guo LY, Panchenko T, Dawicki-Mckenna JM, Heun P, Black BE (2015) Both tails and the centromere targeting domain of CENP-A are required for centromere establishment. *J Cell Biol* 208:521–531

Maheshwari S, Tan EH, West A, Franklin FC, Comai L, Chan SW (2015) Naturally occurring differences in CENH3 affect chromosome segregation in zygotic mitosis of hybrids. *PLoS Genet* 11:e1004970

Malik HS, Henikoff S (2003) Phylogenomics of the nucleosome. *Nat Struct Biol* 10:882–891
 Malik HS, Vermaak D, Henikoff S (2002) Recurrent evolution of DNA-binding motifs in the *Drosophila* centromeric histone. *Proc Natl Acad Sci U S A* 99:1449–1454^[11]_{SEP}

Marques A, Pedrosa-Harand A (2016) Holocentromere identity: from the typical mitotic linear

- structure to the great plasticity of meiotic holocentromeres. *Chromosoma* 125(4):669–81
- Meluh PB, Koshland D (1995) Evidence that the MIF2 gene of *Saccharomyces cerevisiae* encodes a centromere protein with homology to the mammalian centromere protein CENP-C. *Mol Biol Cell* 6:793–807^[SEP]
- Meyer GF (1960) Proceedings of the European regional conference on electron microscopy. Die Nederlandse Vereniging voor Electronmicroscopie
- Milks KJ, Moree B, Straight AF (2009) Dissection of CENP-C-directed centromere and kinetochore assembly. *Mol Biol Cell* 20:4246–4255^[SEP]
- Monen J, Maddox PS, Hyndman F, Oegema K, Desai A (2005) Differential role of CENP-A in the segregation of holocentric *C. elegans* chromosomes during meiosis and mitosis. *Nat Cell Biol* 7:1248–1255^[SEP]
- Notredame C, Higgins DG, Heringa J (2000) T-Coffee: a novel method for fast and accurate multiple sequence alignment. *J Mol Biol* 302:205–217
- ^[SEP]Palmer DK, O'Day K, Margolis RL (1990) The centromere specific histone CENP-A is selectively retained in discrete foci in mammalian sperm nuclei. *Chromosoma* 100:32–36^[SEP]
- Palmer DK, O'Day K, Trong HL, Charbonneau H, Margolis RL (1991) Purification of the centromere-specific protein CENP-A and demonstration that it is a distinctive histone. *Proc Natl Acad Sci U S A* 88:3734–3738
- ^[SEP]Ravi M, Chan SW (2010) Haploid plants produced by centromere-mediated genome elimination. *Nature* 464:615–618^[SEP]
- Ravi M, Kwong PN, Menorca RM, Valencia JT, Ramahi JS, Stewart JL, Tran RK, Sundaresan V, Comai L, Chan SW (2010) The rapidly evolving centromere-specific histone has stringent functional requirements in *Arabidopsis thaliana*. *Genetics* 186:461–471^[SEP]
- Ravi M, Shibata F, Ramahi JS, Nagaki K, Chen C, Murata M, Chan SW (2011) Meiosis-specific loading of the centromere-specific histone CENH3 in *Arabidopsis thaliana*. *PLoS Genet* 7:e1002121^[SEP]
- Raychaudhuri N, Dubruielle R, Orsi GA, Bagheri HC, Loppin B, Lehner CF (2012) Transgenerational propagation and quantitative maintenance of paternal centromeres depends on Cid/Cenp-A presence in *Drosophila* sperm. *PLoS Biol* 10:e1001434
- Sanei M, Pickering R, Kumke K, Nasuda S, Houben A (2011) Loss of centromeric histone H3 (CENH3) from centromeres precedes uniparental chromosome elimination in interspecific barley hybrids. *Proc Natl Acad Sci U S A* 108:E498–E505
- Schittenhelm RB, Althoff F, Heidmann S, Lehner CF (2010) Detrimental incorporation of excess Cenp-A/Cid and Cenp-C into *Drosophila* centromeres is prevented by limiting amounts of the bridging factor Cal1. *J Cell Sci* 123:3768–3779
- Schubert V, Lermontova I, Schubert I (2014) Loading of the centromeric histone H3 variant during meiosis-how does it differ from mitosis? *Chromosoma* 123:491–497
- Schuh M, Lehner CF, Heidmann S (2007) Incorporation of *Drosophila* CID/CENP-A and CENP-C into centromeres during early embryonic anaphase. *Curr Biol* 17:237–243
- Silva MC, Bodor DL, Stellfox ME, Martins NM, Hohegger H, Foltz DR, Jansen LE (2012) Cdk activity couples epigenetic centromere inheritance to cell cycle progression. *Dev Cell* 22:52–63
- Smoak EM, Stein P, Schultz RM, Lampson MA, Black BE (2016) Long-term retention of CENP-A nucleosomes in Mammalian oocytes underpins transgenerational inheritance of centromere identity. *Curr Biol* 26:1110–1116
- ^[SEP]Stoler S, Keith KC, Curnick KE, Fitzgerald-Hayes M (1995) A mutation in CSE4, an essential gene encoding a novel chromatin-associated protein in yeast, causes chromosome nondisjunction and cell cycle arrest at mitosis. *Genes Dev* 9:573–586^[SEP]
- Takahashi K, Chen ES, Yanagida M (2000) Requirement of Mis6 centromere connector for localizing a CENP-A-like protein in fission yeast. *Science* 288:2215–2219^[SEP]
- Takeo S, Lake CM, Morais-De-sá E, Sunkel CE, Hawley RS (2011) Synaptonemal complex-

Appendices

- dependent centromeric clustering and the initiation of synapsis in *Drosophila* oocytes. *Curr Biol* 21:1845–1851^{[1][SEP]}
- Tanaka K, Chang HL, Kagami A, Watanabe Y (2009) CENP-C functions as a scaffold for effectors with essential kinetochore functions in mitosis and meiosis. *Dev Cell* 17:334–343^{[1][SEP]}
- Tanneti NS, Landy K, Joyce EF, McKim KS (2011) A pathway for synapsis initiation during zygotene in *Drosophila* oocytes. *Curr Biol* 21:1852–1857^{[1][SEP]}
- Torras-Llort M, Moreno-Moreno O, Azorín F (2009) Focus on the centre: the role of chromatin on the regulation of centromere identity and function. *EMBO J* 28:2337–2348^{[1][SEP]}
- Tsubouchi T, Macqueen AJ, Roeder GS (2008) Initiation of meiotic chromosome synapsis at centromeres in budding yeast. *Genes Dev* 22:3217–3226^{[1][SEP]}
- Unhavaithaya Y, Orr-Weaver TL (2013) Centromere proteins CENP-C and CAL1 functionally interact in meiosis for centromere clustering, pairing, and chromosome segregation. *Proc Natl Acad Sci U S A* 110:19878–19883^{[1][SEP]}
- Valente LP, Silva MC, Jansen LE (2012) Temporal control of epigenetic centromere specification. *Chromosome Res* 20:481–492^{[1][SEP]}
- Von Stetina JR, Orr-Weaver TL (2011) Developmental control of oocyte maturation and egg activation in metazoan models. *Cold Spring Harb Perspect Biol* 3:a005553^{[1][SEP]}
- Watanabe Y (2012) Geometry and force behind kinetochore orientation: lessons from meiosis. *Nat Rev Mol Cell Biol* 13:370–382^{[1][SEP]}
- Zeitlin SG, Patel S, Kavli B, Slupphaug G (2005) *Xenopus* CENP-A assembly into chromatin requires base excision repair proteins. *DNA Repair (Amst)* 4:760–772

Appendices

8.2. Chemical reagents and common buffers

Reagent	Composition	Note
Immunostaining and FISH		
Fixation	4 % (v/v) paraformaldehyde in 1X PBS (for PFA fixation). 100 % Methanol & 100 % acetone (for methanol/acetone fixation).	4 % PFA followed by 10 minute 0.4 % PBSTx wash for removal of cytoplasm. 4 % PFA followed by ethanol series (-20 °C) for cytoplasm preservation.
Immunofluorescence (IF) permeabilisation buffer	0.3 % (w/v) sodium deoxycholate in 0.4 % (v/v) PBS-Triton-X (for PFA fixation). 1X PBS with 1 % (v/v) Triton-X and 0.5 % (v/v) acetic acid (For methanol/acetone fix).	Use 0.3 % (w/v) sodium deoxycholate with 0.4 % PBSTx for PFA in combination with ethanol series. Really permeabilises cell membrane, improves DAPI staining. Sodium deoxycholate need stock solution (10 %) needs to be made fresh every 30 days.
IF wash buffer (0.1% PBSTX)	1X PBS with 0.1 % (v/v) Triton-X or 1X PBS with 0.4 % (v/v) Triton-X	
IF blocking buffer	1 % or 3 % (w/v) Bovine serum albumin (BSA) in 0.4 % (v/v) PBS-Triton-X	Make fresh every 2-3 days.
FISH wash buffer	2X saline-sodium citrate (SSC) with 0.1 % (v/v) Tween 20	
FISH pre-hybridisation buffer 1	2X SCC-Tw with 25 % (v/v) formamide	Pre-hybridisation buffers can be retained after use and re-used as post-hybridisation wash buffers. Store overnight at 4 °C.
FISH pre-hybridisation buffer 2	2X SCC-Tw with 50 % (v/v) formamide	
FISH hybridisation buffer	3X SCC with 50 % (v/v) formamide, 10 % (w/v) dextran sulfate and 20 - 40 ng of DNA probes.	
FISH post-hybridisation wash buffer 1	2X SCC-Tw with 50 % (v/v) formamide	
FISH post-hybridisation wash buffer 2	2X SCC-Tw with 25 % (v/v) formamide	
DAPI staining buffer	1X PBS with 1 ug/ml DAPI	

Appendices

Mounting medium		
DNA / RNA / ATP Extraction		
DNA extraction buffer	100 mM Tris-HCl pH 7.5 with 1 % SDS, 100 mM NaCl and 100 mM EDTA	
RNA extraction buffer	Trizol reagent (100 %)	Toxic, classified as CMR. Use appropriate PPE.
ATP extraction buffer	100 mM Tris pH 7.8 with 6 M Guanidine Hydrochloride and 4 mM EDTA	Long term storage at 4 °C.
Dilution buffer (ATP assay)	25 mM Tris HCL pH 7.8 and 100 µM EDTA	
Reaction buffer (ATP assay)	500 mM Tricine buffer, pH 7.8, 100 mM MgSO ₄ , 2 mM EDTA and 2 mM sodium azide	
Reaction solution (ATP assay)	1X Reaction buffer with 0.01 mM DTT, 0.005 mM D-luciferin and 12.5 µg of firefly luciferase	Only make as much reaction solution as needed, any extra can be stored for up to one week at 4 °C.
Protein Extraction & Pulldown Experiments		
Testis digestion buffer	PBS containing 1 mg/ml collagenase, 1.5 mM CaCl ₂ , 2 % BSA and 100 µg/ml DNase	Make fresh for each use.
Hypotonic buffer	10 mM HEPES, 1.5 mM NaCl, 1.5 mM MgCl ₂ , 0.1 mM EGTA, 1 mM DTT, 0.1 % Triton-X, 1 % protease inhibitor cocktail	
Lysis buffer	20 mM Tris-HCl pH 7.5, 300 mM NaCl, 0.5 mM EDTA, 0.05 % Triton-X, 0.1 % NP-40, 1 mM PMSF and 1 % protease inhibitor cocktail	
Interaction buffer (Pull-down experiments)	20 mM Tris-HCl pH 7.5, 300 mM NaCl, 0.5 mM EDTA, 0.05 % NP-40, 1 mM PMSF and 1 % protease inhibitor cocktail	
Wash buffer (Pull-down experiments)	20 mM Tris-HCl pH 7.5, 500 mM NaCl, 0.5 mM EDTA, 0.05 % NP-40, 1 mM PMSF and 1 % protease inhibitor cocktail	
Protein Expression & purification		

Appendices

Luria-Bertani medium (LB)	1 % tryptone, 0.5% yeast extract, 1 % NaCl at pH 7.0. LB was supplemented with 25 µg/ml ampicillin, kanamycin or chloramphenicol.	
Bacterial cell lysis buffer	1X PBS with 1 mM EDTA, 1mM EGTA, 1mM PMSF, 200 µg/ml lysozyme and protease inhibitors	
Wash buffer (GST-tag purification)	PBS with 0.25 M KCL, 0.5 mM DTT and 1 % protease inhibitor cocktail.	
GST-tag elution buffer	50 mM Tris-HCL pH 8.0, 40 mM glutathione and 0.25 M KCL	Make fresh each time. Glutathione is reduced at Ph 8.0, to ensure efficient elution check Ph each time you make buffer and adjust as required.
Inclusion body wash buffer	50 mM Tris-HCL pH 8.0 with 1 % protease inhibitor cocktail.	
Inclusion body solubilisation buffer	50 mM Tris-HCL pH 8.0, 5 M urea and 50 mM DTT	
Wash buffer (His-tag purification)	50 mM Tris-HCL pH 8.0, 5 M urea and 20 mM imidazole	
His-tag elution buffer (denaturing conditions)	50 mM Tris-HCL pH 8.0, 5 M urea and 200 mM imidazole	
Dialysis buffer (soluble proteins)	1X PBS with 20 % glycerol.	
Dialysis buffer 1 (renaturing)	50 mM Tris-HCL pH 8.0 and 3 M urea	
Dialysis buffer 2 (renaturing)	50 mM Tris-HCL pH 8.0 and 1.5 M urea	
Dialysis buffer 3 (renaturing)	50 mM Tris-HCL pH 8.0	
Direct interaction assay & Peptide array assay		
Interaction buffer (in vitro)	50 mM Tris-HCL pH 8.0, 250 mM NaCl, 0.05 % NP-40 and 1 % protease inhibitor cocktail	
Wash buffer (Invitro)	50 mM Tris-HCL pH 8.0, 400 mM NaCl and 0.05 % NP-40 and 1 % protease inhibitor cocktail	

Appendices

Elution buffer (in vitro)	50 mM Tris-HCL pH 8.0, 40 mM glutathione and 0.25 M KCL	
Binding buffer (His-ATPsyn- α vs. CENP-A peptide array)	His-ATPsyn- α (5 μ g/ml) in 1X PBS with 0.1 % (v/v) Triton-X and 1 % (w/v) milk powder	
Western blotting		
Loading buffer	NuPAGE LDS sample buffer containing 1X Bolt sample reducing agent (Invitrogen)	
SDS running buffer	NuPAGE MES SDS running buffer	
Transfer buffer		
Ponceau S	0.5 % (w/v) Ponceau S with 5 % acetic acid	
Blocking buffer	5 % (w/v) milk powder in 0.1% TBS-Tween20	
Wash buffer (0.1 % TBSTw)	1X TBS with 0.1 % Tween20	

Appendices

8.3. Fly stocks used during this study

Genotype	Gene	Source BL# / VDRC#	Balancer	RNAi construct type	Appropriate control	Target region
<i>y[1] v[1]; P{y[+t7.7] v[+t1.8]=TRiP.JF02896}attP2</i>	<i>ATPsyn-α</i>	BL28059; Trip JF02896		Hairpin, 1stGeneration, Valium10. TripSoma	#36303	bp 1019-1424, C-term
<i>y[1] v[1]; P{y[+t7.7] v[+t1.8]=TRiP.JF02792}attP2</i>	<i>ATPsyn-β</i>	BL27712; TripJF02792		Hairpin, 1stGeneration, Valium10. TripSoma	#36303	bp 503-761, targets all isoforms of ATPsyn-β. 73% identity with β-like
<i>y[1] v[1]; P{y[+t7.7] v[+t1.8]=TRiP.GLC01662}attP2</i>	<i>ATPsyn-γ</i>	BL50543; TripGLC01662	TM3, Sb	dsRNA, 2nd Generation, Valium22. TripGermline	#36303	
<i>y[1] v[1]; P{y[+t7.7] v[+t1.8]=TRiP.JF02899}attP2</i>	<i>ATPsyn-b</i>	BL28062; TripJF02899		dsRNA, 1st generation, Valium10. TripSoma	#36303	
<i>y[1] sc[*] v[1]; P{y[+t7.7] v[+t1.8]=TRiP.HM05229}attP2</i>	<i>ND-23</i>	BL30487; TripHM05229		dsRNA, 1st generation, Valium10. TripSoma	#36303	
<i>y[1] v[1]; P{y[+t7.7] v[+t1.8]=TRiP.HM05213}attP2</i>	<i>ND-51</i>	BL29534; HM05213		dsRNA, 1st generation, Valium10. TripSoma	#36303	
<i>w[1118]; P{GD11030}v34664</i>	<i>ATPsyn-α</i>	v34664; GD library		Hairpin	#60000	328bp, targets mid gene bp670-998
<i>w[1118] P{GD4967}v37812</i>	<i>ATPsyn-β</i>	v37812; GD library		Hairpin	#60000	bp 82-394, (312bp target) Nterm. Low homology with β-Like
<i>w[1118]; P{GD6339}v16538</i>	<i>ATPsyn-γ</i>	v16538; GD Library		Hairpin	#60000	356bp target region.

Appendices

<i>w</i> [1118]; <i>P</i> {GD11634} <i>v</i> 22111/ <i>TM3</i>	<i>ATPsyn-β-Like</i>	V22111; GD Library	TM3, Sb	Hairpin	#60000	348bp hairpin, Cterminus
<i>P</i> {KK106259} <i>VIE-260B</i>	<i>ATPsyn-β-Like</i>	V106718; KK Library		Hairpin	#60100	342bp hairpin, Nterminus target
<i>w</i> [1118]; <i>P</i> {GD4436} <i>v</i> 43857	<i>cid</i>	v43857; GD Library		Hairpin	#60000	<i>cid</i> bp 295-371
<i>P</i> {KK110670} <i>VIE-260B</i>	<i>cid</i>	v102090; KK library		Hairpin	#60100	<i>cid</i> bp 141-413
<i>y</i> [+] <i>ry</i> [+]						
<i>y</i> [1] <i>v</i> [1]; <i>P</i> { <i>y</i> [+7.7]= <i>CaryP</i> } <i>attP2</i>		BL36303				
<i>y</i> [1] <i>v</i> [1]; <i>P</i> { <i>y</i> [+7.7] <i>v</i> [+1.8]= <i>TRiP.HMC04808</i> } <i>attP2</i>		v60000				
<i>y</i> [1] <i>sc</i> [*] <i>v</i> [1]; <i>P</i> { <i>y</i> [+7.7] <i>v</i> [+1.8]= <i>TRiP.HMC05094</i> } <i>attP40</i>		v60100				

Genotype	Gene	Bloomington Stock #	Balancer	Control	Reference
<i>w</i> ¹¹¹⁸ ; <i>P</i> Bac{RB} <i>ATPsyn-βLike</i> ^{e01800} / <i>Tb</i>	<i>ATPsyn-β-Like</i>	#17989	<i>Tb</i>	<i>y+ry+</i>	Thibault <i>et al.</i> , 2004; Bellen <i>et al.</i> , 2011

Appendices

8.4. Information on cloning and cloning strategy

Construct	Method	Vector	Primers used	Additional information
Constructs for transgenic fly lines				
<i>pcopia_egfp_ATPsyn-βlike</i>	Gibson Assembly	pCaSpeR5 (Ampicillin resistant)	FRAG1. FOR: CCGCATAGGCCACTAGTGGATCTGTGTTGGAATATACTATTCAAC FRAG1. REV: AGCTCCTCGCCCTTGCTCACCATAACCTGTTGTAATTTATAATTT FRAG2. FOR: AATATAAATTACAACAGGTTATGGTGAGCAAGGGCGAGGAGCT FRAG2. REV: TTAGCCCATGATACCAACATCTTGACAGCTCGTCCATGCCGAGA FRAG3. FOR: GCATGGACGAGCTGTACAAGATGTTGGTATCATGGGCTAAAATGG FRAG3. REV: AGCTTTAGAGCTCTTCTTAAGTTAATCTTTCTTTCCGGTTC	Inserted at BamH1 site
<i>pATPsynβlike_egfp_ATPsyn-βlike</i>	Gibson Assembly	pCaSpeR5 (Ampicillin resistant)	FRAG1. FOR: GCATAGGCCACTAGTGGATCTGTTTTAGCTGCTGATCCACATGCT FRAAG1. REV: AGCTCCTCGCCCTGGCTCACCATTTTTACTTTAGTTTTTTATTCT FRAG2. FOR: AGAATAAAAAAATAAGTAAAAATGGTGAGCAAGGGCGAGGAGCT FRAG2. REV: CATTTTAGCCCATGATACCAACATCTTGACAGCTCGTCCATGCC FRAG3. FOR: AAGCTTTAGAGCTCTTCTTAAGAAGAGGTGGGTTTCCCTTCTCC FRAG3. REV: TCGGCATGGACGAGCTGTACAAGATGTTGGTATCATGGGCTAAAA	Inserted at BamH1 site
<i>pATPsynβ_mcherry_ATPsyn-β Variant C</i>	Gibson Assembly	pCaSpeR5 (Ampicillin resistant)	FRAG1. FOR: GCCGCATAGGCCACTAGTGGATCTGAGCCGAGTCGATCTACACAT FRAG1. REV: ATCCTCCTCGCCCTTGCTCACCATTTTTCTCGAACTAACTGAGAA FRAG2. FOR: CACTTCTCAGTTAGTTCGAGAAAAATGGTGAGCAAGGGCGAGGAG FRAG2. REV: TAGATGCAGCACGTAACGCGAACATCTTGACAGCTCGTCCATGC FRAG3. FOR: GGCGCATGGACGAGCTGTACAAGATGTTTCGCGTTACGTGCTGCA FRAG3. REV: GCTTTAGAGCTCTTCTTAAGAAGGAACCCGCTACCTATAGTAT	Inserted at BamH1 site
<i>pATPsynβ_mcherry_ATPsyn-β Variant D</i>	Gibson Assembly	pCaSpeR5 (Ampicillin resistant)		

Appendices

<i>pcep-a_egfp_cenpa</i> $\Delta 118$	Gibson Assembly	pCaSpeR5 (Ampicillin resistant)	FRAG1. FOR: ATAGGCCACTAGTGGATCTGccgacatggctgtatcttcagt FRAG1. REV: AACAGCTCCTCGCCCTTGCTCACCATtttcaaatttcggtatttGCTT FRAG2. FOR: ttaagcaaataccgaaaatttgaatGGTGAGCAAGGGCGAGGAGCT FRAG2. REV: GATTGGCCGCTTTGCGCCCTACCACCACCTTGTACAGCTCGTCCAT FRAG3. FOR: ATGGACGAGCTGTACAAGGGTGGTGGTAGGCGGCGCAAAGCGGCCAATC FRAG3. REV: AAGCTTTAGAGCTCTTCTTAAGAAGCCTAATCCTAGCTGAAACCCTATG	Inserted at BamH1 site
Constructs for protein purification				
<i>gst-cenp-a</i> (FL)	Restriction Cloning	pGEX-4T-1 (Ampicillin resistant)	FORWARD: ATGATGGGATCCATGCCACGACACAGCAGAG REVERSE: CGATGCGGCCGCTAAAATTGCCGACCCCGGTC	Inserted in-line with N-terminal GST-tag at BAMH1 (5') and NOT1 (3') restriction sites
<i>gst-cenp-a n terminus</i> (a.a 1-126)	Restriction Cloning	pGEX-4T-1 (Ampicillin resistant)	FORWARD: ATGATGGGATCCATGCCACGACACAGCAGAG	Inserted in-line with N-terminal GST-tag at BAMH1 (5') and NOT1 (3') restriction sites
<i>gst-cenp-a hfd</i> (a.a 127-225)	Restriction Cloning	pGEX-4T-1 (Ampicillin resistant)	FORWARD: CCGCGTGGATCCATGAGCAGAGCCAAGAGAATGGATCG REVERSE: CGATGCGGCCGCTAAAATTGCCGACCCCGGTC	Inserted in-line with N-terminal GST-tag at BAMH1 (5') and NOT1 (3') restriction sites
<i>gst-histone h3.1</i>	Restriction Cloning	pGEX-4T-1 (Ampicillin resistant)	FORWARD: CGCGTGGATCCATGGCTCGTACCAAGCAAAT REVERSE: GTCGACCCGGGAATTCTTAAGCACGCTCGC	Inserted in-line with N-terminal GST-tag at BAMH1 (5') and ECOR1 (3') restriction sites
<i>His-ATPsyn-α</i>	Gibson Assembly	pET-30 a (-) (Kanamycin resistant)	FORWARD: ATATGCACCATCATCATCATATGTGATTTTTTCCGCCCGCC REVERSE: CCGCGTGGCACCAGACCAGAAGATTACCCTGGAAGGTGGACATG	Inserted in-line with N-terminal His-tag
<i>His-ATPsyn-β</i>	Gibson Assembly	pET-30 a (-) (Kanamycin resistant)	FORWARD: CATATGCACCATCATCATCATATGTTGCGTTACGTGCTGCA REVERSE: ACCGCGTGGCACCAGACCAGAAGACTAGGCAGCTTCTTTGCCAG	Inserted in-line with N-terminal His-tag
<i>His-ATPsyn-βlike</i>	Gibson Assembly	pET-30 a (-) (Kanamycin resistant)	FORWARD: ACATATGCACCATCATCATCATATGTTGGTATCATGGGCTAAAATG REVERSE: GCGTGGCACCAGACCAGAAGATTAATCTTTCTTTCCGGTCTTTTGGC	Inserted in-line with N-terminal His-tag
<i>gst-mst35ba</i> (a.a 6 - 123)	Restriction	pGEX-4T-1 (Ampicillin resistant)	FORWARD: tctacggaattcATGGTAAATGAgtgcaagag REVERSE: cccgggCtacATCCGGCGGTAT	Inserted in-line with N-terminal GST-tag at ECOR1 (5') and PST1 (3') restriction

Appendices

				sites
<i>gst-mst35bb</i> (a.a 6-127)	Restriction	pGEX-4T-1 (Ampicillin resistant)	FORWARD: GaattcatgGTAATGAGTGCAAGAGCC REVERSE: cccgggctaGACCTTGCATGCCAT	Inserted in-line with N-terminal GST-tag at ECOR1 (5') and PST1 (3') restriction sites
<i>gst-mst77f</i>	Restriction	pGEX-4T-1 (Ampicillin resistant)	FORWARD: ATGATagaattcATGAGTAATCTGAAACAAAAGGATA REVERSE: cccgggTTACATCGAGCACTTGGGCTTGG	Inserted in-line with N-terminal GST-tag at ECOR1 (5') and XHO1 (3') restriction sites

Appendices

8.5. Primary and secondary antibodies

Primary antibodies				
Target	Antibody Description	Product Identifier	Immunofluorescence	Western Blot
CENP-A (CID)	Rabbit pAb (Active Motif)	#39713	1/500	1/2000
CENP-C	Guinea Pig pAb (Erhardt <i>et al.</i> , 2008)	n/a	1/500	1/2000
ATPsyn- α	Mouse monoclonal 15H4C4 (Abcam)	ab14748	1/200	1/1000
ATPsyn- β	Mouse monoclonal 3D5 (Abcam)	ab14730	1/200	1/1000
ATPsyn- γ	Goat Polyclonal-C terminal (Abcam)	ab190310	1/200	
GST	Rat monoclonal 6G9 (Chromotek)	6G9		1/1000
mCherry (WB)	Mouse monoclonal 6G6 (Chromotek)	6G6	1/1000	
mCherry (IF)	Rat monoclonal 5F8 (Chromotek)	5F8		1/1000
GFP	Rabbit polyclonal (FL) (Santa Cruz)	SC-8334		
Poly-HIS	Mouse monoclonal (Sigma Aldrich)	H1029		1/1000
Tubulin (IF)	Mouse monoclonal (Abcam)	Ab44928	1/500	
Tubulin (WB)	Mouse monoclonal DM1-A (Sigma Aldrich)	T5168		1/10,000

Appendices

Secondary antibodies				
Target	Antibody Description	Product Identifier	Immunofluorescence	
Mouse IgG	Goat Anti-Mouse Alexa 488 (Life Technologies)	A-11029	1/500	
Mouse IgG	Goat Anti-Mouse Alexa 546 (Life Technologies)		1/500	
Mouse IgG	Goat Anti-Mouse Alexa 647 (Life Technologies)	A-21236	1/500	
Rabbit IgG	Goat Anti-Rabbit Alexa 488 (Life Technologies)	A-11034	1/500	
Rabbit IgG	Goat Anti-Rabbit Alexa 546 (Life Technologies)	A-11035	1/500	
Rabbit IgG	Goat Anti-Rabbit Alexa Cy-5 (Bethyl)	A120-201C5	1/500	
GunieaPig IgG	Goat Anti Guniea Pig Alexa 647(Life Technologies)	A-21450	1/500	
GunieaPig IgG	Goat Anti Guniea Pig Alexa 488 (Life Technologies)	A-11073	1/500	

Appendices

8.6. Fluorescence in-situ Hybridization (FISH) DNA probes

Target	DNA Probe Sequence	Reference
1.686 g/cm ³ satellite; Chromosomes 2L and 3L	(AATAACATAG) ₃	Tsai <i>et al.</i> , 2011
4th Chromosome	(AATAT) ₆	Tsai <i>et al.</i> , 2011
X (L) Chromosome	359 bp Repeat	Tsai <i>et al.</i> , 2011
Y (L) Chromosome	(AATAC) ₆	Tsai <i>et al.</i> , 2011

8.7. C. M Collins and E. M Dunleavy, under review.

Book Title:

Histone Variants: Centromeric Histone Dynamics in the Cell Cycle and Development

Chapter Title: Imaging of Centromere Assembly and Chromosome Dynamics in *Drosophila melanogaster* Testis by Immunofluorescence In Situ Hybridisation (Immuno-FISH).

Authors: Caitríona M Collins and Elaine M Dunleavy

i. Summary/Abstract

This chapter describes a method used to assay the cell cycle dynamics of centromeres in meiosis using *Drosophila* males as the experimental system. Specifically, we describe a method to combine Fluorescence in-situ Hybridisation (FISH) and Immunofluorescence (IF) protocols, performed on fixed *Drosophila* testes. An advantage of this protocol is the ability to localize individual centromeres on the four *Drosophila* chromosomes that form distinct nuclear territories in spermatocytes. We also describe a method to quantify CENP-A focal intensities using Image J software.

ii. Key Words

Drosophila melanogaster; Centromere; Chromosome segregation; CENP-A; Meiosis; Prophase I; Spermatogenesis

1. Introduction

At centromeres, the canonical histone H3 is replaced by the centromeric histone H3 variant CENP-A (Westhorpe and Straight 2014). Correct levels of CENP-A at the centromere are essential for centromere function in both mitotic and meiotic cell division cycles. Additionally, as centromeres are not determined by DNA sequence, CENP-A provides the key epigenetic mark that defines centromere location on the chromosome (Allshire and Karpen 2008; Panchenko and Black 2009). To ensure centromere function, CENP-A nucleosomes at centromeres must be replenished each

cell cycle. Unlike canonical histone H3 that is assembled at DNA replication, the de novo assembly of CENP-A at centromeres is a DNA replication independent process occurring outside of S phase. Strikingly, investigations so far indicate that the cell cycle timing of CENP-A assembly differs between mitosis and meiosis. In mitosis in most somatic cells, CENP-A is assembled at late telophase/early G₁ phase (Valente et al. 2012). Yet, in meiosis in germ cells, CENP-A is assembled at prophase of meiosis I (Dunleavy et al. 2012; Raychaudhuri et al. 2012). Here we describe a method to assay CENP-A assembly and localization dynamics in *Drosophila* cell meiosis.

Drosophila melanogaster males are an excellent model system in which to study centromere dynamics in meiosis and development. Advantages of this model system include the ease of genetic manipulation and the sequential progression of meiosis through the tubular shaped testes, which allows for easy identification of different cell stages. At the tip of *Drosophila* testes, germ-line stem cells divide asymmetrically giving rise to pre-meiotic primary spermatogonia. These cells are then amplified in number through a series of mitotic divisions producing a cyst of 16 cells, which synchronously undergo a single round of DNA replication prior to entering into meiosis I (Fuller 1993). *Drosophila* males do not follow the standard meiotic prophase I script whereby homologous chromosomes pair, assemble a synaptonemal complex, recombine and are held together until anaphase I by chiasma (McKee et al. 2012). Instead, male fruit flies opt for an alternative (and not very well understood) method of conjoining homologous chromosomes in distinct nuclear territories. Therefore, stages of meiotic prophase I have a unique classification (designated S1 to S6) which is based on the formation of these chromosome territories (Cenci et al. 1994; figure 1). In this system, previous studies have shown that CENP-A is assembled at centromeres between S1 and S6 stages (Dunleavy et al. 2012; Raychaudhuri et al. 2012; Kwenda et al. 2016). During this stage different levels of CENP-A are observed at centromeres of different chromosomes; Firstly, the 4th chromosomes are usually paired at this stage and display a brighter CENP-A signal as a result. Secondly, the nucleolar-associated sex chromosomes display a higher level of CENP-A compared to the more ‘peripherally’ located autosomes (figure 1) and interestingly, disruption of CENP-A assembly mechanisms at this time have been shown to reduce CENP-A assembly at peripheral centromeres but not nucleolar-associated centromeres (Kwenda *et al.*, 2016). Thus alternative CENP-A assembly mechanisms for different chromosomes have been proposed (Kwenda *et al.*, 2016).

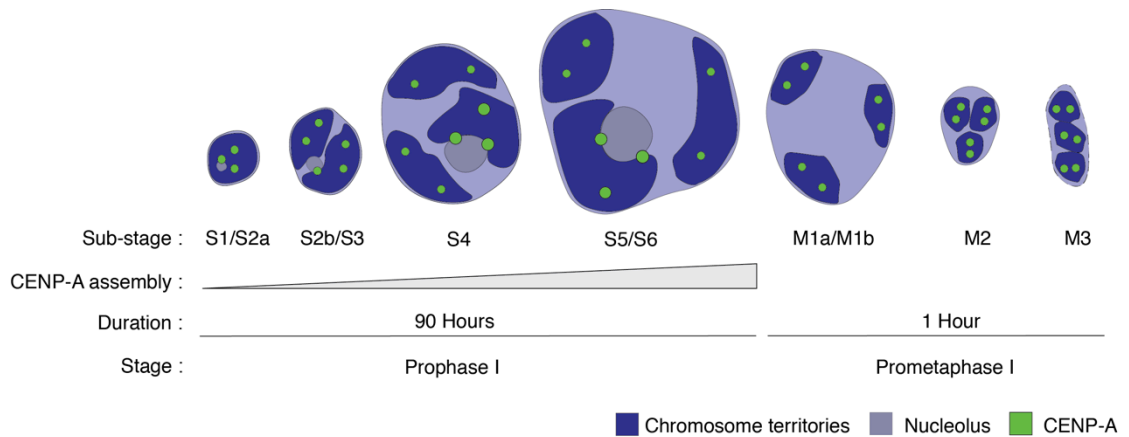


Figure 1: Schematic illustrating nuclear morphology, centromere organization and CENP-A dynamics during meiosis prophase and prometaphase I in *Drosophila* spermatocytes. At prophase S1/S2a homologous and non-homologous centromeres cluster. Between S2b and S5/6 wide homologous centromeres separate and distinct nuclear territories form. Widespread chromatin decondensation results in the formation of DAPI-light regions. In prometaphase I chromosome territories condense and centromeres align at the metaphase plate. Sister centromeres remain cohesed throughout.

Here we describe procedures for immuno-staining S1 and S6 stage spermatocytes for CENP-A, combined with chromosome specific FISH, to enable the tracking of centromere and CENP-A dynamics on each of the four *Drosophila* homologs during meiosis. Here we use FISH probes recognizing distinct heterochromatic sites (1.686g/cm^3) on the 2nd and 3rd autosomes and a known pairing site on the 4th chromosome (AATAT) (Tsai *et al.*, 2011; figure 2). Using Immuno-FISH it is possible to study CENP-A assembly dynamics at the centromeres of distinct chromosomes. In addition to this is it possible to study meiotic centromere and chromosome dynamics including (but not limited to); homologous centromere and chromosome pairing or clustering, sister centromere and arm cohesion, chromosome segregation in meiotic divisions I or II and the correct formation of chromosome territories.

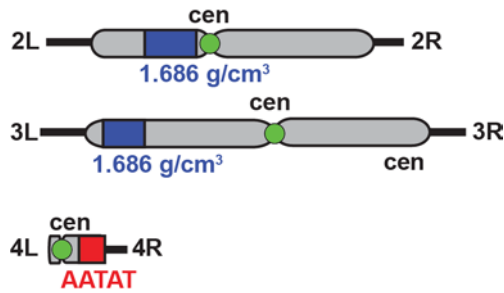


Figure 2: Schematic illustrating the location 1.686g/cm³ and AATAT FISH probe targets.

2. Materials

2.1 Fly culture

1. 25 mm polystyrene vials containing standard cornmeal medium (Nutri-Fly™) preserved with 0.5 % propionic acid and 0.1 % Tegosept (APEX Bioresearch Products) (note 1).
2. Incubator (20°C) under 12-hour light-dark cycle.

2.2 Dissection

1. Stereomicroscope and light source.
2. One pair of ultra-fine dissecting forceps.
3. Translucent glass 1 ml dissecting dishes.
4. Tungsten needle (diameter 0.125 mm).
4. Dissection buffer: 1X PBS.

2.3 Fixation

1. Poly-L-lysine coated glass slides.
2. Liquid Nitrogen and 1 L dewar container.
3. Cryogenic safety goggles and gloves.
4. Hydrophobic coverslips (note 2).
5. Sharp razor blade.
6. 4 % paraformaldehyde.
8. Glass coplin staining jars.
9. 70 % ethanol (-20°C).
10. 75 %, 85 % and 95 % ethanol at -20°C.

11. Permeabilisation buffer: PBS with 0.4 % Triton-X (0.4 % PBTX).

2.4 FISH

1. FISH wash buffer: 2X Saline-Sodium Citrate with 0.1 % Triton X (0.1 % SSC-TX).
2. Pre-hybridization buffer 1: 0.1 % SCC-TX with 25 % formamide (note 3).
4. Pre-hybridization buffer 2: 0.1 % SCC-TX with 50 % formamide, solutions at 23°C and 37°C (Note 4).
5. Fluorescently labeled oligonucleotides or DNA probes. Oligonucleotides were end labeled with Alexa fluorophores. Oligonucleotides recognizing the 2nd and 3rd chromosome 1.686g.cm³ site were (AATAACATAG)₃ labeled with Alexa-555, the 4th chromosome oligonucleotide (AATAT)₆ was labeled with Alexa-647. The X (359bp repeat) and Y (AATAC)₆ chromosome probes were labeled with Alexa-555 and Alexa-488 respectively (Tsai *et al.* 2011).
6. Hybridisation buffer: 3X SSC, 50 % formamide and 10 % dextran sulphate.
7. Rubber cement (Marabu Fixo-gum).
8. Hot plate at 95°C.
9. Incubators at 37°C and 25°C.
10. Post-hybridization wash buffer 1: 0.1 % SCC-TX and 50 % formamide (solutions at 23°C and 37°C).
11. Post-hybridization wash buffer 2: 0.1 % SCC-TX and 25 % formamide (solution at 23°C)

2.5 Immunostaining

1. IF wash buffer: 0.4 % PBTX.
2. Blocking buffer: 0.4 % PBTX with 3 % BSA.
3. Humid chamber.
4. Hydrophobic barrier (EVO-STIK Impact or PAP pen).
5. Primary antibody: rabbit anti-CENP-A, Active Motif, #39713.
6. Secondary antibody: Alexa-546 conjugated goat anti-rabbit.
7. DAPI: 1 µg/ml solution in 1X PBS.
8. 1X PBS.
9. Mounting medium: SlowFade® Gold antifade reagent (Life Technologies™).
10. Coverslips (22 x 22 mm, 0.13-0.17 mm thick).
11. Sealing varnish.

2.6 Imaging, image quantification and processing.

1. Fluorescent microscope.

2. Image J software (NIH).

3. Methods

3.1 Dissection

1. Sex larval or adult flies and transfer males to 1 ml of dissecting buffer in a dissecting dish. Dissect 12-16 testes per sample being careful to remove any excess fat and/or any associated tissues as well as testes associated seminal vesicles (notes 5 & 6).
2. Individually transfer testes using forceps (note 7) to a 10 μ l drop of dissecting buffer on a poly-L-lysine coated slide.
3. Tear open testes using forceps and/or tungsten wire to release cell cysts from inside. Separate testes on the slide so that the tissues are not overlapping (note 8).
4. Place a hydrophobic coverslip (note 2) over the sample, being careful to avoid air bubbles. Squash the sample beneath the coverslip (note 9).

3.2 Fixation & Permeabilisation

1. Immediately freeze the slides with squashed testes in liquid nitrogen using a large forceps.
2. Remove the frozen slide from the liquid Nitrogen, place on the bench on a piece of paper towel and immediately remove the coverslip with a sharp blade (note 10).
3. While the slide is still frozen, pipette 500 μ l of 4 % paraformaldehyde over the samples and incubate at room temperature for 10 minutes.
4. Drain the paraformaldehyde from the slide into a waste container and immediately transfer the slide into 70 % ethanol at -20°C (Note 11).
5. Pass slides through a series of ethanol concentrations (at -20°C); 2 minutes in 75 % ethanol, 2 minutes in 85 % ethanol and 2 minutes in 95 % ethanol.
6. Remove slides from ethanol and place on paper towel; tap excess ethanol from the slide and dry by evaporation for 2 minutes.
7. Incubate the sample at room temperature for 1 x 15 minutes in permeabilisation buffer.

3.3. FISH

1. Transfer sample to FISH wash buffer and at room temperature carry out a 1 x 10 minute wash.
2. Incubate the sample at room temperature for 10 minutes in pre-hybridization buffer 1, followed by 10-minutes in pre-hybridization buffer 2.
3. Incubate the sample at 37 °C for 2 hours in pre-hybridization buffer 2.

4. Prepare 20 μl of hybridization buffer containing FISH probes per slide. Use 20 ng of DNA probe for the 1.686g/cm³ (AATAACATAG)₃ probe and 40 ng of DNA probe for 4th chromosome (AATAT)₆ per sample (Figure 2).
5. Remove slides from pre-hybridization buffer (in the fume hood) and transfer to paper towel to dry slightly.
6. Pipette 20 μl of hybridization buffer onto a coverslip, invert slide over the coverslip and gently mount onto slide being careful to avoid air bubbles.
7. Seal the edges of the coverslip with rubber cement and denature the slide on a hotplate at 95°C for 4 minutes.
8. Incubate slides overnight at 20°C in a humid chamber (note 12).
9. After probe hybridization, gently remove coverslip from slide using a sharp blade. Wash the sample at 20°C for 10 minutes in post-hybridization wash buffer 1 (note 13).
10. Incubate sample for a further 2 x 30-minutes at 20°C in post-hybridization wash buffer 1.
11. Incubate sample at room temperature for 10 minutes in post-hybridization wash buffer 2.
12. Finally, carry out 3 x 10-minute washes at room temperature in FISH wash buffer.

3.4 Immunofluorescence

1. After FISH protocol, transfer sample to IF wash buffer and incubate at room temperature for 10 minutes.
2. Place a hydrophobic barrier (using EVO-STIK Impact or a PAP pen) around the samples on the slide to create a well (note 14). Fill the well with 200 μl of blocking buffer and incubate in the dark at room temperature for 1 hour in a humid chamber.
3. Drain blocking buffer from the slide and add 200 μl of anti-CENP-A primary antibody solution. Incubate overnight at 4°C.
4. Following primary antibody incubation remove hydrophobic barrier from slides with a blade/sharp forceps and wash for 3 x 15-minutes at room temperature in IF wash buffer.
5. Prior to secondary antibody staining, replace the hydrophobic ring around the samples and add 200 μl of the secondary antibody solution.
6. Incubate the samples in the dark for 1 hour at room temperature in a humid chamber.
7. Remove hydrophobic ring and wash in the dark at room temperature for 3 x 15-minutes in IF wash buffer.

8. Stain DNA with 1 $\mu\text{g/ml}$ DAPI in the dark at room temperature for 10-minutes in a humid chamber. (note 15)
9. Wash samples in the dark for 10 minutes in 1X PBS.
10. To mount, allow slides to dry slightly for 2-3 minutes then place 20 μl of mounting medium on the coverslip and 20 μl on the sample and invert slide onto the coverslip being careful to avoid air bubbles (note 16).
11. Seal coverslips with varnish.

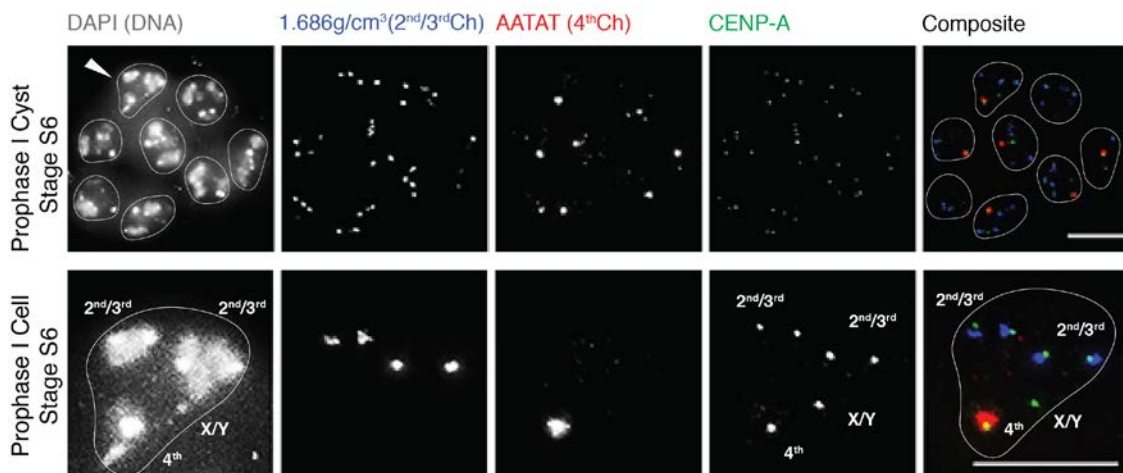


Figure 3: Immuno-FISH on meiotic prophase I (S6 stage) spermatocytes. CENP-A (green) in combination with the 2nd and 3rd chromosome probe (1.686 g/cm³, blue) and the 4th chromosome probe (AATAT)₆, red). Nuclear membrane and specific chromosome centromeres are illustrated. Scale bar 10 μm .

3.5 Imaging

Fluorescent imaging was carried out using a DeltaVision Elite wide-field microscope system (Applied Precision). The images were acquired with a 60X lens. As centromeres have a diameter of $< 5 \mu\text{m}$ images were acquired as z-stacks with a step size of 0.2 μm in order to ensure capture of all CENP-A foci. Raw data files were deconvolved using a conservative maximum intensity algorithm (10 cycles) and 3D z-stack images were represented in 2D by projection using SoftWorx (Applied Precision). RGB images were exported in TIFF format for further quantification analysis.

3.6 Quantitation of Fluorescent Intensity

Focal fluorescent intensities were measured as corrected total cellular fluorescence (CTCF) using Image J software (NIH).

1. Export RGB image from microscope software in TIFF format.
2. Import TIFF image to Image J.
3. Split the channels of the composite RGB image. Image > colour > split channels.
4. For quantification of CENP-A signal, select channel displaying CENP-A and select nucleus of interest (figure 4, step 1).
5. Copy and paste selected nucleus into a new 8-bit file.
6. Apply a threshold to the image (figure 4, step 2) and reduce the background reading to visualize the particles of interest (figure 4, step 3).
7. Set parameters to be analysed. Analyse > set measurements > select area, integrated density and mean grey value > OK.
8. Analyse selected particles. Analyse > analyse particles > OK (figure 4, step 4).
9. Export results to a Microsoft Excel workbook.
10. To generate background readings return to original CENP-A image and select an area of fixed size. Take 10 background readings in the area surrounding your particles of interest. Analyse > measure (figure 4, step 5).
11. Export background readings to a Microsoft Excel workbook.
12. Calculate the corrected total cellular fluorescence (CTCF) using the following formula:

$$\text{CTCF} = \text{Integrated Density}_{(\text{CENP-A})} - (\text{Area}_{(\text{CENP-A})} \times \text{Average Mean}_{(\text{Background})}).$$

13. For identification of CENP-A levels on a specific chromosome identify the chromosome from the composite FISH image and extract the CTCF pertaining to that centromere. TO determine the average centromeric CENP-A sum the CTCF of each centromere per nucleus.

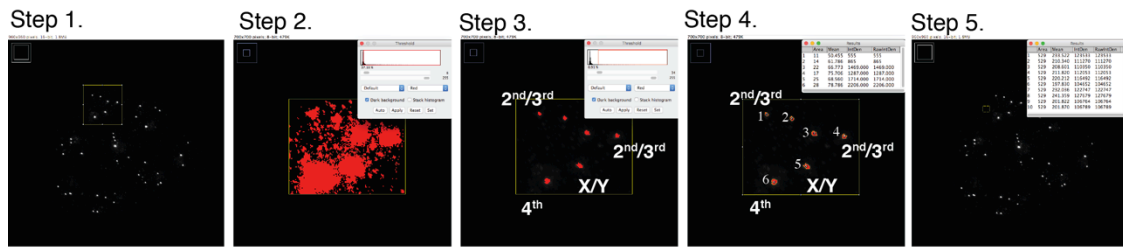


Figure 4: Steps required to calculate the corrected total cellular fluorescence (CTCF) of centromeric foci using the image processing software Image J. Specific centromeres are illustrated.

4. Notes

1. In humid climates/conditions the addition of low concentrations of Tegosept (0.1 %) helps to prevent growth of contaminating moulds in fly stocks.
 2. To reduce sticking of the coverslip during squashing, coverslips (22 mm x 22 mm) are treated with a hydrophobic substance such as Rain-X rain repellent. The coverslips are coated with thin layer of the rain repellent and allowed to dry at room temperature. Hydrophobic coverslips can be stored for later use.
 3. SAFETY: formamide (CAS 75-12-7). Formamide is characterized as CMR (carcinogenic, mutagenic and reprotoxin). To avoid exposure wear appropriate PPE and prepare all solutions and carry out all incubations in a fume hood. When removing coplin staining jars from the fume hood seal lids with Parafilm to avoid leakage/spillage.
 4. Pre-hybridization buffers containing formamide can be collected after use and stored overnight at 4°C for re-use during washing steps.
 5. For analysis of the early stages of spermatogenesis including early and late prophase I, dissect testes from third instar larval testes. To enrich for the later stages of meiosis including late prophase, meiosis I and II and all stages of spermatid differentiation dissect testes from newly eclosed adult males (< 1 day old).
 6. To cleanly remove larval testes; identify the testes, which are visible on the ventral surface towards the aboral end of the larvae. Place one set of dissecting forceps on each side of the testes and gently tease apart the larvae. The released testes are surrounded by fat tissue; using the forceps remove as much of this as possible.
- For dissection of the whole adult testes; place anaesthetized adult males in 500 µl of dissecting buffer with the dorsal surface facing upwards. Secure the fly by placing one forceps on the upper third of the abdomen; the testes are removed from the abdomen

by gently removing the epididymium. Remove the attached accessory glands and seminal vesicles from the testes.

7. Transferring testes individually prevents loss of sample, as the testes are prone to sticking to the inside of the plastic pipette tip. For transfer by pipette, this can be minimized by coating the inside of the pipette tip with 1% BSA in 1X PBS.

8. During transfer of testes additional buffer can carry over to the slide, additional buffer should be removed with a pipette to prevent over spreading of the sample when squashed.

9. To squash, place the slide on the bench with a folded sheet of paper towel on top and give a relatively firmly squash. If the sample is not squashed enough, the cysts of cells remain inside the tissue and are difficult to visualize. Over-squashing leads to distorted nuclear morphology.

10. To avoid damaging/losing the sample the coverslip needs to be removed quickly, before the slide thaws, leaving the slide on paper towel insulates the slide and stops it from thawing immediately. To remove the coverslip, firmly hold the slide down (being careful to avoid cold burn) and quickly flick off the coverslip with a sharp blade.

11. At this point, slides can be stored in 70 % ethanol at -20°C until all samples are collected or until further processing.

12. Incubating slides over a period of 48 hours (12 hours FISH + 12 hours IF) in a humid chamber can lead to bacterial growth on the slide, to avoid this ensure to replace water, moist tissue and wash down the chamber surfaces with 70 % ethanol prior to use.

13. Pre-warm buffers to 20°C before washing steps. Washing at specific temperatures was found to be critical for probe retention on DNA.

14. Creating a well around the samples on the slide allows for full immersion of the sample in the primary antibody solution and leads to more uniform antibody staining.

15. Steps involved in FISH protocol reduce the permeability of the sample to DAPI staining and this gives a blurry appearance when the cells are visualised by fluorescence microscopy. Increased permeabilisation steps with stronger permeabilisation chemicals led to reduced visibility of the highly decondensed DNA of these cells.

16. Placing mounting medium on both surfaces (slide and coverslip) acts to prevent formation of air bubbles.

5. References

- Allshire RC, Karpen GH. 2008. Epigenetic regulation of centromeric chromatin: old dogs, new tricks? *Nat Rev Genet* **9**: 923-937.
- Cenci G, Bonaccorsi S, Pisano C, Verni F, Gatti M. 1994. Chromatin and microtubule organization during premeiotic, meiotic and early postmeiotic stages of *Drosophila melanogaster* spermatogenesis. *J Cell Sci* **107** (Pt 12): 3521-3534.
- Dunleavy EM, Beier NL, Gorgescu W, Tang J, Costes SV, Karpen GH. 2012. The cell cycle timing of centromeric chromatin assembly in *Drosophila* meiosis is distinct from mitosis yet requires CAL1 and CENP-C. *PLoS Biol* **10**: e1001460.
- Fuller M. 1993. *The Development of Drosophila melanogaster*. Cold Spring Harbor Press.
- Kwenda L, Collins CM, Dattoli AA, Dunleavy EM. 2016. Nucleolar activity and CENP-C regulate CENP-A and CAL1 availability for centromere assembly in meiosis. *Development* **143**: 1400-1412.
- McKee BD, Yan R, Tsai JH. 2012. Meiosis in male *Drosophila*. *Spermatogenesis* **2**: 167-184.
- Panchenko T, Black BE. 2009. The epigenetic basis for centromere identity. *Prog Mol Subcell Biol* **48**: 1-32.
- Raychaudhuri N, Dubruille R, Orsi GA, Bagheri HC, Loppin B, Lehner CF. 2012. Transgenerational propagation and quantitative maintenance of paternal centromeres depends on Cid/Cenp-A presence in *Drosophila* sperm. *PLoS Biol* **10**: e1001434.
- Tsai, JH., Yan, R. & McKee, B.D. 2011 Homolog pairing and sister chromatid cohesion in heterochromatin in *Drosophila* male meiosis I. *Chromosoma* **120**: 335.
- Valente LP, Silva MC, Jansen LE. 2012. Temporal control of epigenetic centromere specification. *Chromosome Res* **20**: 481-492.
- Westhorpe FG, Straight AF. 2014. The centromere: epigenetic control of chromosome segregation during mitosis. *Cold Spring Harb Perspect Biol* **7**: a015818.

Acknowledgements

This work was supported by Science Foundation Ireland (SFI)-Health Research Board-Wellcome Trust Research Career Development Fellowship and SFI-President of Ireland Young Research Award to EMD. CMC is funded by a College of Science Scholarship from National University of Ireland Galway.

8.8. IP and MS results from Experiment 1 (FL GFP-CENP-A)

Mass Spectrometry performed by the Imhof Laboratory, LMU, Munich

Description	Accession #	MW (kDa)	Control	GFP-TRAP IP (FL-GFP-CENP-A)
Trypsin OS=Sus scrofa PE=1 SV=1	TRYP_PIG	24 kDa	100% (100%)	100% (100%)
Keratin, type II cytoskeletal 1 OS=Homo sapiens GN=KRT1 PE=1 SV=6	K2C1_HUMAN	66 kDa	100% (100%)	100% (100%)
Keratin, type I cytoskeletal 9 OS=Homo sapiens GN=KRT9 PE=1 SV=3	K1C9_HUMAN	62 kDa	100% (100%)	100% (100%)
Serum albumin OS=Bos taurus GN=ALB PE=1 SV=4	ALBU_BOVIN	69 kDa	100% (100%)	100% (100%)
Cluster of Keratin, type I cytoskeletal 10 OS=Homo sapiens GN=KRT10 PE=1 SV=6 (K1C10_HUMAN)	K1C10_HUMAN [2]	59 kDa	100% (100%)	100% (100%)
Keratin, type I cytoskeletal 10 OS=Homo sapiens GN=KRT10 PE=1 SV=6	K1C10_HUMAN	59 kDa	100% (100%)	87% (87%)
sp P13645 K1C10_HUMAN Keratin, type I cytoskeletal 10 OS=Homo sapiens GN=KRT10 PE=1...	HUMANKeratin, type I cytoskeletal 10 OS=Homo sapiens GN=KRT10 PE=1...	?	99% (99%)	35% (35%)
Unknown protein 14 (Fragment) OS=Pseudotsuga menziesii PE=1 SV=1	UP14_PSEMZ	1 kDa	99% (99%)	99% (99%)
Tubulin alpha-1 chain OS=Drosophila melanogaster GN=alphaTub84B PE=2 SV=1	TBA1_DROME (+11)	50 kDa	100% (100%)	100% (100%)
Cluster of Collagen alpha-2(I) chain OS=Bos taurus GN=COL1A2 PE=1 SV=2 (CO1A2_BOVIN)	CO1A2_BOVIN [5]	129 kDa	100% (100%)	100% (100%)
Collagen alpha-2(I) chain OS=Bos taurus GN=COL1A2 PE=1 SV=2	CO1A2_BOVIN (+4)	129 kDa	99% (99%)	98% (98%)
sp O46392 CO1A2_CANFA Collagen alpha-2(I) chain OS=Canis familiaris GN=COL1A2 PE=2...	sp O46392 CO1A2_CANFACollagen alpha-2(I) chain OS=Canis familiaris GN=COL1A2 PE=2...	?	70% (70%)	90% (90%)
Dihydrolypoyllysine-residue succinyltransferase component of 2-oxoglutarate dehydrogenase complex OS=Escherichia coli O157:H7 GN=sucB PE=1 SV=2	ODO2_ECO57 (+1)	44 kDa		100% (100%)
Tubulin beta-1 chain OS=Gallus gallus PE=2 SV=1	TBB1_CHICK (+35)	50 kDa	100% (100%)	100% (100%)
Pancreatic trypsin inhibitor OS=Bos taurus PE=1 SV=2	BPT1_BOVIN	11 kDa	100% (100%)	100% (100%)
Cluster of Glycinin G1 OS=Glycine max GN=GY1 PE=1 SV=2 (sp P04776 GLYG1_SOYBNGlycinin G1 OS=Glycine max GN=GY1 PE=1 SV=2)	sp P04776 GLYG1_SOYBNGlycinin G1 OS=Glycine max GN=GY1 PE=1 SV=2 [2]	?	100% (100%)	
Glycinin G1 OS=Glycine max GN=GY1 PE=1 SV=2	sp P04776 GLYG1_SOYBNGlycinin G1 OS=Glycine max GN=GY1 PE=1 SV=2	?	100% (100%)	
Glycinin G1 OS=Glycine max GN=GY1 PE=1 SV=2	GLYG1_SOYBN	56 kDa	99% (99%)	

Appendices

ATP synthase subunit beta, mitochondrial OS=Drosophila melanogaster GN=ATPsyn-beta PE=1 SV=3	ATPB_DROME	54 kDa		100% (100%)
Keratin, type II cytoskeletal 2 epidermal OS=Homo sapiens GN=KRT2 PE=1 SV=2	K22E_HUMAN	65 kDa	100% (100%)	100% (100%)
Keratin, type II cytoskeletal 5 OS=Homo sapiens GN=KRT5 PE=1 SV=3	K2C5_HUMAN	62 kDa	100% (100%)	100% (100%)
Actin-10 OS=Dictyostelium discoideum GN=act10 PE=1 SV=1	ACT10_DICDI (+121)	42 kDa		100% (100%)
Cluster of 60 kDa heat shock protein, mitochondrial OS=Drosophila melanogaster GN=Hsp60 PE=1 SV=3 (CH60_DROME)	CH60_DROME [3]	61 kDa	100% (100%)	100% (100%)
60 kDa heat shock protein, mitochondrial OS=Drosophila melanogaster GN=Hsp60 PE=1 SV=3	CH60_DROME	61 kDa	100% (100%)	75% (75%)
60 kDa heat shock protein homolog 2, mitochondrial OS=Drosophila melanogaster GN=Hsp60C PE=2 SV=2	CH60C_DROME	62 kDa		100% (100%)
sp Q9VMN5 CH60C_DROME 60 kDa heat shock protein homolog 2, mitochondrial OS=Drosophila...	sp Q9VMN5 CH60C_DROME 60 kDa heat shock protein homolog 2, mitochondrial OS=Drosophila...	?		100% (100%)
Cluster of ATP synthase subunit alpha, mitochondrial OS=Drosophila melanogaster GN=blw PE=1 SV=2 (ATPA_DROME)	ATPA_DROME	59 kDa		100% (100%)
Keratin, type II cytoskeletal 3 OS=Homo sapiens GN=KRT3 PE=1 SV=3	K2C3_HUMAN	64 kDa	44% (44%)	100% (100%)
Protein l(2)37Cc OS=Drosophila melanogaster GN=l(2)37Cc PE=1 SV=2	L2CC_DROME	30 kDa		100% (100%)
sp P02533 K1C14_HUMAN Keratin, type I cytoskeletal 14 OS=Homo sapiens GN=KRT14 PE=1...	sp P02533 K1C14_HUMANKeratin, type I cytoskeletal 14 OS=Homo sapiens GN=KRT14 PE=1...	?	100% (100%)	99% (99%)
RNA-directed RNA polymerase L OS=Hendra virus (isolate Horse/Australia/Hendra/1994) GN=L PE=3 SV=2	L_HENDH	257 kDa	98% (98%)	99% (99%)
Cluster of Chaperone protein htpG OS=Rickettsia bellii (strain OSU 85-389) GN=htpG PE=3 SV=1 (HTPG_RICB8)	HTPG_RICB8	71 kDa	100% (100%)	99% (99%)
sp Q7Z794 K2C1B_HUMAN Keratin, type II cytoskeletal 1b OS=Homo sapiens GN=KRT77 PE=1...	sp Q7Z794 K2C1B_HUMANKeratin, type II cytoskeletal 1b OS=Homo sapiens GN=KRT77 PE=1...	?	100% (100%)	
Keratin, type II cytoskeletal 1b OS=Homo sapiens GN=KRT77 PE=1 SV=3	K2C1B_HUMAN	62 kDa	100% (100%)	7% (7%)
Succinate dehydrogenase [ubiquinone] flavoprotein subunit, mitochondrial OS=Drosophila melanogaster GN=SdhA PE=2 SV=3	DHSA_DROME	72 kDa		100% (100%)
Serum basic protease inhibitor OS=Bos taurus PE=1 SV=1	IBPS_BOVIN	7 kDa	100% (100%)	100% (100%)
Histone H1.1 (Fragment) OS=Bos taurus PE=1 SV=1	H11_BOVIN (+7)	10 kDa		100% (100%)

Appendices

Rubber elongation factor protein OS=Hevea brasiliensis PE=1 SV=2	REF_HEVBR	15 kDa	100% (100%)	
sp P02538 K2C6A_HUMAN Keratin, type II cytoskeletal 6A OS=Homo sapiens GN=KRT6A PE=1...	sp P02538 K2C6A_HUMANKeratin, type II cytoskeletal 6A OS=Homo sapiens GN=KRT6A PE=1...	?	100% (100%)	11% (11%)
Eukaryotic initiation factor 4A-10 OS=Nicotiana tabacum PE=2 SV=1	IF410_TOBAC (+37)	47 kDa		100% (100%)
Putative cytochrome c oxidase subunit II PS17 (Fragments) OS=Pinus strobus PE=1 SV=1	PS17_PINST	2 kDa	99% (99%)	
Hornerin OS=Homo sapiens GN=HRNR PE=1 SV=2	HORN_HUMAN	282 kDa	98% (98%)	99% (99%)
Elongation factor 1-alpha, somatic form OS=Xenopus laevis GN=eef1as PE=2 SV=1	EF1A0_XENLA (+81)	50 kDa		99% (99%)
40S ribosomal protein S13 OS=Anopheles gambiae GN=RpS13 PE=2 SV=2	RS13_ANOGA (+16)	17 kDa		100% (100%)
40S ribosomal protein S14-1 OS=Arabidopsis thaliana GN=RPS14A PE=2 SV=1	RS141_ARATH (+20)	16 kDa		100% (100%)
Plasma serine protease inhibitor OS=Bos taurus GN=SERPINA5 PE=1 SV=1	IPSP_BOVIN	45 kDa	100% (100%)	
Catalase HP11 OS=Escherichia coli (strain K12) GN=katE PE=1 SV=1	CATE_ECOLI	84 kDa		100% (100%)
sp Q05707 COEA1_HUMAN Collagen alpha-1(XIV) chain OS=Homo sapiens GN=COL14A1 PE=1...	sp Q05707 COEA1_HUMANCollagen alpha-1(XIV) chain OS=Homo sapiens GN=COL14A1 PE=1...	?	100% (100%)	
60 kDa chaperonin 2 OS=Sinorhizobium medicae (strain WSM419) GN=groL2 PE=3 SV=1	CH602_SINMW	58 kDa		100% (100%)
Glyceraldehyde-3-phosphate dehydrogenase 1 OS=Kluyveromyces lactis GN=GAP1 PE=1 SV=1	G3P1_KLULA (+15)	35 kDa	100% (100%)	
Beta-conglycinin, beta chain OS=Glycine max GN=CG-4 PE=1 SV=1	GLCB_SOYBN	51 kDa	100% (100%)	
Trypsin inhibitor A OS=Glycine max GN=KTI3 PE=1 SV=2	ITRA_SOYBN (+2)	24 kDa	100% (100%)	
sp P04405 GLYG2_SOYBN Glycinin G2 OS=Glycine max GN=Gy2 PE=1 SV=2	sp P04405 GLYG2_SOYBNGlycinin G2 OS=Glycine max GN=Gy2 PE=1 SV=2	?	100% (100%)	
Filaggrin-2 OS=Homo sapiens GN=FLG2 PE=1 SV=1	sp Q5D862 FILA2_HUMANFilaggrin-2 OS=Homo sapiens GN=FLG2 PE=1 SV=1	?	100% (100%)	
Superoxide dismutase [Mn], mitochondrial OS=Drosophila melanogaster GN=Sod2 PE=2 SV=3	SODM_DROME	25 kDa		100% (100%)
Alkaline phosphatase OS=Escherichia coli (strain K12) GN=phoA PE=1 SV=1	PPB_ECOLI	49 kDa		99% (99%)
30S ribosomal protein S18, chloroplastic OS=Lobularia maritima GN=rps18 PE=3 SV=1	RR18_LOBMA	12 kDa		99% (99%)
Trans-cinnamate 4-monooxygenase OS=Arabidopsis thaliana GN=CYP73A5 PE=2 SV=1	TCMO_ARATH	58 kDa		99% (99%)

Appendices

Succinate dehydrogenase [ubiquinone] iron-sulfur subunit, mitochondrial OS=Drosophila melanogaster GN=SdhB PE=2 SV=2	DHSB_DROME	34 kDa		99% (99%)
Heat shock 70 kDa protein 1A OS=Bos taurus GN=HSPA1A PE=2 SV=2	HS71A_BOVIN (+63)	70 kDa		99% (99%)
40S ribosomal protein S3-1 OS=Arabidopsis thaliana GN=RPS3A PE=1 SV=1	RS31_ARATH (+15)	28 kDa		99% (99%)
Polyadenylate-binding protein OS=Drosophila melanogaster GN=pAbp PE=1 SV=3	PABP_DROME	70 kDa		99% (99%)
sp Q8SWU7 Y1354_DROME GTP-binding protein CG1354 OS=Drosophila melanogaster GN=CG1354...	sp Q8SWU7 Y1354_DROME GTP-binding protein CG1354 OS=Drosophila melanogaster GN=CG1354...	?		99% (99%)
tRNA(Met) cytidine acetyltransferase Tmca OS=Shigella flexneri serotype 5b (strain 8401) GN=tmca PE=3 SV=1	TMCA_SHIF8	75 kDa		99% (99%)
Heat shock protein 26 OS=Drosophila melanogaster GN=Hsp26 PE=1 SV=2	HSP26_DROME	23 kDa		99% (99%)

8.9. IP and MS results from Experiment 2

MS analysis performed by the Proteomics Facility, The University of Bristol. (Dr. Kate Heesom)

Appendices

Description	A5: Area (GST)	B5: Area (GST-CID a.a 1-126)	Score A2	Coverage A2	# Peptides A2	# PSM A2	Score B2	Coverage B2	# Peptides B2	# PSM B2	# AAs	MW [kDa]	calc. pI
Glutathione S-transferase S1 OS=Drosophila melanogaster GN=GstS1 PE=1 SV=2 - [GST1_DROME]	6.314E9	4.372E9	353.21	62.65	18	98	402.25	65.46	20	123	249	27.6	4.65
Aldehyde dehydrogenase (Fragment) OS=Drosophila melanogaster GN=Aldh PE=4 SV=1 - [B0F5B2_DROME]	0.000E0	2.961E6					17.71	47.50	3	6	80	8.6	9.31
RH09938p OS=Drosophila melanogaster GN=RpL30 PE=2 SV=1 - [Q8MT23_DROME]	0.000E0	6.037E6					12.84	42.34	3	4	111	12.3	9.47
Glutathione S-transferase 1-1 OS=Drosophila melanogaster GN=GstD1 PE=1 SV=1 - [GSTT1_DROME]	1.715E8	1.233E8	56.97	39.23	8	16	52.77	35.41	8	16	209	23.9	7.23
Histone H3-like centromeric protein cid OS=Drosophila melanogaster GN=cid PE=1 SV=2 - [CID_DROME]	3.169E7	4.127E10	7.71	20.44	2	3	940.25	38.67	11	275	225	26.0	10.20
AT03383p OS=Drosophila melanogaster GN=S-Lap1 PE=2 SV=2 - [Q9VSM6_DROME]	3.659E6	5.835E7	2.52	1.80	1	1	63.11	38.56	14	22	555	61.5	7.80
GH13849p OS=Drosophila melanogaster GN=S-Lap2 PE=2 SV=1 - [Q9VSM7_DROME]	3.659E6	5.835E7	2.52	1.81	1	1	62.13	36.41	15	21	552	61.3	6.92
Alpha tubulin 84B (Fragment) OS=Drosophila melanogaster PE=2 SV=1 - [K7WKV0_DROME]	0.000E0	5.148E7					80.30	36.39	10	25	415	46.1	6.13
Tubulin beta-1 chain OS=Drosophila melanogaster GN=betaTub56D PE=1 SV=2 - [TBB1_DROME]	0.000E0	2.275E7					79.59	34.23	12	28	447	50.1	4.86
Ribosomal protein S11 (Fragment) OS=Drosophila melanogaster GN=RPS11 PE=3 SV=1 - [LOCPE3_DROME]	0.000E0	6.374E6					13.24	33.77	5	8	151	17.6	11.15
40S ribosomal protein S8 OS=Drosophila melanogaster GN=RpS8 PE=1 SV=1 - [RS8_DROME]	0.000E0	4.396E6					32.06	32.69	5	10	208	23.7	10.48
Histone H2A OS=Drosophila melanogaster GN=His2A PE=1 SV=2 - [H2A_DROME]	4.419E6	2.633E7	2.55	7.26	1	1	13.70	31.45	3	5	124	13.4	10.73

Appendices

Tubulin beta-2 chain OS=Drosophila melanogaster GN=betaTub85D PE=1 SV=1 - [TBB2_DROME]	0.000E0	2.700E7					78.90	31.17	11	27	446	49.8	4.83
Histone H4 OS=Drosophila melanogaster GN=His4 PE=1 SV=2 - [H4_DROME]	0.000E0	1.602E7					11.92	31.07	3	6	103	11.4	11.36
LD04994p1 OS=Drosophila melanogaster GN=Act57B PE=2 SV=1 - [E1JGP0_DROME]	1.266E7	2.528E7	4.88	5.00	1	2	43.18	30.28	7	16	360	40.2	5.83
Heat shock 70 kDa protein cognate 4 OS=Drosophila melanogaster GN=Hsc70-4 PE=1 SV=3 - [HSP7D_DROME]	2.460E7	3.251E7	36.54	10.29	6	11	62.72	30.26	15	26	651	71.1	5.52
RE62581p OS=Drosophila melanogaster GN=RpL21 PE=1 SV=1 - [Q9V9M7_DROME]	0.000E0	7.164E6					16.78	30.19	5	7	159	18.5	10.55
Beta-Tubulin at 60D, isoform B OS=Drosophila melanogaster GN=betaTub60D PE=4 SV=1 - [A0A0B4LGH1_DROME]	0.000E0	1.130E7					65.32	27.81	9	23	453	50.7	4.88
BcDNA.GH02250 OS=Drosophila melanogaster GN=ocn PE=2 SV=1 - [Q9Y170_DROME]	0.000E0	7.137E6					23.33	27.70	4	8	148	16.9	9.94
GrpE protein homolog, mitochondrial OS=Drosophila melanogaster GN=Roe1 PE=2 SV=2 - [GRPE_DROME]	1.688E7	6.336E6	25.96	25.82	5	9	13.16	20.66	4	6	213	23.9	8.50
CG6459 protein OS=Drosophila melanogaster GN=CG6459 PE=4 SV=1 - [A0APE4_DROME]	0.000E0	9.973E6					20.97	24.71	5	8	263	29.0	5.16
Ubiquitin-40S ribosomal protein S27a OS=Drosophila melanogaster GN=RpS27A PE=1 SV=2 - [RS27A_DROME]	3.178E6	7.308E6	7.45	10.26	1	2	13.44	24.36	3	5	156	17.9	9.77
ATP synthase subunit gamma, mitochondrial OS=Drosophila melanogaster GN=ATPsyn-gamma PE=2 SV=2 - [ATPG_DROME]	0.000E0	7.280E6					34.53	23.91	5	10	297	32.9	9.22
Stress-sensitive B, isoform E OS=Drosophila melanogaster GN=sesB PE=3 SV=1 - [X2JB48_DROME]	1.386E6	3.060E7	3.28	4.35	1	1	27.10	23.41	7	11	299	32.9	9.77
AT02348p OS=Drosophila melanogaster GN=UQCR-C2 PE=2 SV=1 -	0.000E0	3.369E6					41.28	23.41	7	12	440	45.4	9.44

Appendices

[Q9VV75_DROME]													
60S ribosomal protein L14 OS=Drosophila melanogaster GN=RpL14 PE=1 SV=1 - [RL14_DROME]	0.000E0	1.057E7					7.74	22.89	4	5	166	19.2	11.18
Glutathione S-transferase D3 OS=Drosophila melanogaster GN=GstD3 PE=2 SV=1 - [GSTT3_DROME]	4.285E6	6.935E6	13.78	12.06	2	4	2.17	22.61	3	3	199	22.9	5.47
40S ribosomal protein S16 OS=Drosophila melanogaster GN=RpS16 PE=1 SV=1 - [RS16_DROME]	0.000E0	5.434E6					9.48	22.30	3	4	148	16.8	10.17
60S ribosomal protein L15 OS=Drosophila melanogaster GN=RpL15 PE=1 SV=1 - [RL15_DROME]	0.000E0	1.097E7					9.93	22.06	4	4	204	24.3	11.47
Elongation factor 1-alpha 1 OS=Drosophila melanogaster GN=Ef1alpha48D PE=1 SV=2 - [EF1A1_DROME]	4.299E6	1.568E7	2.94	2.38	1	1	33.20	22.03	8	14	463	50.3	9.07
40S ribosomal protein S26 OS=Drosophila melanogaster GN=RpS26 PE=1 SV=1 - [RS26_DROME]	0.000E0	7.904E6					4.68	21.05	2	2	114	13.3	11.15
AT13329p (Fragment) OS=Drosophila melanogaster GN=RpS29 PE=2 SV=1 - [Q8IHD2_DROME]	0.000E0	3.621E6					1.62	20.93	1	1	43	5.1	9.52
Heat shock protein 83 OS=Drosophila melanogaster GN=Hsp83 PE=1 SV=1 - [HSP83_DROME]	0.000E0	1.620E7					71.99	20.78	13	25	717	81.8	5.02
Cytochrome c oxidase subunit II OS=Drosophila melanogaster GN=COX2 PE=3 SV=1 - [A0A0A0RZ60_DROME]	0.000E0	3.234E6					17.91	20.18	3	5	228	26.2	5.10
60S ribosomal protein L4 OS=Drosophila melanogaster GN=RpL4 PE=1 SV=2 - [RL4_DROME]	0.000E0	9.958E6					19.81	18.95	5	6	401	45.0	11.47
AT30376p OS=Drosophila melanogaster GN=loopin-1 PE=2 SV=1 - [Q7K2S9_DROME]	1.222E6	3.329E7	7.54	2.85	1	2	40.19	18.44	8	14	526	56.7	8.87
Arginine kinase OS=Drosophila melanogaster GN=Argk PE=2 SV=2 - [KARG_DROME]	0.000E0	1.273E7					20.76	17.42	5	7	356	39.8	6.47
60S ribosomal protein L36 OS=Drosophila melanogaster GN=RpL36 PE=1 SV=1 -	0.000E0	7.216E6					4.86	17.39	2	2	115	13.5	11.37

Appendices

[RL36_DROME]													
60S ribosomal protein L28 OS=Drosophila melanogaster GN=RpL28 PE=1 SV=1 - [RL28_DROME]	0.000E0	8.375E6					6.90	17.36	2	4	144	16.0	11.09
Heat shock protein 26 OS=Drosophila melanogaster GN=Hsp26 PE=1 SV=2 - [HSP26_DROME]	0.000E0	2.955E6					11.59	17.31	3	5	208	23.0	7.56
CG9010 OS=Drosophila melanogaster GN=CG9010 PE=2 SV=1 - [Q7JY07_DROME]	0.000E0	4.121E6					17.25	16.91	5	6	343	37.0	8.51
26S protease regulatory subunit 4 OS=Drosophila melanogaster GN=Rpt2 PE=1 SV=2 - [PRS4_DROME]	0.000E0	5.161E6					16.34	16.86	5	7	439	49.3	6.58
40S ribosomal protein S3 OS=Drosophila melanogaster GN=RpS3 PE=1 SV=1 - [RS3_DROME]	0.000E0	4.801E6					9.72	16.67	4	4	246	27.5	9.39
RE10515p OS=Drosophila melanogaster GN=CG9117 PE=2 SV=1 - [Q8SZ99_DROME]	0.000E0	0.000E0					0.00	16.67	1	1	228	25.2	5.22
40S ribosomal protein S14 OS=Drosophila melanogaster GN=RpS14a PE=1 SV=1 - [RS14_DROME]	0.000E0	5.317E6					5.41	16.56	2	2	151	16.3	10.35
60S ribosomal protein L18a OS=Drosophila melanogaster GN=RpL18A PE=1 SV=1 - [RL18A_DROME]	0.000E0	4.628E6					8.70	16.38	3	4	177	21.0	10.62
Probable cytochrome P450 6d5 OS=Drosophila melanogaster GN=Cyp6d5 PE=2 SV=1 - [CP6D5_DROME]	0.000E0	4.626E6					19.02	16.34	6	7	508	57.3	8.84
CG32063-PA, isoform A OS=Drosophila melanogaster GN=S-Lap3 PE=2 SV=1 - [Q961W5_DROME]	0.000E0	2.297E7					39.80	16.07	7	14	535	57.7	7.87
60S ribosomal protein L13 OS=Drosophila melanogaster GN=RpL13 PE=1 SV=1 - [RL13_DROME]	0.000E0	8.288E6					8.68	16.06	4	4	218	24.9	10.99
AT20029p OS=Drosophila melanogaster GN=S-Lap7 PE=2 SV=1 - [Q500X4_DROME]	0.000E0	2.657E7					16.87	15.56	5	5	527	57.4	8.40
AT09752p OS=Drosophila melanogaster GN=S-Lap4 PE=2 SV=1 -	0.000E0	1.045E7					13.80	15.46	6	6	524	57.5	8.10

Appendices

[Q95R35_DROME]													
Glycoprotein 93 OS=Drosophila melanogaster GN=Gp93 PE=2 SV=1 - [Q9VAY2_DROME]	0.000E0	1.059E7					37.95	15.25	11	17	787	90.2	5.02
60S ribosomal protein L3 OS=Drosophila melanogaster GN=RpL3 PE=1 SV=3 - [RL3_DROME]	0.000E0	6.907E6					24.90	15.14	4	9	416	46.9	10.24
MIP08013p1 OS=Drosophila melanogaster GN=Mpcp PE=2 SV=1 - [QOE8E8_DROME]	0.000E0	6.211E6					16.14	14.89	5	6	356	38.8	8.88
Cofilin/actin-depolymerizing factor homolog OS=Drosophila melanogaster GN=tsr PE=2 SV=1 - [CADF_DROME]	0.000E0	3.602E6					2.74	14.86	2	2	148	17.1	7.17
AT29272p OS=Drosophila melanogaster GN=CG31924 PE=2 SV=1 - [Q8MZ65_DROME]	0.000E0	3.204E7					0.00	14.83	1	1	236	26.5	7.17
IP06876p1 OS=Drosophila melanogaster GN=CG30005 PE=2 SV=1 - [Q4V5M6_DROME]	0.000E0	6.225E6					0.00	14.78	1	1	115	13.3	8.68
60 kDa heat shock protein homolog 2, mitochondrial OS=Drosophila melanogaster GN=Hsp60C PE=2 SV=2 - [CH60C_DROME]	0.000E0	4.148E6					33.56	14.76	5	9	576	61.5	7.06
Protein disulfide-isomerase OS=Drosophila melanogaster GN=Pdi PE=2 SV=1 - [PDI_DROME]	0.000E0	4.564E6					20.87	14.52	6	9	496	55.7	4.82
60S ribosomal protein L7a OS=Drosophila melanogaster GN=RpL7A PE=1 SV=2 - [RL7A_DROME]	0.000E0	5.664E6					17.83	14.39	4	6	271	30.7	10.71
60S ribosomal protein L38 OS=Drosophila melanogaster GN=RpL38 PE=1 SV=1 - [RL38_DROME]	0.000E0	0.000E0					2.02	14.29	1	1	70	8.2	10.29
GH07689p OS=Drosophila melanogaster GN=S-Lap8 PE=2 SV=1 - [Q7K5K9_DROME]	0.000E0	5.531E6					27.79	13.30	5	9	534	57.7	8.46
LD37859p OS=Drosophila melanogaster GN=RpS27 PE=1 SV=1 - [Q9VBU9_DROME]	0.000E0	3.708E6					0.00	13.10	1	1	84	9.4	9.52
Zipper, isoform H OS=Drosophila melanogaster GN=zip PE=4 SV=1 -	0.000E0	4.085E6					82.99	12.58	19	30	1964	226.6	5.52

Appendices

[A0A0B4JD95_DROME]														
Heat shock 70 kDa protein cognate 3 OS=Drosophila melanogaster GN=Hsc70-3 PE=2 SV=2 - [HSP7C_DROME]	2.448E7	3.216E7	20.38	4.27	3	6	44.58	12.50	7	15	656	72.2	5.36	
CG7424-PA OS=Drosophila melanogaster GN=RpL36A PE=1 SV=2 - [Q9VLT7_DROME]	0.000E0	7.915E6					0.00	12.50	1	1	104	12.5	10.80	
AT14166p OS=Drosophila melanogaster GN=CG4434 PE=2 SV=2 - [Q9VCN3_DROME]	0.000E0	5.811E6					32.38	12.34	7	13	535	59.9	8.56	
60S ribosomal protein L18 OS=Drosophila melanogaster GN=RpL18 PE=1 SV=1 - [RL18_DROME]	0.000E0	1.141E7					5.52	12.23	2	3	188	21.7	11.53	
CG7920, isoform A OS=Drosophila melanogaster GN=CG7920 PE=2 SV=1 - [Q9VAC1_DROME]	0.000E0	7.322E6					11.25	12.16	4	6	477	51.8	8.12	
IP16013p (Fragment) OS=Drosophila melanogaster GN=CG5261 PE=2 SV=1 - [Q1WWF8_DROME]	0.000E0	2.511E6					8.78	11.61	2	3	224	24.7	9.32	
CG12079-PA OS=Drosophila melanogaster GN=ND-30 PE=2 SV=1 - [Q9VZU4_DROME]	0.000E0	2.076E6					4.67	11.32	2	3	265	30.0	7.84	
LD46344p OS=Drosophila melanogaster GN=Phb2 PE=2 SV=2 - [Q0E924_DROME]	0.000E0	1.228E6					8.22	11.04	3	4	299	33.0	9.54	
GM13757p OS=Drosophila melanogaster GN=ND-39 PE=2 SV=1 - [Q86NN5_DROME]	0.000E0	1.949E6					9.53	11.01	2	3	327	37.8	8.76	
40S ribosomal protein S7 OS=Drosophila melanogaster GN=RpS7 PE=1 SV=1 - [RS7_DROME]	0.000E0	3.651E6					5.82	10.82	2	3	194	22.2	9.80	
40S ribosomal protein S17 OS=Drosophila melanogaster GN=RpS17 PE=1 SV=2 - [RS17_DROME]	9.439E5	4.216E6	2.04	10.69	1	1	4.92	10.69	1	2	131	15.3	9.94	
Myosin heavy chain, isoform U OS=Drosophila melanogaster GN=Mhc PE=4 SV=1 - [M9ND95_DROME]	0.000E0	4.694E6					75.28	10.67	16	23	1949	222.8	6.25	
Myosin heavy chain, isoform O OS=Drosophila melanogaster GN=Mhc PE=4 SV=1 - [E1JHJ3_DROME]	0.000E0	4.694E6					74.53	10.60	16	23	1962	224.4	6.19	

Appendices

40S ribosomal protein S13 OS=Drosophila melanogaster GN=RpS13 PE=1 SV=3 - [RS13_DROME]	0.000E0	3.326E6					1.85	10.60	2	2	151	17.2	10.55
ATP synthase subunit alpha, mitochondrial OS=Drosophila melanogaster GN=blw PE=1 SV=2 - [ATPA_DROME]	0.000E0	8.880E6					22.41	10.51	5	9	552	59.4	9.01
Ribosomal protein L6, isoform A OS=Drosophila melanogaster GN=RpL6 PE=1 SV=1 - [Q9V9W2_DROME]	0.000E0	5.078E6					5.87	9.88	2	2	243	27.7	10.68
60S ribosomal protein L37a OS=Drosophila melanogaster GN=RpL37A PE=1 SV=3 - [RL37A_DROME]	0.000E0	3.496E6					2.10	9.78	1	1	92	10.3	10.61
CG10944-PA, isoform A OS=Drosophila melanogaster GN=RpS6 PE=2 SV=1 - [Q95TP9_DROME]	0.000E0	6.709E6					2.44	9.68	2	2	217	24.7	11.06
F119901p1 OS=Drosophila melanogaster GN=S-Lap5 PE=2 SV=1 - [A1Z9G3_DROME]	0.000E0	4.773E6					8.04	9.65	4	5	549	59.6	7.96
Glutathione S transferase D9, isoform A OS=Drosophila melanogaster GN=GstD9 PE=3 SV=1 - [Q9VGA0_DROME]	1.059E7	0.000E0	13.18	9.63	1	3					218	25.4	5.34
MIP20559p (Fragment) OS=Drosophila melanogaster GN=CG11963-RB PE=2 SV=1 - [D6W4K6_DROME]	0.000E0	4.088E6					11.40	9.51	2	4	263	28.4	8.73
Serine protease SER4 OS=Drosophila melanogaster GN=Jon25Bi PE=2 SV=1 - [O16101_DROME]	0.000E0	0.000E0					2.13	9.43	1	1	265	28.9	6.70
AT04852p OS=Drosophila melanogaster GN=eIF-4a-RD PE=2 SV=1 - [C8VV33_DROME]	0.000E0	2.334E6					7.02	9.23	3	5	390	44.3	5.53
CG9437 protein OS=Drosophila melanogaster GN=CG9437 PE=4 SV=1 - [A0AQF9_DROME]	0.000E0	0.000E0					0.00	9.21	1	1	315	36.5	5.64
AT14585p OS=Drosophila melanogaster GN=mil PE=2 SV=2 - [Q9VAZ1_DROME]	0.000E0	4.211E6					4.75	9.19	2	2	283	33.2	4.67
RE59324p OS=Drosophila melanogaster GN=RpS24 PE=1 SV=1 - [Q9W229_DROME]	0.000E0	9.002E6					3.13	9.16	1	1	131	15.0	11.22
60S ribosomal protein L7 OS=Drosophila	0.000E0	3.410E6					9.48	9.13	3	3	252	29.5	10.89

Appendices

melanogaster GN=RpL7 PE=1 SV=2 - [RL7_DROME]													
RE05501p OS=Drosophila melanogaster GN=CG12896 PE=2 SV=1 - [Q8SY26_DROME]	0.000E0	1.067E6					2.18	9.03	1	1	155	17.3	6.98
CG4389-PB, isoform B OS=Drosophila melanogaster GN=Mtalpha PE=3 SV=1 - [Q8IPE8_DROME]	0.000E0	4.680E6					16.55	9.01	5	6	744	79.6	8.85
Dolichyl-diphosphooligosaccharide--protein glycosyltransferase subunit 1 (Fragment) OS=Drosophila melanogaster GN=rho-5 PE=2 SV=1 - [Q8IH64_DROME]	0.000E0	2.430E6					5.72	8.89	3	3	371	42.3	9.11
IP19605p (Fragment) OS=Drosophila melanogaster GN=Dox-A2 PE=2 SV=1 - [A8E6V2_DROME]	0.000E0	1.169E6					5.24	8.84	1	2	147	16.6	9.70
Polyadenylate-binding protein OS=Drosophila melanogaster GN=pAbp PE=1 SV=3 - [PABP_DROME]	0.000E0	4.566E6					22.77	8.68	4	8	634	69.9	9.31
40S ribosomal protein S25 OS=Drosophila melanogaster GN=RpS25 PE=1 SV=3 - [RS25_DROME]	0.000E0	4.005E6					1.77	8.55	1	1	117	13.2	10.27
ADP/ATP translocase OS=Drosophila melanogaster GN=Ant2 PE=2 SV=1 - [O62526_DROME]	0.000E0	1.592E7					6.06	8.47	3	3	307	33.7	9.57
CG31021 OS=Drosophila melanogaster GN=CG31021 PE=4 SV=2 - [Q8IMH8_DROME]	0.000E0	2.211E6					9.01	8.39	3	3	453	52.6	5.25
HDC13853 OS=Drosophila melanogaster GN=HDC13853 PE=4 SV=1 - [Q6IK11_DROME]	2.719E9	7.172E9	165.04	8.25	1	65	204.91	8.25	1	94	194	21.4	10.08
CG6543, isoform A OS=Drosophila melanogaster GN=CG6543 PE=2 SV=1 - [Q7JR58_DROME]	0.000E0	2.928E6					4.81	8.14	2	2	295	31.6	8.63
Heat shock protein 23 OS=Drosophila melanogaster GN=Hsp23 PE=2 SV=2 - [HSP23_DROME]	0.000E0	5.651E6					2.24	8.06	1	1	186	20.6	5.85
40S ribosomal protein S18 OS=Drosophila melanogaster GN=RpS18 PE=1 SV=1 - [RS18_DROME]	0.000E0	3.576E6					6.65	7.89	1	2	152	17.6	10.48

Appendices

Heat shock 70 kDa protein cognate 5 OS=Drosophila melanogaster GN=Hsc70-5 PE=1 SV=2 - [HSP7E_DROME]	2.438E6	2.813E6	37.78	7.87	4	10	14.30	5.83	3	4	686	74.0	6.35
TA01212p OS=Drosophila melanogaster GN=RpL17A PE=2 SV=1 - [A8E792_DROME]	0.000E0	2.608E6					3.09	7.86	1	2	140	14.9	10.83
40S ribosomal protein S3a OS=Drosophila melanogaster GN=RpS3A PE=1 SV=4 - [RS3A_DROME]	0.000E0	8.804E6					3.16	7.84	2	3	268	30.3	9.61
40S ribosomal protein S23 OS=Drosophila melanogaster GN=RpS23 PE=1 SV=1 - [RS23_DROME]	0.000E0	8.075E6					3.06	7.69	1	1	143	16.0	10.59
CG6891, isoform C OS=Drosophila melanogaster GN=CG6891 PE=4 SV=1 - [Q81QX5_DROME]	0.000E0	3.072E5					0.00	7.53	1	1	146	16.6	5.01
LD28840p OS=Drosophila melanogaster GN=Rab35 PE=2 SV=1 - [Q95RH7_DROME]	0.000E0	7.108E5					2.35	7.48	1	1	147	17.0	8.85
60S ribosomal protein L32 OS=Drosophila melanogaster GN=RpL32 PE=1 SV=3 - [RL32_DROME]	0.000E0	1.041E6					2.66	7.46	1	1	134	16.0	11.40
Hsp90-related protein TRAP1 OS=Drosophila melanogaster GN=Trap1 PE=2 SV=1 - [Q7KNF3_DROME]	0.000E0	6.728E6					24.36	7.43	4	8	686	77.4	7.39
AT14183p OS=Drosophila melanogaster PE=2 SV=1 - [Q8T462_DROME]	0.000E0	7.049E8					2.50	7.34	1	1	286	30.8	9.80
RE10012p OS=Drosophila melanogaster GN=wor PE=2 SV=1 - [Q8SXL3_DROME]	0.000E0	8.718E7					0.00	7.12	1	1	548	61.8	6.38
CG11876, isoform A OS=Drosophila melanogaster GN=CG11876 PE=2 SV=1 - [Q7K5K3_DROME]	0.000E0	2.097E6					5.46	6.85	2	2	365	39.3	7.80
HDC06432 OS=Drosophila melanogaster GN=HDC06432 PE=4 SV=1 - [Q61GF6_DROME]	0.000E0	0.000E0					2.58	6.80	1	1	250	27.1	9.33
Heat shock protein 27 OS=Drosophila melanogaster GN=Hsp27 PE=1 SV=2 - [HSP27_DROME]	0.000E0	3.443E6					10.16	6.57	1	3	213	23.6	7.44
60S ribosomal protein L24 OS=Drosophila melanogaster GN=RpL24 PE=1 SV=1 -	0.000E0	3.424E6					1.83	6.45	1	1	155	17.5	11.06

Appendices

[RL24_DROME]													
Maternal protein exuperantia OS=Drosophila melanogaster GN=exu PE=1 SV=2 - [EXU_DROME]	0.000E0	5.015E6					3.77	6.39	3	3	532	57.9	9.54
CG1633 (Fragment) OS=Drosophila melanogaster GN=CG1633 PE=4 SV=1 - [F6J6B9_DROME]	5.060E6	1.796E6	8.40	6.29	1	3	2.92	6.29	1	1	175	19.8	5.43
CG8197, isoform A OS=Drosophila melanogaster GN=CG13743-RA PE=2 SV=1 - [A1Z7N0_DROME]	1.915E8	0.000E0	2.60	6.20	1	1					387	44.8	9.09
L71-8 protein OS=Drosophila melanogaster GN=Eig71Eh PE=4 SV=1 - [Q24059_DROME]	0.000E0	1.943E8					1.62	6.12	1	1	98	11.1	9.17
Mitochondrial import inner membrane translocase subunit TIM44 OS=Drosophila melanogaster GN=CG11779-RB PE=2 SV=1 - [C9QP57_DROME]	0.000E0	2.228E6					3.27	6.07	2	2	428	48.9	6.48
NADH-ubiquinone reductase 75 kDa subunit (Fragment) OS=Drosophila melanogaster GN=ND-75 PE=4 SV=1 - [Q8MM97_DROME]	0.000E0	1.279E6					7.00	6.03	2	2	514	55.5	6.73
Ribosomal protein L13A, isoform C OS=Drosophila melanogaster GN=RpL13A PE=4 SV=1 - [A0A0B4KFM7_DROME]	0.000E0	5.511E6					0.00	5.94	1	1	101	11.5	11.25
Fatty acid (Long chain) transport protein, isoform A OS=Drosophila melanogaster GN=Fatp PE=2 SV=2 - [Q9VKU1_DROME]	0.000E0	1.231E6					5.38	5.91	3	3	626	70.1	8.84
Teyrha-meyrha, isoform D OS=Drosophila melanogaster GN=tey PE=4 SV=1 - [M9PFP2_DROME]	0.000E0	1.631E7					2.54	5.77	1	1	745	79.4	6.71
CG11294, isoform A OS=Drosophila melanogaster GN=CG11294 PE=2 SV=1 - [Q9W3C6_DROME]	0.000E0	0.000E0					2.55	5.75	1	1	261	28.6	7.18
Glycosyltransferase 25 family member OS=Drosophila melanogaster GN=CG31915 PE=2 SV=1 - [GLT25_DROME]	4.405E7	0.000E0	2.67	5.56	1	1					612	71.1	5.40
Peroxisome oxidin 3 OS=Drosophila melanogaster GN=Prx3 PE=2 SV=2 -	0.000E0	2.148E6					3.65	5.56	1	1	234	26.4	7.49

Appendices

[Q9VEJ0_DROME]													
TNF-receptor-associated factor 2 OS=Drosophila melanogaster GN=Traf6 PE=2 SV=1 - [Q9XYQ9_DROME]	0.000E0	2.785E7					2.21	5.40	1	1	463	52.4	7.18
60S ribosomal protein L17 OS=Drosophila melanogaster GN=RpL17 PE=1 SV=1 - [RL17_DROME]	0.000E0	8.319E6					2.69	5.38	1	1	186	21.6	10.30
Guanine nucleotide-binding protein subunit beta-like protein OS=Drosophila melanogaster GN=Rack1 PE=1 SV=2 - [GBLP_DROME]	0.000E0	1.416E6					2.92	5.35	1	1	318	35.6	7.47
40S ribosomal protein S19a OS=Drosophila melanogaster GN=RpS19a PE=1 SV=3 - [RS19A_DROME]	0.000E0	2.079E6					1.82	5.13	1	1	156	17.3	10.11
Transmembrane emp24 domain-containing protein eca OS=Drosophila melanogaster GN=eca PE=2 SV=2 - [TMEDE_DROME]	0.000E0	1.349E6					3.12	5.09	1	1	216	25.1	7.05
Adenylate kinase isozyme 3 OS=Drosophila melanogaster GN=Adk3 PE=2 SV=1 - [Q9VGU6_DROME]	0.000E0	1.046E6					2.63	5.09	1	1	216	24.1	9.32
Calcium ATPase at 60A, isoform I OS=Drosophila melanogaster GN=Ca- P60A PE=4 SV=1 - [A0A0B4LGB7_DROME]	0.000E0	1.361E6					11.48	5.01	4	5	999	109.3	5.45
CG9172, isoform A OS=Drosophila melanogaster GN=ND-20 PE=2 SV=1 - [Q9VXK7_DROME]	0.000E0	1.078E6					4.83	4.98	1	2	221	24.6	9.74
RE63456p OS=Drosophila melanogaster GN=RpL34a PE=2 SV=1 - [Q8SYG0_DROME]	0.000E0	6.420E6					6.20	4.94	1	3	162	18.0	11.44
Thiolase OS=Drosophila melanogaster GN=Thiolase PE=2 SV=1 - [O77466_DROME]	0.000E0	7.749E6					3.29	4.90	2	2	469	50.6	9.14
V-type proton ATPase subunit E OS=Drosophila melanogaster GN=Vha26 PE=2 SV=1 - [VATE_DROME]	0.000E0	6.457E5					2.03	4.87	1	1	226	26.1	6.15
Isocitrate dehydrogenase, isoform A OS=Drosophila melanogaster GN=Idh PE=3 SV=1 - [Q7KUB0_DROME]	0.000E0	3.028E6					3.60	4.81	2	2	416	46.6	6.74

Appendices

AT28327p OS=Drosophila melanogaster GN=CG14736 PE=2 SV=1 - [Q8T3W1_DROME]	0.000E0	6.866E6					4.87	4.78	1	2	335	36.8	7.88
Voltage-dependent anion-selective channel OS=Drosophila melanogaster GN=porin PE=1 SV=3 - [VDAC_DROME]	0.000E0	5.891E5					5.73	4.61	1	2	282	30.5	6.96
AT13777p OS=Drosophila melanogaster GN=CG12861 PE=2 SV=1 - [Q8T465_DROME]	0.000E0	6.705E6					3.14	4.60	1	1	239	28.0	9.03
Importin subunit alpha OS=Drosophila melanogaster GN=Pen PE=1 SV=2 - [IMA_DROME]	0.000E0	9.145E4					0.00	4.41	1	1	522	57.8	5.35
HDC07503 OS=Drosophila melanogaster GN=HDC07503 PE=4 SV=1 - [Q6IM45_DROME]	0.000E0	1.253E6					1.71	4.41	1	1	227	25.8	7.99
Calcium-binding protein 1, isoform A OS=Drosophila melanogaster GN=CaBP1 PE=2 SV=1 - [Q9V438_DROME]	0.000E0	0.000E0					0.00	4.39	1	1	433	46.7	5.69
CG2065, isoform A OS=Drosophila melanogaster GN=CG2065 PE=2 SV=1 - [Q7JYX2_DROME]	0.000E0	1.279E6					6.34	4.33	1	2	300	33.4	9.25
AT27831p OS=Drosophila melanogaster GN=CG31538 PE=2 SV=1 - [Q8I0F1_DROME]	0.000E0	8.835E5					0.00	4.26	1	1	563	63.8	9.82
Glyceraldehyde-3-phosphate dehydrogenase 1 OS=Drosophila melanogaster GN=Gapdh1 PE=2 SV=2 - [G3P1_DROME]	0.000E0	2.029E6					2.86	4.22	1	1	332	35.3	8.18
LD12501p OS=Drosophila melanogaster GN=CG11089 PE=2 SV=1 - [Q95RT1_DROME]	7.358E6	0.000E0	0.00	4.18	1	1					383	41.4	7.94
CG11999 OS=Drosophila melanogaster GN=CG11999 PE=2 SV=1 - [Q9VNA3_DROME]	0.000E0	1.190E6					1.81	4.17	1	1	216	23.6	6.80
60S ribosomal protein L10 OS=Drosophila melanogaster GN=RpL10 PE=1 SV=1 - [RL10_DROME]	0.000E0	4.471E6					4.08	4.13	1	2	218	25.5	9.85
Globin 2, isoform C OS=Drosophila melanogaster GN=glob2-RB PE=2 SV=1 -	0.000E0	2.572E7					1.81	4.11	1	1	219	24.9	7.83

Appendices

[H8F4P7_DROME]													
GH09538p OS=Drosophila melanogaster GN=CG7441 PE=2 SV=1 - [Q8SZU2_DROME]	0.000E0	1.097E6					5.94	4.07	2	3	516	57.0	9.92
Failed axon connections, isoform E OS=Drosophila melanogaster GN=fax PE=4 SV=1 - [M9PFH6_DROME]	0.000E0	0.000E0					1.90	4.06	1	1	271	31.2	5.62
Serine protease inhibitor (Serpin-3) OS=Drosophila melanogaster GN=Spn38F PE=2 SV=1 - [Q9U116_DROME]	0.000E0	5.520E7					7.26	4.03	1	3	372	41.6	8.25
26-29kD-proteinase OS=Drosophila melanogaster GN=26-29-p PE=2 SV=1 - [Q9V3U6_DROME]	0.000E0	4.030E6					8.17	4.01	2	3	549	62.1	6.74
GH13039p OS=Drosophila melanogaster GN=gammaSnap1 PE=2 SV=1 - [Q9U6R9_DROME]	0.000E0	0.000E0					1.94	3.97	1	1	302	33.7	5.33
Succinyl-CoA ligase [ADP/GDP-forming] subunit alpha, mitochondrial OS=Drosophila melanogaster GN=Scsalpha PE=2 SV=3 - [SUCA_DROME]	0.000E0	2.854E5					2.09	3.96	1	1	328	34.4	8.98
Caf1-105 OS=Drosophila melanogaster GN=Caf1-105 PE=4 SV=1 - [A1Z898_DROME]	0.000E0	3.633E6					2.22	3.88	1	1	747	83.3	8.22
CG5660, isoform B OS=Drosophila melanogaster GN=CG5660 PE=2 SV=1 - [Q9VSR7_DROME]	0.000E0	2.334E6					1.89	3.82	3	3	994	113.0	6.70
CG4691 OS=Drosophila melanogaster GN=BG:DS06874.1 PE=2 SV=1 - [Q9V3K5_DROME]	0.000E0	6.959E5					2.79	3.82	1	1	262	30.8	9.79
CG11913 OS=Drosophila melanogaster GN=ND-49L PE=3 SV=2 - [Q9VBR4_DROME]	0.000E0	2.548E6					5.56	3.82	2	2	523	60.1	7.01
Aspartate aminotransferase OS=Drosophila melanogaster GN=Got2 PE=2 SV=1 - [Q8T0M9_DROME]	0.000E0	2.497E6					4.90	3.82	1	3	393	43.7	8.43
Glutamate carrier 1, isoform A OS=Drosophila melanogaster GN=GC1 PE=2 SV=1 - [Q9VGF7_DROME]	0.000E0	1.273E6					3.44	3.74	1	1	321	34.5	9.55

Appendices

Hsc70-interacting protein 2 OS=Drosophila melanogaster GN=HIP-R PE=1 SV=2 - [F10A2_DROME]	0.000E0	2.748E5					2.31	3.71	1	1	377	41.0	5.35
60S ribosomal protein L22 OS=Drosophila melanogaster GN=RpL22 PE=1 SV=2 - [RL22_DROME]	0.000E0	3.688E6					1.77	3.68	1	2	299	30.6	10.11
Protein painting of fourth OS=Drosophila melanogaster GN=Pof PE=1 SV=1 - [POF_DROME]	0.000E0	0.000E0					3.48	3.64	1	1	495	55.1	6.23
RE21586p OS=Drosophila melanogaster GN=CG9480 PE=2 SV=1 - [Q8IGV8_DROME]	0.000E0	2.094E7					8.31	3.62	1	4	387	43.4	6.30
Sluggish A, isoform N OS=Drosophila melanogaster GN=slgA PE=4 SV=1 - [M9NHG9_DROME]	0.000E0	1.388E6					6.02	3.52	2	2	681	77.2	8.90
Beta4GalNAcTB OS=Drosophila melanogaster GN=beta4GalNAcTB PE=2 SV=1 - [Q9VAQ8_DROME]	0.000E0	0.000E0					0.00	3.41	1	1	323	37.8	7.09
CG32479, isoform B OS=Drosophila melanogaster GN=Usp10 PE=4 SV=1 - [M9PDK3_DROME]	0.000E0	0.000E0					1.64	3.26	1	1	797	85.9	9.11
Probable isocitrate dehydrogenase [NAD] subunit alpha, mitochondrial OS=Drosophila melanogaster GN=I(1)G0156 PE=2 SV=1 - [IDH3A_DROME]	0.000E0	3.035E6					2.67	3.18	1	1	377	40.8	7.36
HDC13886 OS=Drosophila melanogaster GN=HDC13886 PE=4 SV=1 - [Q6IK08_DROME]	0.000E0	1.901E6					1.63	3.18	1	2	314	35.3	7.02
Odorant receptor OS=Drosophila melanogaster GN=Or7a PE=3 SV=1 - [E2E4R0_DROME]	0.000E0	5.724E7					2.04	3.15	1	1	413	47.6	8.24
GH23452p OS=Drosophila melanogaster GN=I(2)tid-RA PE=2 SV=1 - [D3DN23_DROME]	0.000E0	8.047E5					7.31	3.15	1	2	445	49.2	9.16
ATP synthase subunit beta OS=Drosophila melanogaster GN=ATPsyn-beta-RA PE=2 SV=1 - [D3DMY7_DROME]	0.000E0	6.502E6					2.19	3.12	1	1	353	38.0	5.12
Probable medium-chain specific acyl-CoA	0.000E0	1.144E6					7.26	3.10	1	2	419	45.8	7.94

Appendices

dehydrogenase, mitochondrial OS=Drosophila melanogaster GN=CG12262 PE=1 SV=1 - [ACADM_DROME]													
RE40293p OS=Drosophila melanogaster GN=CG7668 PE=2 SV=1 - [Q8SYR0_DROME]	0.000E0	9.896E5					3.82	3.08	1	2	422	48.0	5.99
Flotillin-1 OS=Drosophila melanogaster GN=Flo-1 PE=2 SV=1 - [FLOT1_DROME]	0.000E0	1.422E6					8.66	3.05	1	3	426	47.1	5.64
CG8642 (Fragment) OS=Drosophila melanogaster GN=CG8642 PE=4 SV=2 - [A1Z7G6_DROME]	0.000E0	0.000E0					2.21	3.03	1	1	429	49.1	7.96
Elongation factor 1-gamma OS=Drosophila melanogaster GN=Ef1gamma PE=2 SV=2 - [EF1G_DROME]	0.000E0	1.276E6					3.54	3.02	1	1	431	48.9	7.05
Pi3K21B, isoform B OS=Drosophila melanogaster GN=Pi3K21B PE=4 SV=1 - [Q7KTZ2_DROME]	0.000E0	5.966E5					0.00	3.02	1	1	496	56.3	6.20
26S proteasome regulatory complex subunit p48B OS=Drosophila melanogaster GN=Rpt1 PE=2 SV=1 - [Q7KMQ0_DROME]	0.000E0	1.654E6					7.61	3.00	1	2	433	48.5	6.04
NADH dehydrogenase (ubiquinone) complex I, assembly factor 6 homolog OS=Drosophila melanogaster GN=sicily PE=2 SV=1 - [NDUF6_DROME]	0.000E0	4.134E5					1.76	2.99	1	1	334	38.2	9.54
MIP27737p (Fragment) OS=Drosophila melanogaster GN=cin-RA PE=2 SV=1 - [E4NKI3_DROME]	0.000E0	1.239E6					0.00	2.94	1	1	374	40.7	7.17
F124005p1 OS=Drosophila melanogaster GN=RanBPM-RC PE=2 SV=1 - [X5D3H6_DROME]	0.000E0	5.302E6					2.27	2.84	1	1	598	66.4	6.68
60S acidic ribosomal protein P0 OS=Drosophila melanogaster GN=RpLP0 PE=1 SV=1 - [RLA0_DROME]	0.000E0	1.072E6					0.00	2.84	1	1	317	34.2	6.95
Glutamate dehydrogenase, isoform D OS=Drosophila melanogaster GN=Gdh PE=4 SV=1 - [A0A0C4DHE7_DROME]	0.000E0	1.519E6					1.90	2.81	1	1	391	43.0	7.30
CG30438, isoform A OS=Drosophila	0.000E0	1.084E6					2.18	2.76	1	1	435	49.9	9.29

Appendices

melanogaster GN=CG30438 PE=2 SV=1 - [Q7K142_DROME]														
GM1404Op OS=Drosophila melanogaster GN=Smg6 PE=2 SV=1 - [Q8MZ10_DROME]	0.000E0	8.952E6					0.00	2.76	1	2	688	79.3	8.18	
CG8841, isoform A OS=Drosophila melanogaster GN=CG8841 PE=4 SV=1 - [Q0E9B5_DROME]	0.000E0	6.160E6					2.45	2.75	1	1	837	95.5	5.78	
AT16994p OS=Drosophila melanogaster GN=pdm3 PE=2 SV=1 - [Q7JUR9_DROME]	0.000E0	0.000E0	2.41	2.72	1	1					994	106.3	8.00	
Cytoplasmic protein 89BC OS=Drosophila melanogaster GN=bor PE=2 SV=1 - [Q7KJ37_DROME]	0.000E0	1.038E6					4.99	2.71	1	2	554	63.1	9.19	
CG14945, isoform B OS=Drosophila melanogaster GN=CG14945 PE=4 SV=1 - [Q9VKC3_DROME]	5.065E10	0.000E0	0.00	2.70	1	1					482	54.8	6.90	
Aconitase, isoform B OS=Drosophila melanogaster GN=Acon PE=2 SV=2 - [Q9VIE8_DROME]	0.000E0	2.300E6					2.65	2.67	2	2	787	85.3	8.24	
Malate dehydrogenase OS=Drosophila melanogaster GN=Mdh1 PE=2 SV=1 - [Q8MQS7_DROME]	0.000E0	9.217E5					1.68	2.67	1	1	337	36.0	7.39	
Elongation factor Tu mitochondrial, isoform A OS=Drosophila melanogaster GN=EftuM PE=3 SV=1 - [A1Z9E3_DROME]	0.000E0	1.592E6					0.00	2.66	1	1	489	54.0	8.03	
LD46175p OS=Drosophila melanogaster GN=sea PE=2 SV=1 - [Q7KSQ0_DROME]	0.000E0	3.520E6					1.91	2.52	1	1	317	34.1	9.42	
CG11893 OS=Drosophila melanogaster GN=CG11893 PE=2 SV=1 - [Q9VBT2_DROME]	0.000E0	1.693E7					2.41	2.40	1	1	416	48.9	5.64	
CG32855 OS=Drosophila melanogaster GN=CG32855 PE=4 SV=1 - [Q8INCO_DROME]	0.000E0	0.000E0					2.13	2.36	1	1	552	60.3	9.26	
Desaturase 1, isoform A OS=Drosophila melanogaster GN=Desat1 PE=2 SV=1 - [Q7K4Y0_DROME]	0.000E0	0.000E0					0.00	2.35	1	1	383	43.4	8.82	
CG6255 protein OS=Drosophila	0.000E0	2.360E6					1.64	2.34	1	1	342	35.9	9.36	

Appendices

melanogaster GN=CG6255 PE=3 SV=1 - [A0AMMO_DROME]													
CG8036, isoform D OS=Drosophila melanogaster GN=CG8036 PE=4 SV=1 - [Q7KSU6_DROME]	0.000E0	2.747E6					5.19	2.24	1	2	580	63.0	6.80
MICOS complex subunit Mic60 OS=Drosophila melanogaster GN=CG6455 PE=2 SV=4 - [MIC60_DROME]	0.000E0	1.758E6					7.71	2.17	1	2	739	82.0	8.94
60 kDa heat shock protein homolog 1, mitochondrial OS=Drosophila melanogaster GN=Hsp60B PE=2 SV=1 - [CH60B_DROME]	0.000E0	8.149E5					4.10	2.16	1	1	648	68.6	5.64
CG5718 OS=Drosophila melanogaster GN=SdhAL PE=2 SV=1 - [Q8SX97_DROME]	0.000E0	6.851E5					3.54	2.15	1	1	651	71.7	8.35
Drosocrystallin OS=Drosophila melanogaster GN=Cry PE=4 SV=1 - [O96967_DROME]	0.000E0	2.622E6					1.73	2.12	1	1	472	55.1	5.66
Ferrochelatase, mitochondrial OS=Drosophila melanogaster GN=FeCh PE=2 SV=1 - [HEMH_DROME]	0.000E0	3.095E6					4.09	2.08	1	2	384	43.6	8.40
Succinate dehydrogenase [ubiquinone] iron-sulfur subunit, mitochondrial OS=Drosophila melanogaster GN=SdhBL PE=2 SV=1 - [Q8SXL9_DROME]	0.000E0	9.336E5					2.06	2.06	1	1	437	46.6	9.55
AT03614p (Fragment) OS=Drosophila melanogaster GN=opa1-like-RA PE=2 SV=1 - [FOJAK2_DROME]	0.000E0	4.904E5					2.96	2.04	1	1	540	63.2	7.31
Sphingosine-1-phosphate lyase OS=Drosophila melanogaster GN=Sply PE=2 SV=1 - [SGPL_DROME]	0.000E0	2.358E6					0.00	2.02	1	1	545	60.3	8.46
Protein fem-1 homolog CG6966 OS=Drosophila melanogaster GN=CG6966 PE=2 SV=2 - [FEM1A_DROME]	0.000E0	1.851E6					2.61	1.96	1	1	664	73.7	7.08
RE71183p OS=Drosophila melanogaster GN=SRm160 PE=2 SV=1 - [Q6AWQ1_DROME]	0.000E0	5.351E6					0.00	1.89	1	1	954	107.5	11.60
CG42570, isoform B OS=Drosophila melanogaster GN=CG42570 PE=4 SV=1 -	0.000E0	0.000E0	0.00	1.81	1	1					609	70.6	5.44

Appendices

[M9PFC9_DROME]														
IP08220p OS=Drosophila melanogaster GN=CG15655 PE=2 SV=1 - [Q1WWA9_DROME]	3.330E7	0.000E0	2.03	1.81	1	1						496	55.3	7.58
Major facilitator superfamily transporter 3 OS=Drosophila melanogaster GN=MFS3 PE=2 SV=1 - [Q9VPX2_DROME]	0.000E0	1.587E7					4.59	1.76	1	2		512	55.0	7.46
CG5353-PB, isoform B OS=Drosophila melanogaster GN=Aats-thr PE=3 SV=1 - [Q8IP94_DROME]	0.000E0	4.684E5					1.75	1.74	1	1		690	79.3	6.90
CG10366 OS=Drosophila melanogaster GN=CG10366 PE=4 SV=1 - [Q9VIS9_DROME]	0.000E0	1.264E7					2.57	1.73	1	1		578	65.4	6.52
CG6512-PB, isoform B OS=Drosophila melanogaster GN=CG6512 PE=3 SV=1 - [Q81QQ9_DROME]	0.000E0	7.138E5					1.85	1.72	1	1		697	76.0	7.09
Eater OS=Drosophila melanogaster GN=eater PE=4 SV=1 - [D9IQC5_DROME]	4.054E7	1.687E7	5.04	1.71	1	2	2.20	1.71	1	1		876	93.6	5.77
CG1970, isoform B OS=Drosophila melanogaster GN=ND-49 PE=2 SV=2 - [Q9V4E0_DROME]	0.000E0	1.105E6					0.00	1.71	1	1		468	52.9	6.67
LD22885p OS=Drosophila melanogaster GN=Gcn2 PE=2 SV=1 - [Q7YU14_DROME]	0.000E0	0.000E0	0.00	1.68	1	1						1312	147.4	6.02
AT28279p OS=Drosophila melanogaster GN=CG13382 PE=2 SV=1 - [Q8T3H5_DROME]	0.000E0	1.121E6					1.78	1.57	1	1		509	58.8	9.33
BcDNA.LD34343 OS=Drosophila melanogaster GN=wdb PE=2 SV=2 - [Q9VB23_DROME]	0.000E0	6.156E6					1.82	1.53	1	1		524	59.7	7.49
IP09048p OS=Drosophila melanogaster GN=CG6118 PE=2 SV=1 - [Q4V732_DROME]	0.000E0	1.359E6					0.00	1.47	1	1		882	99.4	6.73
Muscle wasted, isoform D OS=Drosophila melanogaster GN=mute PE=2 SV=1 - [Q8MS31_DROME]	0.000E0	4.894E7					3.81	1.35	1	2		665	74.4	6.55
Probable ATP-dependent RNA helicase Dbp73D OS=Drosophila melanogaster GN=Dbp73D PE=2 SV=3 - [DDX51_DROME]	0.000E0	0.000E0					0.00	1.31	1	1		687	77.5	8.19

Appendices

CG10073, isoform A OS=Drosophila melanogaster GN=CG10073-RA PE=2 SV=1 - [A1ZBK4_DROME]	1.730E6	0.000E0	2.70	1.26	1	1					873	97.5	6.80
LD17482p OS=Drosophila melanogaster GN=Atg4b PE=2 SV=1 - [Q8T0A2_DROME]	0.000E0	0.000E0	0.00	1.23	1	1					653	73.0	6.01
Homeobox protein cut-like OS=Drosophila melanogaster GN=onecut PE=2 SV=1 - [Q95TW5_DROME]	0.000E0	1.125E6					1.85	1.23	1	1	976	106.3	5.43
Dynein regulatory complex protein 1 homolog OS=Drosophila melanogaster GN=CG10958 PE=2 SV=1 - [DRC1_DROME]	0.000E0	0.000E0					1.77	1.21	1	1	743	88.1	8.07
Terrribly reduced optic lobes, isoform AX OS=Drosophila melanogaster GN=trol PE=4 SV=1 - [X2JAC7_DROME]	0.000E0	1.715E6					2.75	1.19	3	3	2853	316.6	4.88
RH57795p (Fragment) OS=Drosophila melanogaster PE=2 SV=1 - [Q6NKL9_DROME]	0.000E0	1.154E6					1.88	1.19	1	1	589	64.7	6.14
Paramyosin, long form OS=Drosophila melanogaster GN=Prm PE=1 SV=1 - [MYS1_DROME]	0.000E0	4.409E5					2.88	1.14	1	1	879	102.3	5.58
Dystrophin, isoform L OS=Drosophila melanogaster GN=Dys PE=4 SV=1 - [A0A0B4KGB9_DROME]	0.000E0	7.261E6					2.47	1.13	1	1	1323	149.8	6.35
IP16232p (Fragment) OS=Drosophila melanogaster GN=CG6214-RE PE=2 SV=1 - [A2RVE8_DROME]	0.000E0	1.338E7					1.76	1.01	1	1	594	68.4	9.32
Raf homolog serine/threonine-protein kinase phl OS=Drosophila melanogaster GN=phl PE=1 SV=6 - [KRAF1_DROME]	0.000E0	1.597E7					0.00	0.95	1	1	739	83.7	8.73
TEP1 protein OS=Drosophila melanogaster GN=Tep1 PE=2 SV=1 - [Q9NFV8_DROME]	0.000E0	2.991E8					2.29	0.89	1	1	1354	151.8	8.35
CG14441, isoform A OS=Drosophila melanogaster GN=CG14441 PE=4 SV=2 - [Q9W3X0_DROME]	0.000E0	1.852E7					0.00	0.87	1	1	1149	128.2	6.57
RE10062p OS=Drosophila melanogaster GN=Cad74A PE=2 SV=1 - [Q8IGX4_DROME]	4.956E6	3.540E6	2.76	0.66	1	1	2.45	0.66	1	1	1820	200.9	4.97

Appendices

LP19492p OS=Drosophila melanogaster GN=trio-RA PE=2 SV=1 - [C6TP86_DROME]	0.000E0	7.528E6					0.00	0.60	1	1	1987	225.9	6.57
CG17150, isoform D OS=Drosophila melanogaster GN=CG17150 PE=4 SV=3 - [Q9VZ77_DROME]	0.000E0	0.000E0					0.00	0.59	1	1	4385	504.3	6.24
CG3280 OS=Drosophila melanogaster GN=CG46121 PE=4 SV=1 - [M9NDN5_DROME]	0.000E0	9.778E6					0.00	0.52	1	1	1932	216.5	6.57
CG42795, isoform C OS=Drosophila melanogaster GN=CG42795 PE=4 SV=1 - [A0A0B4KG40_DROME]	0.000E0	6.654E6					4.80	0.52	1	2	2904	328.3	8.37
Crossveinless c, isoform C OS=Drosophila melanogaster GN=cv-c PE=4 SV=1 - [A8JR05_DROME]	0.000E0	0.000E0	2.61	0.51	1	1					2351	255.8	8.46
Enhancer of polycomb, isoform C OS=Drosophila melanogaster GN=E(Pc) PE=4 SV=1 - [A0A0B4KEK1_DROME]	0.000E0	1.776E7					0.00	0.25	1	1	1974	216.2	6.24